

FEDERAL UNIVERSITY OF PELOTAS
Faculty of Agronomy Eliseu Maciel
Crop Protection Graduate Program



Thesis

**Partial resistance, fungicide and mineral nutrition on wheat: effect on
cytological and biochemical defenses, chlorophyll a fluorescence, yield and
technological grain quality**

Andrea Elizabeth Román Ramos

Pelotas

2021

Universidade Federal de Pelotas / Sistema de Bibliotecas
Catalogação na Publicação

R175p Ramos, Andrea Elizabeth Román

Resistência parcial, fungicida e nutrição mineral em trigo: efeito nas defesas citológicas e bioquímicas, fluorescência da clorofila a, rendimento e qualidade tecnológica do grão / Andrea Elizabeth Román Ramos ; Leandro José Dallagnol, orientadora ; Daniel Debona, coorientador. — Pelotas, 2021.

217 f.

Tese (Doutorado) — Programa de Pós-Graduação em Fitossanidade, Faculdade de Agronomia Eliseu Maciel, Universidade Federal de Pelotas, 2021.

1. Fontes de inóculo. 2. Fluorescência de clorofila a. 3. Qualidade tecnológica de trigo. 4. Análise citológica. 5. Doenças de trigo. I. Dallagnol, Leandro José, orient. II. Debona, Daniel, coorient. III. Título.

CDD : 633.11

Elaborada por Gabriela Machado Lopes CRB: 10/1842

Andrea Elizabeth Román Ramos

Partial resistance, fungicide and mineral nutrition on wheat: effect on cytological and biochemical defenses, chlorophyll a fluorescence, yield and technological grain quality

Thesis submitted to the Crop Protection Graduate Program of the Faculty of Agronomy Eliseu Maciel of the Federal University of Pelotas, as a partial requirement for obtaining the title of Doctor of Science (Area: Plant Pathology).

Advisor: Prof.Dr. Leandro José Dallagnol.

Co-advisor: Prof.Dr. Daniel Debona.

Andrea Elizabeth Román Ramos

Partial resistance, fungicide and mineral nutrition on wheat: effect on cytological and biochemical defenses, chlorophyll a fluorescence, yield and technological grain quality

Thesis approved as a partial requirement, to obtain the degree of Doctor of Science (Area: Plant Pathology).

Crop Protection Graduate Program, Faculty of Agronomy Eliseu Maciel, Federal University of Pelotas.

Dec 16, 2021

Examination committee:

Prof. Dr. Leandro José Dallagnol (advisor)

Doctor in Science - Plant Pathology by University of São Paulo, Esalq

Dra. Martha Zavariz de Miranda

Doctor in Science - Food Technology by State University of Campinas

Dr. Carlos Eduardo Aucique-Perez

Doctor in Science - Plant Physiology by Federal University of Viçosa

Prof. Dr. Alessandro Antonio Fortunato

Doctor in Science - Plant Pathology by Federal University of Viçosa

Dr. Paulo Kuhnem

Doctor in Science - Plant Pathology by Federal University of Rio Grande do Sul

Acknowledgements

I would like to thank God for giving me the courage and strength; and my family for their support during these years.

I would like to thank the Postharvest Laboratory of the Brazilian Agricultural Research Corporation's National Wheat Research Center (Embrapa Trigo) for their partnership, BIOTRIGO for providing seeds for experiments and Passo Fundo University for providing the *Pyrenohora tritici-repentis* isolates used in the greenhouse experiments.

I also wish to thank to my co advisor and advisor for their supervision of the research; and my committee examination members for critical review and suggestions.

I would like to thank to the staff of Centro Agropecuário da Palma, the Laboratory of Phytopathogenic Fungus and Seed Pathology, and the Laboratory of Virology of the Veterinary School of UFPEL for support in conducting the field and lab experiments.

I want to thank the Organization of American States (OAS) and Office to Coordinate Improvement of Higher Education Personnel (CAPES) for funding the scholarship of my doctorate studies.

Finally, I thank all who in any way contributed to the realization of this research.

"If A is success in life, then $A = x + y + z$. Work is x, play is y,
and z is keeping your mouth shut."

-Albert Einstein, 1929

Resumo

Román Ramos, Andrea Elizabeth. **Resistência parcial, fungicida e nutrição mineral em trigo: efeito nas defesas citológicas e bioquímicas, fluorescência da clorofila a, rendimento e qualidade tecnológica do grão. 2021. Tese (Doutorado).** – Programa de Pós-graduação em Fitossanidade, Faculdade de Agronomia Eliseu Maciel, Universidade Federal de Pelotas, Pelotas, 2021.

O trigo é afetado por diversas doenças. Dentre elas, a mancha amarela causada por *Pyrenohora tritici-repentis* (Died.) (*Ptr*) é uma das principais e causa danos significativos na produtividade. Estudos indicam que a adubação nitrogenada e a aplicação de fungicidas diminuem a severidade dessa doença. No entanto, há poucas informações sobre o aumento de nitrogênio (N) na interação com doenças do trigo ou com elementos minerais como o silício (Si). Neste estudo, foram realizados experimentos de campo nas safras de 2019 e 2020, com a ocorrência natural do patógeno e experimentos em casa de vegetação, no Rio Grande do Sul, Brasil. No primeiro capítulo foram determinadas as principais fontes de inoculo de *Ptr*. Os resultados de experimentos em campo mostraram que as potenciais fontes de inóculo, foram os pseudotécios encontrados em restos de palha e conídios de *Drechslera* sp. em etapas de desenvolvimento específicas. No capítulo 2, foram testadas três doses de N e a pré-mistura (bixafem+protioconazol+trifloxistrobina) em cultivares de trigo com resistência contrastante, considerando a intensidade da doença e o retorno econômico na eficiência de uso de nitrogênio (EUN). Os resultados mostraram que a cultivar moderadamente resistente e a dose recomendada de N (130 kg ha^{-1}), aumentaram a duração da área sadia, mantendo a EUN e o retorno econômico adequado, reduzindo a área abaixo da curva de progresso da doença (AACPD) da mancha amarela. No entanto, a maior AACPD de oídio foi observada com altas doses de nitrogênio. Para a ferrugem da folha e giberela, a cultivar moderadamente resistente e a aplicação de fungicida reduziram a AACPD. No terceiro capítulo, foram avaliadas medidas de manejo de doenças considerando as mudanças na fluorescência de *Chla*, os componentes de rendimento e a qualidade tecnológica do trigo. Os resultados mostraram que a eficiência do fotossistema II (*Fv/Fm*) que avaliou disfunções fotossintéticas decorrentes da doença, estava correlacionada com parâmetros de qualidade tecnológica de trigo. A dose recomendada de N aumentou o teor de proteína, o glúten seco e o glúten úmido, mantendo o tempo de estabilidade e absorção de água adequados, demonstrando a resistência da massa à mistura e melhorando a qualidade tecnológica do grão de trigo. No quarto capítulo, realizado em casa de vegetação, foi avaliado o efeito do N na resistência e na eficiência fotossintética de plantas infectadas pelas raças 1 e 2 de *Ptr*. O resultado demonstrou que o N alto está associado a um maior período de incubação, reduzindo a eficiência relativa da infecção e o tamanho final da lesão causada por *Ptr* quando comparado à dose

de N recomendada. Nas plantas inoculadas com a raça 1, as concentrações de clorofila foram menores que das plantas inoculadas com a raça 2 e a fluorescência da clorofila avaliou danos causados por *Ptr* raça 1 e 2, observou-se uma diminuição da Fv/Fm e um aumento de variáveis relacionadas com transporte de elétrons. No quinto capítulo, a interação da fertilização de N com Si, foi avaliada por meio das respostas histocitológicas e mecanismos bioquímicos de defesa ativadas em trigo infectado por *Ptr*. O experimento mostrou que a atividade enzimática foi associada ao acúmulo de H_2O_2 e de calose em resposta à infecção por *Ptr* no tratamento com +Si e N baixo. No entanto, em plantas com N alto, a concentração de +Si diminuiu nas folhas. Esses resultados indicaram que cada elemento pode atuar de forma independente na ativação das respostas de defesa da planta e na ativação de mecanismos de defesa antioxidantes. Os resultados desta pesquisa mostram o uso adequado da fertilização nitrogenada no manejo de doenças de trigo especialmente em doenças da folha, suas implicações na interação com outros elementos e o efeito na qualidade tecnológica do grão.

Palavras-chave: fontes de inóculo, fluorescência de clorofila *a*, qualidade tecnológica de trigo, análise citológica, doenças de trigo.

Abstract

Román Ramos, Andrea Elizabeth. **Partial resistance, fungicide and mineral nutrition on wheat: effect on cytological and biochemical defenses, chlorophyll a fluorescence, yield and technological grain quality.** Thesis (Doctorate). – Crop Protection Graduation Program, Faculty of Agronomy Eliseu Maciel, Federal University of Pelotas, Pelotas, 2021.

Wheat is affected by several diseases. Among them, tan spot caused by *Pyrenohora tritici-repentis* (Died.) (*Ptr*) is one of the main ones and causes significant damage to productivity. Studies indicate that nitrogen (N) fertilization and the application of fungicides decrease the severity of this disease. However, there is few information about nitrogen (N) increase and its interaction with wheat disease or with mineral elements such as silicon (Si). In this study, field experiments were conducted in the 2019 and 2020 growing seasons, with the natural occurrence of the pathogen and in greenhouse, in Rio Grande do Sul, Brazil. In the first chapter, the main sources of *Ptr* inoculum were determined. Results from field experiments showed that potential inoculum sources were pseudothecia found in straw remains and conidia of *Drechslera* sp. in specific plant develop stages. In the second chapter, three N rates and the premix (bixafen+prothioconazole+trifloxystrobin) were tested on wheat cultivars with contrasting resistance, considering the disease intensity and the economic return in nitrogen use efficiency (NUE). The results of nitrogen fertilization showed that the moderately resistant cultivar and the recommended N rate (130 kg ha⁻¹), increased the healthy area duration while maintaining NUE and adequate economic return, reducing the area under the disease progress curve (AUDPC) of the tan spot. However, the highest AUDPC of powdery mildew was observed with high nitrogen doses. For leaf rust and FHB, a moderately resistant cultivar and fungicide application reduced the AUDPC. In the third chapter, disease management measures considering changes in *Chla* fluorescence, yield components, and technological quality of wheat were evaluated. The results showed that photosystem II efficiency (*Fv/Fm*) that evaluated photosynthetic dysfunction arising from disease was correlated with wheat technological quality parameters. The recommended N rate increased protein content, dry and wet gluten, while maintaining adequate stability time and water absorption, demonstrating dough resistance to mixing and improving the technological quality of wheat grain. In the fourth chapter, conducted in the greenhouse, the effect of N on resistance and photosynthetic efficiency of plants infected by *Ptr* races 1 and 2 was evaluated. The result showed that high N is associated with a longer incubation period, reducing the relative efficiency of infection and the final size of the lesion caused by *Ptr* when compared to the recommended N. In plants

inoculated with race 1, chlorophyll concentrations were lower than in plants inoculated with race 2 and chlorophyll fluorescence evaluated the damage caused by *Ptr* race 1 and 2, demonstrating a decrease in Fv/Fm and increase of variables related to electron transport. In the fifth chapter, the interaction of N with Si fertilization was evaluated through histocytological responses and biochemical defense mechanisms activated in *Ptr*-infected wheat. The experiment showed that enzyme activity was associated with H_2O_2 and callose accumulation in response to *Ptr* infection in the +Si and low N treatment. However, in plants with high N, the concentration of +Si decreased in the leaves. These results indicated that each element may act independently in activating plant defense responses and activating antioxidant defense mechanisms. The results of this research show the adequate use of nitrogen fertilization in the management of wheat diseases especially with leaf diseases, its implications in the interaction with other elements and the effect on the grain technological quality.

Keywords: sources of inoculum, chlorophyll a fluorescence, wheat technological quality, cytological analysis, wheat diseases.

Table of Contents

Introduction.....	1
Chapter 1	
Detection of potential inoculum sources of tan spot under field condition	10
Abstract	10
Introduction.....	11
Materials and methods	12
Results	17
Discussion	19
Conclusions.....	21
References	23
Chapter 2	
Nitrogen fertilization, fungicide application and genetic resistance in wheat disease management	43
Abstract	43
Introduction.....	44
Materials and methods	46
Results	50
Discussion	55
Conclusion.....	57
References	58
Chapter 3	
Disease management maintains adequate chlorophyll a fluorescence and enhances wheat grain technological quality	82
Abstract	82
Introduction.....	83
Materials and methods	85
Results	89
Discussion	92
Conclusion.....	95

References	96
------------------	----

Chapter 4

Effect of nitrogen on wheat cultivars with contrasting resistance infected by <i>Pyrenophora tritici-repentis</i>	121
Abstract	121
Introduction.....	122
Materials and methods	124
Results	130
Discussion	133
References	137

Chapter 5

Abstract	161
Introduction.....	162
Materials and methods	164
Results	174
Discussion	177
References	182

General conclusions	203
---------------------------	-----

Introduction

Wheat (*Triticum aestivum* L.) is one of the most important crops as well as the cereal most consumed worldwide (USDA 2021a; 2021b). In Brazil, the southern region is the most important for wheat production, and Rio Grande do Sul is the second-largest producing state after Paraná, accounting for 36% of Brazil's total production (CONAB 2021). However, weather conditions in southern Brazil are usually very favorable to some diseases affecting wheat (Del Ponte *et al.* 2009). In this context, the main biotic factors affecting the crop during the growing stages are leaf diseases, caused by *Pyrenophora tritici-repentis* (Died.) Drechs (tan spot), *Puccinia striiformis* (stripe rust), *Puccinia triticina* (leaf rust), and *Blumeria graminis* (DC.) f. sp. *tritici* (powdery mildew), and spike diseases, caused by the *Fusarium graminearum* complex (fusarium head blight – FHB), and *Magnaporthe oryzae* pathotype *Triticum* (blast). These pathogens threaten the grain yield and technological quality. To counteract these damages, integrated disease management is employed, which includes the use of resistant genotypes, healthy seeds, fungicides and fertilization practices (Fleitas *et al.* 2018; Dallagnol *et al.* 2020; Pazdiora *et al.* 2021). Besides reducing disease prevalence and severity, these measures also have an effect on wheat technological quality (Kweon *et al.* 2011). Changes in the fertilization is an option to reduce disease progress and increase fungicide efficiency or reduce the number of applications per crop cycle (Pazdiora *et al.* 2021), and can also influence wheat technological quality.

Several studies have demonstrated that nitrogen (N) is an essential element for plant growth and plays a key role in plant health and yield (Malhi *et al.* 2001; Castro *et al.* 2018; Fleitas *et al.* 2018; Schierenbeck *et al.* 2019). In this context,

the variation in the N concentration in plant tissues has shown contrasting effects on disease development (Huber and Thompson 2007; Veresoglou *et al.* 2013; Simon *et al.* 2020). For necrotrophic pathogens such as *Pyrenophora tritici-repentis* (*Ptr*), some studies have demonstrated the reduction of disease severity and increase of green leaf area in wheat by increasing the nitrogen rate (Huber *et al.* 1987; Jones *et al.* 1990; Bockus and Davis 1993; Fernandez *et al.* 1998; Krupinsky and Tanaka 2001; Fleitas *et al.* 2018). However, increasing the N rates can also increase the levels of biotrophic pathogens such as *Blumeria graminis* (Jensen and Munk 1997; Stadnik and Buchenauer 2000) and *Puccinia striiformis* f. sp. tritici (Ash and Brown 1991). Little is known about the effect of increasing N rate for the tan spot control and its interaction with other diseases under natural infection in the field; as well as the effects on the physiological process, grain yield and technological quality.

Tan spot is a globally important disease (Wiese 1987; Turner *et al.* 2021), causing yield losses up to 75% in severe cases (Rees and Platz 1980; Reis and Casa 2007). The no-till system currently used favors the survival of the fungus and increases the intensity of tan spot over the years (Ciuffetti *et al.* 2014). However, little is known about the amount of primary inoculum under field conditions and its dynamic during the crop cycle.

Furthermore, *Ptr* produces proteinaceous (Tox A and Tox B) and non-proteinaceous (Tox C) host-specific toxins, also known as necrotrophic effectors (NEs) (Friesen *et al.* 2008). Those toxins are associated with inducement of cell death, preceded by changes in the photosynthetic machinery and accumulation of reactive oxygen species (ROS), likely due to the disruption of homeostasis of the two photosystems (PSI and II) (Manning *et al.* 2009). In this sense, *Ptr* can affect

energy dissipation via chlorophyll (Chl) a fluorescence due to the toxin production during host-pathogen interaction. However, there is no information related to changes in the chlorophyll a fluorescence in the *Ptr*-wheat interaction.

In addition, recent studies have described the application of N and silicon (Si) amendment for disease management (White *et al.* 2017; Wu *et al.* 2017; Galindo *et al.* 2021; Pazdiora *et al.* 2021). Silicon is considered a non-essential plant nutrient that plays a beneficial role in promoting plant growth and increasing yield by alleviating biotic and abiotic stresses in many plant species (Rodrigues *et al.* 2015; Debona *et al.* 2017; Coskun *et al.* 2019; Dallagnol *et al.* 2020). Therefore, it is important to understand the interaction between Si and N when they are used for *Ptr* management in wheat.

In this context, N is one of the most limiting factors in crop production systems, so it is often applied in large amounts (White 2015; Ying *et al.* 2017). Thus, the increase of the cost of N fertilizer and the pollution caused by its wide-scale use in agriculture make it necessary to manage N rates carefully. The correct dose of nitrogen used for disease management and higher grain yield requires understanding the nitrogen use efficiency (NUE). In this respect, understanding the effect of N on diseases is important to determine effective management strategies.

In this study, field and greenhouse experiments were carried out from 2019 to 2021. The methods used in this investigation and the results obtained from them are described in five chapters. Regarding field experiments, the first three chapters present the results relating of the following topics: 1) the detection of possible sources of *Ptr* inoculum; 2) the effect of nitrogen fertilization, genotype

resistance and the application of fungicides on the severity of the tan spot and grain yield; and 3) the application of comprehensive disease management measures and their effect on chlorophyll a fluorescence and the improvement of the technological quality of wheat grains. Those topics aim to address the following research questions: a) What are the potential inoculum sources for tan spot epidemics under field conditions? b) What is the effect of increasing by 50% the recommended nitrogen rate associated with two sprayings of fungicide pre-mix (carboxamide + triazole + strobilurin) for tan spot control on cultivars with contrasting resistance and their interaction with other wheat diseases? and c) What is the effect of disease management measures on changes in the chlorophylla (Chla) fluorescence, yield components, and technological quality of early-maturing wheat cultivars?

Chapters 4 and 5 describe greenhouse experiments to assess the following topics: a) the effect of nitrogen doses on contrasting wheat genotypes during the infection of *Pyrenophora tritici-repentis* races 1 and 2; and b) the effect of N and Si interaction on histocytological defense responses and biochemical defense mechanisms during *Ptr* infection. In this case, the following questions were answered: d) What is the effect of nitrogen rates, using urea as ammonium source, on resistance-contrasting wheat genotypes during the infection of *Pyrenophora tritici-repentis* races 1 and 2 on tan spot resistance components and photosynthesis parameters (Chla fluorescence and chlorophyll content)? and e) What is the effect of Si amendment (calcium silicate) and its interaction with N (urea) on the histocytological defense responses and biochemical defense mechanisms activated during *Pyrenophora tritici-repentis* infection in a susceptible

wheat cultivar through callose and hydrogen peroxide accumulation as well as on the activity of antioxidant enzymes?

References

- Ash, G J, Brown, J F. (1991). Effect of nitrogen nutrition of the host on the epidemiology of *Puccinia striiformis* f. sp. *tritici* and crop yield in wheat. *Australasian Plant Pathology*, **20**, 108-114.
- Bockus W, Davis M A. (1993). Effect of nitrogen fertilizers on severity of tan spot of winter wheat. *Plant Disease*, **77**, 508.
- Castro A C, Fleitas, M C, Schierenbeck M, Gerard, G S, Simón M R. 2018. Evaluation of different fungicides and nitrogen rates on grain yield and bread-making quality in wheat affected by *Septoria tritici* blotch and yellow spot. *Journal of Cereal Science*, **83**, 49-57.
- Ciuffetti L M, Manning, V A, Pandelova I, Faris J D, Friesen T L, Strelkov S E, Weber G L, Goodwin S B, Wolpert T J, Figueroa M. (2014). *Pyrenophora tritici-repentis*: a plant pathogenic fungus with global impact. In: *Genomics of Plant-Associated Fungi: Monocot Pathogens*. Springer, pp. 1–39.
- CONAB. 2021. Acompanhamento da Safra Brasileira de Grãos, safra 2020/21, quinto levantamento, fev. 2021. Available at: <https://www.conab.gov.br/info-agro/safras/graos/boletim-da-safra-de-graos> [Accessed January 25, 2020].
- Coskun D, Deshmukh R, Sonah H, Menzies J G, Reynolds O, Ma J F, Kronzucker H J, Bélanger R R. (2019). The controversies of silicon's role in plant biology. *New Phytologist*, **221**, 67–85.
- Dallagnol L J, Román A E, da Rosa Dorneles K. (2020). Silicon Use in the Integrated Disease Management of Wheat: Current Knowledge. *Current Trends in Wheat Research*. [Online First], IntechOpen, Available at: <https://www.intechopen.com/online-first/74509>.
- Debona D, Rodrigues F A, Datnoff L E. (2017). Silicon's role in abiotic and biotic plant stresses. *Annual Review of Phytopathology. Annual Reviews*, **55**, 85–107.
- Del Ponte E M, Fernandes J M, Pavan W, Baethgen W E. (2009). A model based assessment of the impacts of climate variability on fusarium head blight seasonal risk in Southern Brazil. *Journal of Phytopathology*, **157**, 675–681.
- Fernandez M R, Zentner R P, McConkey B G, Campbell C A. (1998). Effects of crop rotations and fertilizer management on leaf spotting diseases of spring wheat in southwestern Saskatchewan. *Canadian Journal of Plant Science*, **78**, 489–496.

- Fleitas M C, Schierenbeck M, Gerard G S, Dietz J I, Golik S I, Simón M R. (2018). Breadmaking quality and yield response to the green leaf area duration caused by fluxapyroxad under three nitrogen rates in wheat affected with tan spot. *Crop Protection*, **106**, 201–209.
- Friesen T L, Xu S S, Harris M O. (2008). Stem rust, tan spot, *Stagonospora nodorum* blotch, and hessian fly resistance in langdon durum– synthetic hexaploid wheat lines. *Crop Science*, **48**, 1062.
- Galindo F S, Pagliari P H, Rodrigues W L, Fernandes G C, Boleta E H, Santini J M, Teixeira Filho M C.(2021). Silicon amendment enhances agronomic efficiency of nitrogen fertilization in maize and wheat crops under tropical conditions. *Plants*, **10**, 1329.
- Huber D M, Lee T S, Ross M A, Abney T S. (1987). Amelioration of tan spot-infected wheat with nitrogen. *Plant Disease*, **71**, 49.
- Huber D, Thompson I. (2007). Nitrogen and plant disease. In: Datnoff L, Elmer W, Huber D. (Eds) *Mineral Nutrition and Plant Disease*. St Paul, MA: APS Press, pp. 31–44.
- Jensen B, Munk L. (1997). Nitrogen induced changes in colony density and spore production of *Erysiphe graminis* f. sp. hordei on seedlings of six spring barley cultivars. *Plant Pathology*, **46**, 191-202.
- Jones J, Monem M A, Ryan J. (1990). Nitrogen fertilization in relation to durum wheat and tan spot (*Pyrenophora tritici-repentis*)* development. *Arab Journal of Plant Protection*, **8**, 110–113.
- Krupinsky J M, Tanaka D L. (2001). Leaf spot diseases on winter wheat influenced by nitrogen, tillage, and haying after a grass-alfalfa mixture in the conservation reserve program. *Plant Disease*, **85**, 785–789.
- Kweon M, Slade L, Levine H. (2011). Solvent retention capacity (SRC) testing of wheat flour: Principles and value in predicting flour functionality in different wheat based food processes and in wheat breeding-A review. *Cereal Chemistry*, **88**, 537–552.
- Malhi S S, Grant C A, Johnston A M, Gill K S. (2001). Nitrogen fertilization management for no-till cereal production in the Canadian Great Plains: a review. *Soil and Tillage Research*, **60**, 101–122.
- Manning V A, Chu A L, Steeves J E, Wolpert T J, Ciuffetti L M. (2009). A host-selective toxin of *Pyrenophora tritici-repentis*, *Ptr ToxA*, induces photosystem changes and reactive oxygen species accumulation in sensitive wheat. *Molecular Plant-Microbe Interactions*, **22**, 665–676.
- Pazdiora, P C, da Rosa Dorneles K, Morello T N, Nicholson P, Dallagnol L J. (2021). Silicon soil amendment as a complement to manage tan spot and fusarium head blight in wheat. *Agronomy for Sustainable Development*, **41**, 1–13.
- Rees R G, Platz G J. (1980). The epidemiology of yellow spot of wheat in southern

- Queensland. *Australian Journal of Agricultural Research*, **31**, 259–267.
- Reis, E M, Casa R T. (2007). *Doenças dos cereais de inverno: diagnose, epidemiologia e controle*. 2nd ed. Lages: Graphel, pp. 176.
- Rodrigues F A, Resende R S, Dallagnol L J, Datnoff L E. (2015). Silicon potentiates host defense mechanisms against infection by plant pathogens. In *Silicon and plant diseases*. Springer, pp. 109–138.
- Schierenbeck M, Fleitas M C, Simón M R. 2019. Nitrogen fertilization and fungicide mixtures in wheat: how do they affect the severity, yield and dynamics of nitrogen under leaf rust infections?. *European Journal of Plant Pathology*, **155**, 1061-1075.
- Simón M R, Fleitas M C, Castro A C, Schierenbeck M. (2020). How foliar fungal diseases affect nitrogen dynamics, milling and end-use quality of wheat. *Frontiers in Plant Science*, **11**, 1568.
- Stadnik M J, Buchenauer H. (2000). Inhibition of phenylalanine ammonia-lyase suppresses the resistance induced by benzothiadiazole in wheat to *Blumeria graminis* f. sp. *tritici*. *Physiological and Molecular Plant Pathology*, **57**, 25-34.
- Turner J A, Chantry T, Taylor M C, Kennedy M C. (2021). Changes in agronomic practices and incidence and severity of diseases in winter wheat in England and Wales between 1999 and 2019. *Plant Pathology*, **70**, 1759-1778.
- USDA (2021a) *Index mundi - Mundial production of wheat, Index mundi*. Available at:
<https://www.indexmundi.com/agriculture/?producto=trigo&variable=produccion&l=es> [Accessed August 8, 2021].
- USDA (2021b) *Index mundi - wheat consumption worldwide, Index mundi*. Available at:
<https://www.indexmundi.com/agriculture/?producto=trigo&variable=consumo-domestico&l=es> [Accessed August 8, 2021].
- Veresoglou S D, Barto E K, Menexes G, Rillig M C. (2013). Fertilization affects severity of disease caused by fungal plant pathogens. *Plant Pathology*, **62**, 961–969.
- White B. (2015) *Evaluating the Effects of Silicon and Nitrogen Fertilization on Wheat Production*. Louisiana State University. Available at:
https://digitalcommons.lsu.edu/gradschool_theses/2607. [Accessed August 10, 2021].
- White B, Tubana B S, Babu T, Mascagni H, Agostinho F, Datnoff L E, Harrison S. (2017). Effect of silicate slag application on wheat grown under two nitrogen rates. *Plants*, **6**, 47.
- Wiese M V. (1987) *Compendium of wheat diseases*. 2nd ed. St. Paul, MN:

American Phytopathological Society. St. Paul, MN.

Wu X, Baerson S R, Song Y, Liang G, Ding C, Niu J, Pan Z, Zeng R (2017). Interactions between nitrogen and silicon in rice and their effects on resistance toward the brown planthopper *Nilaparvata lugens*. *Frontiers in plant science*, **8**, 28.

Ying H, Ye Y, Cui Z, Chen, X. (2017). Managing nitrogen for sustainable wheat production. *Journal of Cleaner Production*, **162**, 1308–1316.

The chapter 1 was formatted under the guidelines of the **European Journal of Plant Pathology**

Detection of potential inoculum sources of tan spot under field condition

Andrea Román^{1,2} and Leandro José Dallagnol^{1*}

¹ Federal University of Pelotas, Eliseu Maciel Faculty of Agronomy, Crop Protection Department, Laboratory of Plant Pathogen Interaction, 96010-900, Pelotas, Rio Grande do Sul, Brazil.

² Bolivar State University, Agricultural Sciences Natural Resources and the Environment Faculty, Laboratory of Phytopathology, EC020150, Guaranda, Ecuador.

*Corresponding author: leandro.dallagnol@ufpel.edu.br

Abstract

The main inoculum sources of *Pyrenophora tritici-repentis* (*Ptr*) are wheat stubble, conidia and contaminated seeds. However, there is no information about the contribution of each one on the epidemic. In this regard, field experiments involving natural infection were conducted in Rio Grande do Sul, Brazil, in the 2019 and 2020 seasons using susceptible (TBIO Tibagi) and moderately resistant (TBIO Audaz) wheat cultivars. Pathogen inoculum was evaluated in the seeds, field stubble and air dispersion, the last using spore collectors placed 30, 45, and 60 cm above the soil. The seed health testing showed that incidence of *Drechslera* sp. on seeds was 5 to 6% per lot, without statistical differences ($p > 0.05$) regarded the year. Collectors at 30 cm height captured the largest portion of *Drechslera* sp. conidia, and the highest conidial frequencies occurred during early seedling growth (ZGS13), tillering (ZGS20) and after flowering (ZGS65) stages. The increment of 56% in pseudothecia per m² and 48% in pseudothecia per g of stubble each year indicated the prevalence of sexual structures. A positive linear relationship determined that the presence of >1000 pseudothecia per m² would show a severity and incidence that ranged from 2.4 to 3.6% and 5.1 to 5.4% for the TBIO Audaz and 3.4 to 4.6% and 5.8 to 6.6% for TBIO Tibagi. As a result, management of *Ptr* should be associated with stubble management, since the successive wheat planting for more than the two years favored the increase in the inoculum from pseudothecia. The findings about the initial inoculum *Ptr* have implications for tan spot integrated management in the South region of Brazil.

Keywords: inoculum, seed, straw, pseudothecia, collector, selective-medium

Introduction

Tan spot, caused by the necrotrophic fungi *Pyrenophora tritici-repentis* (*Ptr*) (Died.) *Drechs.* (teleomorph) and *Drechslera tritici-repentis* (Died.) Shoem. (anamorph) (Kirk, 2019) is one of the most important diseases of wheat worldwide (Wiese, 1987; Turner et al., 2021), and in southern Brazil it is the major wheat spot leaf disease (Moffat & Santana, 2019). The wheat yield losses in severe cases of tan spot range up to 75% (Rees & Platz, 1980; Reis & Casa, 2007). The greatest yield losses and seed quality reduction are recorded when the pathogen infects plants during the booting and flowering stages (De Wolf et al., 1998; Wegulo et al., 2009). The environment and crop practices play important roles in the severity of leaf spots diseases, hence resulting in variable impact on yield depending on the year and location (MacLean et al., 2018). No-till management to maximize soil conservation and crop rotation to reduce the damage of tan spot can be employed, as is the case in Brazil (Moffat & Santana, 2019). However, over the past three decades tan spot has become increasingly important globally, and its prevalence is associated with conservation tillage practices, frequent wheat production in crop rotation and mono-cropping, as well as cultivation of susceptible wheat genotypes (Ciuffetti et al., 2014; Turner et al., 2021).

Ptr can survive in infected wheat stubble as mycelia or pseudothecia (Ciuffetti et al., 2014; Wegulo, 2011). Ascospores are formed on infested residue throughout the growing season, infecting leaves of nearby young plants, and repeated cycles of conidia production during the growing season can also play a primary role in the initial stages of infection (Krupinsky, 1992). After the first infection by the primary inoculum, mature lesions on leaves are the source of conidia, and this secondary inoculum plays an important role in the progress of tan spot during the growing season (Moffat & Santana, 2019). Conidia are produced on wet leaves in the dark, and are dispersed during the day (Francel, 1998). Conidial germination is possible over a temperature range of 10 to 28°C. The latent period ranges from three to six days after conidia are deposited and penetrate host tissue, depending on the cultivar's resistance and weather conditions (Riaz et al., 1991; Dorneles et al., 2017; Pazdiora et al., 2018). Additional sources of primary inoculum include infected seeds, conidia in infested crop residues, alternative grass hosts, and volunteer wheat plants (Schilder & Bergstrom, 1993; Reis et al., 1997; Ali & Langham, 2015).

Some studies have been conducted to understand the effect of the primary inoculum on the start of tan spot outbreaks. For example, a two-year experiment showed that the severity of tan spot disease was related to the amount of primary inoculum, which varied (25.000-100.000 pseudothecia per m²) depending on weather conditions (Adee & Pfender, 1989). Furthermore, 12.700-31.200 pseudothecia per m² were required to produce moderate to severe tan spot damage (Wright & Sutton, 1990). However, little is known about relationship of the primary inoculum with tan spot severity and it is not clear which factors are involved in the field.

In addition, infected seeds are suspected of playing an important role in the epidemiology of the disease. However, the pathogen transmission from seed to seedling can be affected by many factors, such as the cultivar's susceptibility, percentage of seed infection, aggressiveness of the isolate, soil moisture, temperature, crop practices, sowing depth, rainfall and light (Schilder & Bergstrom, 1995). Recently, a study conducted by See et al. (2020) found that *Ptr* seed infection is not as common as foliar infection. However, infected seeds are still a source of inoculum and screening for pathogen contamination is advisable to properly distinguish among the *Pyrenophora* species (Bertagnolli et al., 2019; See et al, 2020).

Therefore, much uncertainty exists about the importance of the potential sources of inoculum variously associated with stubble, contaminated seeds, and airborne conidia for the onset of disease damage to wheat. For this reason, the aims of this study were: (1) to quantify the incidence of *Drechslera* sp. from seed lots before sowing; (2) to quantify the sexual structure of *Ptr* from stubble and the relation as primary inoculum with incidence or severity; (3) to examine if spore collectors placed at varied heights are suitable to monitor airborne conidia of *Drechslera* sp. in wheat canopies; and (4) to analyze the disease progress curve of severity associated with cultivars having contrasting resistance to tan spot.

Materials and methods

Study site, and agronomy

Experiments were conducted in the field at the Palma Agriculture Center (31°48'06.4"S 52°30'18.6"W) belonging to Federal University of Pelotas, Brazil, during two successive growing seasons (2019 and 2020). Plots were established in an area previously sown with wheat-soybean succession crops in 2018 to ascertain natural tan

spot occurrence. The trial plots were planted with wheat on July 11, 2019 and July 14, 2020, without tillage. Seeds were sown (9 rows, 0.17 m spacing) with a plot seeder (Semeato, SHP model) at a rate of 300 seeds m^{-2} to achieve plant density of approximately 275 plants m^{-2} . The soil was an Argissol (Ultisol), with the following characteristics: 658 g kg^{-1} of sand, 242 g kg^{-1} of clay; 101 g kg^{-1} of silt; organic matter: 1.0 and 1.79%; nitrogen: 0.73 and 0.93 g kg^{-1} ; NO_3 : 3.23 and 4.11 g kg^{-1} ; NH_4 : 0.94 and 1.19 g kg^{-1} ; phosphorus: 20 and 14 ppm; potassium: 99 and 115 mg dm^{-3} ; calcium: 1.7 and 1.8 cmolc dm^{-3} ; magnesium: 1.2 and 1.3 cmolc dm^{-3} ; copper: 1.0 and 0.9 mg dm^{-3} ; zinc: 1.1 and 0.8 mg dm^{-3} ; manganese: 12.7 and 21.0 mg dm^{-3} ; and pH H_2O 5.7 and 6.0, in 2019 and 2020, respectively.

Fertilizer was applied at sowing as required for maximum crop yield according to soil test recommendations phosphorus was applied at a rate of 40 $kg ha^{-1}$, in the form of triple superphosphate, and potassium at rate of 30 $kg ha^{-1}$, as potassium chloride. Nitrogen was applied (granular urea, N, 45%) at a 130 $kg ha^{-1}$. It was applied as base fertilizer (50% in each treatment) 15 days after sowing and the remainder (50%) was top-dressed at the tillering stage (ZGS23).

Field experimental design and treatments

The experimental design was a complete block design with four replicates. Each plot had area of 3 m^2 (2 m long \times 1.5 m wide). The wheat (*Triticum aestivum*) cultivars TBIO Audaz (Biotrigo®) and TBIO Tibagi (Biotrigo®) were chosen among regionally adapted cultivars with similar anthesis and maturity dates, but contrasting in disease resistance, the former being more resistant to tan spot, powdery mildew, leaf rust and fusarium head blight (FHB) than the latter.

The experimental design used for seedborne inoculum, and crop residue inoculum was completely randomized with four and eight repetitions, respectively. For airborne inoculum, a complete block design was used with four repetitions. Each experiment was repeated twice.

Experimental measurements

Seed health testing

Wheat seeds of TBIO Audaz and TBIO Tibagi were used in the experiment for detection of *Ptr*. A semi-selective medium (Reis, 1983) was used for *Ptr* detection with some modifications. Briefly, the fungicides used in this experiment were 0.133 g of

captan [Captan 500 WP[®], 500 g kg⁻¹; UPL], 0.175 g of tricyclazole [Bim 750 BR[®], 750 g kg⁻¹; Dow AgroSciences], and 0.25 mL of carbendazim [Carbendazim Nortox[®], 500 g L⁻¹; Nortox]. For each fungicide, a stock solution of 100 mL in distilled water was prepared and reserved in a freezer. The antibiotics used were 0.5 g of streptomycin sulfate and 0.3 g of neomycin, dissolved in 100 mL of cold autoclaved distilled water. The main stock solution of 140 mL was prepared with 100 mL of antibiotic mixture, to which was added each stock solution of fungicide (3 mL of captan, 5 mL of tricyclazole, and 32 mL of carbendazim), and was kept in the freezer until use. For each 100 mL of PDA medium (supplemented with 14 g of sucrose L⁻¹), 11.66 mL of the main stock solution was added to prepare the modified semi-selective medium.

Twenty-five seeds, without surface sterilization, were distributed equidistantly with sterile tweezers in germination boxes (11 × 11 × 3.5 cm) containing 40 mL of selective medium. Four replicates of 100 seeds per treatment, totaling 400 seeds, were used. All boxes were incubated at 20 ± 2°C for up to 7 days under 12-h photoperiod in an incubator. After 5-7 days' incubation, a stereomicroscope at 200× magnification revealed the presence of white aerial mycelia and dark olive creeping mycelia forming a colony on the infected seeds (Wiese 1987). *Drechslera* sp. conidiophores and conidia were observed under a microscope at 400× magnification, and compared with those described in the literature (Barnett & Hunter 1972). The incidence was expressed in percentage.

Crop residue inoculum

The inoculum present in crop residues for tan spot development was evaluated by quantifying the amount of sexual structures of *Pyrenophora tritici-repentis* in the crop debris. For this, debris samples were collected from the field plot before sowing, in June 2019 and May in 2020. Debris samples were collected in an area of 1 m² (4 quadrants of 50 cm × 50 cm) in 16 plots (14 × 1.5 m). The debris samples were homogenized to form pooled samples. In the laboratory, these samples were weighed to quantify the total debris, expressed in grams. Then, the stubble was identified and separated from debris samples and immediately placed in 10% (vol/vol) NaOCl for 2 min, followed by washing three times with sterilized water for 3 min, and air drying for 5 min. Then, each stubble sample was separated in four repetitions per plot, and stored in Ziploc bags until use.

After this procedure, stubble samples were weighed and then incubated in a humidified chamber in clear plastic boxes of 20 cm × 10 cm × 13 cm, at 20 ± 2 °C and 12-h photoperiod. After 5 days, a stereoscopic microscope (200× magnification) was used to identify the sexual structures (pseudothecia) of *Pyrenophora tritici-repentis*. Pseudothecia were black, globose to flattened, bearing dark brown setae on the upper surface around ostioles. This morphology corresponded to the descriptions in the literature (Hanlin 1990, 1998; Zhang et al. 2012). The number of structures per stubble sample was expressed in number of pseudothecia per gram of stubble and number of pseudothecia per m² of stubble.

Airborne inoculum

The presence of secondary inoculum during the crop cycle and its relation with the disease development was evaluated by quantifying the number of conidia of *Drechslera* sp. in the air above the field during 17 weeks, starting at seedling emergence. The evaluation was performed in both years using a collector design following the specification of Pontes et al. (2018). Briefly, plastic tubes with 50 cm length and 100 mm diameter were supported by metal rods to keep them fixed in the ground (Supporting information, Figure S1). The junction of the tube and rod allowed the collector to have circular movements. Four collectors were placed in a zigzag pattern separated by 8 meters each inside the plots (24 m × 4 m). The height of the collectors from the ground was adjusted according to the plant height during the growth stage of the crop, being 30 cm [ZGS10; first leaf through coleoptile]; 45 cm [ZGS33; third node detected]; and 60 cm [ZGS65; flowering]. Airborne particles were collected using glass microscope slide traps (7.5 × 2.5 cm) with a double-sided tape of 5 × 2 cm². The slide traps were replaced weekly. The slides were then analyzed under a light microscope (400 × magnification) to quantify the number of spores of *Drechslera* sp. The conidia were identified by comparing their structure with those described in the literature (Barnett & Hunter 1972; Ariyawansa et al., 2014).

Disease assessment

The incidence and severity of tan spot were estimated weekly. Incidence was determined through 15 evaluations during all stages of development of the crop. For this purpose, symptomatic plants were counted in a linear meter of the center line of each experimental plot and expressed as percentage. Tan spot severity was determined

through eight evaluations of severity by examining ten plants of each experimental unit from stem elongation (ZGS30) to hard dough stage (ZGS87) using the midpoint of the Horsfall-Barratt scale (Horsfall & Barratt, 1945), and expressed as percentage of leaf area affected in relation to total area of the plant. The disease progress curve of severity was analyzed by ordinary least squares regression for each possible model fit (Campbell & Madden, 1990; Madden et al., 2007). The relationship of crop residue inoculum, severity and incidence were examined by linear regression analysis.

Weather data

Weather data (daily rainfall; relative humidity, minimum, maximum and mean temperatures) were recorded at the Pelotas weather station, located at coordinates latitude 31° 52' 00" S and longitude 52° 21' 24" W. GRW, at altitude of 13.24 m.

Data analysis

The statistical analyses were conducted with R version 4.0.4 (RStudio, 2021). For seed test health and crop residue inoculum, the base aov function for analysis of variance (ANOVA) of completely randomized design data was used. Before the analyses, data distribution assumptions were verified by the Shapiro-Wilk test and q-q plots for data normality. Levene's test was used to determine homoscedastic residual variance. Outliers were identified graphically by boxplots using the ggplot2 package (Wickham, 2016). For the seedborne inoculum data, incidence and severity were transformed by arcsine-square root to obtain the assumptions of ANOVA.

The relationship of the crop residue inoculum with disease incidence and severity were analyzed using the base *lm* of R. Each model was determined by examining the coefficient of determination (R^2) and the best fitting model was selected to describe the relationship of primary inoculum incidence and severity by goodness of fit criteria: lowest Akaike information criterion (AIC) and lowest Bayesian information criterion (BIC).

For the airborne conidia, a generalized linear model (GLM) with a logit link and Poisson family was used to analyze the data, using the 'glm' function of the lme4 package (Bates et al., 2014). Data assumptions were verified graphically using plots of fitted values versus the residuals for homogeneity of variance and using normal Q-Q plots for normality of residuals and graphically by using the 'simulateResiduals' function of the DHARMA package (Hartig, 2021). The mean values

of experiments 1 and 2 were estimated with the emmeans package (Lenth, 2021) and compared with the Tukey test using 'cld' from the multcomp package (Hothorn et al., 2008).

For the disease progress curve was analyzed by ordinary linear regression for each possible model fit (exponential, monomolecular, logistic or Gompertz) using the 'fit_lin' and 'fit_multi' functions of the epifit package (dos S. Alves & Del Ponte, 2021). The data on disease severity as proportion, time and curve identifier (cultivars) were used to compare the tan spot outbreaks. Each model's goodness of fit was determined according to model fitting functions to ascertain the coefficient of determination (R^2), residual standard error (RSE), and Lin's concordance correlation coefficient (CCC), using the 'fit_lin' function of the epifit package. The outbreaks were described with parameters representing the amount of the disease (y), time of incidence (t), rate of disease increase (r) and initial level of disease (y_0).

Results

Seed health testing

There was no difference ($p>0.05$) in the incidence of *Drechslera* sp. on seeds of TBIO Audaz and TBIO Tibagi (Table 1, Fig. 1). For seeds of both cultivars, the fungal incidence ranged from 5 to 6% in 2019, and 6 to 7 % in 2020. The selective medium allowed the identification of the pathogen in seeds in seven days.

Crop residue inoculum

There were significant differences ($p<0.05$) in the number of sexual structures of *Ptr* observed in the stubble between 2019 and 2020. The number of pseudothecia per m^2 and number of pseudothecia per g of stubble were 75 and 56% higher, respectively, in 2020 compared to 2019 (Table 2, Fig. 2). However, there was no difference in the amount of stubble measured in g per m^2 ($p>0.05$) (Table 2).

Airborne inoculum and weather variables

The influence of collector height was significant ($p<0.05$) for *Drechslera* sp., with 30 cm being the height with the greatest amount of conidia collected, compared to heights of 45 and 60 cm (Fig. 3 and 4). The largest number of *Drechslera* sp. conidia was observed at initial planting in 2019, while in 2020 this peak was observed three weeks after planting (Fig. 5). During the 2020 crop season, the number of conidia of

Drechslera sp. was 5% lower than observed in 2019 (Fig. 5). The ascospores were observed only in the first weeks after sowing at 30 cm height (data not shown).

The weather variables (temperature, humidity and rainfall) were favorable for development of *Drechslera* sp. conidia in 2019 and 2020 (Fig. 6). In 2019, the temperature during July varied from 6.5 to 17°C, with average temperature of 11.6°C (Fig. 6A). Likewise, in 2020 the temperature during July varied from 4 to 17 °C, with average of 10.5°C. However, in 2020 the colder temperatures were registered than in 2019 (Fig. 6B).

In 2020, the rainfall during August was less (49 mm) than in 2019 (103 mm) (Fig. 6A and B). In both years, the fewest sexual spores of *Ptr* were observed in August (data not shown), but conidia of *Drechslera* sp. increased at the end of August and during September (Fig. 5). The temperatures in September 2020 varied from 9.9 to 18.7°C (mean of 14.3°C), lower than August (8.9 to 21.5, average of 15.2°C), being favorable to conidia of *Drechslera* sp. to develop (Fig. 6A). The rainfall in September 2019 was 147 mm compared to 189 mm registered in the same month in 2020 (Fig. 6A and B). The reduction in rainfall during the growth season (July to November) from 748.2 mm in 2019 to 482.5 mm in the same period in 2020 resulted in the later observation of conidia of *Drechslera* sp. during 2020 (Fig. 5). The humidity varied from 64 to 94% daily in both years, but no differences were observed in mean humidity, being 83 to 86% in 2019 and 2020 (Fig. 6C). The difference of approximately 300 mm in rainfall was related to the earlier development of conidia of *Drechslera* sp. in 2019 compared to 2020 (Fig. 5 and 6).

Relationship of crop residue inoculum (CRI) with disease incidence and severity

The relations of crop residue inoculum (CRI) with disease incidence and severity were significant ($p < 0.05$). The relationship of CRI with incidence and severity was positive, meaning that an increase in the number of pseudothecia per m² was accompanied by an increase in disease severity or incidence (Table 3). According to the equations in Table 3, in the case of severity, the presence of pseudothecia per m² between 1.000 and 1.600 showed severity ranging from 2.4 to 3.6% for the cultivar TBIO AUDAZ and from 3.4 to 4.6% for the cultivar TBIO Tibagi regarding the year. Conversely, with respect to the incidence, for the same number pseudothecia per m²,

TBIO Audaz showed values ranging from 5.1 to 5.4%, whereas in TBIO Tibagi the incidence ranged from 5.8 to 6.6%.

Evaluations of disease progress curve

The tan spot disease severity data according to treatment with and without fungicide spraying were analyzed by the exponential, monomolecular, logistic and Gompertz models. The linearized form allowed choosing the model that best described the disease development. The statistical criteria considered for evaluation and selection of the models are presented in Table 4. Inspection of the R^2 , RSE and CCC values confirms the Gompertz model best described the tan spot disease severity curves, according cultivar in 2019 and 2020 (Fig.7).

Table 5 reports the regression model equation and adjustment of initial inoculum (y_0^*) estimated for TBIO Audaz and TBIO Tibagi. For TBIO Audaz, the y_0^* values were 156 and 87% higher in 2019 and 2020, respectively, compared to TBIO Tibagi (Table 5; Fig.7A and B). The regression statistics in Table 5, show, that TBIO Audaz was lower by 26 and 12% regarding the apparent rate of disease severity (0.014 – 0.016 gompits/day), in 2019 and 2020, respectively, compared to TBIO Tibagi (Fig. 7A and B). As a result, there was a reduction of the apparent rate of the disease severity in 2020 compared to 2019.

Discussion

In this study, different types of primary and secondary inoculum sources under field conditions were investigated in two growing seasons. Theseed health testingshowed that incidence of *Drechslera* sp. on seeds was under the tolerance limit according to the seed phytosanitary standard, which is 5% per lot (Brasil 2004). However, seed health testingis necessary to detect the pathogen, because seeds from poor quality lots can be a primary source of inoculum and act to disseminate the pathogen to other regions (See et al. 2020).

For *Ptr*, which survives as pseudothecia and mycelia on wheat debris, wheat seedlings developing near infested debris may be exposed to high concentrations of primary inoculum during the development stage, when the plant has a low number of leaves, compromising plant development and increasing the risk of a high amount of secondary inoculum in later stages.Previous reports have indicated that 25.000-100.000 pseudothecia per m^2 (Adee &Pfender, 1989) and 12.700-31.200 pseudothecia per

m²(Wright & Sutton, 1990) are considered as minimums to be considered as primary inoculum. In contrast, our results showed that the pseudothecia per m² was lower (1.031 – 1.600 pseudothecia per m²) compared to previous reports, but this was still important as an inoculum source for the onset of tan spot epidemic, probably enhanced by environmental conditions favorable to disease development. One explanation for the differences in the number of pseudothecia among studies, regarding disease onset, is associated with the real condition and the quantity of the stubble collected each year in the experimental area.

However, our study indicated that the increment in wheat stubble was associated with increased presence of pseudothecia. This observation agrees with the fact that no-till wheat production increases the amount of wheat straw on the soil surface and slightly increases the severity of tan spot compared with conventional tillage (Bailey, 1996; Krupinsky et al., 1997; Kutcher & Malhi, 2010). It has been suggested that the number of pseudothecia per m² present in accumulated stubble also depends on the type of residue, time of decay, and the influence of environment (Kutcher et al., 2010). In this study, the number of pseudothecia per g of stubble and pseudothecia per m² each year demonstrated an increase in the inoculum after continuous wheat sowing. This finding agrees with previous reports that tan spot severity increases with the adoption of minimum and no-till sowing (Gilbert et al., 1998; Ciuffetti et al., 2014; Turner et al., 2021). Numerous studies have shown that growing a crop on its own stubble usually leads to greater disease severity of residue-borne inocula compared with production on crop stubble of different species (Johnston et al., 2005; Krupinsky et al., 2006, 2007; Kutcher et al., 2011). In this sense, further studies of the influence of previous crop rotation, crop residues, and time of decay are necessary to determine the best crop sequence to reduce the risk of leaf spot diseases.

The collectors used allowed the quantification of conidia of *Drechslera* sp., but the ascospores were observed only in the first weeks after sowing. In this regard, our study clearly shows that conidia were collected during all development stages, but a higher number was detected during the seedling growth (ZGS13), tillering (ZGS20) and late season after flowering (ZGS65). Interestingly, in this study the collector placed at 30 cm above ground during the early season collected a greater number of conidia of *Drechslera* sp. than sexual spores. However, ascospores from pseudothecia can be involved in the production of the primary lesion at the beginning of growth, increasing

the early formation of asexual spores (conidia) on the lesions and increasing the secondary inoculum in the area. In fact, only a small quantity of ascospores can be formed due to the immaturity of the pseudothecia formed in wheat debris (Adee & Sutton, 1989). A possible explanation for this result is that the ascospores may be dispersed in the lower canopy but rarely to the upper leaves (Wright & Sutton, 1990), resulting in lack of ascospores collected. After the formation of primary lesions, the production of conidia increases, being important for the development of secondary inoculum.

Despite of the increment in the amount of primary inoculum found in this study, the severity in 2020 was lower than in 2019, but it was accompanied by differences in the amount of rainfall, associated with later development of the symptoms during flag leaf (ZGS39) and flowering (ZGS65) in 2020 compared to tillering (ZGS20) in 2019. These observations agree with reports indicating no observed differences in leaf disease development due to tillage system in years when the climate is not favorable for disease development (Reis & Santos, 1993; Krupinsky & Tanaka, 2001; Bankina et al., 2015). Nevertheless, the disease progress curve corroborated the relation of the inoculum density of stubble with the disease severity. In fact, the number of pseudothecia per m^2 ranging from 1.031 to 1.600 was associated to the development of the disease within a plant population in the field. This number of pseudothecia, although lower than reported in other studies (Adee & Pfender, 1989; Wright & Sutton, 1990), was enough to start the disease outbreak. This effect is very important because wheat seedlings developing near infested debris can be exposed to high concentrations of ascospores in the beginning of the growing season, compromising plant development and increasing the risk of secondary inoculum, especially in susceptible cultivars. For instance, the higher apparent rate and lower adjustment of initial inoculum (y_0^*) for TBIO Tibagi showed higher disease severity. This result indicated the importance of selecting moderately resistant cultivars that reduce the formation of repetitive asexual cycles on upper leaves, delaying the outbreak and reducing the time for the pathogen to cause damage, suggesting a strategy for managing tan spot.

Conclusions

The seed health test is important to check the seed sanitary quality for better plant development under field conditions. Furthermore, spore collectors in the field at

different heights from the soil revealed that the largest portion of conidia of *Drechslerasp.* was collected at 30 cm height and the greatest conidia frequencies occurred during early seedling growth (ZGS13), tillering (ZGS20) and late in the season after flowering (ZGS65). In addition, the crop residue from successive wheat cropping was associated with the presence of pseudothecia, which is associated with first lesions observed near the ground and in the development of secondary inoculum. As a result, management of *Ptr* should be associated with the management of the crop residues, since the successive wheat planting for more than the two years favored the increase in the inoculum from the sexual stage.

Acknowledgements

We are thankful to Phytopathology laboratory of Federal University of Pelotas for technical assistance in seeds healthy experiments. Grow Green for the digital design planning of collectors and the staff of Centro Agropecuário da Palma for facilities and collectors manufacturing.

Funding

The authors are thankful to the Office to Coordinate Improvement of Higher Education Personnel (CAPES) for financial support and the student scholarship (Finance code 001) to A. Román; and L. J. Dallagnol is supported by a fellowship (grant number 308149/2018-1) from the Brazilian National Council for Scientific and Technological Development (CNPq). We are thankful to BIOTRIGO for providing wheat seeds for the experiments.

CRedit

Conceptualization: A.R. and L.J.D; Methodology: A.R.; Investigation: A.R.; Writing – original draft: A.R. Formal analysis: A.R.; Writing–review and editing: L.J.D. and A.R.; Resources: L.J.D.; Funding acquisition: L.J.D.; Supervision: L.J.D.

Conflict of interest

The authors declare that they have no known competing financial interests or personal relationships that could have appeared to influence the work reported in this paper.

References

- Adee, E.A. & Pfender, W. (1989). The effect of primary inoculum level of *Pyrenophora tritici-repentis* on Tan Spot Epidemic Development in Wheat. *Phytopathology*, 79, 873-77. <https://doi.org/10.1094/Phyto-79-873>.
- Ali, S. & Langham, M.A.C. (2015). Reaction of Five Non-cereal Grasses to Five Races and Two Host Selective Toxins of *Pyrenophora tritici-repentis*. *The Plant Pathology Journal*, 31:245-251. <https://doi.org/10.5423/PPJ.OA.03.2015.0028>.
- Ariyawansa H.A., Kang, J.C., Alias, S.A., Chukeatirote, E., & Hyde, K.D. (2014). *Pyrenophora*. *Mycosphere*, 5,351-362.
- Bailey, K.L. (1996). Diseases under conservation tillage systems. *Canadian Journal of Plant Science*, 76, 635-639. <https://doi.org/10.4141/cjps96-113>.
- Bankina, B., Ruža, A., Paura, L., & Priekule, I. (2015). The effects of soil tillage and crop rotation on the development of winter wheat leaf diseases. *Zemdirbyste-Agriculture*, 102:67-72. <https://doi.org/10.13080/z-a.2015.102.008>.
- Barnett, H.L. & Hunter, B.B. (1972). Illustrated genera of imperfect fungi., 3rd ed. Minneapolis, Burgess Publishing Company. pp 211.
- Bates, D., Mächler, M., Bolker, B. & Walker, S. (2014). Fitting linear mixed-effects models using lme4. arXiv preprint arXiv:14065823.
- Bertagnolli, V. V., Ferreira, J. R., Liu, Z., Rosa, A.C., & Deuner, C.C. (2019). Phenotypical and genotypical characterization of *Pyrenophora tritici-repentis* races in Brazil. *European Journal of Plant Pathology*, 154, 995-1007. <https://doi.org/10.1007/s10658-019-01720-3>.
- Brasil (2004) Decreto nº 5.153, 2004, de 23 de julho de 2004. Aprova o Regulamento da Lei nº 10.711, de 5 de agosto de 2003, que dispõe sobre o Sistema Nacional de Sementes e Mudas – SNSM, e dá outras providências. Available from: <https://www2.camara.leg.br/legin/fed/decret/2004/decreto-5153-23-julho-2004-533120-norma-pe.html>. [Accessed January 30, 2020].
- Campbell, C.L. & Madden, L. V. (1990). Introduction to plant disease epidemiology. John Wiley & Sons.
- Ciuffetti, L.M., Manning, V.A., Pandelova, I., Faris, J.D., Friesen, T.L., Strelkov, S.E., Weber G.L., Goodwin S. B., Wolpert T.J. & Figueroa, M. (2014). *Pyrenophora tritici-repentis*: a plant pathogenic fungus with global impact. In: Dean R., Lichens-Park A., Kole C. (Eds.) *Genomics of Plant-Associated Fungi: Monocot*

- Pathogens*. Springer, pp 1-39.
- De Wolf, E.D., Effertz, R.J., Ali, S., Francl, L.J. (1998). Vistas of tan spot research. *Canadian Journal of Plant Pathology* 20,349-370. <https://doi.org/10.1080/07060669809500404>.
- Dorneles, K.R., Dallagnol, L.J., Pazdiora, P.C., Rodrigues, F.A. & Deuner, S. (2017). Silicon potentiates biochemical defense responses of wheat against tan spot. *Physiological and molecular plant pathology*, 97,69-78.
- dos S. Alves, K. & Del Ponte, E.M. (2021). Epifitter: Analysis and Simulation of Plant Disease Progress Curves. R package version 0.3.0.
- Francl, L.J. (1998). Genesis and liberation of conidia of *Pyrenophora tritici-repentis*. *Canadian Journal of Plant Pathology*, 20,387-393. <https://doi.org/10.1080/07060669809500408>.
- Gilbert, J., Woods, S.M. & Tekauz, A. (1998). Relationship between environmental variables and the prevalence and isolation frequency of leaf-spotting pathogens in spring wheat. *Canadian Journal of Plant Pathology*, 20,158-164. <https://doi.org/10.1080/07060669809500421>.
- Hanlin, R.T. (1990). Illustrated genera of Ascomycetes. American Phytopathological Society Press, Saint Paul, MN, USA, pp 66.
- Hanlin, R.T. (1998). Combined keys to illustrated genera of Ascomycetes. American Phytopathological Society Press, Saint Paul, MN, USA, pp118.
- Hartig, F. (2021). DHARMA: Residual Diagnostics for Hierarchical (Multi-Level / Mixed) Regression Models. R package version 0.4.1.
- Horsfall, J.G., Barratt, R.W. (1945). An improved grading system for measuring plant diseases. *Phytopathology*, 35, 65.
- Hothorn, T., Bretz, F. & Westfall, P. (2008). Simultaneous inference in general parametric models. *Biometrical Journal: Journal of Mathematical Methods in Biosciences*, 50, 346-363. <https://doi.org/10.1002/bimj.200810425>.
- Hyndman, R.J. (2013). fpp: Data for “Forecasting: principles and practice”. R package version 0.5. <http://pkg.robjhyndman.com/forecast>.
- Johnston, A.M., Kutcher, H.R. & Bailey, K.L. (2005). Impact of crop sequence decisions in the Saskatchewan Parkland. *Canadian Journal of Plant Science*, 85, 95-102. <https://doi.org/10.4141/P04-090>.
- Kirk, P.M. (2019) *Species Fungorum (version Oct 2017)*. In: *Species 2000 & ITIS Catalogue of Life, 2019 Annual Checklist*. Edited by Y. Roskov et al. Digital

resource at www.catalogueoflife.org/annual-checklist/2019. Leiden, the Netherlands: Species 2000: Naturalis. Available at: www.catalogueoflife.org/annual-checklist/2018. [Accessed Dec 9, 2019].

- Krupinsky, J.M. (1992). Collection of conidia and ascospores of *Pyrenophora tritici-repentis* from wheat straw. In: Second International Wheat Tan Spot and Spot Blotch Workshop. North Dakota Agricultural Experiment Station, North Dakota State University, Fargo, North Dakota, pp 91-95.
- Krupinsky, J.M. (1997). Aggressiveness of *Stagonospora nodorum* isolates obtained from wheat in the northern Great Plains. *Plant Disease*, 81, 1027-1031. <https://doi.org/10.1094/PDIS.1997.81.9.1027>.
- Krupinsky, J.M., & Tanaka, D.L. (2001). Leaf spot diseases on winter wheat influenced by nitrogen, tillage, and haying after a grass-alfalfa mixture in the conservation reserve program. *Plant Disease*, 85, 785-789. <https://doi.org/10.1094/PDIS.2001.85.7.785>.
- Krupinsky, J.M., Tanaka, D.L., Merrill, S.D., Liebig, M.A. & Hanson, J.D. (2006). Crop sequence effects of 10 crops in the northern Great Plains. *Agricultural Systems*, 88, 227-254. <https://doi.org/10.1016/j.agsy.2005.03.011>.
- Krupinsky, J.M., Halvorson, A.D., Tanaka, D.L. & Merrill, S.D. (2007). Nitrogen and tillage effects on wheat leaf spot diseases in the northern Great Plains. *Agronomy Journal*, 99, 562-569. <https://doi.org/10.2134/agronj2006.0263>.
- Kutcher, H.R. & Malhi, S.S. (2010). Residue burning and tillage effects on diseases and yield of barley (*Hordeum vulgare*) and canola (*Brassica napus*). *Soil and Tillage Research*, 109, 153-160. <https://doi.org/10.1016/j.still.2010.06.001>.
- Kutcher, H.R., Warland, J.S. & Brandt, S.A. (2010). Temperature and precipitation effects on canola yields in Saskatchewan, Canada. *Agricultural and Forest Meteorology*, 150, 161-165. <https://doi.org/10.1016/j.agrformet.2009.09.011>.
- Kutcher, H.R., Johnston, A.M., Bailey, K.L. & Malhi, S.S. (2011). Managing crop losses from plant diseases with foliar fungicides, rotation and tillage on a Black Chernozem in Saskatchewan, Canada. *Field Crops Research*, 124, 205-212. <https://doi.org/10.1016/j.fcr.2011.05.018>.
- Kuznetsova, A., Brockhoff, P.B. & Christensen, R.H.B. (2017). lmerTest package: tests in linear mixed effects models. *Journal of statistical software*, 82, 1-26. <https://doi.org/10.18637/jss.v082.i13>.
- Lenth R. 2021. emmeans: Estimated Marginal Means, aka Least-Squares Means. R package version 1.6.0. <https://cran.r-project.org/package=emmeans>.
- MacLean, D.E., Lobo, J.M., Coles, K., Harding, M.W., May, W.E., Peng, G.,

- Turkington, T.K. & Kutcher, H.R. (2018). Fungicide application at anthesis of wheat provides effective control of leaf spotting diseases in western Canada. *Crop protection* 112, 343-349. <https://doi.org/https://doi.org/10.1016/j.cropro.2018.06.019>.
- Madden, L.V., Hughes, G., Van Den Bosch, F. (2007). *The study of plant disease epidemics*. The American Phytopathological Society, St. Paul, Minnesota, MN.
- Moffat, C.S. & Santana, F.M. (2019). *Diseases affecting wheat: tan spot*. In: Oliver R. (ed) Integrated disease management of wheat and barley. Burleigh Dodds Science Publishing Limited, Cambridge, UK, pp 1-13.
- Pazdiora, P.C., da Rosa Dorneles, K., Forcelini, C.A., Del Ponte, E.M. & Dallagnol, L. J. (2018). Silicon suppresses tan spot development on wheat infected by *Pyrenophora tritici-repentis*. *European Journal of Plant Pathology*, 150, 49-56. <https://doi.org/https://doi.org/10.1007/s10658-017-1251-4>.
- Pontes, K.B., Amaral, H.F. & Igarashi, S. (2018). Qualidade do solo associada ao monitoramento e manejo da *Phakopsora pachyrhizie* em áreas de diferentes sucessões da cultura da soja. *Revista Terra & Cultura: Cadernos de Ensino e Pesquisa* 34:333-359. Available from: <http://periodicos.unifil.br/index.php/Revistateste/article/view/525>. [Accessed March 30, 2019].
- Rees, R.G. & Platz, G.J. (1980). The epidemiology of yellow spot of wheat in southern Queensland. *Australian Journal of Agricultural Research*, 31, 259-267.
- Reis, E.M. & Casa, R.T. (2007). *Doenças dos cereais de inverno: diagnose, epidemiologia e controle*, 2nd ed. Lages: Graphel, pp 176.
- Reis, E.M. (1983). Selective medium for isolating *Cochliobolus sativus* from soil. *Plant Disease*, 67, 68-70. <https://doi.org/10.1094/PD-67-68>.
- Reis, E. & Santos, H.D. (1993). Interações entre doenças de cereais de inverno e sistema plantio direto. *Plantio direto no Brasil*. Centro Nacional de Pesquisa de Trigo, EMBRAPA, 105-110.
- Reis, E.M., Madeiros, C., Casa, R.T. (1997). Control of leaf blights of wheat by elimination of the inoculum source. In: Proc. Int. Workshop helminthosporium diseases of wheat: spot blotch and tan spot, CIMMYT, El Batan, Mexico. pp 327-332.

- Riaz, M., Bockus, W.W. & Davis, M.A. (1991). Effects of wheat genotype, time after inoculation, and leaf age on conidia production by *Drechslera tritici-repentis*. *Phytopathology*, 81, 1298-1302.
- RStudio. 2021. RStudio: Integrated development environment for R. RStudio, PBC, Boston, MA. <http://www.rstudio.com/>.
- See, P.T., Schultz, N. & Moffat, C.S. (2020). Evaluation of *Pyrenophora tritici-repentis* Infection of Wheat Heads. *Agriculture*, 10, 417. <https://doi.org/10.3390/agriculture10090417>.
- Schilder, A.M.C. & Bergstrom, G.C. (1993). Tan spot. In: Mathur SB, Cunfer BM (Eds) Seedborne diseases and seed health testing of wheat. Danish Government Institute of Seed Pathology for Developing Countries, Copenhagen, Denmark, pp 113–122.
- Schilder, A.M.C. & Bergstrom, G.C. (1995). Seed transmission of *Pyrenophora tritici-repentis*, causal fungus of tan spot of wheat. *European Journal of Plant Pathology*, 101, 81-91. <https://doi.org/https://doi.org/10.1007/BF01876096>.
- Turner, J.A., Chantry, T., Taylor, M.C., Kennedy, M.C. (2021). Changes in agronomic practices and incidence and severity of diseases in winter wheat in England and Wales between 1999 and 2019. *Plant Pathology*, 70, 1759-1778. <https://doi.org/https://doi.org/10.1111/ppa.13433>.
- Wegulo, S.N. (2011). Tan spot of cereals. In: The Plant Health Instructor. Retrieved September 20, 2019, from: <https://www.apsnet.org/edcenter/disandpath/fungalasco/pdlessons/Pages/TanSpot.aspx>.
- Wegulo, S.N., Breathnach, J.A., Baenziger, P.S. (2009). Effect of growth stage on the relationship between tan spot and spot blotch severity and yield in winter wheat. *Crop Protection*, 28, 696-702. <https://doi.org/https://doi.org/10.1016/j.cropro.2009.04.003>.
- Wickham, H. (2016). ggplot2: Elegant Graphics for Data Analysis. Springer-Verlag, New York.
- Wiese, M.V. (1987). Compendium of wheat diseases, 2nd ed. American Phytopathological Society, St. Paul, MN, USA, pp 152.
- Wright, K.H. & Sutton, J.C. (1990). Inoculum of *Pyrenophora tritici-repentis* in relation to epidemics of tan spot of winter wheat in Ontario. *Canadian Journal of Plant Pathology*, 12, 149-157. <https://doi.org/https://doi.org/10.1080/07060669009501018>.
- Zadoks, J.C., Chang, T.T. & Konzak, C.F. (1974). A decimal code for the growth stages

of cereals. *Weed research*, 14,415-421.

Zhang, Y., Crous, P.W., Schoch, C.L. & Hyde, K.D. (2012). Pleosporales. *Fungal diversity*, 53, 1-221. <https://doi.org/10.1007/s13225-011-0117-x>.

Table 1. Mean squares and standard errors of the incidence, in percentage of *Dreschlera* sp. on seeds of TBIO Audaz and TBIO Tibagi in modified Reis selective medium.

Cultivar seeds	Incidence (%) 2019	Incidence (%) 2020
TBIO Audaz	5.75 ± 1.62 a	5.5 ± 1.08a
TBIO Tibagi	5.0 ± 1.62 a	6.5 ± 1.08 a
<i>p</i> value	0.8815	0.4904

Means followed by the same letter within the same source of variation are not statistically different (Tukey test, $p < 0.05$)

Table 2. Mean values and standard errors of the stubble number of pseudothecia of *Pyrenophora tritici-repentis* by year.

Year	stubble g per m²	Number of pseudothecia per g^a stubble	Number of pseudothecia per m²
2019	119 ± 10.3a	9.04 ± 1.57 b	1031 ± 187 b
2020	125 ± 10.3a	13.56 ± 1.57 a	1624 ± 187 a
<i>p</i> value	0.703	0.0458	0.0287

Means followed by the same letter within the same source of variation are not statistically different (Tukey test, $p < 0.05$)

^a variation of weight of 20 stubbles of 10 cm = 1.75-3.50 g

Table 3. Regression statistics (coefficient of determination (R^2), Akaike information criterion (AIC) and lowest Bayesian information criterion (BIC)) and model parameters (intercept, slope) of incidence and severity of tan spot in relation to crop residue inoculum (CRI) of the TBIO Audaz and TBIO Tibagi cultivars during 2019 and 2020 growing seasons.

Cultivar	Relation	Year	Model	Equation	Regression Statistics				
					Intercept(b0)	Slope (b1)	R^2 (%)	AIC	BIC
TBIO Audaz	Severity vs CRI*	2019	Linear	$Y = 3.1 + 0.0003X$	3.1	0.0003	0.90	381.3	384.84
TBIO Audaz	Severity vs CRI	2020	Linear	$Y = 2 + 0.0004X$	2	0.0004	0.91	352.67	356.20
TBIO Tibagi	Severity vs CRI	2019	Linear	$Y = 4.0 + 0.0004X$	4.0	0.0004	0.81	359.15	362.69
TBIO Tibagi	Severity vs CRI	2020	Linear	$Y = 2.8 + 0.0006X$	2.8	0.0006	0.87	334.97	338.50
TBIO Audaz	Incidence vs CRI	2019	Linear	$Y = 4.7 + 0.0004X$	4.7	0.0004	0.75	367.28	370.81
TBIO Audaz	Incidence vs CRI	2020	Linear	$Y = 4.8 + 0.0004X$	4.8	0.0004	0.82	341.82	345.36
TBIO Tibagi	Incidence vs CRI	2019	Linear	$Y = 6.1 + 0.0003X$	6.1	0.0003	0.86	374.72	378.26
TBIO Tibagi	Incidence vs CRI	2020	Linear	$Y = 5.2 + 0.0006X$	5.2	0.0006	0.88	343.69	347.23

* number of pseudothecia per m^2

Table 4. Model fit statistics being coefficient of determination (R^2), residual standard deviation (RSE) and Lin's concordance correlation coefficient (CCC) of tan spot severity data for the best fitted models of the treatments of TBIO Audaz and TBIO Tibagi cultivars during 2019 and 2020 growing seasons.

Cultivar	Model	R^2		RSE		CCC	
		2019	2020	2019	2020	2019	2020
TBIO Audaz	Gompertz	0.815	0.802	0.243	0.224	0.898	0.890
	Logistic	0.801	0.788	1.374	1.338	0.890	0.881
	Exponential	0.800	0.787	1.365	1.332	0.889	0.881
	Monomolecular	0.664	0.665	0.021	0.014	0.798	0.799
TBIO Tibagi	Gompertz	0.802	0.814	0.224	0.243	0.890	0.898
	Logistic	0.788	0.803	1.338	1.359	0.881	0.891
	Exponential	0.787	0.801	1.332	1.350	0.881	0.890
	Monomolecular	0.665	0.550	0.014	0.028	0.799	0.710

Table 5. Model coefficients intercept (b1), apparent infection rate (r) and initial inoculum (y_0^*) estimate of tan spot severity data of the best Gompertz model of TBIO Audaz and TBIO Tibagi cultivars during the 2019 and 2020 growing seasons.

Cultivar	Intercept (b1)	r	y_0^*
TBIO Audaz	-2.56	0.016	0.0000023
TBIO Tibagi	-2.63	0.020	0.0000009
TBIO Audaz	-2.51	0.014	0.0000043
TBIO Tibagi	-2.56	0.016	0.0000023

*y-intercept is an estimate of tan spot severity at the start of an epidemic

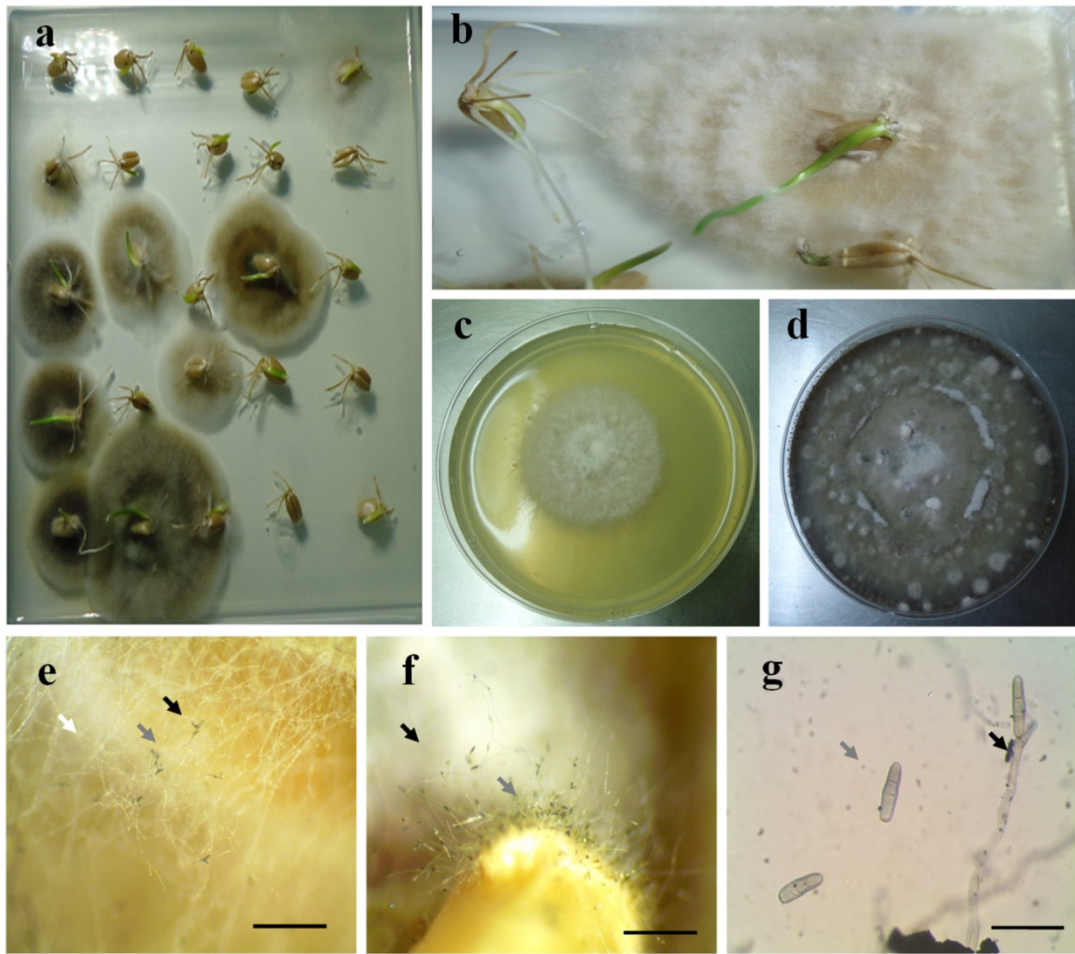


Fig. 1 Pathogen growth from infected seeds seven days after incubation in modified Reis selective medium (a); aspect of mycelial growth at seven days on seed (b); aspects of mycelial growth of after five days (c); and twelve days (d) after isolation of *Drechslera* sp. Conidia (gray arrows), conidiophores (black arrows) and mycelium (white arrows) observed in seeds infected by *Drechslera* sp. Scale bar, 1.5 mm (e,f); conidia (gray arrows) containing three septa, and conidiophores (black arrows). Scale bar, 50 μ m (g).

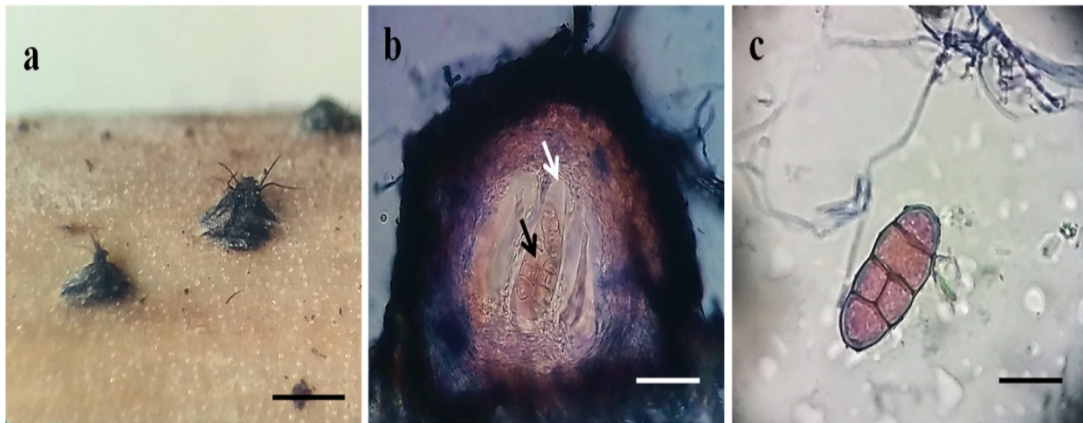


Fig. 2 Immature pseudothecia of *Phryrenophora tritici-repentis* showing globose shape and dark brown, setae. Scale bar, 1.5 mm (a); pseudothecia showing bitunicate asci (white arrows) with ascospores (black arrows), Scale bar, 50 μm (b), ascospores with three or four transverse septa and one or two longitudinal septa in the median cells. Scale bar, 100 μm (c).

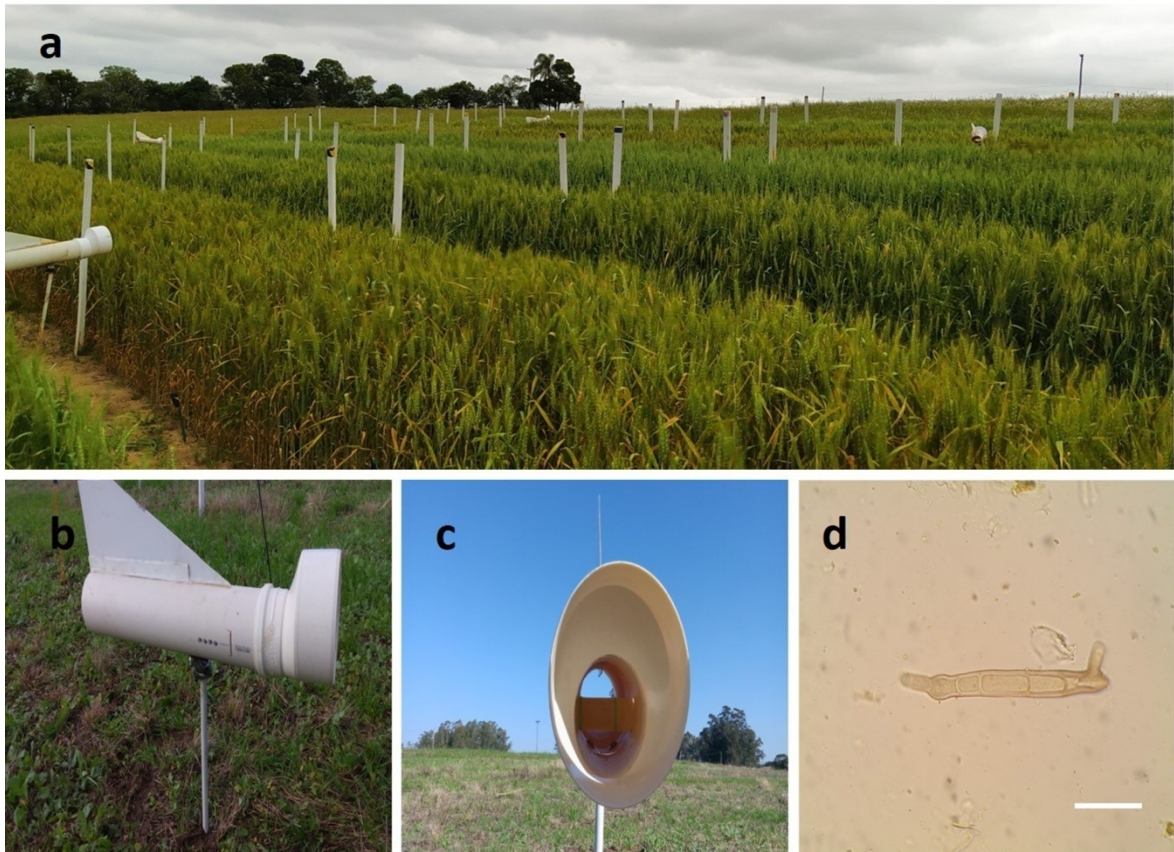


Fig. 3 Collectors in the field experiment with separation of eight meters between each other(a); collector structure located in the field experiment (b); inside of collector, with a slide that collected spores (c);conidia of *Drechslera* sp. observed on slides, characterized by dark multiple-celled and bipolar germination of conidia. Scale bar, 50 μm (d).

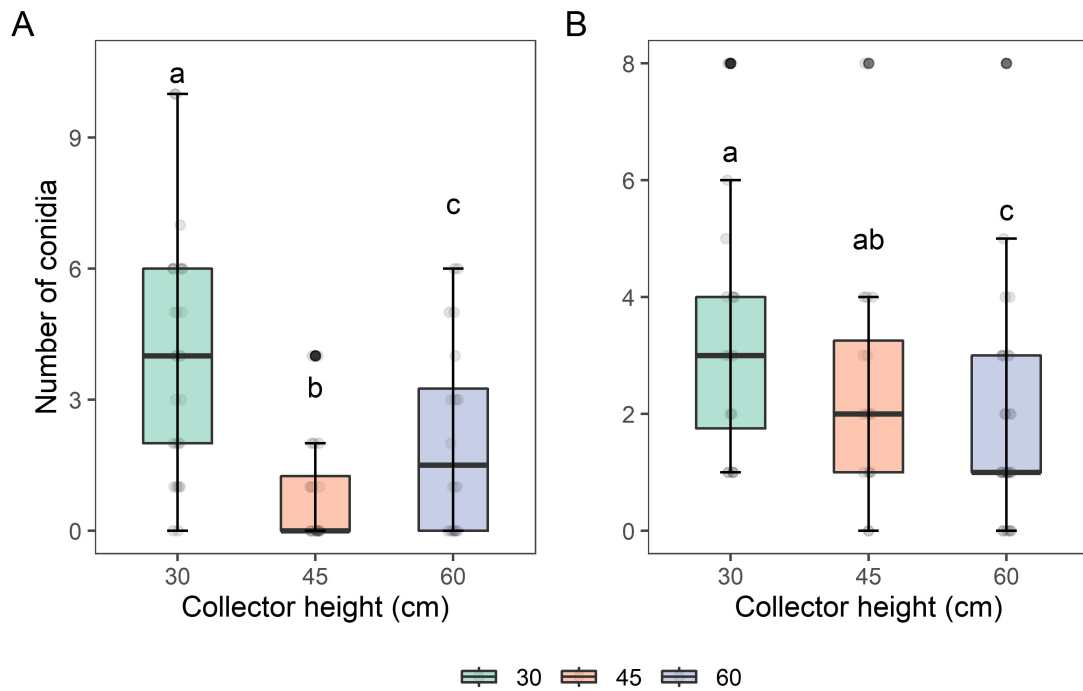


Fig. 4 Mean values of the number of conidia of *Drechslera* sp. according to collector height during 2019 (A) and 2020 (B) growing season. The horizontal line inside the box represents the median, the limits of the box represent the lower and upper quartiles, and the circles represent the observation of each treatment. Data points of experiments (n = 4) are the means and error bars represent standard deviation of means. Point (•) corresponds to outliers. Different lowercase letters indicate statistical differences according to the Tukey test at $p < 0.05$.

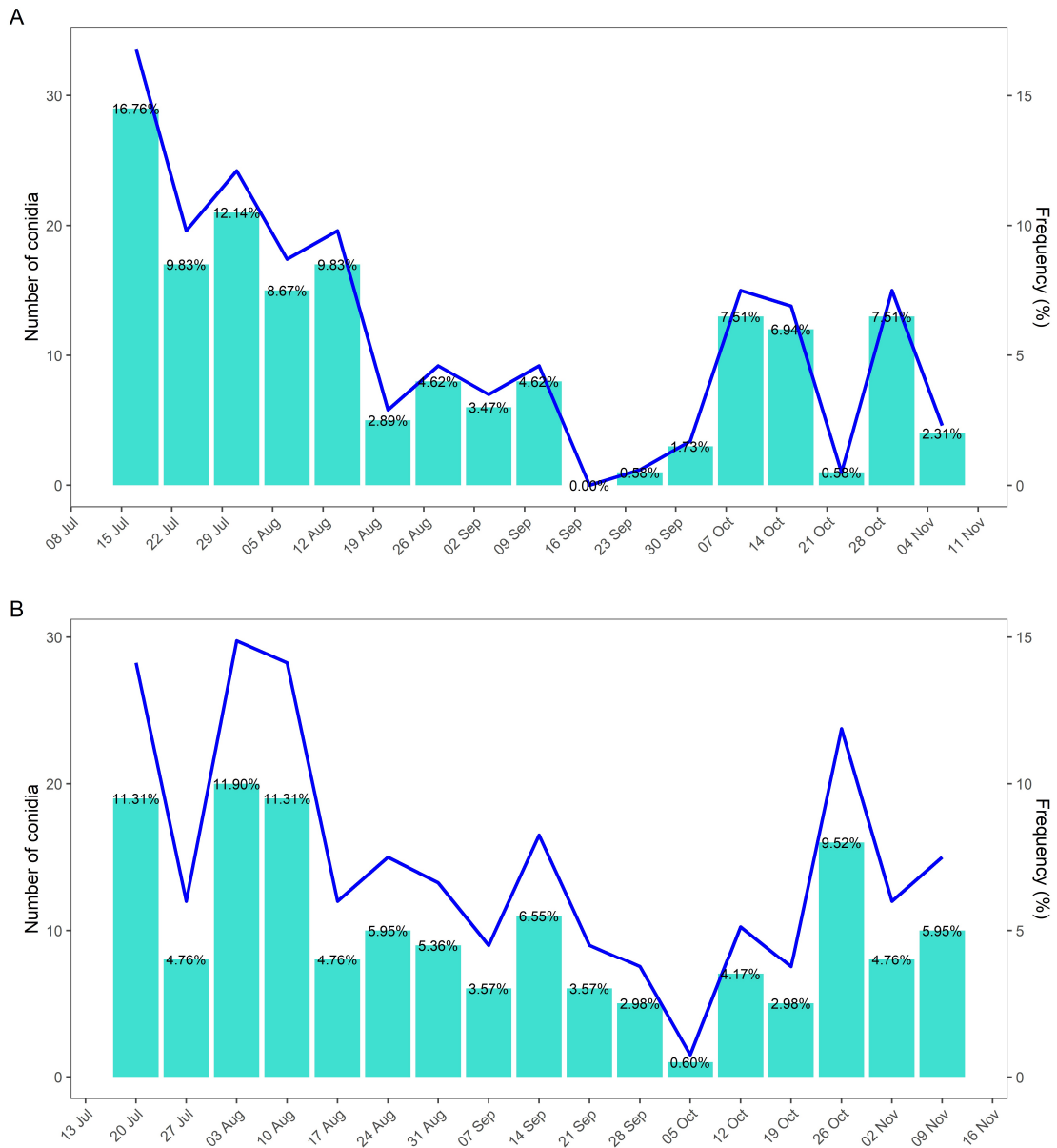


Fig. 5 Number of conidia (—) and frequency (—) of *Drechslera* sp. conidia collected weekly in 2019 (A), and 2020 (B).

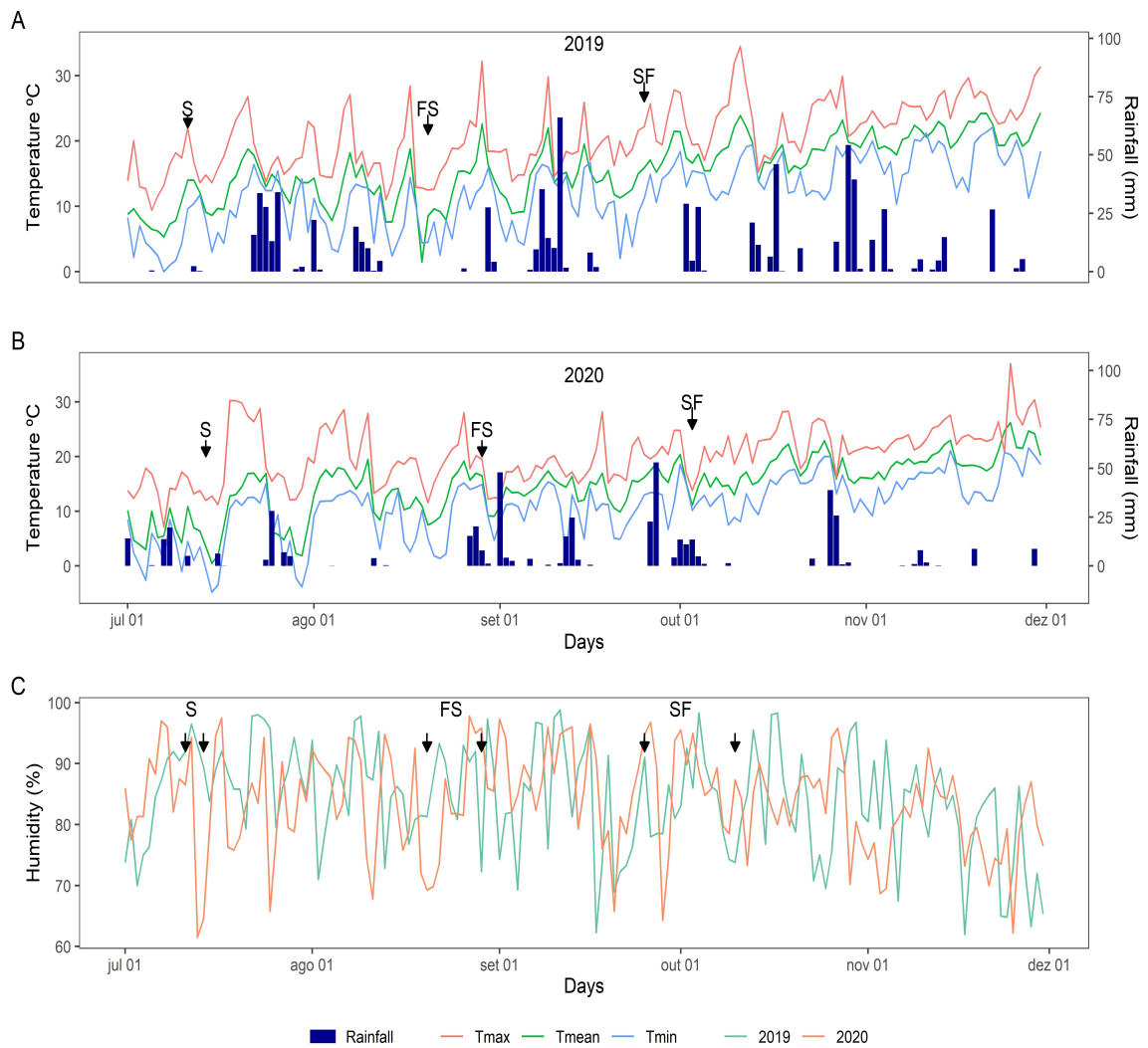


Fig. 6 Climate conditions of the experimental area in Capão de Leão, RS, Brazil. Rainfall (mm), temperature: mean (Tmean), minimum (Tmin) and maximum (Tmax) during the growing cycle of wheat in 2019 (A) and 2020 (B); humidity during the growing cycle of wheat in 2019 and 2020 (C). S = date of sowing; FF = date of first fungicide spraying at flag leaf stage (ZGS39); SF = date of second fungicide spraying at flowering (ZGS65).

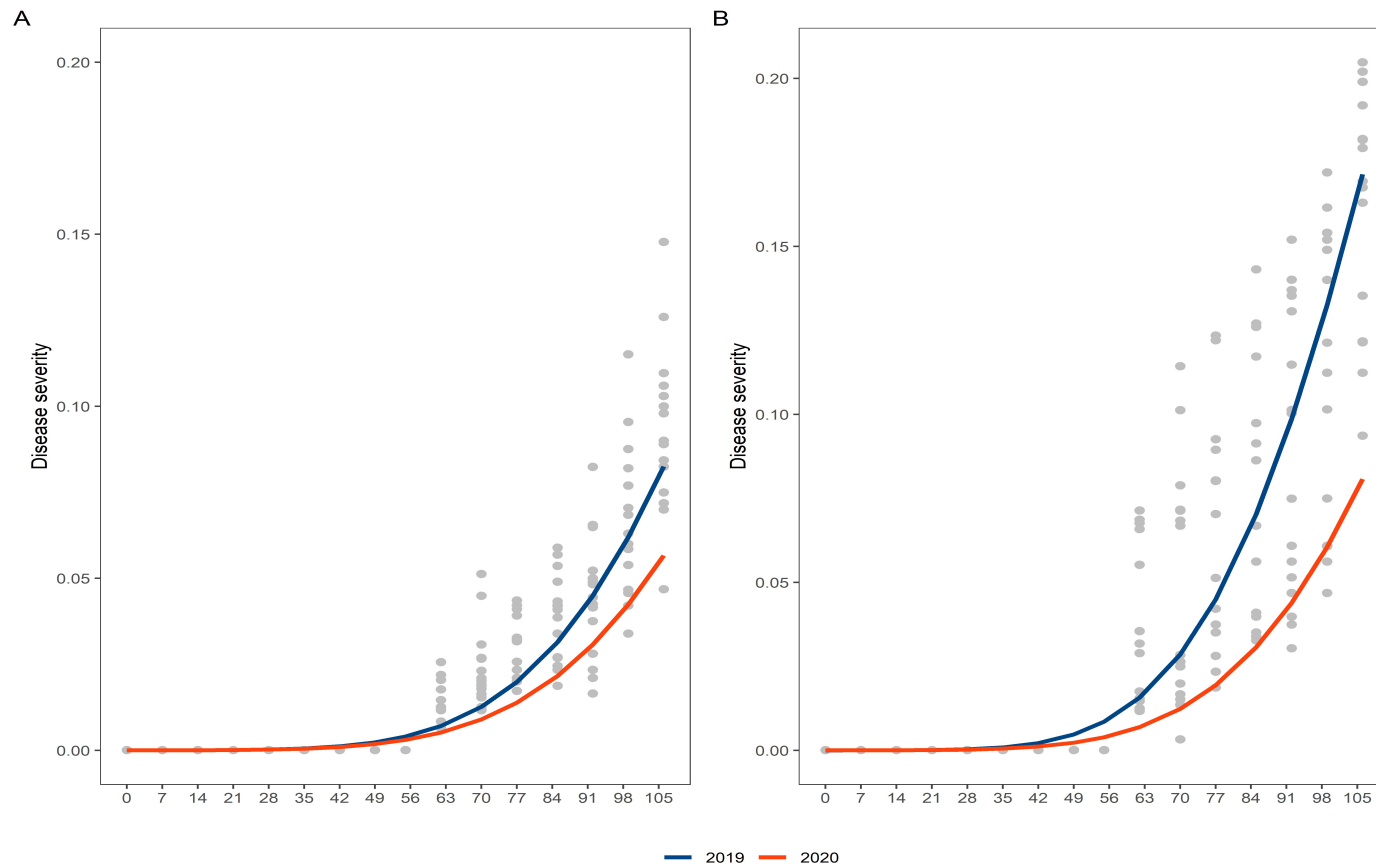
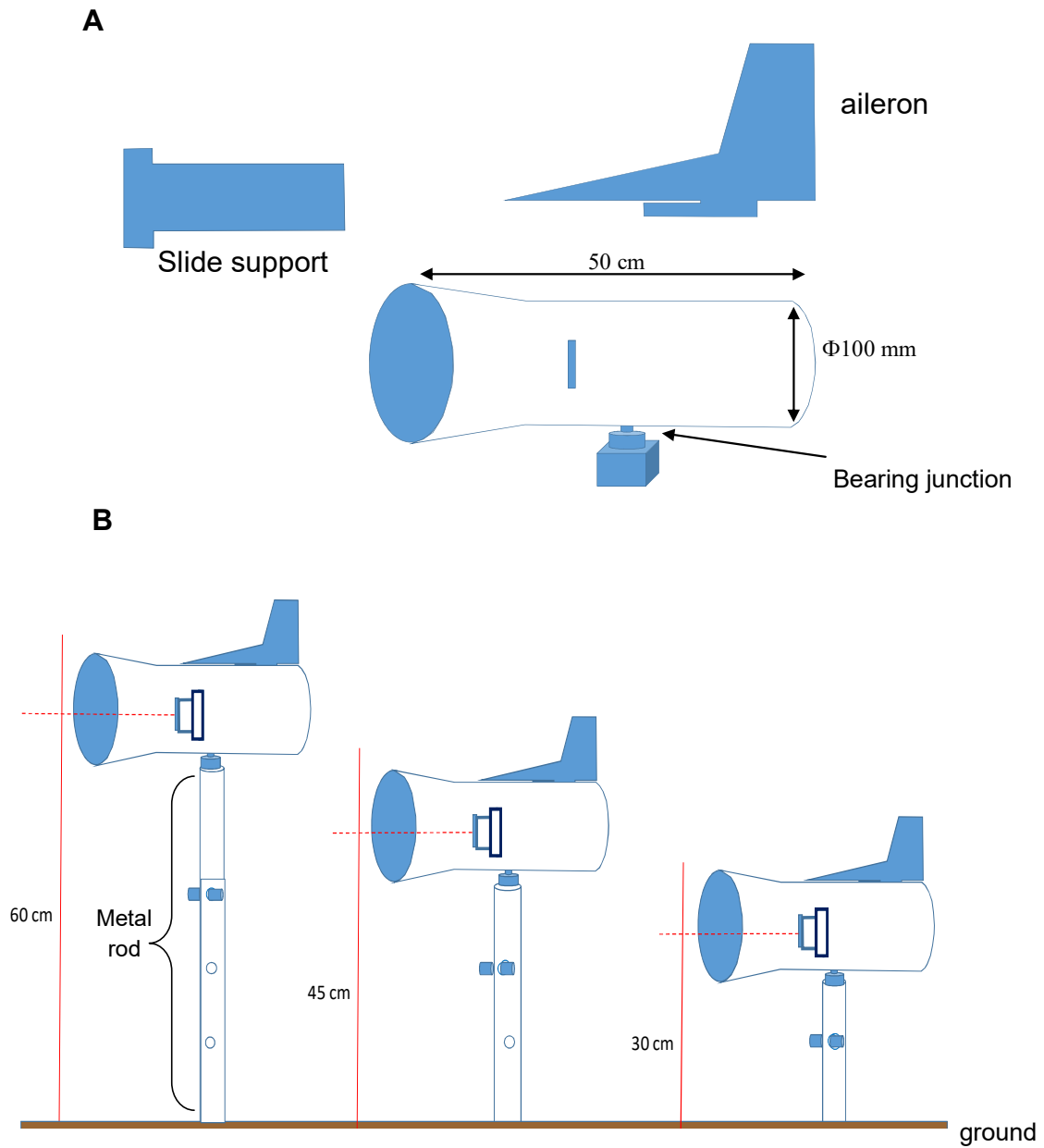


Fig. 7 Curves fitted by Gompertz model (lines) of disease progress data (•) of tan spot severity plotted against time for TBIO Audaz during 2019 and 2020 growing seasons (A), TBIO Tibagi during 2019 and 2020 growing seasons (B).



Supporting information

Figure S1. Collector for quantification of airborne inoculum. A) Collector design and *specification*. B) Height of the collectors about the ground.

The chapter 2 was formatted under the guidelines of the **Journal of Integrative
Agriculture**

Nitrogen fertilization, fungicide application and genetic resistance in wheat disease management

Andrea ROMÁN^{1,3}, Daniel DEBONA², Eduardo RODRIGUEZ⁴ and Leandro José DALLAGNOL^{1*}

¹ *Federal University of Pelotas, Eliseu Maciel Faculty of Agronomy, Crop Protection Department, Laboratory of Plant Pathogen Interaction, 96010-900, Pelotas, Rio Grande do Sul, Brazil.*

² *Universidade Tecnológica Federal do Paraná - Campus Santa Helena, Agronomy Department, 85892-000, Santa Helena, Paraná, Brazil.*

³ *Bolivar State University, Agricultural Sciences Natural Resources and the Environment Faculty, Laboratory of Phytopathology, EC020150, Guaranda, Ecuador.*

⁴ *Grow Green Agricultural Technologies, EC0103, Riobamba, Ecuador.*

***Corresponding author:** leandro.dallagnol@ufpel.edu.br

Abstract

Nitrogen (N) fertilization is a common practice adopted worldwide to increase grain yield and disease control. This study was carried out to determine the effect three N rates (70, 130 and 200 kg ha⁻¹, referred as low, recommended and high, respectively) and a pre-mix fungicide (bixafen + prothioconazole + trifloxystrobin) on disease intensity and grain yield of the two early-maturing wheat cultivars TBIO Audaz and TBIO Tibagi, which which are moderately resistant and susceptible to most diseases, respectively. Two experiments involving natural infection were conducted in the field during 2019 and 2020 in a split-split plot design. Tan spot, powdery mildew, leaf rust, and Fusarium head blight (FHB) were the main diseases observed in the experiments. Recommended N reduced the area under the disease progress curve (AUDPC) of tan spot by 23%, which was similar to high N. Nevertheless, AUDPC of powdery mildew was increased at high N in both cultivars, whereas N rates did not affect leaf rust or FHB. The use of early-maturing wheat cultivars did not allow escaping to FHB damage, except TBIO Audaz, which is moderately resistant. Associated with fertilization, the fungicide application decreased AUDPC of tan spot, powdery mildew, leaf rust and FHB by 31, 33, 75 and 40%, respectively, in comparison with the unsprayed treatment. The results indicated that cultivar × fungicide and cultivar × nitrogen were significant ($p < 0.05$) for AUDPCs, and yield variables. Yield was not

increased by increasing the N rate by 50%; however, recommended N increased yield, health area duration (HAD), and improved tan spot control relative to low N. These findings, associated with economic and cost-efficiency analysis, indicate that the use of a moderately resistant cultivar and recommended N maintain adequate nitrogen use efficiency (NUE) and economic returns.

Keywords: early-maturing wheat cultivars, wheat diseases, nitrogen use efficiency, fungicide mixture, economic analysis.

1. Introduction

Wheat (*Triticum aestivum* L.) is one of the most important crops as well as the most consumed cereal worldwide. However, several diseases and pests are estimated to decrease yield by 21.5% at the global level, threatening food security (Savary *et al.* 2019). In Brazil, South is the most important region for wheat production. Rio Grande do Sul state is the second producing state, accounting for 36% of the total Brazilian production (CONAB 2021a). Nevertheless, weather conditions in southern Brazil are usually very favorable to some diseases affecting wheat (Del Ponte *et al.* 2009). The main leaf diseases that can occur are tan spot (*Pyrenophora tritici-repentis* (Died.) Drechs.), powdery mildew (*Blumeria graminis* (DC.) f. sp. *tritici*), yellow (stripe) rust (*Puccinia striiformis* West.), and leaf rust (*P. triticina* Eriks. (= *P. recondita* Rob. Ex Desm. f. sp. *tritici* Eriks & Henn.). Moreover, Fusarium head blight (FHB) (*Fusarium graminearum* species complex) affects wheat during anthesis to late stages of grain development (Del Ponte *et al.* 2007), and wheat blast (*Magnaporthe oryzae* *Triticum pathotype*) mainly infects spikes (Debona *et al.* 2012; Cruz *et al.* 2015), although the latter is less common in Rio Grande do Sul.

Prevalence of pathogens causing leaf spots varies with weather conditions such as rainfall and range of daily temperatures, as well as the disease resistance of wheat genotypes (Fernandez *et al.* 2016). The use of resistant genotypes is the most important and economic method to reduce yield losses due to diseases (Li *et al.* 2011; Faris *et al.* 2012), while the use of early-maturing cultivars allows to escape from spike diseases occurring at the maturity time besides enabling to grow more than one crop per season (Patel and Monpara 2007; Gilbert and Haber 2013). In Brazil, only cultivars with moderate resistance are available to manage tan spot, FHB, and wheat blast, while resistant cultivars are available to manage powdery mildew and rusts (Santana *et al.* 2008; Dorneles *et al.* 2018; Pazdiora *et al.* 2018; Reunião da Comissão Brasileira de Pesquisa de Trigo e

Triticale 2018; Bertagnolli *et al.* 2019). Fungicide application is often employed to mitigate yield losses arising from wheat diseases (Jorgensen and Olsen 2007; Fleitas *et al.* 2018; MacLean *et al.* 2018; Reunião da Comissão Brasileira de Pesquisa de Trigo e Triticale 2018). Likewise, the reduction of disease damage depends on the efficiency of the fungicide associated with the level of cultivar susceptibility (Ruskeet *et al.* 2003).

In general, growing susceptible cultivars under optimal weather conditions for pathogens increases the risk of disease outbreak and the dependence on the use of fungicides. For wheat, strategies to protect flag leaves and delay its senescence are important to guarantee high grain yield, because the flag leaf is the main contributor to grain development and filling (Blandino and Reyneri 2009). However, under conditions favorable to diseases (monoculture vs. no-till, use of susceptible cultivars, etc.), tan spot can occur before tillering, requiring to anticipate fungicide spraying to delay the increase of the secondary inoculum, which can infect flag leaves. On the other hand, diseases such as FHB and blast which affect mainly wheat spikes make fungicide spray a difficult task for wheat growers. For instance, the efficacy of chemical control of FHB has been reported as low as 50 to 60%, often being unsatisfactory (Machado *et al.* 2017; Barro *et al.* 2020), due to the difficulty of the required amount of fungicide reaching the biological target. This is related to a long flowering period and a low persistence of the product on the surface of the flower organ (Reis *et al.* 1996).

Wheat fertilization is an option to reduce disease progress and increase fungicide efficiency or reduce its demand (Pazdiora *et al.* 2021). For example, nitrogen (N) fertilization has been found to decrease tan spot severity and increase green leaf area in wheat (Huber *et al.* 1987; Jones *et al.* 1990; Bockus and Davis 1993; Fernandez *et al.* 1998; Krupinsky and Tanaka 2001). Furthermore, the use of pre-mix of fungicides of different chemical groups (triazoles, strobilurins and carboxamides) in combination with higher N rates reduced the damage of some diseases and increased grain yield (Castro *et al.* 2018; Fleitas *et al.* 2018; Schierenbeck *et al.* 2019). Nevertheless, the effect of N fertilization varies according to the pathosystem, N rates and sources used, and wheat cultivars, resulting in different yields depending on the plant pathogen interaction (Huber and Thompson 2007; Mur *et al.* 2017).

N fertilizers are used throughout the world to increase the yield of cereals. However, field studies regarding N fertilization and its effect on the efficiency of the use of

nitrogen (NUE) as well as the impact of the implementation of other disease management strategies, including the use of premixes of fungicides or early-maturing wheat cultivars with contrasting resistant, remain scarce. Therefore, the objective of this study was to investigate the effect of alteration of the N fertilization rate, compared to the recommended dose, associated with two sprayings of a pre-mix fungicide (carboxamide + triazolintione + strobilurin) on disease intensity and grain yield of two early-maturing wheat cultivars with contrasting disease susceptibility.

2. Materials and methods

2.1. Field trials

Experiments were conducted in the field at the Centro Agropecuário da Palma (31°48'06.4"S 52°30'18.6"W) belonging to the Pelotas Federal University, Brazil, during two successive growing seasons (2019 and 2020). Plots were established in an area previously sown in a wheat-soybean succession system in 2018 for naturalinfection of diseases. The trials plots were sown on July 11, 2019, and July 14, 2020, under no-till. Wheat seeds were sown (9 rows, 0.17 m spacing) with a plot seeder (Semeato, SHP model) at a seeding rate of 300 seeds m⁻² to achieve plant density of approximately 275 plants m⁻². The soil was an Argis soil (Ultisol), with 658 g kg⁻¹ of sand, 242 g kg⁻¹ of clay; 101 g kg⁻¹ of silt. Chemical characteristics were as they follow: organic matter: 1.0 and 1.79%, nitrogen: 0.73 and 0.93 g kg⁻¹; NO₃: 3.23 and 4.11 g kg⁻¹; NH₄: 0.94 and 1.19 g kg⁻¹; phosphorus: 20 and 14 ppm, potassium: 99 and 115 mg dm⁻³; calcium: 1.7 and 1.8 cmolc dm⁻³; magnesium: 1.2 and 1.3 cmolc dm⁻³; copper: 1 and 0.9 mg dm⁻³; zinc: 1.1 and 0.8 mg dm⁻³; manganese: 12.7 and 21 mg dm⁻³; pH_{H2O} 5.7 and 6, in 2019 and 2020 respectively.

Weather data (daily rainfall; relative humidity, minimum, maximum and mean temperatures) were recorded at the Pelotas weather station, located at coordinates latitude 31° 52' 00" S and longitude 52° 21' 24" W. GRW and altitude of 13.24 m.

2.2. Experimental design and treatments

The experimental design was a split-split plot arrangement with four replications. Main plots consisted in plants that were sprayed with fungicide or unsprayed plants. Subplots were wheat cultivars (TBIO Audaz and TBIO Tibagi), and sub-sub-plots were nitrogen rates (low N: 70 kg ha⁻¹, recommended N: 130 kg ha⁻¹ and high N: 200 kg ha⁻¹).

Each sub-sub-plot had an area of 3 m² (2 m long × 1.5 m wide). Cultivars TBIO Audaz (Biotrigo®) and TBIO Tibagi (Biotrigo®) were chosen among regionally adapted cultivars showing similar anthesis and maturity times, but contrasting in disease resistance (the former being more resistant to tan spot, powdery mildew, leaf rust and FHB than the latter).

Fertilizer was applied at sowing as required for maximum crop yield according to soil test recommendations at 40 kg ha⁻¹ phosphorus supplied as triple superphosphate, and 30 kg ha⁻¹ potassium supplied as potassium chloride. Nitrogen (granular urea, 45% N) was applied 15 days after sowing and at tillering stage (ZGS23), being applied 50% of the rate of each treatment in each time.

The pre-mix fungicide containing bixafen (125 g L⁻¹; carboxamide) + prothioconazole (175 g L⁻¹; triazolinthione) + trifloxystrobin (150 g L⁻¹; strobirulin) (Fox Xpro®; Bayer CropScience) was applied at 0.5 L ha⁻¹ on flag leaf (ZGS 39) and flowering (ZGS65) (Zadoks *et al.* 1974). The fungicide was applied using a CO₂ pressure sprayer, with four nozzles (TTJ60 11002; Teejet®), delivering 200 L ha⁻¹.

2.3. Experimental measurements

2.3.1. Diseases assesses

The main diseases recorded during the two growing seasons were tan spot, powdery mildew, leaf rusts and FHB. Disease incidence was determined in a linear meter of the center line of each experimental plot counting the total and symptomatic plants for each disease. Incidence was expressed as percentage. For severity of leaf diseases, up to eight evaluations were performed in each year. Tan spot and powdery mildew severities were estimated using the midpoint of the Horsfall-Barratt scale based on whole plants (Horsfall and Barratt 1945) and expressed as percentage of leaf area showing disease symptoms on ten plants in each plot from stem elongation stage (ZGS30) to hard dough stage (ZGS87). For leaf rust, six and seven evaluations were performed in 2019 and 2020, respectively. Rust severity was estimated based on Cobb's scale as modified by Peterson *et al.* (1948) from flowering stage (ZGS65) to hard dough stage (ZGS87). For FHB, 20 spikes at random were assessed from each plot from flowering stage (ZGS65) to hard dough stage (ZGS87). FHB severity (proportion of the spike bleached) was determined as the average disease severity (%) of 20 spikes per plot using the scale of Stack and McMullen (2011), and four estimations were considered for analyses. For each disease, the area under disease

progress curve (AUDPC) was calculated to summarize the disease progress with time, according to Shaner and Finney (1977).

2.3.2. Healthy area duration (HAD)

Leaf area of the fourth and flag leaves was estimated at ZGS39, ZGS60 and ZGS80 and calculated by multiplying the length \times width \times 0.835 (Miralles and Slafer 1990). In each experimental plot, the number of plants m^2 was counted in order to calculate the leaf area index (LAI), by multiplying the total leaf area per total shoot per number of plants per m^2 and divided by the area used for plants per m^2 . LAI was used to estimate HAD, using the following equation:

$$HAD = \sum_{i=0}^{n-1} [LAI t_i (1 - X_i) + LAI_{i+1} (1 - X_{i+1})] / 2(t_{i+1} - t_i)$$

where n is the number of evaluations, X_i is severity proportion, LAI is leaf area per m^2 and $(t_{i+1} - t_i)$ is the interval between two consecutive assessments (Waggoner and Berger 1987).

2.3.3. Nitrogen determination

Leaf samples were taken at ZGS60 in the central rows in all plots. Samples were dried at 60°C for 72 h and ground using an R-TE-350 mill. A subsample of 1 g was used for the determination of plant nitrogen level (PNL, $g\ kg^{-1}$) according to the micro-Kjeldahl method (Bremner and Mulvaney 1982). A sample of grains was ground using a mill (R-TE-350, Tecnal) to determinate the total nitrogen per grain (TNG; $g\ kg^{-1}$) by the micro-Kjeldahl method (Bremner and Mulvaney 1982).

2.3.4. Yield determinations

Wheat was harvested from five central rows with length of 1 m (totaling 1 m^2) of each plot and threshed in a mechanical grain thresher (EDA, model TR, Parcela). Samples were air-dried for approximately 48 h and cleaned. The grain moisture content of a representative subsample was measured with a moisture tester (AgraTronix, MT-PRO). The grain yield ($kg\ ha^{-1}$) was estimated after harvesting the useful area of each plot and it was adjusted to 13% moisture content. The thousand kernel weight (TKW; g) was measured by counting 250 grains in quadruple from each plot sample and weighed on an analytical balance to an accuracy of 0.001g (Shimadzu model BL 3200H). The test weight

(TW; kg hL⁻¹) was determined using a Dallemolle type 40 hectoliter balance, according to Method 55-10.01 (AACC, 1999).

2.3.5. Economic analysis

Economic analysis of the treatments was done using the dominance analysis technique according to Perrin *et al.* (1979). Production costs were based on CONAB (2021b) including fixed costs: transport, preharvest and harvest machinery, labor, land, assistance, and sprays; and variable costs: seeds, fungicides, fertilizers, and other agrochemical. Variable costs were adjusted to prices of treatment used according to the local sellers. Other variable production costs revenues were calculated using data in the AGROLINK database for three wheat-producing states (Rio Grande do Sul, Paraná and Santa Catarina) in November 2019 to 2020 (AGROLINK 2021a). Variable costs and wheat prices were transformed into USD at the exchange rate in November 2020 (5.33 BRL = 1 USD), obtained from <http://es.investing.com>. Wheat price was considered as US\$ 14.47 per 60 kg (AGROLINK 2021b).

Partial budget was estimated for each treatment according to the yield obtained; adjusted yield to efficiency of 90%; variable total costs; gross income; and net profit (Appendix A).

For the dominance analysis, total variable costs of each treatment were ordered in function of variable cost (lowest to highest). Non-dominated (ND) treatments were considered those that, compared to the immediately previous treatment, obtained a greater net benefit.

The ND treatments were compared, and the marginal costs were determined as the difference between the highest variable cost and the previous treatment that reported the lowest cost. In addition, the marginal net benefit was determined as the difference between the net benefit of the treatment (between highest to lowest net benefit of the preceding treatment). Finally, the marginal return was calculated as the ratio between the marginal net benefit and the marginal variable cost, expressed as a percentage. In this way, the treatment with the highest percentage was considered the most viable from an economic standpoint (Appendix B).

2.3.6. Nitrogen use efficiency (NUE)

Nitrogen use efficiency (NUE) was calculated according Meena *et al.* (2016) using the following equation:

$$\text{Nitrogen use efficiency (NUE)} = \frac{\text{YieldF(kg)} - \text{YieldC (kg)}}{\text{Quantity of nutrient applied (kg)}}$$

where F is plant receiving fertilizers and C is plants receiving no fertilizer.

Then the NUE of each treatment was used to calculate the cost-efficiency index (Appendix C).

2.3.7. Cost-efficiency

The cost-benefit index was determined as the ratio between the NUE and the variable costs of each of the treatment (Sermeño *et al.* 2001). For this purpose, the treatments were arranged in descending order of the NUE. According to the variable costs, the lower-cost treatments were considered as ND. In this way, the treatment with the lowest rate was considered the best in terms of efficiency.

2.4. Data analyses

Data analyses were performed with R version 4.0.4. (RStudio 2021) using mixed-effects linear models with the ‘lmer’ function of the lme4 (Bates *et al.* 2014) and lmerTest (Kuznetsova *et al.* 2017) packages. The data were analyzed separately for the years. Fungicide, cultivar and nitrogen treatment were considered as fixed factors. Blocks, the nesting of plots within blocks and subplots within plots were considered as random factors. Data assumptions were verified graphically using plots of fitted values *versus* the residuals for homogeneity of variances and using normal Q-Q plots for normality of residuals and graphically by using simulate the ‘simulateResiduals’ of the DHARMA package (Hartig 2021). Fixed treatment effects were considered significant at $p < 0.05$. Estimated marginal means were computed with the emmeans function of the emmeans package (Lenth 2021) and pairwise comparisons were performed with the Tukey test using the ‘cld’ function of the multcomp package (Hothorn *et al.* 2008). The economic analysis was performed in Excel 2013 ©Microsoft.

3. Results

3.1 Weather conditions during the growing season and disease recording

Weather conditions differed between the years regarding the temperatures as well as frequency and amount of rainfall. In 2020, lower temperatures were recorded at the end

of July and the first half of August compared to the same period in 2019 (Fig. 1A and B). Accordingly, diseases occurred earlier in 2019 in comparison to 2020. The main difference between the years was the amount and distribution of rainfall in growing season. In 2019, the rainfall was frequent, and October was the wettest month. Tan spot was the main leaf spot observed during tillering and displayed higher intensity after the flag leaf formation during 2019; however, in 2020 tan spot was observed just before the flag leaf formation with lower intensity. In 2020, the rainfall was 35% lower than in 2019, with August being the month with less rainfall, but it increased in September. As a result, the development of tan spot was observed only after the flag leaf formation and during flowering (ZGS60). Powdery mildew was recorded at the same time as tan spot, and it was displayed a higher intensity in 2019, during tillering, compared to 2020. Leaf rust was observed during flowering in 2019, while in 2020 it began with flag leaf formation (ZGS39), likely due to a slight decrease in temperature in 2020 compared to 2019. This effect was most pronounced in the susceptible cultivar. FHB occurred in both years, but in 2020 high amounts of rainfall during anthesis favored the increase of the severity in the susceptible cultivar (TBIO Tibagi).

3.2 Effect of cultivar, fungicide and nitrogen rate on the area under disease progress curve

The diseases recorded in this study included tan spot, powdery mildew, leaf rust and FHB (Fig. 2, and 3). The factor cultivar was significant ($p < 0.05$) for all AUDPCs, regardless of crop season (Table 1). Fungicide was significant ($p < 0.05$) for AUDPC of tan spot in 2019, and for all AUDPCs, except powdery mildew, in 2020. Nitrogen levels were significant ($p < 0.05$) for tan spot and powdery mildew AUDPCs (Table 1). Some interactions of factors were also significant, especially in 2020 (Table 1).

Cultivars showed differences for all AUDPCs (Table 1; Fig. 2, and 3). The cultivar TBIO Audaz showed lower AUDPC of tan spot (Figure 2C and 3C), powdery mildew (Fig. 2F and 3F), leaf rust (Figure 2I and 3I), and FHB (Figure 2L and 3L) by 56 and 34%, 52 and 38%, 83 and 73%, and 47 and 66%, respectively, for 2019 and 2020, compared to TBIO Tibagi (Table 2). N rate displayed differences for tan spot, and powdery mildew (Table 2). The AUDPC of tan spot was reduced by 20 and 25% by recommended and high N rate, respectively, compared to low N (Table 2). However, high N had a similar effect on AUDPC of tan spot with the recommended N rate. In contrast, AUDPC of powdery

mildew was increased by 15 and 22% at high N and recommended N, respectively, in comparison to low N (Table 2). Fungicide application influenced all AUDPCs. Fungicide application reduced the AUDPC of tan spot by 33% in 2019 and 29% in 2020, whereas the AUDPC of powdery mildew was reduced by 33% due to fungicide application only in 2020. AUDPCs of leaf rust and FHB, were decreased 76 and 74% in 2019 and 47 and 35% in 2020, respectively, due to fungicide application (Table 2).

The most significant interactions observed were cultivar \times fungicide, and cultivar \times nitrogen, which varied between the variables (Table 1; Fig. 4, and 5). The interaction cultivar \times fungicide was significant for AUDPC of tan spot and AUDPC of leaf rust (Fig. 4A, and B). For TBIO Audaz, fungicide application decreased AUDPC of tan spot by 27%. A similar result was observed for TBIO Tibagi, in which AUDPC of tan spot in plots treated with fungicide was 34% lower than in unsprayed plots (Fig. 4A). For AUDPC of leaf rust, fungicide application decreased it by 40% in TBIO Audaz. A similar trend was observed for TBIO Tibagi sprayed with fungicide, which had an AUDPC of leaf rust 80% lower than unsprayed control (Fig. 4B). By contrast, the AUDPC of FHB was influenced by none interactions in both years.

The interaction fungicide \times nitrogen was significant for AUDPC of tan spot ($p < 0.05$) in 2019 (Table 1). In contrast, the interaction of cultivar \times nitrogen rate was significant for AUDPC of tan spot. For TBIO Audaz, high N decreased AUDPC of tan spot by 20% relative to the low N, while the AUDPC of tan spot was 23% lower at high N than for low N for TBIO Tibagi (Fig. 5A).

3.3. Effect of cultivar, fungicide and nitrogen rate on grain yield and yield components

There were significant ($p < 0.05$) differences for the fixed factors fungicide, cultivar and nitrogen rate on the grain yield and quality variables, as well as for the interactions cultivar \times fungicide and cultivar \times nitrogen (Table 3). Cultivar and fungicide were significant ($p < 0.05$) for TKW, TW and yield in 2019 and 2020 (Table 3).

TBIO Audaz performed better than TBIO Tibagi regarding the yield components TKW, TW and yield, with increases of 14 and 29%, 4 and 7%, and 40 and 74% in 2019 and 2020, respectively (Table 4). Fungicide application increased TKW, TW and yield by 25 and 37%, 8 and 6%, and 27 and 44% in 2019 and in 2020, respectively, in comparison

to the unsprayed treatment (Table 4). N rate produced higher yield of 29% in 2019 and 36% in 2020 between a low N to recommended N.

There were significant ($p < 0.05$) differences for the fixed factors cultivar and N rate for HAD, PNL, and TNG in both years (Table 5). However, for HAD, nitrogen rates showed significant differences, but it was not consistent between the years. HAD in TBIO Audaz was higher by 88% in 2019 and 23% in 2020 compared to TBIO Tibagi, which is an increase of 8 to 15 days (Table 6). These results indicate that cultivar has a major effect on the increment in the time of healthy area duration. High N increased HAD by 9% relative to low N in 2019. The PNL was 9% higher for TBIO Audaz compared to TBIO Tibagi in 2020, but no differences were observed in 2019. In contrast, for TBIO Tibagi TNG was 15% in 2019 and 9% higher in 2020 compared to TBIO Audaz. There were differences according to N rates. For PNL, high N showed increases of 21 and 8% in 2019 and 2020, respectively, compared to low N (Table 6). Moreover, increases of 15 and 12% for TNG in 2019 and 2020, respectively, were observed for high N compared to low N.

The interaction of cultivar \times fungicide was significant ($p < 0.05$) for TKW, TW, and HAD in both years (Table 5). There were no differences in TKW between plants sprayed or unsprayed with fungicide for TBIO Audaz. For TBIO Tibagi, however, fungicide application increased TKW by 37% (Figure 4C). TBIO Audaz sprayed with fungicide displayed an increase in 4% in TW relative to unsprayed treatment, whereas fungicide application increased TW by 12% in TBIO Tibagi (Fig. 4D). Yield was increased by 54% in response to fungicide application for TBIO Audaz (Fig. 4E). Regarding the HAD, there were no differences between treatments with or without fungicide for both cultivars. However, TBIO Audaz displayed increases of 76 and 90% in HAD for treatments with and without fungicide, respectively, compared with TBIO Tibagi (Fig. 4F).

The interaction cultivar \times nitrogen was significant ($p < 0.05$) for TKW, yield, PNL, and TNG in 2019 and 2020 (Fig. 5). For TKW, the interaction between cultivar TBIO Audaz \times N rate had no significant differences among the rates, but for TBIO Tibagi, recommended N decreased TKW by 4% compared to low N (Fig. 5B). For yield, TBIO Audaz supplied with recommended N had a value 37% higher compared to low N. Moreover, recommended N resulted in a yield that was 11% higher than high N. For TBIO Tibagi, yield was increased by 30% at recommended N compared to low N (Fig. 5C). For PNL, there were increases of 21 and 20% for TBIO Audaz and TBIO Tibagi, respectively, at high N compared to low N. There were no differences between cultivars at high and

recommended N for PNL (Fig. 5D). High N increased TNG of TBIO Audaz and TBIO Tibagi, respectively, by 13 and 16% compared to low N. There were no significant differences between cultivars regarding the high N and recommended N for TNG (Fig. 5E).

3.4. Economic analysis

According to the partial budget analysis (Appendix A), TBIO Tibagi treatment without the application of fungicide and the application of low N had the lowest variable cost (USD 633.41), whereas the highest variable cost was observed for TBIO Audaz sprayed with fungicide and supplied with high N (USD 726.30).

The TBIO Audaz sprayed with fungicide and supplied with recommended N presented the highest net profit (USD 271.04), while the TBIO Tibagi plants without fungicide application supplied with low N showed a negative performance with a net loss (-USD 337.77).

According to the dominance analysis, treatments with TBIO Audaz without fungicide application supplied with recommended N, TBIO Audaz with fungicide application supplied with low N and TBIO Audaz with fungicide application supplied with recommended N were not dominated (ND) (Appendix B). The remaining treatments were dominated (D) and were excluded from further analyses.

The economic analysis regarding the marginal net benefits showed that TBIO Audaz supplied with recommended N (130 kg ha⁻¹) and sprayed with fungicide showed the highest net marginal benefit (193.74 USD) compared to TBIO Audaz without fungicide application supplied with low N (Table 7).

3.5. Nitrogen use efficiency and cost-efficiency

In this study the treatments with low and recommended N showed higher NUE compared with high N treatments. TBIO Audaz had higher NUE than TBIO Tibagi. Furthermore, unsprayed treatments showed a higher NUE compared with fungicide treatments (Table 8).

Dominance analysis of NUE and variable cost showed that the treatments TBIO Audaz without fungicide application and low N, TBIO Audaz without fungicide application and recommended N, and TBIO Audaz without fungicide application and recommended N were not dominated (ND) (Appendix C). The remaining treatments were dominated (D) and excluded from further analyses. Therefore, the cost-efficiency analysis showed that the

treatment TBIO Audaz without fungicide application and low N had the lowest cost-efficiency index (Table 8).

4. Discussion

In this study, four diseases occurred during the wheat development, displaying varied intensities. Weather conditions had a strong effect on disease development. Tan spot was the main leaf spot disease observed, similar to the observations made in spring wheat by Pazdiora *et al.* (2021). During 2019, the higher temperature during winter was conducive to higher intensity of powdery mildew compared to 2020. On the other hand, a higher intensity of leaf rust was observed during 2020 compared to 2019. The use of early-maturing wheat cultivars had an effect on the four diseases. Their use is indicated to escape from diseases such as FHB (Gilbert and Haber 2013); however, in this study, their use did not reduce the damage, probably due to the increase in the rainfall during the anthesis, thereby favoring FHB severity. The final intensity of the four diseases was related by the susceptibility level of the cultivar as well as its interaction with fungicide and N rate.

The results of this study clearly indicate the effects of the treatment interactions on the diseases during the course of wheat growth. Tan spot appeared since early stages of wheat development, while leaf rust appeared just before flowering, and both diseases were more severe for TBIO Tibagi than TBIO Audaz. The cultivar \times fungicide interaction demonstrated that two applications of fungicide on the susceptible cultivar reduced the damage stemming from diseases. However, TBIO Audaz without fungicide application showed AUDPCs relatively lower than TBIO Tibagi sprayed with fungicide. TBIO Audaz was less prone to the diseases regardless of fungicide application, and its resistance level can be adequate for management of diseases under high disease pressure. These results indicate that choice of wheat cultivars suitable for the region and the proper management measures can enhance wheat production, including successive crops.

In this study, the fertilization with recommended and high N, especially in a moderately resistant cultivar, decreased AUDPC of tan spot. These findings are consistent with those of Fleitas *et al.* (2018), who reported reduction of tan spot at high N. In this sense, results of this study corroborate to others researchers that indicated that at higher N, the N modified crop canopy, increasing the greenleaf area index (GLAI) and delaying senescence due to a higher radiation interception and radiation use efficiency (RUE), thus reducing the disease severity of necrotrophic pathogens (Hawkesford 2014; Schierenbeck *et al.* 2016; Fleitas *et al.* 2018).

However, the effect of N rate differs according to the pathosystem; while there was a reduction for AUDPC of tan spot at high N, this rate increased AUDPC of powdery mildew in both cultivars. Leaf rust and FHB, in turn, were not influenced by N rate. Increases in plant susceptibility to biotrophic pathogens, including *B. graminis* f. sp. *tritici*, due to high N supply are well-documented in literature and may be associated to increases in the availability of N compounds with low molecular weight for pathogen exploitation (Huber and Thompson 2007; Mur *et al.* 2017). Furthermore, high N is associated to decrease in the activity of key enzymes of the phenylpropanoid pathway (Matsuyama 1973), reducing the synthesis of resistance-related phenolics (Dixon and Paiva 1995), suggesting the increase of powdery mildew damage. However, the phenylpropanoid derivatives accumulation at the infection site has been reported to reduce *P. tritici-repentis* (necrotrophic) (Dorneles *et al.* 2017, 2018). The contrasting result between diseases suggested that high N rate, it is not the mainly factor influencing wheat diseases. In this context, the N source may be associated with the activation of different signaling pathways (Huber and Thompson 2007; Hawkesford 2014). Further studies will be necessary to reveal those effects on the *P. tritici-repentis* – wheat interaction.

The effect of the fungicide and N rate on HAD differed between the years, but cultivar was the most important factor for decreasing disease severity, mainly for TBIO Audaz. The interaction cultivar × fungicide observed in this study demonstrated that a pre-mix of fungicides (bixafen + prothioconazole + trifloxystrobin) may be associated with increased HAD. These results agree with the findings of other studies, in which a triple mixture of fungicides (epoxiconazole + pyraclostrobin + fluxapyroxad) was also associated with HAD (Schierenbeck *et al.* 2019; Fleitas *et al.* 2018). In this sense, the fungicide effect may be associated with the maintenance of photosynthetic area of green tissues, improving the CO₂ assimilation rate, and enhancing the concentrations of nitrogen, chlorophylls and proteins (Wu and von Tiedemann 2001; Ruske *et al.* 2003). For instance, previous studies have demonstrated that fungicide application increases GLAI and HAD in wheat, delaying senescence, reducing the disease severity (Serrago *et al.* 2009; Hawkesford 2014; Schierenbeck *et al.* 2016; Fleitas *et al.* 2018).

The fungicide effect was also observed on TKW, TW, yield, and TNG whereas nitrogen had an effect on TKW, yield, and TNG. Two applications with a pre-mix of fungicides during flag leaf and anthesis stages were related to an increase in TKW, TW, and yield. Likewise, Kutcher *et al.* (2018) found that the application of a fungicide mixture reduced leaf spot disease severity and increased yield, TKW, and TW. However, our

findings indicated that increasing the nitrogen rate by 50% regarding the recommended N rate (130 kg ha^{-1}) did not increase yield. This result demonstrated that only 30 to 40% of the applied nitrogen can be utilized by the plants, which means that more than 60% of the nitrogen is lost by leaching, denitrification and volatilization (Malhi *et al.* 2001). For that reason, exceeded the recommended N rate, is not profitable because it increases the cost without improving nitrogen use efficiency (NUE).

In addition, the nitrogen content was influenced by genotype and the management under field conditions. For example, in this study, TBIO Tibagi was the cultivar with highest TNG, but produced lower yields compared with TBIO Audaz, while TBIO Audaz had high PNL and yield. Some studies suggested that the increase in yield may be related with N remobilization before senescence, possibly from storage proteins as opposed to those with metabolic functions, at least up to an amount that does not affect essential physiological processes (Kong *et al.* 2016). These findings are in line with Maillard *et al.* (2015) and Thomas and Howarth (2000), who reported that nitrogen remobilization delayed leaf senescence and increased GLAI (major photosynthesis period), resulting in higher yield.

Our findings suggest that the recommended N rate (130 kg ha^{-1}) for the state of Rio Grande do Sul in Brazil (Silva *et al.* 2017) had a similar effect as the high N rate (200 kg ha^{-1}) on reduction of tan spot. The recommended N rate used in this study was similar to the high N (140 kg ha^{-1}) previously reported by Fleitas *et al.* (2018). Therefore, fertilization with the recommended N rate reduces tan spot and did not favor other leaf diseases, whereas increases the yield. Economic analysis showed that TBIO Audaz fertilized with low N (70 kg ha^{-1}) and recommended N (130 kg ha^{-1}) with fungicide produced better marginal returns, while the cost-benefit relation indicated that TBIO Audaz fertilized with 70 kg ha^{-1} was the most efficient with respect to NUE. These results agree with the findings of other studies, in which indicated that the use of wheat cultivars with higher NUE can contribute to reduce the amounts of N applied without decreasing grain yield (Barraclough *et al.* 2014; Gaju *et al.* 2014).

5. Conclusion

Warmer winters with continuous rainfall favor the occurrence of leaf and spike diseases. Regarding the susceptible cultivar, the fungicide application associated with the incorporation of nitrogen at the recommended N reduced AUDPCs of leaf diseases. On the

other hand, a moderate resistance cultivar reduced AUDPCs of leaf diseases, even in absence of fungicide application, but the fungicide improved yields as a result of the higher HAD. Also, moderate resistance cultivar and fungicide application increase TW and TKW due to lower disease damage. The economic analysis regarding the marginal net benefits showed that the TBIO Audaz with the incorporation of a recommended N (130 kg ha^{-1}) and the fungicide application (pre-mix) increased the economic benefits.

In this sense, higher N amount respect to the recommended N (130 kg ha^{-1}) increases the cost-efficiency index, which reduces economic benefits and produce losses considering that the utilization rate of the N by the plant does not exceed 40%. Therefore, the use of a moderately resistant cultivar with recommended N rate and properly fungicide application had an effect on disease control, and wheat yield respect to the NUE.

Acknowledgements

The authors are thankful to the Office to Coordinate Improvement of Higher Education Personnel (CAPES) for financial support and the student scholarship (Finance code 001) and a fellowship (grant number 308149/2018-1) from the Brazilian National Council for Scientific and Technological Development (CNPq). We are thankful to BIOTRIGO for providing wheat seeds for the experiments.

Declaration of competing interest

The authors declare that they have no conflicts of interest.

References

- AACC. 1999. Approved Methods of Analysis, 11th ed. Cereal and Grains Association, Saint Paul, MN, USA. Method 55-10.01. Test weight per bushel. Approved Nov 3, 1999. [2021-05-02]. <http://methods.aaccnet.org/toc.aspx>.
- AGROLINK, 2021a. Cotações de grãos. [2021-10-12]. <https://www.agrolink.com.br/cotacoes/graos/trigo/>. (in Portuguese)
- AGROLINK, 2021b. Trigo em grão nacional Sc 60 kg. [2021-10-12]. <https://www.agrolink.com.br/cotacoes/historico/rs/trigo-em-grao-nacional-sc-60kg>.
- Barro J, Santana F M, Machado F J, Duffeck M R, Lau D, Sbalcheiro C C, Schipanski C A, Chagas D F, Venancio W S, Dallagnol L J, Guterres C W, Kuhnem P, Feksa H R, Del Ponte E M. 2020. Are DMI+ QoI fungicide premixes during flowering

- worthwhile for fusarium head blight control in Wheat? A Meta-analysis. *Plant Disease*, **105**, 2680-2687.
- Bates D, Mächler M, Bolker B, Walker S. 2014. Fitting linear mixed-effects models using lme4. arXiv preprint arXiv:1406.5823.
- Barracough P B, Lopez-Bellido R, Hawkesford M J. 2014. Genotypic variation in the uptake, partitioning and remobilisation of nitrogen during grain-filling in wheat. *Field Crops Research*, **156**, 242-248.
- Bertagnolli V V, Ferreira J R, Liu Z, Rosa A C, Deuner C C. 2019. Phenotypical and genotypical characterization of *Pyrenophora tritici-repentis* races in Brazil. *European Journal of Plant Pathology*, **154**, 995-1007.
- Blandino M, Reyneri A. 2009. Effect of fungicide and foliar fertilizer application to winter wheat at anthesis on flag leaf senescence, grain yield, flour bread-making quality and DON contamination. *European Journal of Agronomy*, **30**, 275-282.
- Bockus W W, Davis M A. 1993. Effect of nitrogen fertilizers on severity of tan spot of winter wheat. *Plant Disease*, **77**, 508.
- Bremner J M, Mulvaney Y C. 1982. Nitrogen total. In *Methods of Soil Analysis. Part 2. Chemical and Microbiological Properties. Agronomy Monograph*. American Society of Agronomy and Soil Science Society of America, Madison, WI, USA. pp. 595-624.
- Castro A C, Fleitas, M C, Schierenbeck M, Gerard, G S, Simón M R. 2018. Evaluation of different fungicides and nitrogen rates on grain yield and bread-making quality in wheat affected by *Septoria tritici* blotch and yellow spot. *Journal of Cereal Science*, **83**, 49-57.
- CONAB, 2021a. Acompanhamento da safra brasileira de grãos, safra 2020/21, quinto levantamento, fev. 2021. [2021-01-25]. <https://www.conab.gov.br/info-agro/safras/graos/boletim-da-safra-de-graos>. (in Portuguese)
- CONAB. 2021b. Série histórica-custos-trigo-1998 a 2021.[2021-12-20]. <https://www.conab.gov.br/info-agro/custos-de-producao/planilhas-de-custo-de-producao/itemlist/category/828-trigo>. (in Portuguese)
- Cruz M F da Silva L A, Rios J A, Debona D, Rodrigues F Á. 2015. Microscopic aspects of the colonization of *Pyricularia oryzae* on the rachis of wheat plants supplied with silicon. *Bragantia*, **74**, 207-214.
- Debona D, Rodrigues F Á, Rios J A, Nascimento K J. 2012. Biochemical changes in the leaves of wheat plants infected by *Pyricularia oryzae*. *Phytopathology*, **102**, 1121-1129.

- Del Ponte E M, Fernandes J M, Bergstrom G C. 2007. Influence of growth stage on Fusarium head blight and deoxynivalenol production in wheat. *Journal of Phytopathology*, **155**, 577-581.
- Del Ponte E M, Fernandes J M, Pavan W, Baethgen W E. 2009. A model-based assessment of the impacts of climate variability on fusarium head blight seasonal risk in Southern Brazil. *Journal of Phytopathology*, **157**, 675-681.
- Dixon R A, Paiva N L. 1995. Stress-induced phenylpropanoid metabolism. *The plant cell*, **7**, 1085.
- Dorneles K R, Dallagnol L J, Pazdiora P C, Rodrigues F A, Deuner S. 2017. Silicon potentiates biochemical defense responses of wheat against tan spot. *Physiological and Molecular Plant Pathology*, **97**, 69-78.
- Dorneles K R, Pazdiora, P C, Hoffmann J F, Chaves F C, Monte L G, Rodrigues F A, Dallagnol L J. 2018. Wheat leaf resistance to *Pyrenophora tritici-repentis* induced by silicon activation of phenylpropanoid metabolism. *Plant Pathology*, **67**, 1713-1724.
- Faris J D, Abeyssekara N S, McClean P E, Xu S S, Friesen T L. 2012. Tan spot susceptibility governed by the Tsn1 locus and race-nonspecific resistance quantitative trait loci in a population derived from the wheat lines Salamouni and Katepwa. *Molecular Breeding*, **30**, 1669-1678.
- Fernandez M R, Stevenson C F, Hodge K, Dokken-Bouchard F, Pearse P G, Waelchli F, Brown A, Peluola C. 2016. Assessing effects of climatic change, region and agronomic practices on leaf spotting of bread and durum wheat in the western Canadian Prairies, from 2001 to 2012. *Agronomy Journal*, **108**, 1180-1195.
- Fernandez M R, Zentner R P, McConkey B G, Campbell C A. 1998. Effects of crop rotations and fertilizer management on leaf spotting diseases of spring wheat in southwestern Saskatchewan. *Canadian Journal of Plant Science*, **78**, 489-496.
- Fleitas M C, Schierenbeck M, Gerard G S, Dietz J I, Golik S I, Simón M R. 2018. Breadmaking quality and yield response to the green leaf area duration caused by fluxapyroxad under three nitrogen rates in wheat affected with tan spot. *Crop Protection*, **106**, 201-209.
- Gaju O, Allard V, Martre P, Le Gouis J, Moreau D, Bogard M, Hubbart M, Foulkes M J. 2014. Nitrogen partitioning and remobilization in relation to leaf senescence, grain yield and grain nitrogen concentration in wheat cultivars. *Field Crops Research*, **155**, 213-223.
- Gilbert J, Haber S. 2013. Overview of some recent research developments in Fusarium

- head blight of wheat. *Canadian Journal of Plant Pathology*, **35**, 149-174.
- Hartig F. 2021. DHARMA: Residual diagnostics for hierarchical (Multi-Level/Mixed) regression models. R package version 0.4.1. [2021-08-25]. <https://cran.r-project.org/package=DHARMA>.
- Hawkesford M J. 2014. Reducing the reliance on nitrogen fertilizer for wheat production. *Journal of Cereal Science*, **59**, 276-283.
- Horsfall J G, Barratt R W. 1945. An improved grading system for measuring plant diseases. *Phytopathology*, **35**, 65.
- Hothorn T, Bretz F, Westfall P. 2008. Simultaneous inference in general parametric models. *Biometrical Journal*, **50**, 346-363.
- Huber D M, Lee T S, Ross M A, Abney T S. 1987. Amelioration of tan spot-infected wheat with nitrogen. *Plant Disease*, **71**, 49.
- Huber D, Thompson I. 2007. Nitrogen and plant disease. In *Mineral nutrition and plant disease*, eds. L E Datnoff, W H Elmer, and Huber D M. American Phytopathological Society Press, St Paul, Madison. pp. 31-44.
- Jones J, Monem M A, Ryan J. 1990. Nitrogen fertilization in relation to durum wheat and tan spot (*Pyrenophora tritici-repentis*)* development. *Arab Journal of Plant Protection*, **8**, 110-113.
- Jorgensen L N, Olsen L V. 2007. Control of tan spot (*Drechslera tritici-repentis*) using cultivar resistance, tillage methods and fungicides. *Crop Protection*, **26**, 1606-1616.
- Kong L, Xie Y, Hu L, Feng B, Li S. 2016. Remobilization of vegetative nitrogen to developing grain in wheat (*Triticum aestivum* L.). *Field Crops Research*, **196**, 134-144.
- Krupinsky M, Tanaka D L. 2001. Leaf spot diseases on winter wheat influenced by nitrogen, tillage, and haying after a grass-alfalfa mixture in the conservation reserve program. *Plant Disease*, **85**, 785-789.
- Kutcher H R, Turkington T K, McLaren D L, Irvine R B, Brar G S. 2018. Fungicide and cultivar management of leaf spot diseases of winter wheat in western Canada. *Plant Disease*, **102**, 1828-1833.
- Kuznetsova A, Brockhoff P B, Christensen R H B. 2017. lmerTest package: tests in linear mixed effects models. *Journal of Statistical Software*. **82**:1-26.
- Lenth R. 2021. emmeans: Estimated Marginal Means, aka Least-Squares Means. R package version 1.6.0. [2021-04-20]. <https://cran.r-project.org/package=emmeans>.
- Li H B, Yan W, Liu G R, Wen S M, Liu C J. 2011. Identification and validation of

- quantitative trait loci conferring tan spot resistance in the bread wheat variety Ernie. *Theoretical and Applied Genetics*, **122**, 395-403.
- Machado F J, Santana F M, Lau D, Del Ponte E M. 2017. Quantitative review of the effects of triazole and benzimidazole fungicides on Fusarium head blight and wheat yield in Brazil. *Plant Disease*, **101**, 1633-1641.
- MacLean D E, Lobo J M, Coles K, Harding M W, May W E, Peng G, Turkington T K, Kutcher H R. 2018. Fungicide application at anthesis of wheat provides effective control of leaf spotting diseases in western Canada. *Crop protection*, **112**, 343-349.
- Maillard A, Diquélou S, Billard V, Laine P, Garnica M, Prudent M, Garcia-Mina J M, Yvin J C, Ourry A. 2015. Leaf mineral nutrient remobilization during leaf senescence and modulation by nutrient deficiency. *Frontiers in Plant Science*, **6**, 317.
- Malhi S S, Grant C A, Johnston A M, Gill K S. 2001. Nitrogen fertilization management for no-till cereal production in the Canadian great plains: a review. *Soil and Tillage Research*, **60**, 101-122.
- Matsuyama N. 1973. Effect of nitrogenous fertilizer on biochemical processes that could affect lesion size of rice blast. *Phytopathology*, **63**, 1202-1203.
- Meena S K, Rakshit A, Meena V S. 2016. Effect of seed bio-priming and N doses under varied soil type on nitrogen use efficiency (NUE) of wheat (*Triticum aestivum* L.) under greenhouse conditions. *Biocatalysis and Agricultural Biotechnology*, **6**, 68-75.
- Miralles D J, Slafer G A. 1990. Estimación del área foliar en trigo: Generación y validación de un modelo. 11vo Congreso Nacional de Trigo. Pergamino. pp. 76-85. (in Spanish)
- Mur L A J, Simpson C, Kumari A, Gupta A K, Gupta K J. 2017. Moving nitrogen to the centre of plant defence against pathogens. *Annals of Botany*, **119**, 703-709.
- Patel A P, Monpara B A. 2007. Effects of maturity on variation and association for grain filling and yield related traits in durum wheat. *Agricultural Science Digest*, **27**, 178-181.
- Pazdiora P C, da Rosa Dorneles K, Forcelini C A, Del Ponte E M, Dallagnol L J. 2018. Silicon suppresses tan spot development on wheat infected by *Pyrenophora tritici-repentis*. *European Journal of Plant Pathology*, **150**, 49-56.
- Pazdiora P C, da Rosa Dorneles K, Morello T N, Nicholson P, Dallagnol L. J. 2021. Silicon soil amendment as a complement to manage tan spot and fusarium head

- blight in wheat. *Agronomy for Sustainable Development*, **41**, 1-13.
- Perrin R K, Winkelman D L, Moseardi E R, Anderson J R. 1979. Farm agronomic data to farmer's recommendations. *CIMMYT Mexico Project Information Bulletin*, **27**: 63.
- Peterson R F, Campbell A B, Hannah A E. 1948. A diagrammatic scale for estimating rust intensity on leaves and stems of cereals. *Canadian Journal of Research*, **26**, 496-500.
- Reis E M, Blum M M C, Casa R T. 1996. Chemical control of *Gibberella zeae* in wheat, a problem of deposition of fungicides on anthers. *Summa Phytopathol*, **22**, 39-42.
- Reunião da Comissão Brasileira de Pesquisa de Trigo e Triticale. 2018. Informações técnicas para trigo e triticale - safra 2019. In *XII Reunião da Comissão Brasileira de Pesquisa de Trigo e Triticale*, Brasília, DF: Embrapa. p. 240. [2020-01-05]. <https://www.embrapa.br/busca-de-publicacoes/-/publicacao/1108443/informacoes-tecnicas-para-trigo-e-triticale---safra-2019>.(in Portuguese)
- RStudio. 2021. RStudio: Integrated development environment for R. RStudio, PBC, Boston, MA. [2021-08-20]. <http://www.rstudio.com/>.
- Ruske R E, Gooding M J, Jones S A. 2003. The effects of adding picoxystrobin, azoxystrobin and nitrogen to a triazole programme on disease control, flag leaf senescence, yield and grain quality of winter wheat. *Crop Protection*, **22**, 975-987.
- Santana F M, Clebsch C C, Friesen T L. 2008. Caracterização de raças de *Pyrenophora tritici-repentis*, agente etiológico da mancha amarela do trigo, no sul do Brasil. Passo Fundo: Embrapa Trigo. [2021-10-02]. http://www.cnpt.embrapa.br/biblio/bp/p_bp60.htm. (in Portuguese)
- Savary S, Willocquet L, Pethybridge S J, Esker P, McRobert N, Nelson A. 2019. The global burden of pathogens and pests on major food crops. *Nature ecology & evolution*, **3**, 430-439.
- Schierenbeck M, Fleitas M C, Miralles D J, Simón M R. 2016. Does radiation interception or radiation use efficiency limit the growth of wheat inoculated with tan spot or leaf rust?. *Field Crops Research*, **199**, 65-76.
- Schierenbeck M, Fleitas M C, Simón M R. 2019. Nitrogen fertilization and fungicide mixtures in wheat: how do they affect the severity, yield and dynamics of nitrogen under leaf rust infections?. *European Journal of Plant Pathology*, **155**, 1061-1075.
- Sermeno J, Rivas A, Menjivar R. 2001. Manual tecnico manejo integrado de plagas. OIRSA, 632.6 Se675m. [2021-10-02]. <http://usi.earth.ac.cr/glas/sp/Oirsa/50000083.pdf>. (in Spanish)

- Serrago R A, Carretero R, Bancal M O, Miralles D J. 2009. Foliar diseases affect the eco-physiological attributes linked with yield and biomass in wheat (*Triticum aestivum* L.). *European Journal of Agronomy*, **31**,195-203.
- Shaner G, Finney R E. 1977. The effect of nitrogen fertilization on the expression of slow-mildewing resistance in Knox wheat. *Phytopathology*. **67**:1051-1056.
- Silva S R, Bassoi M C, Foloni J S. 2017. *Informações técnicas para trigo e triticale - safra 2017*. Eds. Silva S, Bassoi M, Foloni J S. Brasilia: Embrapa. p. 240.(in Portuguese)
- Stack R W, McMullen M P. 2011. A visual scale to estimate severity of Fusarium head blight in wheat. [2019-01-25]. <https://www.ag.ndsu.edu/ndipm/publications/wheat/documents/pp1095.pdf>.
- Thomas H, Howarth C J. 2000. Five ways to stay green. *Journal of Experimental Botany*, **51**, 329-337.
- Waggoner P E, Berger R D. 1987. Defoliation, disease, and growth. *Phytopathology*,**77**, 393-398.
- Wu Y X, von Tiedemann A. 2001. Physiological effects of azoxystrobin and epoxiconazole on senescence and the oxidative status of wheat. *Pesticide Biochemistry and Physiology*, **71**, 1-10.
- Zadoks J C, Chang T T, Konzak C. F. 1974. A decimal code for the growth stages of cereals. *Weed Research*,**14**, 415-421.

Table 1 Summary statistics from linear mixed model analyses of the effects of fungicide (FU), cultivar (C), nitrogen rate (NR), and their interactions on area under disease progress curve (AUDPC) of tan spot, powdery mildew, leaf rust, and Fusarium head blight (FHB) during 2019 and 2020.

Treatments	df	Tan spot		Powdery mildew		Leaf rust		FHB	
		<i>F-value</i>		<i>F-value</i>		<i>F-value</i>		<i>F-value</i>	
		2019	2020	2019	2020	2019	2020	2019	2020
Cultivar (C)	1	126.80**	203.39**	20.39*	57.63*	20.14*	302.89***	16.02*	55.67**
Fungicide (FU)	1	34.83**	143.69**	2.79ns	41.27**	8.21ns	323.56***	6.20ns	38.29**
Nitrogen rate (NR)	2	25.09***	53.45***	20.60***	4.15*	0.29ns	0.35ns	0.51ns	1.70ns
C × FU	1	8.13*	17.89*	0.067ns	2.11ns	7.91ns	169.22***	1.81ns	2.07ns
C × NR	2	7.28**	5.732***	0.43ns	0.43ns	0.28ns	1.41ns	1.25ns	2.44ns
FU × NR	2	0.08ns	6.21**	0.65ns	0.44ns	0.42ns	0.23ns	2.06ns	1.80ns
C × FU × NR	2	0.15ns	2.18ns	2.75ns	1.73ns	0.68ns	0.81ns	0.261ns	1.02ns

*** $p = 0.001$ highly significant; ** $p = 0.01$ moderately significant; ns $p > 0.05$ not significant

Table 2 Mean squares and standard errors of fungicide (FU), cultivar (C), nitrogen rate (NR)effect on area under disease progress curve (AUDPC) of tan spot, powdery mildew, leaf rust, and Fusarium head blight (FHB)during 2019 and 2020.

Effect/Contrast	Tan spot		Powdery mildew		Leaf rust		FHB	
	2019	2020	2019	2020	2019	2020	2019	2020
Cultivar (C)								
TBIO Audaz	187 ± 39.3 b	131 ± 3.52 b	305 ± 157 b	128 ± 7.58 b	65.8 ± 12.5 b	81.6 ± 8.18 b	134 ± 41.3 b	173 ± 15.5 b
TBIO Tibagi	420 ± 39.3 a	195 ± 3.52 a	633 ± 157 a	205 ± 7.58 a	394.4 ± 12.5 a	301.9 ± 8.18 a	253 ± 41.3 a	322 ± 15.5 a
Fungicide (FU)								
Fungicide (FU)	245 ± 39.3 b	136 ± 3.52 b	424 ± 157	199 ± 7.58 a	90.3 ± 32.6 b	80.2 ± 8.18 b	157 ± 41.3 b	195 ± 15.5 b
Unsprayed (US)	362 ± 39.3 a	190 ± 3.52 a	524 ± 157	134 ± 7.58 b	369.9 ± 12.5 a	303.3 ± 8.18 a	231 ± 41.3 a	300 ± 15.5 a
Nitrogen rate (NR)								
Low N	351 ± 38.6 a	192 ± 3.9 b	425 ± 149 b	150 ± 8.16 b	233 ± 13.8	187 ± 9.38	204 ± 31.5	242 ± 14.6
Recommended N	281 ± 38.6 b	154 ± 3.9 a	490 ± 149 a	180 ± 8.16 a	243 ± 13.8	202 ± 9.38	203 ± 31.5	240 ± 14.6
High N	277 ± 38.6 b	144 ± 3.9 a	490 ± 149 a	170 ± 8.16 ab	215 ± 13.8	186 ± 9.38	196 ± 31.5	261 ± 14.6
	p value	p value	p value	p value	p value	p value	p value	p value
TBIO Audaz × TBIO Tibagi	0.0013	0.0007	0.0501	0.0019	0.0001	0.0003	0.0081	0.0029
FU × US	0.0098	0.0012	0.4473	0.0036	0.0002	0.0003	0.0308	0.0077
Low N × High N	<0.0001	<0.0001	0.0193	0.1307	0.7761	0.4869	0.9907	0.9907
Low N × Recommended N	<0.0001	<0.0001	0.0188	0.0169	0.4453	0.996	0.7170	0.2089
Recommended N × High N	0.9163	0.0799	0.9999	0.6683	0.1456	0.4365	0.7936	0.1642

Means followed by the same letter within the same source of variation are not statistically different (Tukey test $p < 0.05$)

Table 3 Summary statistics from linear mixed model analyses of the effects of fungicide (FU), cultivar (C), nitrogen rate (NR), and their interactions on thousand kernel weight (TKW), test weight (TW), and yield during 2019 and 2020.

Treatments	df	TKW (grams)		TW (kg hL ⁻¹)		Yield (kg ha ⁻¹)	
		<i>F-value</i>		<i>F-value</i>		<i>F-value</i>	
		2019	2020	2019	2020	2019	2020
Cultivar (C)	1	12.92*	102.03***	21.35*	293.40***	29.53*	22.73*
Fungicide (FU)	1	34.86**	157.11***	70.11**	233.19***	14.74*	10.96*
Nitrogen rate (NR)	2	0.40ns	2.01ns	2.48ns	2.36ns	18.67***	14.89**
C × FU	1	10.89*	69.05**	17.17*	330.48***	2.31ns	1.05ns
C × NR	2	3.60*	9.09***	1.73ns	4.29*	4.40*	4.129*
FU × NR	2	0.13ns	3.02ns	1.03ns	0.78ns	0.91ns	1.11ns
C × F × NR	2	0.90ns	1.57ns	0.35ns	0.05ns	1.02ns	0.05ns

*** $p = 0.001$ highly significant; ** $p = 0.01$ moderately significant; ns $p > 0.05$ not significant

Table 4 Mean squares and standard errors of fungicide (F), cultivar (C), and nitrogen rate (NR) on yield, test weight (TW), thousand kernel weight (TKW), and yield during 2019 and 2020.

Effect/Contrast	TKW (grams)		TW (kg hL ⁻¹)		Yield (kg ha ⁻¹)	
	2019	2020	2019	2020	2019	2020
Cultivar (C)						
TBIO Audaz	28.4 ± 0.69 a	31.8 ± 0.501 a	76.2 ± 0.53 a	76.6 ± 0.201 a	2350 ± 107 a	3445 ± 233 a
TBIO Tibagi	24.9 ± 0.69 b	24.6 ± 0.501 b	73.1 ± 0.53 b	71.7 ± 0.201 b	1674 ± 107 b	2090 ± 233 b
Fungicide (FU)						
Fungicide (FU)	29.6 ± 0.69 a	32.6 ± 0.501 a	77.5 ± 0.53 a	76.3 ± 0.201 a	2251 ± 107 a	3231 ± 233 a
Unsprayed (US)	23.8 ± 0.69 b	23.8 ± 0.501 b	71.9 ± 0.53 b	72.0 ± 0.201 b	1774 ± 107 b	2304 ± 233 b
Nitrogen rate (NR)						
Low N	26.5 ± 0.53	28.4 ± 0.379	75.1 ± 0.45	74.6 ± 0.246	1704 ± 101 b	2264 ± 202 b
Recommended N	26.8 ± 0.53	28.2 ± 0.379	74.5 ± 0.45	73.9 ± 0.246	2190 ± 101 a	3090 ± 202 a
High N	26.6 ± 0.53	27.9 ± 0.379	74.4 ± 0.45	74.0 ± 0.246	2143 ± 101 a	2849 ± 202 a
	<i>p</i> value	<i>p</i> value	<i>p</i> value	<i>p</i> value	<i>p</i> value	<i>p</i> value
TBIO Audaz × TBIO Tibagi	0.0369	0.0021	0.0191	0.0004	0.0122	0.0235
FU × US	0.0097	0.0011	0.0036	0.0006	0.0312	0.0657
Low N × High N	0.9140	0.1237	0.0918	0.1908	<0.0001	0.0502
Low N × Recommended N	0.6448	0.7454	0.2315	0.1228	<0.0001	0.0008
Recommended N × High N	0.8757	0.4285	0.8841	0.972	0.8532	0.3304

Means followed by the same letter within the same source of variation are not statistically different (Tukey test $p < 0.05$)

Table 5 Summary statistics from linear mixed model analyses of the effects of fungicide (FU), cultivar (C), nitrogen rate (NR), and their interactions on plant nitrogen level (PNL), and healthy area duration (HAD) during 2019 and 2020.

Treatments	df	HAD (days)		PNL (g kg ⁻¹)		TNG (g kg ⁻¹)	
		<i>F-value</i>		<i>F-value</i>		<i>F-value</i>	
		2019	2020	2019	2020	2019	2020
Cultivar (C)	1	765.71***	58.15**	0.78ns	26.55*	8.40*	14.07*
Fungicide (FU)	1	0.66ns	2.29ns	2.94ns	1.41ns	1.66ns	5.18ns
Nitrogen rate (NR)	2	7.13**	0.24ns	30.01***	17.01***	55.18***	52.06***
C × FU	1	12.29*	0.34ns	1.68ns	0.07ns	0.001ns	0.03ns
C × NR	2	1.56ns	2.16ns	1.66ns	12.17***	6.04**	4.07*
FU × NR	2	0.42ns	2.15ns	0.81ns	1.18ns	2.61ns	2.75ns
C × F × NR	2	0.75ns	2.16ns	1.09ns	0.41ns	0.63ns	1.31ns

*** $p = 0.001$ highly significant; ** $p = 0.01$ moderately significant; ns $p > 0.05$ not significant

Table 6 Mean squares and standard errors of fungicide (FU), cultivar (C), and nitrogen rate (NR) effect on plant nitrogen level (PNL), total nitrogen in grain (TNG), and healthy area duration (HAD) during 2019 and 2020.

Effect/Contrast	HAD (days)		PNL (g kg ⁻¹)		TNG (g kg ⁻¹)	
	2019	2020	2019	2020	2019	2020
Cultivar (C)						
TBIO Audaz	32.2 ± 0.38 a	42.9 ± 0.741 a	32.8 ± 2.09	33.0 ± 0.652 a	22.2 ± 0.52	23 ± 0.391 b
TBIO Tibagi	17.2 ± 0.38 b	34.9 ± 0.741 b	30.4 ± 2.09	28.7 ± 0.652 b	24.3 ± 0.52	25 ± 0.391 a
Fungicide (FU)						
Fungicide (FU)	24.9 ± 0.38	38.1 ± 0.741	29.2 ± 2.09	30.3 ± 0.652	22.8 ± 0.52	23.4 ± 0.391
Unsprayed (US)	24.5 ± 0.38	39.7 ± 0.741	33.9 ± 2.09	31.3 ± 0.652	23.7 ± 0.52	24.6 ± 0.391
Nitrogen rate (NR)						
Low N	23.4 ± 0.64 b	39.2 ± 0.762	28.0 ± 0.81 b	30.1 ± 0.575 b	21.6 ± 0.41 c	22.6 ± 0.313 c
Recommended N	25.8 ± 0.64 a	39.1 ± 0.762	33.1 ± 0.81 a	29.9 ± 0.575 ab	23.5 ± 0.41 b	24.2 ± 0.313 b
High N	25.0 ± 0.64 a	38.6 ± 0.762	33.7 ± 0.81 a	32.5 ± 0.575 a	24.7 ± 0.41 a	25.2 ± 0.313 a
	<i>p</i> value	<i>p</i> value	<i>p</i> value	<i>p</i> value	<i>p</i> value	<i>p</i> value
TBIO Audaz × TBIO Tibagi	0.0001	0.0047	0.4431	0.0142	0.0626	0.0331
FU × US	0.4769	0.2271	0.1848	0.3211	0.2875	0.1073
Low N × High N	0.0436	0.798	<0.0001	<0.0001	<0.0001	<0.0001
Low N × Recommended N	0.0011	0.9951	<0.0001	0.9691	<0.0001	<0.0001
Recommended N × High N	0.4159	0.8484	0.7175	<0.0001	0.0004	0.0009

Means followed by the same letter within the same source of variation are not statistically different (Tukey test $p < 0.05$)

Table 7 Estimation of marginal return of treatments

Treatment	Variable total costs (USD)	Marginal variable cost (USD)	Net profit (USD)	Marginal net benefits (USD)	Marginal return (%)	Income/cost^a
TBIO Audaz + US + Recommended N	662.53		1.31			1.00
TBIO Audaz + FU + Low N	665.34	2.81	77.30	75.99	2701%	1.12
TBIO Audaz + FU + Recommended N	693.48	28.13	271.04	193.74	689%	1.39

^a See Table of Appendice A for complete information of gross income by variable total cost.

FU: Fungicide; US: unsprayed

Low N (70 kg ha⁻¹); recommended N (130 kg ha⁻¹); high N (200 kg ha⁻¹)

Table 8 Nitrogen use efficiency (NUE) and cost-efficiency index for treatment not dominated

Treatment	Nitrogen use efficiency (NUE)	Variable total cost (USD)	Cost- efficient index
TBIO Audaz + US + Low N	31.8	634.4	0.20
TBIO Audaz + FU + Low N	20.6	665.3	0.32
TBIO Audaz + US + Recommended N	15.5	662.5	0.43

FU: Fungicide; US: unsprayed

Low N (70 kg ha⁻¹); recommended N (130 kg ha⁻¹); high N (200 kg ha⁻¹)

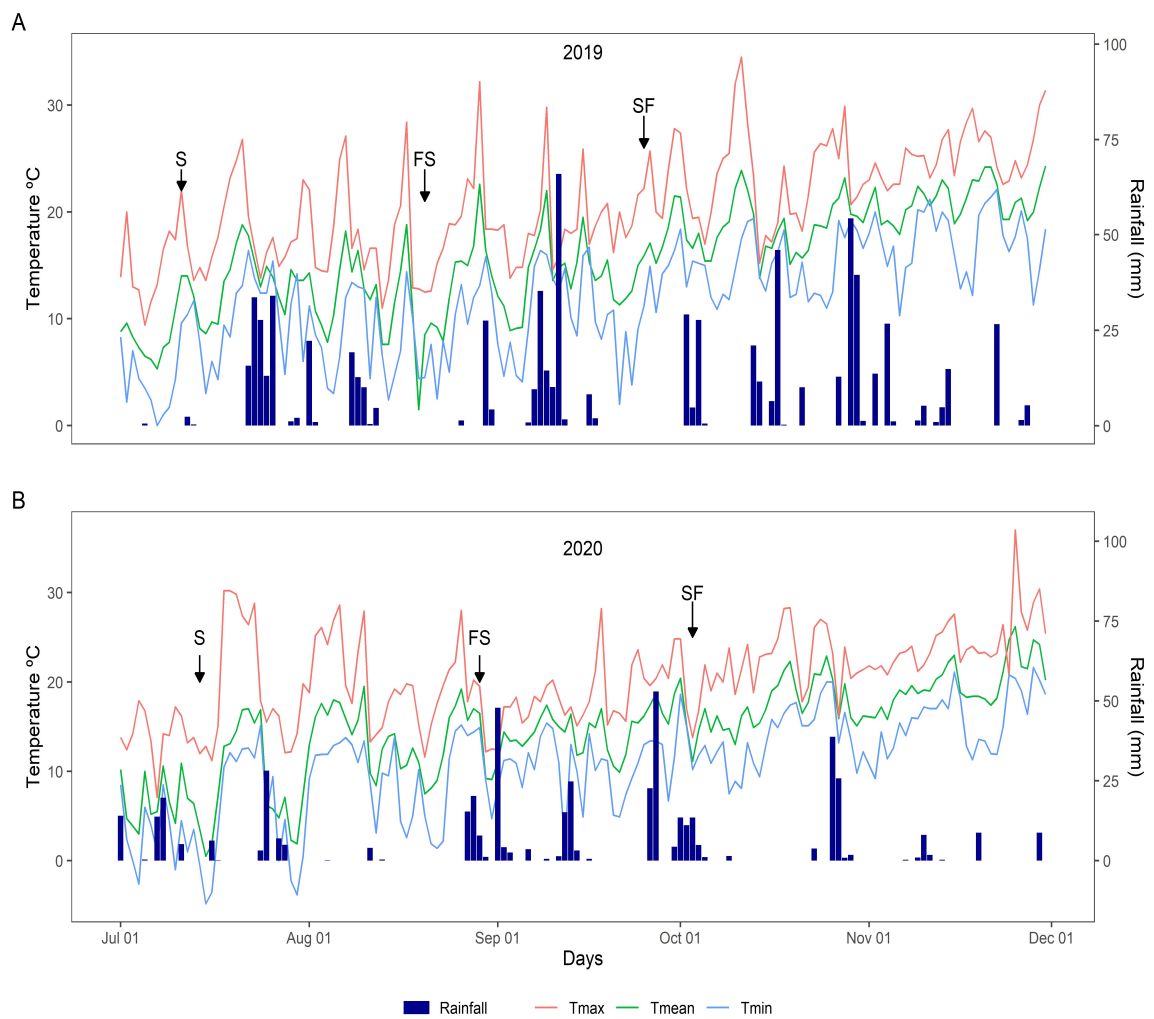


Fig. 1 Climatic conditions of Capão de Leão, RS, Brazil. Rainfall (mm), mean (Tmean), maximum (Tmax), and minimum (Tmin) temperature during the growing cycle of wheat in the two seasons (2019, and 2020). S = date of sowing; FF = date of the first fungicide spraying on flag leaf (ZGS 39); SF = date of the second fungicide spraying, at flowering (ZGS 65).

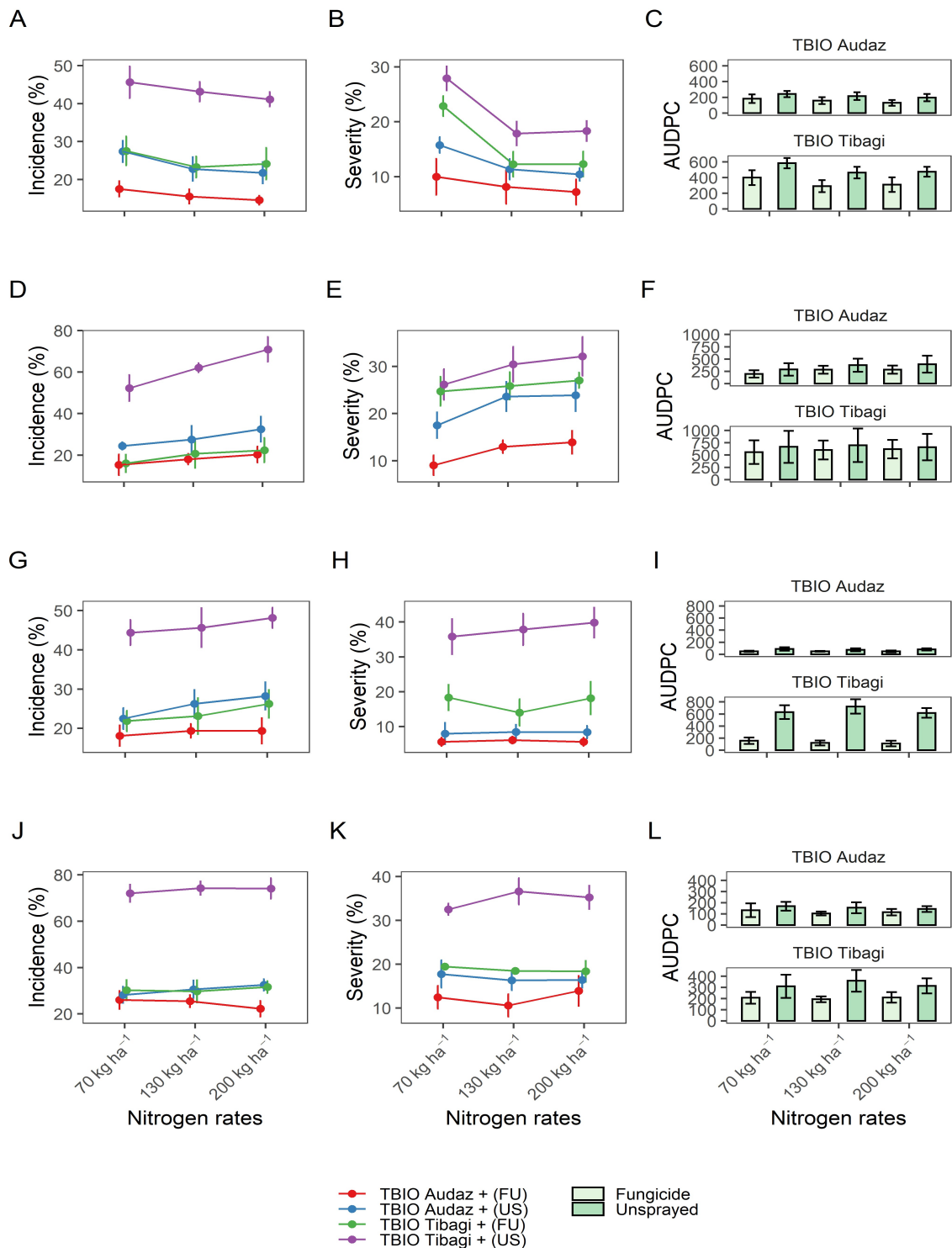


Fig. 2 Final incidence (%), final severity (%), and AUDPC of tan spot (A,B,C), powdery mildew (D,E,F), leaf rust (G,H,I), and FHB (J,K,L) of TBIO Audaz and TBIO Tibagi (fungicide, and unsprayed) in three rates of N during 2019. Data points are the mean and error bars represent standard deviation of means.

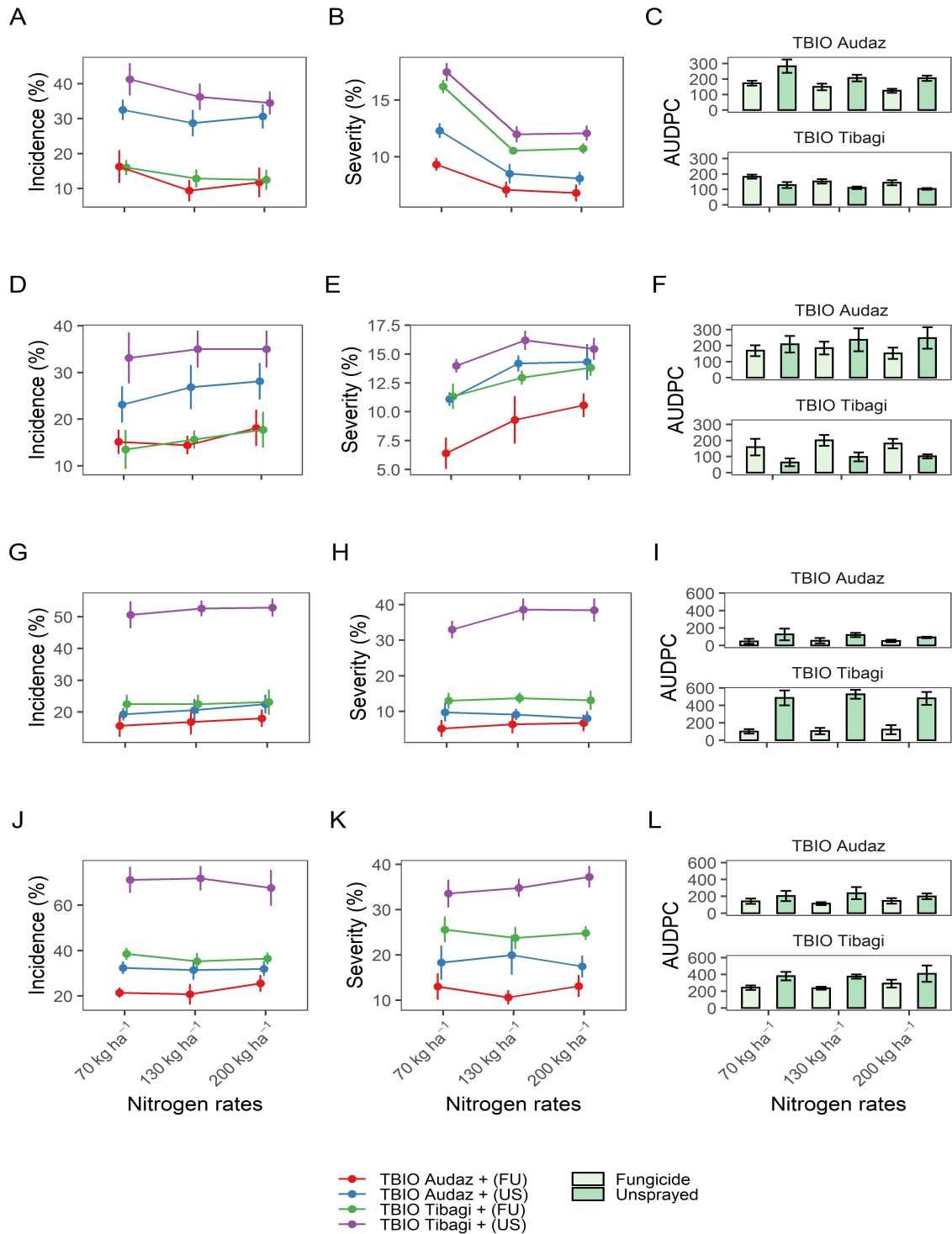


Fig.3 Final incidence (%), final severity (%), and AUDPC of tan spot (A,B,C), powdery mildew (D,E,F), leaf rust (G,H,I), and FHB (J,K,L) of TBIO Audaz and TBIO Tibagi (fungicide, and unsprayed) in three rates of N during 2020. Data points are the mean and error bars represent standard deviation of means.

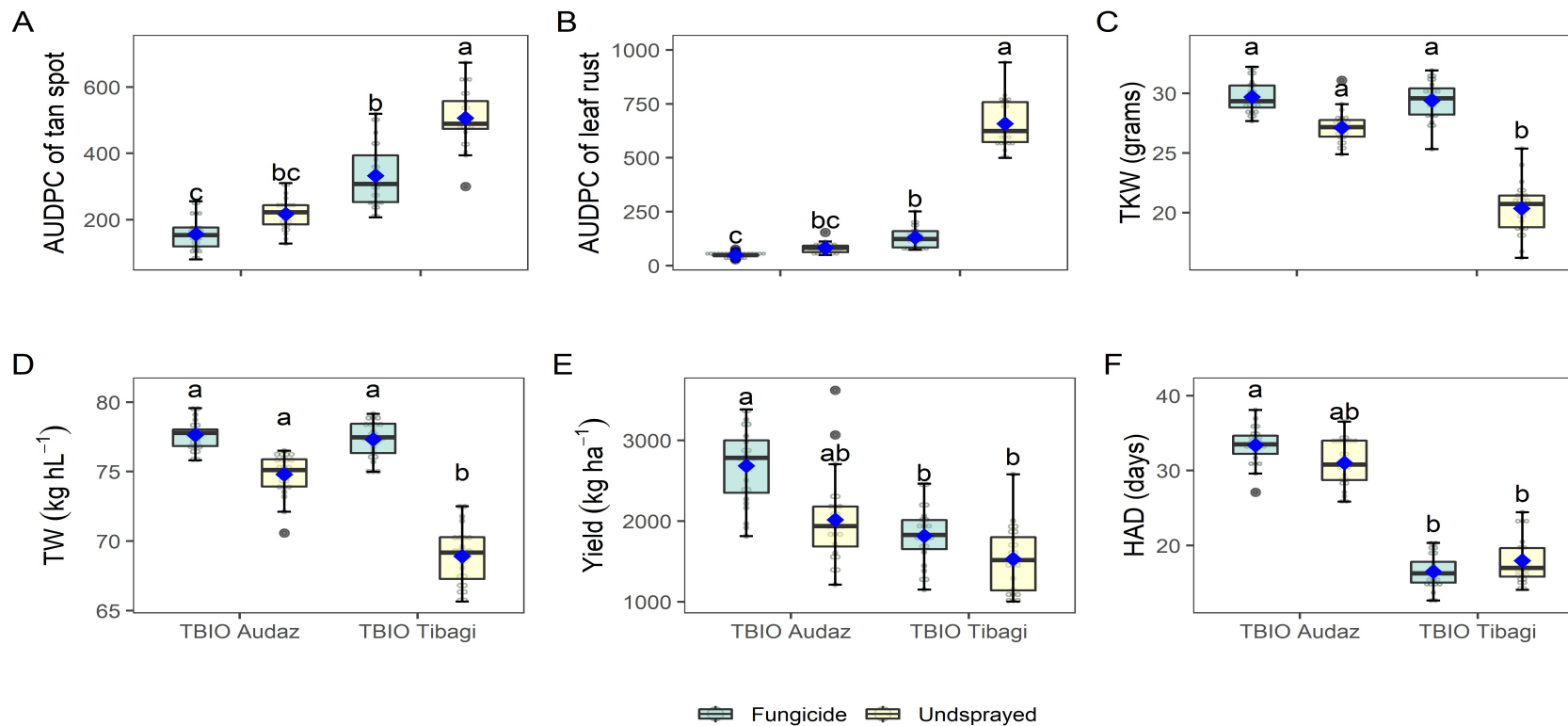


Fig. 4 Effect of the cultivar × fungicide interaction of AUDPC of tan spot (A), AUDPC of rust (B), thousand kernel weight TKW (C), test weight TW (D), Yield (E), and healthy area duration HAD (F). The horizontal line inside the box represents the median, the limits of the box represent the lower and upper quartiles, and the circles represent the observation of each treatment. Data points (♦) are the mean and error bars represent standard deviation of means. Points (*) correspond to outliers. Different lowercase letters indicate statistical differences according to the Tukey test at $p < 0.05$.

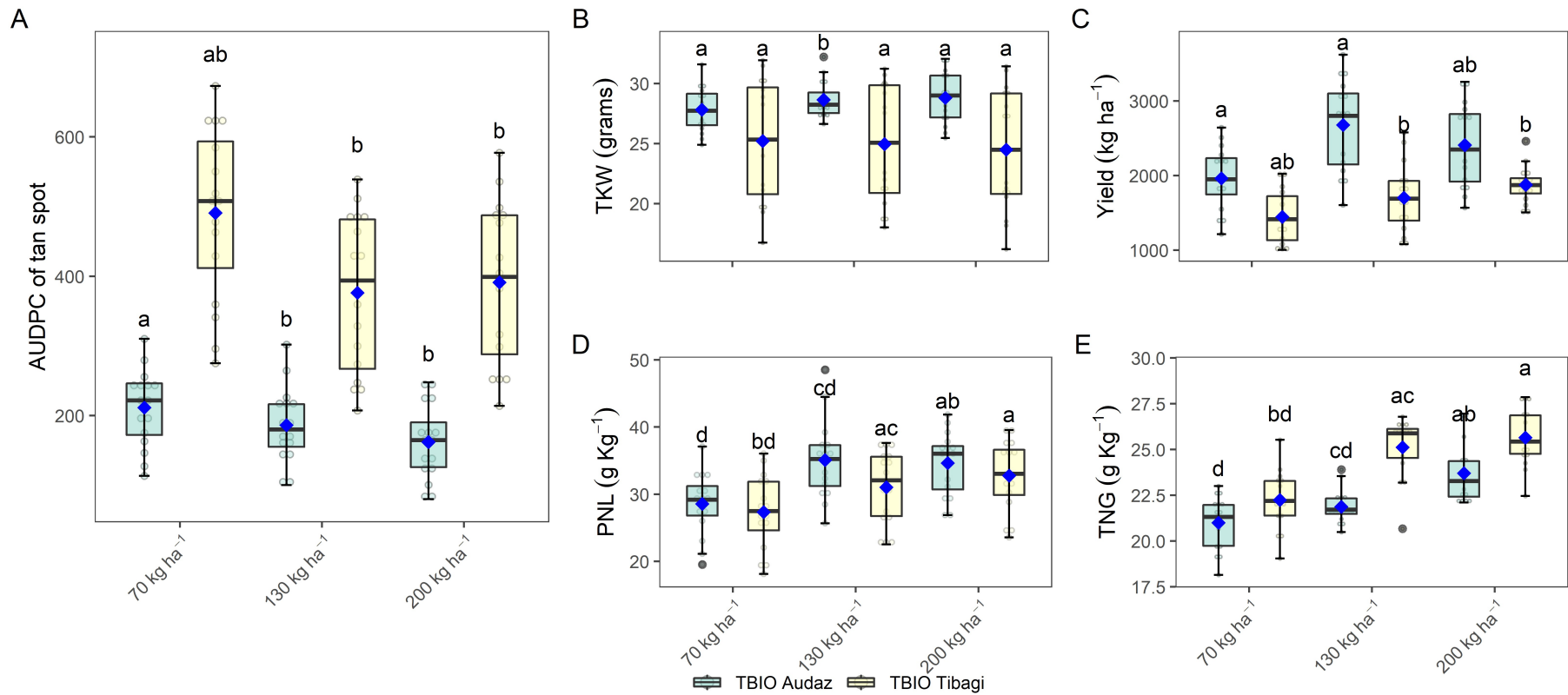


Fig. 5 Effect of the cultivar × nitrogen interaction of AUDPC of tan spot (A), thousand kernel weight TKW (B), Yield (C), plant nitrogen content PNL (D), and total nitrogen in grain TNG (E). The horizontal line inside the box represents the median, the limits of the box represent the lower and upper quartiles, and the circles represent the observation of each treatment. Data points (♦) are the mean and error bars represent standard deviation of means. Points (•) correspond outliers. Different lowercase letters indicate statistical differences according to the Tukey test at $p < 0.05$.

Appendices

Appendix A Summary of partial budget of treatments

Treatment	Yield (kg ha ⁻¹)	Adjusted Yield ^a (kg ha ⁻¹)	Variable total costs (USD)	Gross income ^b (USD)	Net profit (USD)	Inco me/c ost
TBIO Audaz + FU + Low N	3422.73	3080.45	665.34	742.65	77.30	1.12
TBIO Audaz + FU + Recommended N	4445.29	4000.76	693.48	964.52	271.04	1.39
TBIO Audaz + FU + High N	4379.75	3941.77	726.30	950.30	224.00	1.31
TBIO Audaz + US + Low N	1987.21	1788.49	634.40	431.17	-203.22	0.68
TBIO Audaz + US + Recommended N	3059.52	2753.57	662.53	663.84	1.31	1.00
TBIO Audaz + US + High N	3375.27	3037.74	695.35	732.35	37.00	1.05
TBIO Tibagi + FU + Low N	2283.47	2055.12	664.35	495.46	-168.90	0.75
TBIO Tibagi+ FU + Recommended N	2452.28	2207.05	692.49	532.08	-160.40	0.77
TBIO Tibagi + FU + High N	2401.05	2160.95	725.31	520.97	-204.34	0.72
TBIO Tibagi + US + Low N	1362.55	1226.30	633.41	295.64	-337.77	0.47
TBIO Tibagi + US + Recommended N	2085.95	1877.36	661.54	452.60	-208.94	0.68
TBIO Tibagi + US + High N	2005.75	1805.18	694.36	435.20	-259.16	0.63

^a Adjusted grain yield to 10% (possible unforeseen)

^c Estimated according the yield obtained based on the Brazilian grain wheat commercialization (60Kg) at final sale price of grain wheat (USD 14,47)

FU: Fungicide; US: unsprayed

Low N (70 kg ha⁻¹); recommended N (130 kg ha⁻¹); high N (200 kg ha⁻¹)

Appendix B Dominance analysis of treatments for economic analysis

Treatment	Variable total costs (USD)	Net profit (USD)	Dominance analysis
TBIO Audaz + US + Recommended N	\$662.53	\$1.31	ND
TBIO Audaz + FU + Low N	\$665.34	\$77.30	ND
TBIO Audaz + FU + Recommended N	\$693.48	\$271.04	ND
TBIO Audaz + US + High N	\$695.35	\$37.00	D
TBIO Audaz + FU + High N	\$726.30	\$224.00	D

ND: not dominated; D: dominated

FU: Fungicide; US: unsprayed

Low N (70 kg ha⁻¹); recommended N (130 kg ha⁻¹); high N (200 kg ha⁻¹)

Appendix C Dominance analysis of treatments for cost-efficiency

Treatment	Nitrogen use efficiency (NUE)	Variable total cost (USD)	Dominance analysis
TBIO Audaz + US + Low N	31.77	\$634.40	ND
TBIO Audaz + FU + Low N	20.62	\$665.34	ND
TBIO Audaz + US + Recommended N	15.50	\$662.53	ND
TBIO Audaz + US + High N	12.86	\$695.35	D
TBIO Audaz + FU + Recommended N	11.63	\$693.48	D
TBIO Tibagi + FU + Low N	10.45	\$664.35	D
TBIO Audaz + FU + High N	9.99	\$726.30	D
TBIO Tibagi + FU + Recommended N	8.32	\$692.49	D
TBIO Tibagi + FU + High N	5.66	\$725.31	D
TBIO Tibagi + US + Low N	3.92	\$633.41	D
TBIO Tibagi + US + High N	3.70	\$694.36	D
TBIO Tibagi + US + Recommended N	2.38	\$661.54	D

ND: not dominated; D: dominated

FU: Fungicide; US: unsprayed

Low N (70 kg ha⁻¹); recommended N (130 kg ha⁻¹); high N (200 kg ha⁻¹)

The chapter 3 was formatted under the guidelines of the **Journal of Integrative
Agriculture**

Disease management maintains adequate chlorophyll *a* fluorescence and enhances wheat grain technological quality

Andrea ROMÁN^{1,3}, Martha De MIRANDA², Pietra TATSCH², Daniel DEBONA³, Eduardo RODRIGUEZ⁴ and Leandro José DALLAGNOL^{1*}

¹ *Federal University of Pelotas, Eliseu Maciel Faculty of Agronomy, Crop Protection Department, Laboratory of Plant Pathogen Interaction, 96010-900, Pelotas, Rio Grande do Sul, Brazil.*

² *Brazilian Agricultural Research Corporation, Embrapa Trigo, 99050-970 – P.O.Box 3081, Passo Fundo, Rio Grande do Sul, Brazil.*

³ *Universidade Tecnológica Federal do Paraná - Campus Santa Helena, Agronomy Department, 85892-000, Santa Helena, Paraná, Brazil.*

⁴ *Bolivar State University, Agricultural Sciences Natural Resources and the Environment Faculty, Laboratory of Phytopathology, EC020150, Guaranda, Ecuador.*

⁵ *Grow green Agricultural Technologies, EC060103, Riobamba, Ecuador.*

***Corresponding author:** leandro.dallagnol@ufpel.edu.br

Abstract

Leaf and spike diseases are responsible for damage to yield and technological wheat grain quality. To counteract this damage, integrated disease management is employed, involving the use of resistant cultivars along with fungicide and nitrogen application. Therefore, the objective of this study was to determine the effect of these disease management measures on changes in the chlorophyll *a* fluorescence, yield components, and wheat technological quality. The maximum efficiency of PSII photochemistry (F_v/F_m), measured at dough development (ZGS80) under field conditions was correlated with diseases and technological quality parameters. Area under disease progress curve (AUDPC) values of tan spot and powdery mildew were negatively related with thousand kernel weight (TKW) and test weight (TW). High N rate (200 kg ha⁻¹) and recommended N rate (130 kg ha⁻¹) increased the protein content (PC), as well as dry gluten (DG) and wet gluten (WG), maintaining adequate stability time and water absorption, demonstrating the resistance of dough to mixing and improving the wheat grain technological quality. AUDPC values of tan spot, powdery mildew and leaf rust were positively associated with ash content (AC), and higher PC, DG, WG, AC, and falling number, resulting in changes in whole flour color. However, fungicide

application increased the lightness and the yellow tendency of color parameters of the flour. The integrated disease management involving use of a moderately resistant cultivar associated with fungicide and nitrogen application reduced the AUDPCs, reflecting higher Fv/Fm , an indicative of adequate physiological process, while guaranteeing suitable yield components and grain quality.

Keywords: protein,gluten, ash,nitrogen,leaf diseases, Fv/Fm .

1. Introduction

Wheat (*Triticum aestivum* L.) is the most consumed cereal worldwide, with estimated demand of 787.3 million tons in 2021 (USDA 2021b). In Brazil, estimates are that production will be 6.8 million tons in 2021, whereas the national demand will be 12.5 million tons, a deficit of 54.4% in production (USDA 2021a, 2021c). In light of this, the increase in wheat production through more efficient and sustainable disease management tools is needed (Savary *et al.*, 2019), to guarantee wheat quantity and quality.

Several biotic factors caused by pathogens during plant development threaten the grain yield and technological quality of wheat, such as leaf diseases caused by *Pyrenophora tritici-repentis* (Died.) Drechs (tan spot), *Puccinia striiformis* (stripe rust), *Puccinia triticina* (leaf rust), and *Blumeria graminis* (DC.) f. sp. *tritici* (powdery mildew), as well as spike diseases caused by *Fusarium graminearum* complex (fusarium head blight – FHB), and *Magnaporthe oryzae* pathotype *Triticum* (blast). Leaf spot, powdery mildew and rust reduce the leaf photosynthetic area, accelerating leaf senescence and leading to lower grain yield (Serrago *et al.* 2019). Yield losses of up to 75% due to tan spot (Reis and Casa 2007), from 3 to 25% caused by FHB (Reis and Casa, 2007; Duffeck *et al.*, 2020), 40% for powdery mildew (Alam *et al.* 2013), and up to 90% for rusts (Chen 2020) have been recorded.

Likewise, powdery mildew decreases the leaf assimilation index, and negatively affects grain yield by hampering photosynthesis of leaves (Samobor *et al.* 2005). Leaf and spike infection by pathogens can cause grain shriveling, associated with low flour extraction rates from milling (Rose *et al.* 2001; Gooding and Davies 1997).Also, the infection by *P. striiformis* affects the photosynthetic function and accelerates the translocation of assimilation products from leaves to grain filling, causing lower thousand-kernel weight (TKW) and yield (He *et al.* 2019).

In addition, grains from wheat plants affected by diseases such as tan spot, rust, and FHB produce lower protein and gluten content, besides having worse rheological parameters and viscoelastic properties (Castro et al. 2018; Fleitas et al. 2018a; Fleitas et al. 2018b). Johansson et al. (2013, 2020) and Koga et al. (2019) also demonstrated that changes in the viscoelastic properties due to modifications in gluten protein polymerization of the dough were caused by biotic stress, especially of diseases.

To counteract the damage to grain yield and quality, integrated diseases management is employed. This includes the use of resistant genotypes and healthy seeds, besides application of fungicides, and fertilizers (Pazdiora et al. 2021; Fleitas et al. 2018a; Dallagnol et al. 2020). These measures for disease management have an effect on wheat technological quality (Kweon et al. 2011). For instance, for wheat production, characteristics such as flowering time and plant stature are important agronomic traits for adaptation as well as yield potential (Khumalo et al. 2017). In this context, the use of early-maturing cultivars allows the planting of more than one crop per season and reduces hazards that occur at the time of maturity (Patel and Monpara 2007; Gilbert and Haber 2013). Furthermore, application of a pre-mix of fungicides with different action modes (azoles, strobilurins, and carboxamides) significantly increased grain yield as well as grain quality parameters such as thousand kernel weight (TKW), specific weight (TW), and grain starch content (GSC) (Matzen et al. 2019). The application of a similar pre-mix in combination with higher nitrogen (N) rates reduced the damage of some diseases and increased grain yield (Castro et al. 2018; Schierenbeck et al. 2019; Fleitas et al. 2018b).

Chlorophyll *a* (Chl_a) fluorescence is used to determine the physiological status, and specifically the maximum efficiency of photosystem II (PSII) photochemistry (F_v/F_m), also known as the maximum quantum yield of primary photochemistry (Strasser, 2004; Rolfe and Scholes 2010; Ajigboye et al. 2016), is widely used as an indicator of photoinhibition and often used for evaluation of plant disease damage to photosynthesis by providing information about the level of stress to which plants are exposed (Ajigboye et al. 2016; Rolfe and Scholes 2010). In nonstressed plants, the F_v/F_m can fluctuate between 0.80 and 0.83, but it sharply decreases on stressed plants due to photoinhibition and damage to the PSII (Björkman and Powles 1984). In this regard, the reduction of F_v/F_m showed the effect of the biotic stress caused by diseases described in different pathosystems (Fortunato et al. 2018; Rios et al. 2017). Thus, the

use of this parameter may allow associating disease damage and photosynthesis status, especially in PSII, as well as the effect on wheat technological quality parameters (determined through physicochemical and rheological analyses).

Several studies have shown the effect of N and fungicide application on disease management and wheat technological quality (Dimmock and Gooding 2002; Ruske et al. 2003; El Jarroudi et al. 2015; Castro et al. 2018; Fleitas et al. 2018a). Although previous studies have investigated the employment of N fertilization for disease control, there is limited information regarding the changes of PSII and wheat technological quality parameters, as a result of disease management on early-maturing wheat cultivars under field conditions.

The objective of this study was to determine the effect of disease management measures on changes in the Chl a fluorescence, yield components, and wheat technological quality.

2. Materials and methods

2.1. Field experiment and wheat Samples

The field experiment had as split-split plot arrangement with four replications. In each year, the main plots were fungicide treatment (plants receiving fungicide application or unsprayed plants). Sub-plots were two wheat cultivars. Sub-sub plots were nitrogen rates (low N: 70 kg ha⁻¹, recommended N: 130 kg ha⁻¹ and high N: 200 kg ha⁻¹). The nitrogen was applied as the split rate of granular urea (45% N) at sowing and at tillering (ZGS23). Each sub-subplot was 3 m² (2 m long × 1.5 m wide). The diseases occurred due to the inoculum present naturally in the field. Fertilizer was applied at sowing as required for maximum crop yield according to soil test recommendations, as phosphorus at rate of 40 kg ha⁻¹ in the form of triple superphosphate, and potassium at rate of 30 kg ha⁻¹ in the form of potassium chloride at sowing. Glyphosate [Shadow 480 SL® herbicide (Albaugh AgroBrasilLtda), 480 g L⁻¹] applied at 2 L ha⁻¹ was used for weed control 15 days before sowing. In addition, metsulfuron-methyl [Zartan® herbicide (UPL); 600 g kg⁻¹] was applied at 0.006 g L⁻¹ at the three-leaf stage (ZGS13).

The pre-mix of fungicides containing bixafen (125 g L⁻¹; carboxamide) + prothioconazole (175 g L⁻¹; triazolinthione) + trifloxystrobin (150 g L⁻¹; strobirulin) (Fox Xpro®; Bayer) was applied at 0.5 L ha⁻¹ at the time of flag leaf emergence (ZGS39) and flowering (ZGS 65) (Zadoks et al. 1974). The fungicide was applied using

a CO₂ pressure sprayer, with four nozzles (TTJ60 11002; Teejet®), delivering 200 L ha⁻¹.

2.3. Experimental measurements

2.3.1. Disease assessment and area under disease progress curve

During the crop cycle we registered the severity of four diseases: tan spot, powdery mildew, leaf rust, and FHB. The severity was assessed through comparison with scales according to evaluation by Román et al. (2021). In summary, the diseases were monitored from stem elongation (ZGS30) to the hard dough stage (ZGS87). Tan spot and powdery mildew severities were estimated using the Horsfall-Barratt scale on the whole plant (Horsfall and Barratt 1945). For rust, the severity estimation was based on the Cobb scale modified by Peterson et al. (1948). The FHB severity (percentage of bleached spike) was estimated using the scale of Stack and McMullen (2011). For each disease, the area under disease progress curve (AUDPC) was calculated to summarize the disease progress through time, according to Shaner and Finney (1977).

2.3.2. Determination of chlorophyll (Chl) *a* fluorescence (CF)

The CF was determined in the dough development stage (ZGS80) on plants previously marked. The flag leaf of each plant was placed for 30 minutes in the dark before the measurements. The OJIP fluorescence transient was measured using a handheld fluorometer (FluorPen FP110, Photon Systems Instruments, Drásov, Czech Republic). All measurements were made from 5:30 to 6:30 a.m. Polyphasic CF transient was induced by saturating light of 3.000 $\mu\text{mol m}^{-2} \text{s}^{-1}$ and the kinetics were recorded. The measurements were carried out according to Ajigboye et al. (2016), including fluorescence intensity at 50 ms, considered the initial fluorescence value (F_0). The maximum fluorescence level of the OJIP transient (F_m) was measured under saturating light conditions, while intermediate fluorescence values were measured at 300 ms, 2 ms, and 60 ms, and labeled as $F_{300\text{ms}}$, F_j and F_i respectively (Strasser et al. 2000, 2004). The different steps of the OJIP transient were determined with the FluorPen 1.0.0.6 software (Photon Systems Instruments). Only maximum quantum yield of primary photochemistry (F_v/F_m) was used for analysis.

2.3.3. Yield determinations

Wheat was harvested from five central rows with a length of 1 m (totaling 1m²) of each plot and threshed with a mechanical grain thresher (EDA, model TR, Parcela). Samples were air-dried for approximately 48 h and cleaned. The grain moisture content of a representative subsample was measured with a moisture tester (agraTronix MT-PRO). Yield components included test weight (TW; kg hL⁻¹), determined using a Dallemolle type 40 hectoliter balance, according to Method 55-10.01(AACC 1999); and thousand kernel weight, measured by counting 100 seeds, weighing them with an electronic balance with accuracy of 0.001g and multiplying the result by 10 to give the weight of 1000 kernels (TKW; expressed in g).

2.3.4. Physicochemical and rheological quality of wheat samples

From each field plot 40-80 g of grain was separated, which was milled in a hammer mill (LabMill3100, Perten Instruments, Huddinge, Sweden) to obtain whole wheat flour. The replicates of each sample treatment were used to obtain around 1000 g of grain, which was conditioned to 14% moisture for 16-24h before milling in a pilot scale roller mill (Quadrumat Senior, Brabender GmbH & Co. KG, Duisburg, Germany) to obtain white wheat flour, according to Method 26-10.02 (AACC 1999). The protein and ash content, falling number, gluten, and flour color were determined in the whole wheat flour and the farinography was determined in the white flour.

Whole wheat flour protein content (PC), on dry basis, was determined by NIR spectroscopy (XDS-Rapid Content Analyzer, FOSS NIRSystems, Hilleroed, Denmark), with a double detection system (model 6500 monochromator with measuring range: silicon 400–1,100 nm and lead sulfide 1,100–2,500 nm), equipped with the ISIScanTM software (Infrasoft International LLC, State College, PA, USA), following Method 39-10.01(AACC 1999). Ash content (AC), on dry basis, was obtained by the ICC Method 104/1 (ICC, 1990), using a muffle furnace at 900°C for 2.5 hours.

The grain falling number (GFN) was determined with an FN 1900 meter (Perten Instruments, Stockholm, Sweden) according to Method 56-81.03 (AACC, 1999), which is based on the ability of alpha-amylase to liquefy a starch gel. Gluten analysis of whole flour was performed with a Glutomatic System (Perten, Stockholm, Sweden), according

to Method38-12.02 (AACC, 2000), considering the parameters gluten index (GI), wet gluten (WG), and dry gluten (DG).

Whole wheat flour color analysis was performed with a colorimeter (CR-410 Chroma Meter, Minolta, Osaka, Japan), using D_{65} illuminant, \emptyset 50 mm measurement area, and 10° viewing angle (Konica Minolta, 2013). The results were expressed according to the CIEL*a*b* system, considering the parameters: L^* , lightness (0: dark, 100: white); chromaticity coordinates: a^* (-60: green, +60: red) and b^* (-60: blue, +60: yellow); C^* , chroma or color intensity; and h^* , hue or color tonality.

Rheological analyses of samples of each treatment were performed using a farinograph (50 g bowlTyp 820600 model, Brabender GmbH & Co. KG, Duisburg, Germany) according to Method54-21.02 (AACC, 2011), considering the parameters water absorption (WA), dough development time (DDT), dough mixing stability (STB), and, mixture tolerance index (MTI).

2.4. Data analyses

The data were analyzed separately per year using R version 4.0.4. (RStudio 2021). Multivariate analysis was applied using principal component analysis (PCA) with the FactoMineR (Le et al., 2008) and factoextra (Kassambara & Mundt, 2020) packages. The eigenvalues (λ_i), proportion of variance (PV), accumulated proportion of variance (APV) of the components and correlation matrix were used to determinate the relation between AUDPCs, yield components, wheat technological quality variables, whole wheat flour color, and Fv/Fm . Data analyses for TKW and TW, maximum quantum yield of primary photochemistry (Fv/Fm), and wheat technological quality variables (AC, GFN, PC, GI, WG, DG, and whole wheat flour color) were obtained by mixed-effects linear models using the ‘lmer’ function from the lme4 (Bates et al. 2014) and the lmerTest (Kuznetsova et al. 2017) packages. Fungicide, cultivar, and nitrogen rates and interactions were considered as fixed factors. Blocks, the nesting of plots within blocks, and subplots within plots were considered random factors. Data assumptions were verified graphically using plots of fitted values versus the residuals for homogeneity of variance and normal Q-Q plots for normality, as well as the ‘simulateResiduals’ function of the DHARMA package (Hartig 2021). Fixed treatment effects were considered significant at $p < 0.05$. Estimated marginal means were computed with the ‘emmeans’ function from the emmeans package (Lenth 2021) and

pairwise comparisons were performed with the Tukey test using the 'cld' function of the multcomp package (Hothorn et al. 2008). For rheological parameters (WA, DDT, STB, and MTI), descriptive analyses were used.

3. Results

3.1 Multivariate analyses: AUDPCs, *Chla* fluorescence, yield components and wheat grain technological quality

Principal component analysis (PCA) showed a relationship among the attributes of the first three PCs evaluated in our study, since the eigenvalues (λ_i) were greater than 1 (Tables 1 and 2; Figure 1). The first PC explained 56% of the total variance, where the levels of TKW, TW, yield, AC, AUDPC of rust, AUDPC of tan spot, AUDPC of powdery mildew and AUDPC of FHB represented the greatest contribution (Tables 1 and 2). The second PC explained 22%, where the levels of PC, WG, DG, GI, and *Fv/Fm* represented the greatest contribution (Tables 1 and 2; Figure 1).

The correlation matrix among the variables showed that AUDPC of tan spot was positively associated with AC and L^* (Table 3). Also, AUDPC of tan spot and AUDPC of powdery mildew showed negative associations with GFN, a^* , b^* , C^* , TKW, TW, and yield, whereas AUDPC of powdery mildew showed a negative association with PC, and GI. AUDPC of rust had a positive association with AC. AUDPC of FHB was negatively associated with GFN. AUDPC of tan spot and powdery mildew were negatively associated with *Fv/Fm*. AC and GFN showed a negative association with TKW, TW and yield. Regarding the color parameters, L^* was negatively associated with GFN and positively associated with a^* , b^* , C^* and WG. For b^* and C^* , negative associations with PC, WG, and DG, and positive association with GI were observed. PC was positively associated with WG and DG, whereas GI was negatively associated with PC. TKW was positively associated with TW, while yield was positively associated with TKW and TW. In relation to the wheat grain technological quality, *Fv/Fm* was positively associated with GFN and GI, whereas a negative association was observed for PC, WG, and DG. For whole wheat flour color parameters, *Fv/Fm* was positively correlated with a^* , b^* and C^* , and negatively associated with L^* .

3.2. Effect of cultivar, fungicide application, and nitrogen rate on yield components and maximum quantum yield of primary photochemistry (F_v/F_m)

Cultivar and fungicide were significant ($p < 0.05$) for TKW, TW, and F_v/F_m ; however, the fungicide effect on F_v/F_m was not consistent between the years (Table 4). The interaction cultivar \times fungicide was significant ($p < 0.05$) for TKW and TW, whereas cultivar \times nitrogen was significant for TKW and F_v/F_m (Table 4). TBIO Audaz had TKW, TW and F_v/F_m values that exceeded those of TBIO Tibagi by 14 and 29%, 4 and 7%, and 38 and 11%, respectively, in 2019 and 2020 (Table 5). Fungicide application increased TKW in 2019 and 2020, respectively, by 25 and 40%, and TW and F_v/F_m by 8 and 18%, respectively, in 2019 compared with the unsprayed treatment (Table 5).

TBIO Audaz \times fungicide interaction caused no differences for TKW compared to TBIO Audaz \times unsprayed, but the interaction TBIO Tibagi \times fungicide had 37% higher TKW than TBIO Tibagi \times unsprayed (Figure 2A). Likewise, for TW, TBIO Audaz \times fungicide interaction displayed an increase of 4% in relation to TBIO Audaz \times unsprayed; and TBIO Tibagi \times fungicide had an increase of 12% compared to TBIO Tibagi \times unsprayed (Figure 2C). For TKW, the interaction between cultivar TBIO Audaz \times nitrogen had no differences among the rates, but TBIO Tibagi \times recommended N was 4% lower compared to TBIO Tibagi \times low N (Figure 2B). For F_v/F_m , the interaction TBIO Audaz \times nitrogen caused no differences among the rates, but TBIO Tibagi \times recommended N was 5% higher than TBIO Tibagi \times low N (Figure 2D). Nevertheless, there was a noteworthy difference observed for F_v/F_m between cultivar \times nitrogen level, with TBIO Audaz \times recommended N being higher by 24% compared to TBIO Tibagi \times recommended N (Figure 2D).

3.3. Effect of cultivar, fungicide application and nitrogen rate on wheat physicochemical and rheological quality

In this experiment, we observed the effect of cultivar, nitrogen rate and fungicide application for disease management on technological quality parameters. The fixed factors cultivar, fungicide, and nitrogen treatments were significant ($p < 0.05$) among the response variables. The cultivar was significant ($p < 0.05$) for GFN, PC, GI, DG, and WG, whereas fungicide was significant for AC (Table 6). Furthermore, nitrogen level was significant ($p < 0.05$) for PC, GI, DG, WG, and AC (Table 6).

The GFN was higher by 54 and 190% for TBIO Audaz compared to TBIO Tibagi in 2019 and 2020, respectively (Table 7). In contrast, PC was higher by 8 and 15% for TBIO Tibagi than TBIO Audaz in 2019 and 2020, respectively (Table 7). For GI, TBIO Audaz was 29 and 50% higher compared to TBIO Tibagi in 2019 and 2020, respectively. The GD and WG values were higher by 14 and 21%, and 60 and 77% respectively, for TBIO Tibagi compared to TBIO Audaz in 2019 and 2020, respectively (Table 7). In the case of fungicide treatment, AC was lower by 12 and 11% compared to the unsprayed treatment in 2019 and 2020, respectively (Table 7).

For nitrogen rate, AC was higher by 4 and 3% for low N compared to high N in 2019 and 2020, respectively (Table 7). In contrast, PC was higher by 14 and 8% in high N than low N in 2019 and 2020, respectively, but there were no differences regarding recommended N. GI was higher by 10 and 7% in low N compared to high N in 2019 and 2020, respectively. In contrast, DG and WG were higher by 16 and 9%, and 24 and 11%, respectively, in high N compared to low N in 2019 and 2020, respectively.

We observed significant interactions between factors. Cultivar \times nitrogen was significant ($p < 0.05$) for PC, GFN, GI, DG, and WG (Figure 3). For PC, TBIO Tibagi \times high N was higher by 15% compared to TBIO Tibagi \times low N, and TBIO Audaz \times high N was higher by 13% compared to TBIO Audaz \times low N (Figure 3A). In the case of GFN, there were no differences of nitrogen rates for both cultivars, but there were differences of TBIO Audaz \times recommended N, which increased by 60% in time compared to TBIO Tibagi \times recommended N (Figure 3B).

For GI, there were no differences for TBIO Audaz among N rates, but for TBIO Tibagi \times low N was 26% higher compared to TBIO Tibagi \times recommended N. For DG and WG, TBIO Tibagi \times recommended N was higher by 27 and 18%, respectively, compared to TBIO Tibagi \times low N, whereas TBIO Audaz \times high N was 22 and 17% higher compared to TBIO Audaz \times low N (Figures 3C, 3D and 3E).

For color parameters (L^* , a^* , b^* , h^* , and C^*), the cultivar and fungicide were significant ($p < 0.05$), and L^* and a^* were also significant for nitrogen level (Table 8). TBIO Tibagi showed 5 and 4% higher L^* compared to TBIO Audaz in 2019 and 2020, respectively, whereas the parameters a^* and b^* were higher by 33 and 29%, and 30 and 16% in TBIO Audaz compared to TBIO Tibagi in 2019 and 2020, respectively. A similar result was observed for C^* , which was higher by 29 and 19% in TBIO Audaz compared to TBIO Tibagi in 2019 and 2020, respectively. However, treatments with fungicide application showed increases of 1 and 2% for L^* and h^* in 2019 and it was

similar in 2020, compared to unsprayed treatments. In contrast, the unsprayed treatment showed higher values for a^* and b^* by 11 and 12%, and 5 and 2%, in 2019 and 2020, respectively, compared to fungicide treatment. In the case of nitrogen rate, low N was higher by 1% for L^* and h^* compared to high N, whereas high N showed increases of 3% for a^* compared to low N only in 2019; and also, there were no differences between high N and recommended N (Table 9). The cultivar \times fungicide interaction was significant ($p < 0.05$) only for b^* and C^* (Figure 3). For the same two parameters, there were no differences for TBIO Audaz between the plants sprayed with fungicide and unsprayed, whereas TBIO Tibagi \times fungicide was 9% lower than TBIO Tibagi \times unsprayed for both variables (Figure 4A and 4B).

The interaction fungicide \times nitrogen was significant ($p < 0.05$) for WG, b^* and C^* (Figure 5). For WG, unsprayed \times recommended N was higher by 11% than fungicide \times recommended N (Figure 5A). For the color parameters b^* and C^* , unsprayed \times recommended N was 6% higher compared to fungicide \times recommended N for both variables (Figures 5B and 5C). There was a significant triple interaction ($p < 0.05$) only for b^* and C^* color parameters in 2019. For TBIO Audaz at any nitrogen level, with and without fungicide, no differences were observed. However, TBIO Audaz \times fungicide \times high N interaction was 44% higher for both b^* and C^* parameters compared TBIO Tibagi \times fungicide \times high N.

Table 10 shows the results obtained from the rheological analysis of each treatment in 2019 and 2020. At all N rates, TBIO Tibagi unsprayed showed higher DDT compared to TBIO Tibagi with fungicide. In contrast, for MTI the treatment of TBIO Audaz with fungicide with low N was higher compared to unsprayed TBIO Audaz or TBIO Tibagi at all N rates. For STB, TBIO Tibagi unsprayed at all N rates was higher compared to TBIO Tibagi with fungicide, but similar to TBIO Audaz with fungicide and recommended and high N. A notability higher STB value was observed at higher N rates. There were no differences among treatments for WA.

4. Discussion

In this study, the disease registered during the 2019 and 2020 growing seasons, and the disease management measures influenced the photosynthesis parameters and wheat technological quality variables. TBIO Tibagi, a susceptible cultivar, was mainly affected by diseases during 2019 and 2020. The negative association of Fv/Fm and AUDPCs of tan spot and powdery mildew demonstrated that the reduction of this

parameter was caused by leaf diseases and it was associated with lower wheat technological quality parameters. Several studies have indicated that decreases of Fv/Fm in different host pathosystems are related to pathogen infection (Swarbrick et al. 2006; Ajigboye et al. 2016; Chaerle et al. 2007; Fortunato et al. 2018). Differences of Fv/Fm due to the management employed, such as the use of a resistant cultivar along with fungicide and nitrogen application, indicated the use of this strategy limits the effect of diseases. In this regard, the fungicide pre-mix employed reduced the disease's damage and it was associated with the lower Fv/Fm . Those results are in line with Ajigboye (2014), who reported increased PSII efficiency with a positive impact on photosynthesis at the end of the grain filling period due to the use of succinate dehydrogenase inhibitor (SDHI) and triazole fungicide, resulting in higher yield.

The negative association of AUDPC of tan spot and powdery mildew with TKW, TW and yield indicated the effect of the diseases on those parameters. In 2019, the TKW and TW were lower in TBIO Tibagi compared to TBIO Audaz (moderately resistant), but the fungicide application increased TKW and TW in TBIO Tibagi. This result indicated that tan spot and powdery mildew may be responsible for the reduction in TKW and TW. However, the pre-mix of fungicides allowed an increase in these parameters due to the reduction of disease intensity. Those results are in line with Matzenet al. (2019) and Kutcher et al. (2018), who reported increases in TKW and TW due to application of a pre-mix of fungicides belonging to the azoles, strobilurins and carboxamides. Likewise, in treatments with recommended and high N, TKW was higher although the application of N and pre-mix of fungicides reduced the damage of some diseases and increased grain yield. These results agree with the findings of other studies, which have reported a reduction of tan spot with application of fungicide pre-mix and high N (Castro et al. 2018; Schierenbeck et al. 2019; Fleitas et al. 2018a).

The negative relation of Fv/Fm and AUDPCs demonstrated the changes in the efficiency of PSII photochemistry associated with the increase of disease damage, and those values were positively and negatively associated with different parameters of wheat quality. AUDPCs of tan spot, powdery mildew and leaf rust were positively associated with AC, indicating an increase of AC associated with low grain test weight, promoting contamination of flour and semolina, affecting whole wheat flour color. However, fungicide application and higher N decreased AC, improving it to desirable levels, which is less than 2% to meet the acceptable value for baking (Rharrabti et al.

2003). In addition to the positive association with *Fv/Fm*, the negative association with AUDPCs demonstrated decrease of GFN. Indeed, the alpha-amylase enzyme activity associated with GFN is affected by cultivar choice based on genetic background, fertilizers and also by crop management (Kindred et al. 2005; Mares and Mrva 2008; Matzen et al. 2019). In this regard, the delay in leaf senescence and the reduced disease damage suffered by TBIO Audaz was associated with greater GFN compared to the susceptible cultivar, but both were still above 250 seconds, which is the required standard for bread-making (Draper and Stewart 1980).

In this study, the disease management through cultivar choice, nitrogen and fungicide application reduced the disease intensities, with positive effects on protein and gluten content. The positive PC associated with AUDPC of powdery mildew and negative association with *Fv/Fm* indicated increased protein content. Despite the greater susceptibility to leaf diseases, TBIO Tibagi showed higher protein and gluten content compared to TBIO Audaz. However, the cultivar \times N interaction demonstrated that at high N rates, TBIO Audaz and TBIO Tibagi both had increases in PC as well as DG and WG. Differently, at low N the effect differed due to the reduction of protein and gluten content, indicating that the greater disease susceptibility and the less N incorporation affected protein and gluten contents. These results were also consistent with those reported by Matzel et al. (2019), who observed reductions in gluten and grain protein content in wheat due to the presence of leaf diseases.

Also, in association with higher N rates, the use of fungicide pre-mix was related with higher WG and protein compared to low N rate with fungicide application, showing the combined effect of fungicide and nitrogen on the cultivars. Those observations were also described by Castro et al. (2018), who reported PC decreases due to fungicide, but that tended to be lower at higher N rates. Furthermore, Dimmock and Gooding (2002) reported that nitrogen can prevent the reduction of PC that can occasionally result from fungicide use. In this regard, delay in senescence and extension of the grain-filling period of cereals due to fungicides (strobilurins and triazoles), along with genetic improvement of cultivars, may be associated with this result.

The difference observed regarding the cultivar also showed that gain in yield affects quality parameters while reducing protein concentration. This result agreed with other studies that have reported a reduction in protein concentration and loaf volume (Laidig et al. 2017; Rozo-Ortega et al. 2021). This effect can be associated with the

genetics of cultivars due to N remobilization before senescence, which can originate from storage proteins as opposed to those with metabolic functions, at least up to a level that does not affect essential physiological processes (Kong et al. 2016). As a result, TBIO Audaz showed higher TW and TKW, but less protein content compared with TBIO Tibagi. This result can be associated with negative effects on bread-making quality (Gaju et al. 2014), suggesting that the use of fungicide and correct nitrogen rate allows adequate disease control while maintaining protein and gluten content. In this context, the rheological parameters in this study indicated that with the use of recommended N, the gluten content was maintained at an adequate level, while water absorption and stability time demonstrated the resistance of dough to mixing.

In our study, color parameters of the whole wheat flour varied depending on the association among the variables and the cultivar, fungicide application and nitrogen rate. The reduction in Fv/Fm caused by diseases can be reflected in the reduction of L^* , a^* , b^* , and C^* due to the positive association of its variables. Increases in protein content and gluten content, as well as AC, reduced b^* and C^* parameters while variation in GFN reduced L^* . TBIO Tibagi presented darker flour ($< \text{lightness, } L^*$), but it was less reddish ($< a^*$ value) and yellowish ($< b^*$ value) compared to TBIO Audaz. However, the application of fungicide increased the saturation and intensity of flour color, due to the high values of hue and chroma, respectively, increasing the lightness and the yellow tendency. Similarly, low N rates increased the lightness and hue. Those observations of color parameters demonstrated that the effect of the disease management by cultivar \times fungicide interaction improved the color.

5. Conclusion

During the wheat crop cycle, infection by leaf and spike diseases reduced the yield components. In addition, the photosynthesis process was clearly influenced by the diseases. Fv/Fm during the dough development stage (ZGS80) was associated the disease damage under field conditions. The fungicide and nitrogen rate interaction ameliorated plant physiological damage, maintaining adequate Fv/Fm while increasing yield components (TW and TKW). This effect was more evident in the susceptible cultivar. Also, fungicide and nitrogen rate interaction increased the protein and gluten contents while decreasing ash content. However, the moderately resistant cultivar, despite performing better in the field compared to the susceptible cultivar, produced

lower protein content. Likewise, the application of fungicide affected the protein content, especially associated with low N rate, since at recommended N or high N, application of fungicide had a lesser positive effect on protein content. In turn, the nitrogen rate was associated with changes in the color of whole wheat flour, associated with higher PC, DG, WG, AC, and falling number (GFN). The application of the fungicide also increased the lightness and the yellowish color, considered to be improvements. Therefore, the disease management with use of the moderately resistant cultivar improved the yield components, but the use of recommended N rate maintained adequate protein values and fungicide application was necessary, for the susceptible cultivar to reduce the impact of diseases and improve wheat grain technological quality.

Acknowledgements

The authors are thankful to the Office to Coordinate Improvement of Higher Education Personnel (CAPES) for financial support and the student scholarship (Finance code 001) and a fellowship (grant number 308149/2018-1) from the Brazilian National Council for Scientific and Technological Development (CNPq). We thank to Post-Harvest Laboratory of the Brazilian Agricultural Research Corporation National Wheat Research Center (Embrapa Trigo) for the physicochemical and rheological analyses. We are thankful to BIOTRIGO for providing wheat seeds for the experiments.

Declaration of competing interest

The authors declare that they have no conflicts of interest.

References

AACC (Cereals & Grains Association).2010. Approved Methods of Analysis, 11th ed. Method 26-10.02. Experimental milling: introduction, equipment, sample preparation, and tempering. Approved Nov 3,1999; Method 39-10.01. Near-infrared reflectance method for protein determination in small grains. Approved Nov 3, 1999; Method 44-15.02. Moisture-air-oven method. Method 55-10.01. Test weight per bushel. Approved Nov 3, 1999; Method 56-81.03. Determination of falling number. Approved Nov 3, 1999; Method 38-12.02. Wet gluten, dry gluten, water-binding capacity, and gluten index. Approved Nov 8, 2000; Method 54-21.02 Rheological behavior of flour by farinograph: constant flour weight procedure. Approved Jan 6, 2011. [2020-06-28].

<http://methods.aaccnet.org/toc.aspx>.

- Ajigboye O O, Bousquet L, Murchie E H, Ray R V. 2016. Chlorophyll fluorescence parameters allow the rapid detection and differentiation of plant responses in three different wheat pathosystems. *Functional Plant Biology*. **43**:356-369.
- Ajigboye O O, Murchie E, Ray R V. 2014. Foliar application of isopyrazam and epoxiconazole improves photosystem II efficiency, biomass and yield in winter wheat. *Pesticide Biochemistry and Physiology*. **114**:52–60.
- Alam M A, Wang C, Ji W. 2013. Chromosomal location and SSR markers of a powdery mildew resistance gene in common wheat line N0308. *African Journal of Microbiology Research*. **7**:477-482.
- Bates D, Mächler M, Bolker B, Walker S. 2014. Fitting linear mixed-effects models using lme4. arXiv preprint arXiv:1406.5823.
- Björkman O, Powles S B. 1984. Inhibition of photosynthetic reactions under water stress: interaction with light level. *Planta*, **161**:490-504.
- Castro A C, Fleitas M C, Schierenbeck M, Gerard G S, Simón M R. 2018. Evaluation of different fungicides and nitrogen rates on grain yield and bread-making quality in wheat affected by *Septoria tritici* blotch and yellow spot. *Journal of Cereal Science*. **83**:49-57.
- Chaerle L, Hagenbeek D, Vanrobaeys X, Van Der Straeten D 2007. Early detection of nutrient and biotic stress in *Phaseolus vulgaris*. *International Journal of Remote Sensing*. **28**: 3479-3492.
- Chen X. 2020. Pathogens which threaten food security: *Puccinia striiformis*, the wheat stripe rust pathogen. *Food Security*. **12**:239-251.
- Dallagnol L J, Román A, da Rosa Dorneles K. 2020. Silicon Use in the Integrated Disease Management of Wheat: Current Knowledge. *Current Trends in Wheat Research*. [Online First], IntechOpen. [2021-06-28]. <https://www.intechopen.com/online-first/74509>.
- Dimmock J, Gooding M J. 2002. The influence of foliar diseases, and their control by fungicides, on the protein concentration in wheat grain: a review. *The Journal of Agricultural Science*. **138**:349-366.
- Draper S R, Stewart B A. 1980. Procedures for the comparative assessment of quality in crop varieties. III. Methods used in assessing grain protein content, Hagberg

- falling number, ease of milling and the baking quality of wheat varieties. *Journal of the Natural Institute of Agricultural Botany*. **15**:1-14.
- Duffeck M R, dos Santos Alves K, Machado F J, Esker P D, Del Ponte E M. 2020. Modeling yield losses and fungicide profitability for managing fusarium head blight in Brazilian spring wheat. *Phytopathology*. **110**:370-378.
- El Jarroudi M, Kouadio L, Junk J, Beyer M, Pasquali M, Bock C H et al. 2015. Do single, double or triple fungicide sprays differentially affect the grain quality in winter wheat? *Field Crops Research*. **183**:257-266.
- Fleitas MC, Schierenbeck M, Gerard G S, Dietz J I, Golik S I, Campos P E et al. 2018a. How leaf rust disease and its control with fungicides affect dough properties, gluten quality and loaf volume under different N rates in wheat. *Journal of Cereal Science*. **80**:119-127.
- Fleitas M C, Schierenbeck M, Gerard G S, Dietz J I, Golik S I, Simón M R. 2018b. Breadmaking quality and yield response to the green leaf area duration caused by fluxapyroxad under three nitrogen rates in wheat affected with tan spot. *Crop Protection*. **106**:201-209.
- Fortunato A A, Debona D, Aucique-Pérez C E, Fialho Corrêa E, Rodrigues F A. 2018. Chlorophyll a fluorescence imaging of soya bean leaflets infected by *Corynespora cassiicola*. *Journal of Phytopathology*. **166**:782-789
- Gaju O, Allard V, Martre P, Le Gouis J, Moreau D, Bogard M, Hubbart S, Foulkes, M J. 2014. Nitrogen partitioning and remobilization in relation to leaf senescence, grain yield and grain nitrogen concentration in wheat cultivars. *Field Crops Research*. **155**:213-223.
- Gilbert J, Haber S. 2013. Overview of some recent research developments in Fusarium head blight of wheat. *Canadian Journal of Plant Pathology*. **35**:149-174.
- Gooding M J, Davies W P. 1997. *Wheat production and utilization: systems, quality and the environment*. CAB international. New York, p 355.
- Hartig F. 2021. DHARMA: Residual diagnostics for hierarchical (multi-level / mixed) regression models. R package version 0.4.1. [2021-06-09]. <https://cran.r-project.org/package=DHARMA>%0A.
- He C, Zhang Y, Zhou W, Guo Q, Bai B, Shen S et al. 2019. Study on stripe rust (*Puccinia striiformis*) effect on grain filling and seed morphology building of special winter wheat germplasm Huixianhong. *Plos one*. **14**:e0215066.
- Horsfall G, Barratt R W. 1945. An improved grading system for measuring plant

- diseases. *Phytopathology*. **35**:65.
- Hothorn T, Bretz F, Westfall P. 2008. Simultaneous inference in general parametric models. *Biometrical Journal*.**50**:346-363.
- ICC. 1990. Method 104/1. Determination of ash in cereals and cereal products. [2020-06-28]. <https://icc.or.at/publications/icc-standards/standards-overview/104-1-standard-method>.
- Johansson E, Branlard G, Cuniberti M, Flagella Z, Hüsken A, Nurit E, Peña J, Sissons M, Vazquez D. 2020. Genotypic and environmental effects on wheat technological and nutritional quality. In: Igrejas, G., Ikeda, TM, Guzmán, C, eds., *Wheat Quality for Improving Processing and Human Health*. Springer, Switzerland, pp. 171-204.
- Johansson E, Malik A H, Hussain A, Rasheed F, Newson W R, Plivelic T et al. 2013. Wheat gluten polymer structures: the impact of genotype, environment, and processing on their functionality in various applications. *Cereal Chemistry*. **90**:367-376.
- Kassambara A & Mundt F. (2020). factoextra: Extract and visualize the results of multivariate data analyses. R package version 1.0.7. Available at: <https://CRAN.R-project.org/package=factoextra>.
- Khumalo T P, Barnard A, Maphosa L, Tsilo T J. 2017. Impact of growth habit and architecture genes on adaptation and performance of bread wheat. *wheat improvement, Management and Utilization*. IntechOpen. [2021-01-09]. <https://www.intechopen.com/chapters/53971>.
- Kindred D R, Gooding M J, Ellis R H. 2005. Nitrogen fertilizer and seed rate effects on Hagberg falling number of hybrid wheats and their parents are associated with α -amylase activity, grain cavity size and dormancy. *Journal of the Science of Food and Agriculture*. **85**:727-742.
- Koga S, Rieder A, Ballance S, Uhlen A K, Veiseth-Kent E. 2019. Gluten-degrading proteases in wheat infected by *Fusarium graminearum*-protease identification and effects on gluten and dough properties. *Journal of Agricultural and Food Chemistry*.**67**:11025-11034.
- Kong L, Xie Y, Hu L, Feng B, Li S. 2016. Remobilization of vegetative nitrogen to developing grain in wheat (*Triticum aestivum* L.). *Field Crops Research*. **196**:134-144.

- Konica Minolta. 2013. Instruction manual: chroma meter CR-400/410. Tokyo. 156 p.
- Kutcher H R, Turkington T K, McLaren D L, Irvine R B, Brar G S. 2018. Fungicide and cultivar management of leaf spot diseases of winter wheat in western Canada. *Plant Disease*. **102**:1828-1833.
- Kuznetsova A, Brockhoff P B, Christensen R H B. 2017. lmerTest package: tests in linear mixed effects models. *Journal of Statistical Software*. **82**:1-26.
- Kweon M, Slade L, Levine H. 2011. Solvent retention capacity (SRC) testing of wheat flour: Principles and value in predicting flour functionality in different wheat-based food processes and in wheat breeding-A review. *Cereal Chemistry*. **88**:537-552.
- Laidig F, Piepho H P, Rentel D, Drobek T, Meyer U, Huesken A. 2017. Breeding progress, variation, and correlation of grain and quality traits in winter rye hybrid and population varieties and national on-farm progress in Germany over 26 years. *Theoretical and Applied Genetics*. **130**:981-998.
- Le S, Josse J, Husson F. 2008. FactoMineR: An R Package for multivariate analysis. *Journal of Statistical Software*, **25**:1-18.
- Lenth R. 2021. emmeans: Estimated Marginal Means, aka Least-Squares Means. R package version 1.6.0. [2021-07-09]. <https://cran.r-project.org/package=emmeans>.
- Mares D, Mrva K. 2008. Late-maturity α -amylase: low falling number in wheat in the absence of preharvest sprouting. *Journal of Cereal Science*. **47**:6-17.
- Matzen N, Jørgensen J R, Holst N, Jørgensen L N. 2019. Grain quality in wheat-Impact of disease management. *European journal of agronomy*. **103**:152-164.
- Patel A P, Monpara B A. 2007. Effects of maturity on variation and association for grain filling and yield related traits in durum wheat. *Agricultural Science Digest*. **27**:178-181.
- Pazdiora P C, da Rosa Dorneles K, Morello T N, Nicholson P, Dallagnol L J. 2021. Silicon soil amendment as a complement to manage tan spot and fusarium head blight in wheat. *Agronomy for Sustainable Development*. **41**:1-13.
- Peterson R F, Campbell A B, Hannah A E. 1948. A diagrammatic scale for estimating rust intensity on leaves and stems of cereals. *Canadian Journal of Research*. **26**:496-500.
- Reis E M, Casa R T. 2007. *Doenças dos cereais de inverno: diagnose, epidemiologia e*

controle. 2nd ed. Lages: Graphel. (in Portuguese)

- Rharrabti Y, Royo C, Villegas D, Aparicio N, del Moral L F G. 2003. Durum wheat quality in Mediterranean environments: I. Quality expression under different zones, latitudes and water regimes across Spain. *Field Crops Research*.**80**:123-131.
- Rios J A, Aucique-Pérez C E, Debona D, Cruz Neto L B, Rios V S, Rodrigues F A. 2017. Changes in leaf gas exchange, chlorophyll a fluorescence and antioxidant metabolism within wheat leaves infected by *Bipolaris sorokiniana*. *Annals of Applied Biology*. **170**:189-203.
- Rolfe S A, Scholes J D. 2010. Chlorophyll fluorescence imaging of plant–pathogen interactions. *Protoplasma*.**247**:163-175.
- Román A E, Miranda M Z de, Tatsch P O, Debona D, Rodríguez E F, Dallagnol L J. 2021. Efeito da fertilização nitrogenada e fungicida no manejo de doenças e na qualidade da farinha de cultivares precoces do trigo. Congreso Nacional De Trigo. Simpósio De Cereales De Siembra Otoño-Invernal 7. Encuentro Del Mercosul.
- Rose S P, Pirgozliev V R, McCracken K J, McNab J M, Miller H M. 2001. Specific weight and quality measurements on the nutritional value of four wheat cultivars for broiler chickens. *Aspects of Applied Biology*.**64**:85-86.
- Rozo-Ortega G P, Serrago R A, Valvo P J Lo, Fleitas M C, Simón M R, Miralles D J. 2021. Grain yield, milling and breadmaking quality responses to foliar diseases in old and modern Argentinean wheat cultivars. *Journal of Cereal Science*.**99**:103211.
- RStudio. 2021. RStudio: Integrated Development Environment for R. RStudio, PBC, Boston, MA. [2021-04-02]. <http://www.rstudio.com/>.
- Ruske R E, Gooding M J, Jones S A. 2003. The effects of adding picoxystrobin, azoxystrobin and nitrogen to a triazole programme on disease control, flag leaf senescence, yield and grain quality of winter wheat. *Crop Protection*. **22**:975–987.
- Samobor V, Vukobratović M, Jošt M. 2005. Effect of powdery mildew (*Erysiphe graminis* d.c. f.sp. *tritici* Marchal) attack on yield and physical parameters of wheat (*Triticum aestivum* ssp. *vulgare*) grain quality (*Triticum aestivum* ssp. *vulgare*). *Poljoprivreda*. **11**:30-37. (in Bosnian)
- Savary S, Willocquet L, Pethybridge S J, Esker P, McRoberts N, Nelson A. 2019. The global burden of pathogens and pests on major food crops. *Nature Ecology & Evolution*. **3**: 430-439.

- Schierenbeck M, Fleitas M C, Simón M R. 2019. Nitrogen fertilization and fungicide mixtures in wheat: how do they affect the severity, yield and dynamics of nitrogen under leaf rust infections?. *European Journal of Plant Pathology*.**155**:1061-1075
- Serrago R A, Valvo P J Lo, Miralles D J. 2019. Is the source-sink ratio at anthesis a driver to avoid yield reductions caused by late foliar disease in wheat? *Field Crops Research*.**235**:11-17.
- Shaner G, Finney R E. 1977. The effect of nitrogen fertilization on the expression of slow-mildewing resistance in Knox wheat. *Phytopathology*.**67**:1051-1056.
- Stack R W, McMullen M P. 2011. A visual scale to estimate severity of Fusarium head blight in wheat. [2020-01-02]. <https://www.ag.ndsu.edu/ndipm/publications/wheat/documents/pp1095.pdf>.
- Strasser R J, Srivastava A, Tsimilli-Michael M. 2000. The fluorescence transient as a tool to characterize and screen photosynthetic samples. *Probing photosynthesis: mechanisms, regulation and adaptation*. 445-483.
- Strasser R J, Tsimilli-Michael M, Srivastava A. 2004. Analysis of the chlorophyll a fluorescence transient. In: Papageorgiou G, Govindjee C, eds, *Chlorophyll a fluorescence*. Springer, Dordrecht, pp. 321-362.
- Swarbrick P J, Schulze-Lefert P, Scholes J D. 2006. Metabolic consequences of susceptibility and resistance (race-specific and broad-spectrum) in barley leaves challenged with powdery mildew. *Plant, Cell & Environment***29**:1061-1076.
- USDA (United States Department of Agriculture). 2021a. Index mundi - Brazilian wheat production during 1960 to 2021. Index mundi. [2021-08-02]. <https://www.indexmundi.com/agriculture/?pais=br&producto=trigo&variable=produccion&l=es>.
- USDA (United States Department of Agriculture) . 2021b. Index mundi - Mundial production of wheat. Index mundi. [2021-08-02]. <https://www.indexmundi.com/agriculture/?producto=trigo&variable=produccion&l=es>.
- USDA (United States Department of Agriculture). 2021c. Index mundi - wheat consumption worldwide. Index mundi. [2021-08-02]. <https://www.indexmundi.com/agriculture/?producto=trigo&variable=consumo-domestico&l=es>.
- Zadoks J C, Chang T T, Konzak C F. 1974. A decimal code for the growth stages of cereals. *Weed Research*. **14**:415-421.

Table 1 Principal components (PC), eigenvalues (λ_i), proportion of variance (PV), and accumulated proportion of variance (APV) by the components.

PC	λ_i	PV	APV
1	9.9	0.56	0.56
2	3.92	0.22	0.77
3	1.76	0.11	0.87
4	0.87	0.05	0.92
5	0.48	0.03	0.95
6	0.29	0.02	0.96
7	0.20	0.01	0.97
8	0.15	0.01	0.99
9	0.18	0.01	0.99
10	0.06	0.003	0.99
11	0.05	0.0025	0.99
12	0.04	0.0023	1
13	0.03	0.0018	1
14	0.03	0.0017	1
15	0.03	0.0018	1
16	0.0017	0.00051	1
17	0.00016	0.00018	1
18	0.00007	0.0000086	1

Table 2 Contribution, in percentage (%) of each attribute in relation to the first two main principal components (PC)

Attribute	CP1	CP2
Tan spot	0.27	-0.13
Powdery mildew	0.22	-0.16
Giberella	0.08	-0.37
Rust	0.04	-0.43
AC	-0.26	-0.21
GFN	0.29	-0.14
L*	-0.24	0.18
a	0.31	-0.06
b	0.30	0.12
C*	0.08	0.29
<i>h</i> *	0.31	0.06
PC	-0.31	-0.07
GI	0.28	0.11
WG	0.30	-0.04
DG	-0.30	0.05
TKW	-0.08	0.43
TW	0.18	0.43
<i>Fv/Fm</i>	-0.10	0.18

AC: ash content, GFN: grain falling number, L*: lightness, a*and b*: chromaticity coordinates, C*: chroma, *h**: hue angle, PC: protein content, GI: gluten index, WG: wet gluten, DG: dry gluten, TKW: thousand kernel weight, TW: test weight, *Fv/Fm*: maximum efficiency of PSII photochemistry.

Table3 Correlation matrix among the attributes evaluated in the study. AUDPCs of tan spot, powdery mildew, FHB and rust; ash content (AC), gain falling number (GFN); whole wheat flour color parameters: lightness (L*), a* and *b chromaticity coordinates, chroma (C*), and hue (*h**); protein content (PC), gluten index (GI), dry gluten (DG), wet gluten (WG); thousand kernel weight (TKW), test weight (TW), and the maximum efficiency of PSII photochemistry (*Fv/Fm*).

Attribute ^a	Tan spot	Powdery mildew	FHB	Leaf rust	AC	GFN	L*	a*	b*	C*	<i>h</i> *	PC	GI	WG	DG	TKW	TW	<i>Fv/Fm</i>
Tan spot	1																	
Powdery mildew	0.8***	1																
FHB	0.52**	0.65***	1															
Leaf rust	0.75***	0.71***	0.6***	1														
AC	0.78***	0.74***	0.49**	0.73***	1													
GFN	-0.77***	-0.81***	-0.61***	-0.71***	-0.65***	1												
L*	0.73***	0.75***	0.55**	0.54**	0.59***	-0.94***	1											
a	-0.66***	-0.66***	-0.510***	-0.50***	-0.53***	0.91***	-0.98***	1										
b	-0.74***	-0.8***	-0.59***	-0.6***	-0.62***	0.96***	-0.98***	0.94***	1									
C*	-0.74***	-0.79***	-0.58***	-0.59***	-0.62***	0.96***	-0.98***	0.95***	1***	1								
<i>h</i> *	0.09ns	-0.03ns	0.07ns	-0.09ns	-0.03ns	-0.28ns	0.47**	-0.59***	-0.3*	-0.33*	1							
PC	0.21ns	0.53**	0.44**	0.33*	0.34*	-0.51**	0.42**	-0.38**	-0.56***	-0.55**	-0.3*	1						
GI	-0.45ns	-0.64***	-0.59***	-0.54**	-0.52**	0.81***	-0.72***	0.71***	0.8***	0.8***	-0.05ns	0.76***	1					
WG	0.28ns	0.56***	0.5**	0.36*	0.36*	-0.66***	0.6***	-0.58***	-0.7***	-0.69***	-0.04ns	0.9***	-0.85***	1				
DG	0.26ns	0.53**	0.44**	0.35*	0.36*	-0.58***	0.56***	-0.53**	-0.67***	-0.66***	-0.1ns	0.82***	-0.74***	0.91***	1			
TKW	-0.68***	-0.67***	-0.54**	-0.78***	-0.69***	0.46**	-0.27ns	0.19ns	0.35*	0.33*	0.36*	-0.26ns	0.38**	-0.21ns	-0.15ns	1		
TW	-0.61***	-0.62***	-0.55**	-0.79***	-0.68***	0.46**	-0.23ns	0.15ns	0.34*	0.32*	0.46**	-0.38**	0.44**	-0.3*	-0.24ns	0.91***	1	
<i>Fv/Fm</i>	-0.53**	-0.55**	-0.4**	-0.47**	-0.41**	0.71***	-0.65***	0.63***	0.68***	0.68***	-0.13ns	-0.48**	0.71***	-0.57***	-0.48**	0.42**	0.42**	1

Significant at ****p* = 0.001; ***p* = 0.01; * *p* < 0.05; ns = not significant

Table 4 Summary statistics from linear mixed model analyses of the effects of fungicide (FU), cultivar (C), nitrogen rates (NR), and their interactions on thousand kernel weight (TKW), test weight (TW), maximum efficiency of PSII photochemistry (F_v/F_m) during 2019 and 2020 growing seasons.

Treatments	TKW (grams)		TW (kg hL ⁻¹)		F_v/F_m	
	df	F value	F value	F value	F value	F value
2019						
Cultivar (C)	1	12.92*		21.35*		277.23*
Fungicide (FU)	1	34.86**		70.11**		358.53ns
Nitrogen rate (NR)	2	0.40ns		2.48ns		0.62ns
C × FU	1	10.89*		17.12*		0.009ns
C × NR	2	3.60*		1.73ns		0.40ns
F × NR	2	0.13ns		1.03ns		34.77*
C × F × NR	2	0.90ns		0.35ns		12.58ns
2020						
Cultivar (C)	1	102.03***		293.40***		96.56*
Fungicide (FU)	1	157.11***		233.19***		229.51**
Nitrogen rate (NR)	2	2.01ns		2.36ns		0.645ns
C × FU	1	69.05**		330.48***		0.44ns
C × NR	2	9.09***		4.29*		4.00*
FU × NR	2	3.02ns		0.79ns		4.27*
C × FU × NR	2	1.57ns		0.05ns		2.49ns

Significant at *** $p = 0.001$; ** $p = 0.01$; * $p < 0.05$; ns = not significant

Table 5 Mean squares and standard errors of fungicide (FU), cultivar (C), and nitrogen rate (NR) on yield, test weight (TW), thousand kernel weight (TKW), and maximum efficiency of PSII photochemistry (F_v/F_m) during 2019 and 2020 growing seasons.

Effect/Contrast	TKW (grams)		TW (kg hL ⁻¹)		F_v/F_m	
	2019	2020	2019	2020	2019	2020
Cultivar (C)						
TBIO Audaz	28.4 + 0.69 a	31.8 + 0.50 a	76.2 + 0.53 a	76.6 + 0.20	0.68 + 0.03 a	0.73 + 0.01 a
TBIO Tibagi	24.9 + 0.69 b	24.6 + 0.50 b	73.1 + 0.53 b	71.7 + 0.20	0.49 + 0.03 b	0.66 + 0.01 b
Fungicide (FU)						
Fungicide (FU)	29.6 + 0.69 a	23.8 + 0.50 b	77.5 + 0.53 a	72.0 + 0.20	0.62 + 0.03	0.75 + 0.01 a
Unsprayed (US)	23.8 + 0.69 b	32.6 + 0.50 a	71.9 + 0.53 b	76.3 + 0.20	0.55 + 0.03	0.64 + 0.01 b
Nitrogen rate (NR)						
Low N	26.5 + 0.53	28.4 + 0.38	75.1 + 0.45	74.6 + 0.25	0.56 + 0.04	0.69 + 0.01
Recommended N	26.8 + 0.53	28.2 + 0.38	74.5 + 0.45	73.9 + 0.25	0.59 + 0.04	0.70 + 0.01
High N	26.6 + 0.53	27.9 + 0.38	74.4 + 0.45	74.0 + 0.25	0.61 + 0.04	0.70 + 0.01
	P value	P value	P value	P value	P value	P value
TBIO Audaz × TBIO Tibagi	0.0369	0.0021	0.0191	0.0004	0.0134	0.05
FU × US	0.0097	0.0011	0.0036	0.0006	0.1546	0.0173
Low N × High N	0.914	0.1237	0.0918	0.1908	0.5096	0.5065
Low N × Recommended N	0.6448	0.7454	0.2315	0.1228	0.7975	0.9299
Recommended N × High N	0.8757	0.4285	0.8841	0.972	0.8855	0.7323

Means followed by the same letter within the same source of variation are not statistically different (Tukey test $p < 0.05$)

Table 6 Summary statistics from linear mixed model analyses of the effects of fungicide (FU), cultivar (C), nitrogen rate (NR), and their interactions of ash content (AC), grain falling number (GFN), protein content (PC), gluten index (GI), dry gluten (DG), and wet gluten (WG) during 2019 and 2020 growing seasons.

Treatments	df	AC	GFN	PC	GI	DG	WG
		<i>F</i> value	<i>F</i> value	<i>F</i> value	<i>F</i> value	<i>F</i> value	<i>F</i> value
2019							
Cultivar (C)	1	5.77ns	153.90***	9.05*	41.45**	7.99*	9.86*
Fungicide (FU)	1	13.7*	0.16ns	2.95ns	1.017ns	0.47ns	0.66ns
Nitrogen rate (NR)	2	6.64**	0.1ns	106.68***	7.86***	25.67***	52.70***
C × FU	1	2.38ns	0.0001ns	0.023ns	0.22ns	0.32ns	0.06ns
C × NR	2	0.46ns	6.19**	10.67***	3.50*	3.95*	4.82*
FU × NR	2	0.94ns	1.54ns	2.05ns	0.69ns	0.51ns	4.41*
C × FU × NR	2	1.56ns	0.76ns	2.15ns	0.61ns	0.78ns	0.32ns
2020							
Cultivar (C)	1	6.6ns	270.46***	114.17**	19.61*	18.68*	22.79*
Fungicide (FU)	1	6.76**	85.42ns	27.59*	1.41ns	7.31ns	7.31ns
Nitrogen rate (NR)	2	22.96**	0.35ns	94.61***	2.68ns	5.54**	5.57**
C × FU	1	0.88ns	5.51ns	5.791ns	1.138ns	2.61ns	2.05ns
C × NR	2	16.64*	0.11ns	7.612***	2.96ns	6.76**	6.95**
FU × NR	2	57.93**	0.57ns	1.73ns	0.68ns	0.19ns	0.17ns
C × FU × NR	2	84.81***	1.01ns	0.081ns	0.68ns	0.81ns	0.78ns

Significant at *** $p = 0.001$; ** $p = 0.01$; * $p < 0.05$; ns = not significant

Table 7 Mean squares and standard errors of fungicide (FU), cultivar (C), and nitrogen rate (NR) on ash content (AC), grain falling number (GFN), protein content (PC), gluten index (GI), dry gluten (DG), and wet gluten (WG) during 2019 and 2020 growing seasons.

Effect/Contrast	AC		GFN		PC		GI		DG		WG	
	(%)		(sec)		(%)				(%)		(%)	
	2019	2020	2019	2020	2019	2020	2019	2020	2019	2020	2019	2020
Cultivar (C)												
TBIO Audaz	1.60 + 0.04	1.81 + 0.03	341 + 6.83 a	406 + 1.92a	14.7 + 0.26 b	14.5 + 0.20 b	95.8 + 3.03 a	99.0 + 6.54 a	9.06 + 0.32 b	6.01 + 0.83 b	26 + 1.21 b	17.0 + 2.61 b
TBIO Tibagi	1.73 + 0.04	1.92 + 0.03	221 + 6.83 b	140 + 1.92b	15.8 + 0.26 a	16.6 + 0.20 a	68.2 + 3.03 b	66.1 + 6.54 b	10.34 + 0.32 a	9.83 + 0.83 a	31.4 + 1.21 a	30.1 + 2.61 a
Fungicide (FU)												
Fungicide (FU)	1.56 + 0.04 b	1.76 + 0.03 b	283 + 6.83	297 + 14.8	14.9 + 0.26	15.0 + 0.20 b	84.1 + 3.03	78.1 + 6.54	9.54 + 0.32	9.12 + 0.83	28 + 1.21	19.8 + 2.61
Unsprayed (US)	1.77 + 0.04 a	1.97 + 0.03 a	279 + 6.83	249 + 14.8	15.6 + 0.26	16.1 + 0.20 a	79.8 + 3.03	86.9 + 6.54	9.86 + 0.32	6.72 + 0.83	29.4 + 1.21	27.2 + 2.61
Nitrogen rate (NR)												
Low N	1.70 + 0.03 a	1.89 + 0.02a	280 + 5.29	275 + 12.9	14.2 + 0.20 c	14.9 + 0.18 c	88.2 + 2.67 a	85.7 + 5.57	8.83 + 0.26 b	7.44 + 0.71 b	25 + 0.931 b	22.0 + 2.27 b
Recommended N	1.67 + 0.03 ab	1.87 + 0.02 ab	281 + 5.29	273 + 12.9	15.4 + 0.20 b	15.6 + 0.18 b	77.6 + 2.67 b	81.8 + 5.57	10.03 + 0.26 a	8.18 + 0.71 a	30.1 + 0.931 a	24.2 + 2.27 a
High N	1.63 + 0.03 b	1.83 + 0.02 b	282 + 5.29	270 + 12.9	16.1 + 0.20 a	16.1 + 0.18 a	80.2 + 2.67 b	80.1 + 5.57	10.24 + 0.26 a	8.14 + 0.71 a	31 + 0.931 a	24.4 + 2.27 a
TBIO Audaz × TBIO Tibagi	0.0956	0.826	0.0011	0.0005	0.0542	0.0018	0.0076	0.0214	0.0663	0.0228	0.0517	0.0175
FU × US	0.0343	0.0173	0.7161	0.0614	0.1535	0.0134	0.3876	0.3200	0.5403	0.0735	0.4749	0.0736
Low N × High N	0.0014	0.3206	0.8977	0.9213	<0.0001	<0.0001	0.0144	0.2527	<0.0001	0.0112	<0.0001	0.0193
Low N × Recommended N	0.2404	0.0771	0.9783	0.6829	<0.0001	<0.0001	0.0008	0.691	<0.0001	0.0173	<0.0001	0.9685
Recommended N × High N	0.1165	0.0013	0.9678	0.8952	<0.0001	<0.0001	0.6196	0.7915	0.5643	0.9869	0.3543	0.0099

Means followed by the same letter within the same source of variation are not statistically different (Tukey test $p < 0.05$)

Table 8 Summary statistics from linear mixed model analyses of the effects of fungicide (FU), cultivar (C) and nitrogen rate (NR) and their interactions on whole wheat flour color parameters lightness (L^*), a^* and b^* chromaticity coordinates, chroma (C^*), and hue angle (h^*) during 2019 and 2020 growing seasons.

Treatments	df	L^*	a^*	b^*	C^*	h^*
		<i>F</i> value	<i>F</i> value	<i>F</i> value	<i>F</i> value	<i>F</i> value
2019						
Cultivar (C)	1	510.57***	222.0***	560.46***	587.24***	5.96ns
Fungicide (FU)	1	30.38**	32.52**	22.43**	26.51**	13.513*
Nitrogen rate (NR)	2	18.7***	11.41*	0.49ns	0.06ns	21.46***
C × FU	1	7.62ns	0.96ns	9.72*	9.45*	0.081ns
C × NR	2	1.72ns	0.13ns	1.65ns	1.47ns	0.21ns
F × NR	2	0.83ns	0.90ns	3.41*	3.24*	0.28ns
C × F × NR	2	2.45ns	2.21ns	5.07**	5.07**	1.42ns
2020						
Cultivar (C)	1	64.71**	138.56**	157.53**	249.02***	11.89*
Fungicide (FU)	1	10.32*	24.12*	26.48*	41.47**	2.68ns
Nitrogen rate (NR)	2	1.94ns	1.76ns	1.29ns	1.01ns	2.49ns
C × FU	1	14.88*	23.29*	2.03ns	5.19ns	11.39*
C × NR	2	0.35ns	0.19ns	4.27*	3.73*	0.31ns
F × NR	2	0.81ns	0.96ns	1.71ns	1.79ns	0.86ns
C × F × NR	2	0.85ns	1.49ns	2.53ns	2.72ns	0.67ns

Significant at *** $p = 0.001$; ** $p = 0.01$; * $p < 0.05$; ns = not significant

Table 9 Mean squares and standard errors of fungicide (FU), cultivar (C), and nitrogen rate (NR) on wholewheat flour color parameters lightness (L*), a* and *b chromaticity coordinates, chroma (C*), and hue angle (*h**) during 2019 and 2020 growing seasons.

Effect/Contrast	L*		a*		b*		C*		h*	
	2019	2020	2019	2020	2019	2020	2019	2020	2019	2020
Cultivar (C)										
TBIO Audaz	80.09 + 0.13 b	79.8 + 0.30 b	3.44 + 0.04 a	3.61 + 0.06 a	13.9 + 0.09 a	12.5 + 0.20 a	13.9 + 0.09 a	13.0 + 0.20 a	75.7 + 0.2	73.9 + 0.31 b
TBIO Tibagi	84.32 + 0.13 a	83.1 + 0.30 a	2.58 + 0.04 b	2.77 + 0.06 b	10.8 + 0.09 b	10.6 + 0.20 b	10.8 + 0.09 b	10.9 + 0.20 b	76.2 + 0.2	75.4 + 0.31 a
Fungicide (FU)										
Fungicide (FU)	82.72 + 0.13 a	82.1 + 0.30 a	2.85 + 0.04 b	3.01 + 0.061 b	11.7 + 0.09 b	11.1 + 0.20 a	12.0 + 0.09 a	11.5 + 0.20	76.3 + 0.2 a	75.0 + 0.31
Unsprayed (US)	81.69 + 0.13 b	80.8 + 0.30 b	3.17 + 0.04 a	3.36 + 0.061 a	12.3 + 0.09 a	11.9 + 0.20 b	12.7 + 0.09 b	12.4 + 0.20	75.5 + 0.2 b	74.3 + 0.31
Nitrogen rate (NR)										
Low N	82.52 + 0.11 a	81.6 + 0.23	2.94 + 0.03 b	3.14 + 0.06	12.01 + 0.07	11.6 + 0.18	12.4 + 0.07	12.0 + 0.19	76.28 + 0.17 a	74.9 + 0.24
Recommended N	82.14 + 0.11 b	81.4 + 0.23	3.03 + 0.03 a	3.21 + 0.06	11.99 + 0.07	11.6 + 0.18	12.4 + 0.07	12.0 + 0.19	75.83 + 0.17 b	74.6 + 0.24
High N	81.96 + 0.11 b	81.3 + 0.23	3.06 + 0.03 a	3.21 + 0.06	11.97 + 0.07	11.5 + 0.18	12.3 + 0.07	11.9 + 0.19	75.71 + 0.17 b	74.5 + 0.24
TBIO Audaz × TBIO										
Tibagi	0.0002	0.0040	0.0007	0.0013	0.0002	0.0011	0.0002	0.0006	0.0924	0.0410
FU × US	0.0118	0.0489	0.0107	0.0162	0.0179	0.0142	0.0142	0.0076	0.0349	0.1998
Low N × High N										
Low N ×	<0.0001	0.2412	0.0001	0.2503	0.8685	0.8824	0.9608	0.7572	<0.0001	0.3166
Recommended N	0.0003	0.9873	0.0012	0.2336	0.5837	0.5208	0.997	0.7593	<0.0001	0.7422
Recommended N ×										
High N	0.1442	0.1839	0.7025	0.991	0.878	0.2642	0.937	0.3355	0.4395	0.0781

Means followed by the same letter within the same source of variation are not statistically different (Tukey test $p < 0.05$)

Table 10 Rheological analysis considering farinograph parameters: water absorption (WA), dough development time (DDT), dough stability (STB), and, mixture tolerance index (MTI) of TBIO Audaz and TBIO Tibagi with fungicide (FU) and unsprayed (US) with three nitrogen rates (low N: 70 kg ha⁻¹, recommended N: 130 kg ha⁻¹, high N: 200 kg ha⁻¹).

Treatment	WA (%)		DDT (min)		STB (min)		MTI (u)	
	2019	2020	2019	2020	2019	2020	2019	2020
TBIO Audaz + FU + Low N	54.3	54.3	1.5	1.5	3.4	3.4	57	57
TBIO Audaz + FU + Recommended N	53.3	53.3	8.2	8.2	14.2	14.2	18	18
TBIO Audaz + FU + High N	55.2	55.2	10.2	10.2	15.0	15.0	20	20
TBIO Audaz + US + Low N	54.3	53.1	2.5	1.9	8.0	7.2	13	25
TBIO Audaz + US + High N	54.1	53.0	2.8	4.9	7.1	9.0	27	40
TBIO Audaz + US+ Recommended N	54.1	53.9	3.0	3.2	8.4	8.3	17	19
TBIO Tibagi + FU + Low N	53.1	54.3	1.9	2.5	7.2	8.0	25	13
TBIO Tibagi + FU+ Recommended N	53.0	54.1	4.9	2.8	9.0	7.1	40	27
TBIO Tibagi + FU + High N	53.9	54.1	3.2	3.0	8.3	8.4	19	17
TBIO Tibagi + US + Low N	54.5	54.5	7.5	7.5	13.0	13.0	18	18
TBIO Tibagi + US + Recommended N	55.6	55.6	10.0	10.0	17.7	17.7	12	12
TBIO Tibagi + US + High N	56.5	56.5	9.9	9.9	16.6	16.6	13	13

PCA

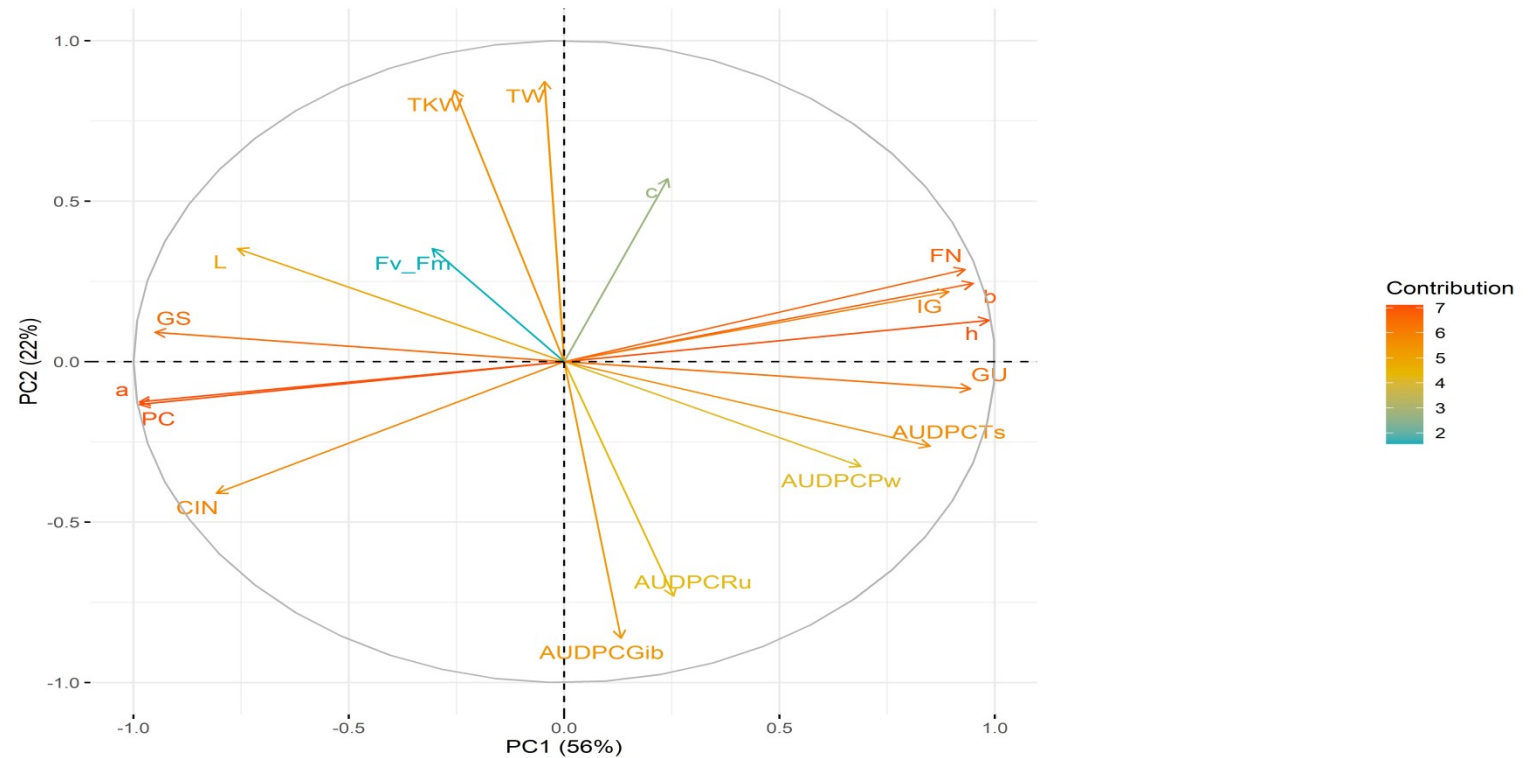


Fig. 1 Principal component analysis with the contribution percentage PC1 and PC2 of AUDPCs of tan spot, powdery mildew, FHB, leaf rust; grain quality variables: ash content (AC), grain falling number (GFN), protein content (PC), gluten index (GI), dry gluten (DG), and wet gluten (WG); color variables: a^* and b^* : chromaticity coordinates, h^* : hue angle, L^* : lightness, C^* : chroma); yield components: TKW: thousand kernel weight, TW: test weight; and F_v/F_m : maximum efficiency of PSII photochemistry. Variables near to orange color show highest contribution to PC1 or 2 than variables near to blue ones.

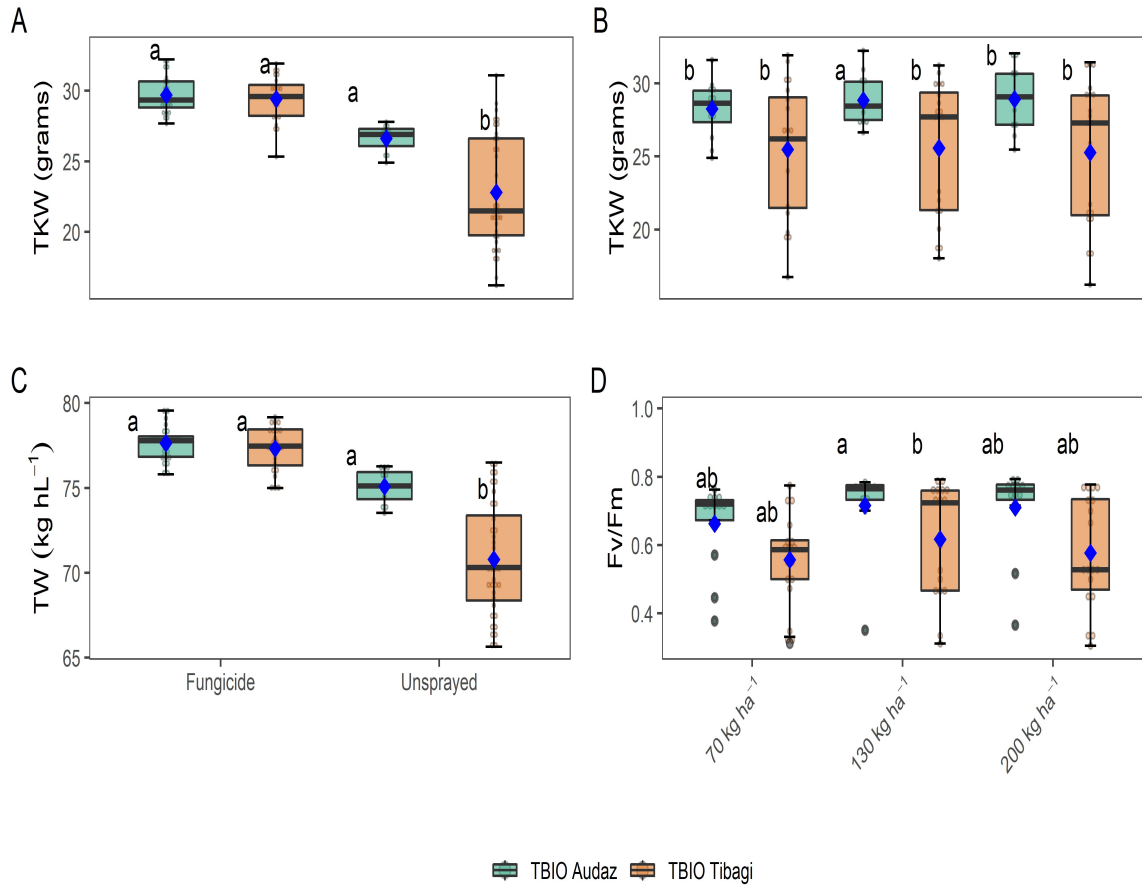


Fig.2 Effect of the cultivar × fungicide interaction on the thousand kernel weight (TKW) (A) and test weight (TW) (C). Cultivar × nitrogen interaction in the thousand kernel weight (TKW) (B) and the maximum efficiency of PSII photochemistry (Fv/Fm) (D). The horizontal line inside the box represents the median, the limits of the box represent the lower and upper quartiles, and the circles represent the observation of each treatment. Data points (♦) are the mean and error bars represent the standard deviation of means. Points (•) correspond to outliers. Different lowercase letters indicate statistical differences according to the Tukey test at $p < 0.05$.

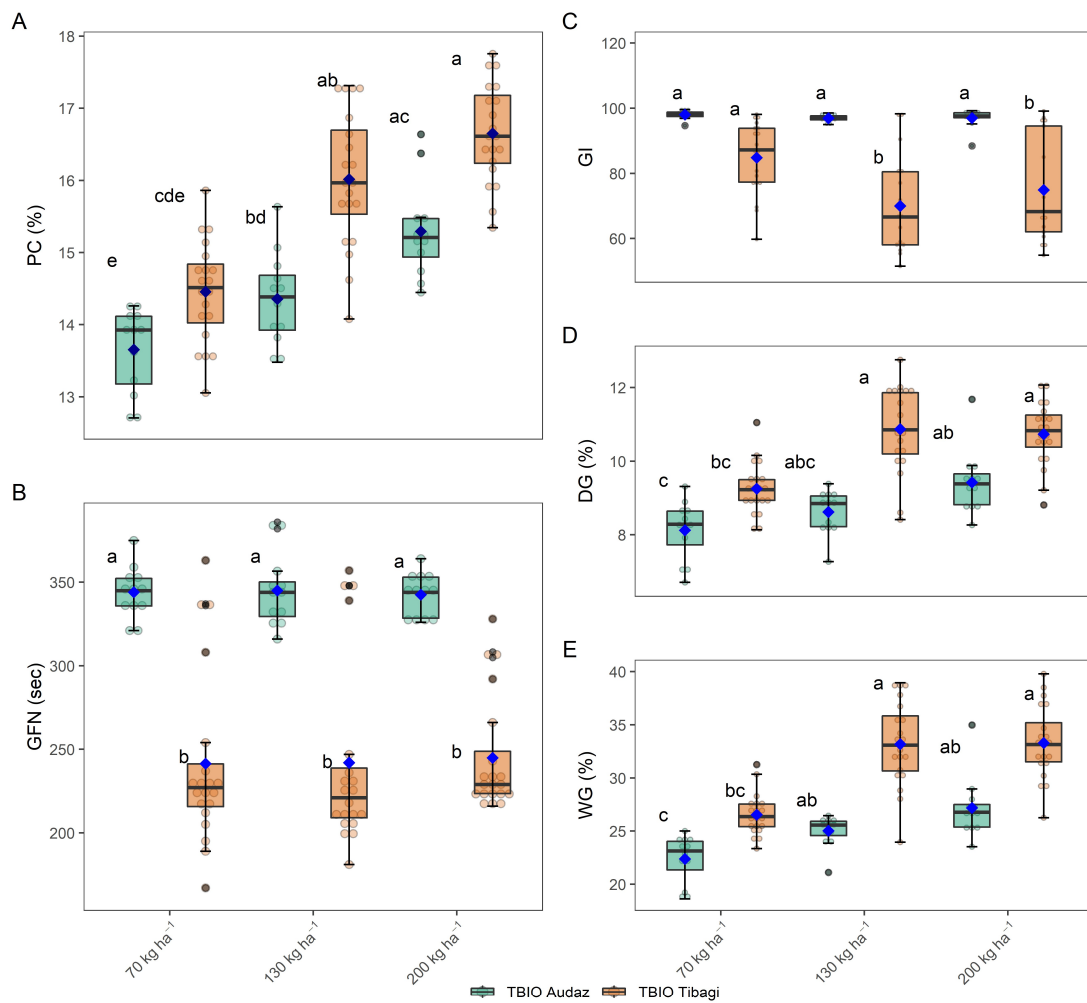


Fig. 3 Effect of cultivar × nitrogen interaction on the protein content (PC) (A), grain falling number (GFN) (B), gluten index (GI) (C), dry gluten (DG) and (D) wet gluten (WG) (E). The horizontal line inside the box represents the median, the limits of the box represent the lower and upper quartiles, and the circles represent the observation of each treatment. Data points (♦) are the mean and error bars represent the standard deviation of means. Points (•) correspond to outliers. Different lowercase letters indicate statistical differences according to the Tukey test at $p < 0.05$.

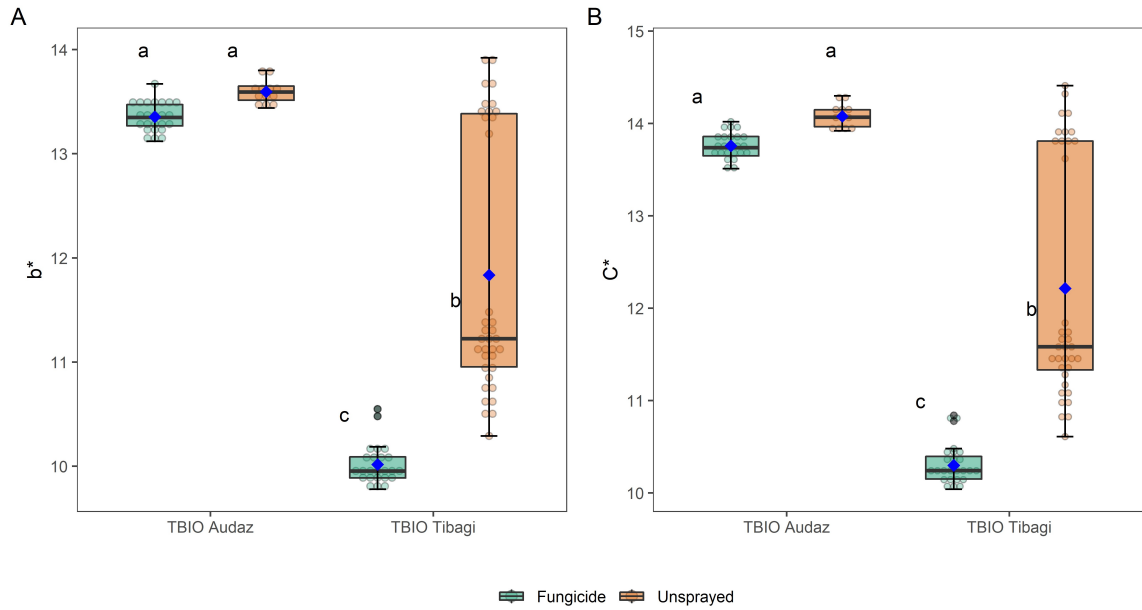


Fig. 4 Effect of cultivar \times fungicide interaction in the whole wheat flour color parameters: b^* chromaticity coordinate (A) and chroma (C^*) (B). The horizontal line inside the box represents the median, the limits of the box represent the lower and upper quartiles, and the circles represent the observations of each treatment. Data points (\blacklozenge) are the mean and error bars represent the standard deviation of means. Points (\bullet) correspond to outliers. Different lowercase letters indicate statistical differences by the Tukey test at $p < 0.05$.

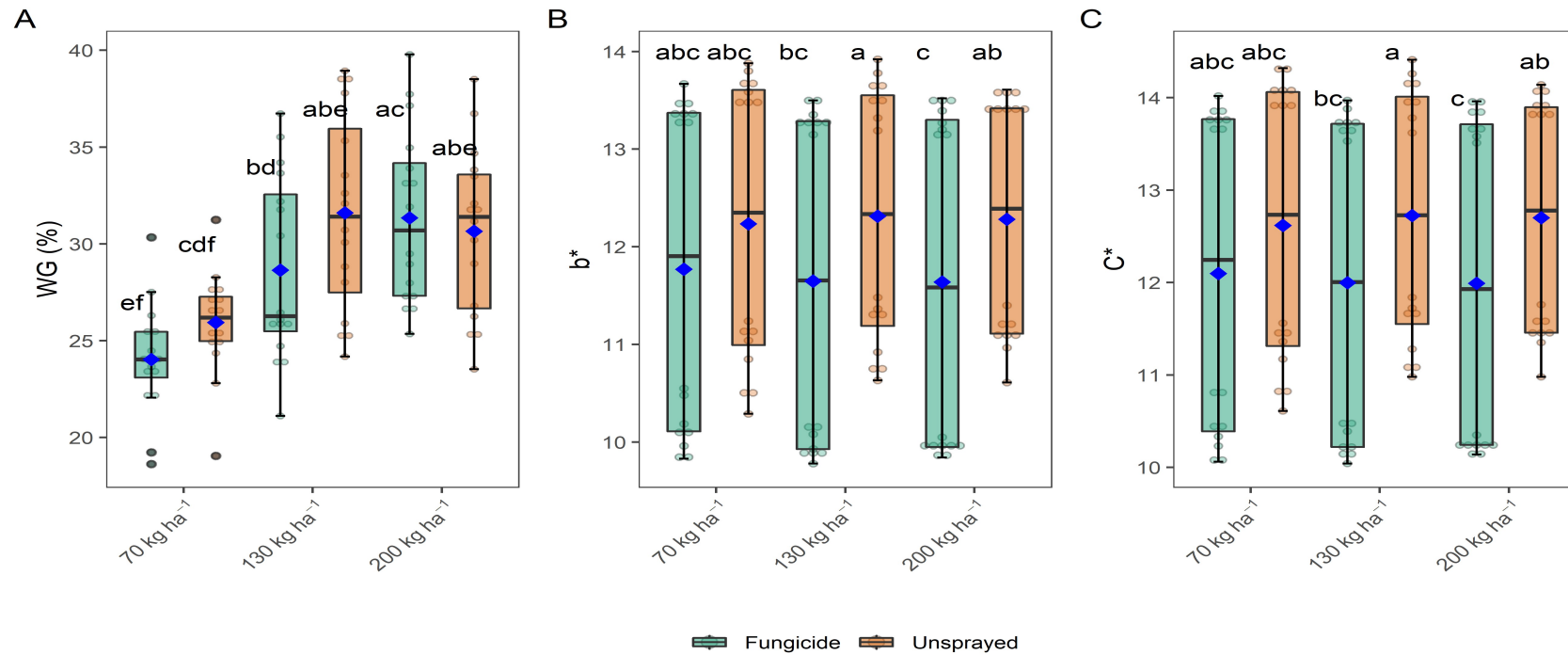


Fig. 5 Effect of fungicide × nitrogen interaction in the wet gluten (WG) (A) and wheat flour color parameters: *b chromaticity coordinate (B) and chroma (C*) (C). The horizontal line inside the box represents the median, the limits of the box represent the lower and upper quartiles, and the circles represent the observation of each treatment. Data points (♦) are the mean and error bars represent the standard deviation of means. Points (•) correspond to outliers. Different lowercase letters indicate statistical differences according to the Tukey test at $p < 0.05$.

Appendix A Soil characteristics of the experiments during 2019 and 2020 growing seasons.

Soil characteristics	2019	2020
Organic matter (%)	1	1,79
Nitrogen (g kg ⁻¹)	0,73	0,93
NO ₃ (g kg ⁻¹)	3,23	4,11
NH ₄ (g kg ⁻¹)	0,94	1,19
Phosphorus (ppm)	20	14
Potassium (mg dm ⁻³)	99	115
Calcium (cmolc.dm ⁻³)	1,7	1,8
Magnesium (cmolc.dm ⁻³)	1,2	1,3
Copper (mg dm ⁻³)	1	0,9
Zinc (mg dm ⁻³)	1,1	0,8
Manganese (mg dm ⁻³)	12,7	21
pH H ₂ O	5,7	6

NO₃: nitrate; NH₄⁺: ammonium

Appendix B Mean of temperature, humidity and total precipitation (July to November) during 2019 and 2020 growing seasons.

Month	2019					2020				
	Temperature maximum (°C)	Temperature minimum (°C)	Temperature mean (°C)	Humidity (%)	Rainfall (mm)	Temperature maximum (°C)	Temperature minimum (°C)	Temperature mean (°C)	Humidity (%)	Rainfall (mm)
July	17.2	4.3	11.6	87.3	130.8	17.2	4.3	11.8	83.5	103.1
August	19.6	9.6	12.5	86.1	103	19.2	10.0	13.7	84.5	49.4
September	18.7	10.4	14.6	83	147.8	18.67	10.41	14.6	86.6	184.2
October	21.9	13.8	18.6	85.1	264.9	21.85	17.27	17.3	82.8	116.7
November	24.5	15.7	21.1	79.1	101.7	24.50	19.85	19.8	79.1	29.1
Mean	20.4	10.8	15.7	84.1	748.2*	20.3	12.4	15.4	83.3	482.5*

*total

The chapter 4 was formatted under the guidelines of the **Plant Pathology**

Effect of nitrogen on wheat cultivars with contrasting resistance infected by *Pyrenophora tritici-repentis*

Andrea Román^{1,3}, Daniel Debona², Eduardo Rodríguez⁴ and Leandro José Dallagnol^{1*}

¹ Pelotas Federal University, Eliseu Maciel Faculty of Agronomy, Crop Protection Department, Laboratory of Plant Pathogen Interaction, 96010-900, Pelotas, Rio Grande do Sul, Brazil.

² Universidade Tecnológica Federal do Paraná - Campus Santa Helena, Agronomy Department, 85892-000, Santa Helena, Paraná, Brazil.

³ Bolívar State University, Agricultural Sciences Natural Resources and the Environment Faculty, Laboratory of Phytopathology, EC020150, Guaranda, Ecuador.

⁴ Grow Green Agricultural Technologies, EC0103, Riobamba, Ecuador.

***Corresponding author:** leandro.dallagnol@ufpel.edu.br

Abstract

Nitrogen (N) fertilization is associated with reduction of tan spot in wheat caused by *Pyrenophora tritici-repentis* (*Ptr*). Therefore, in this study we examined the effect of nitrogen rates, using urea as ammonium source, in wheat genotypes with contrasting resistance during infection by *Ptr* races 1 and 2, by quantifying plant resistance components to tan spot, determining chlorophyll (Chl) *a* fluorescence parameters, and alterations in the chlorophyll content. High N (200 kg ha⁻¹) was associated with increases in the incubation period (IP) of 13% whereas it reduced relative infection efficiency (RIE) and final lesion size (LS) by 34 and 32%. Also, high N was associated with lower severity and area under the disease progress curve (AUDPC) of 39 and 22% compared to low N (70 kg ha⁻¹) respectively, which were associated with higher maximum efficiency of PSII photochemistry (*Fv/Fm*). Despite the high N effect, TBIO Audaz showed lower AUDPC and tan spot severity. Plants inoculated with race 2 suffered slightly higher severity and AUDPC compared to race 1. However, in plants inoculated with race 1, the concentrations of Chl*a*, Chl*b*, carotenoids, Chl*a+b*, and the Chl*a+b*/carotenoids ratio were lower by 32, 54, 39, 40 and 9% compared to plants inoculated with race

2. The chlorophyll a fluorescence (CF), regardless of *Ptr* race, decreased F_v/F_m , the probability of a trapped exciton moving an electron further than Q_A^- (Ψ_o), and the quantum yield of electron transport (ϕE_o). In turn, increase in flux of absorbed (ABS/RC), trapped (TRo/RC), transported (ETo/RC), and dissipated (Dlo/RC) energy per active reaction center were associated with damage caused by necrotrophic *Ptr* races 1 and 2. The result resistance contrasting indicated that the application of the recommended N rate and the use of moderately resistant cultivars maintained adequate CF parameters and enhanced the cultivar resistance.

KEY WORDS: photosystem II, necrotrophic, resistance components, races.

1 INTRODUCTION

Tan spot caused by the necrotrophic fungus *Pyrenophora tritici-repentis* (*Ptr*) (Died.) Drechs. is one of the most important diseases of wheat worldwide (Ciuffetti *et al.*, 2014). In southern Brazil, it is the major leaf disease, as is the case in several other wheat-producing countries (Danelli *et al.*, 2011; Moffat & Santana, 2019), where its prevalence is increasing worldwide (Turner *et al.*, 2021). The pathogen induces tan-colored, necrotic lesions that are often surrounded by chlorotic borders or halos with small dark-brown infection sites (De Wolf *et al.*, 1998). However, in highly resistant or moderately resistant genotypes, reduction of lesion size and lack of chlorotic and necrotic symptoms have been observed, despite the production of toxins (Lamari & Bernier, 1989).

Ptr produces proteinaceous (ToxA and ToxB) and non-proteinaceous (ToxC) host-specific toxins also known as necrotrophic effectors (NEs) (Friesen *et al.*, 2008). *Ptr* ToxA causes necrosis (Meinhardt, 2002; Pandelova *et al.*, 2009) while *Ptr* ToxB and *Ptr* ToxC cause chlorotic lesions (Ciuffetti *et al.*, 2010) in sensitive cultivars. The differential symptoms induced by the absence or secretion of one or more toxins (*Ptr* ToxA, *Ptr* ToxB, or *Ptr* ToxC) that act as pathogenicity/virulence factors in a set of wheat genotypes are used to define the *Ptr* race (Manning & Ciuffetti, 2005; Aboukhaddour *et al.*, 2013). As a result, eight races of *Ptr* are recognized globally (Lamari & Strelkov, 2010). In Brazil, races 1 and 2 are the main ones observed in wheat crops (Bertagnolli *et al.*, 2019). Race 1

(ToxA and ToxC) induces necrosis and chlorosis whereas race 2 (ToxA) causes necrosis.

The chlorosis or necrosis of infected leaves caused by three toxins (ToxA, ToxB, and ToxC), can significantly reduce the total photosynthetic area (Lamari & Strelkov, 2010). Studies of toxin infiltration have demonstrated that ToxA induces cell death, preceded by changes in the photosynthetic machinery and accumulation of reactive oxygen species (ROS), likely due to the disruption of homeostasis of the two photosystems (PSI and II) (Manning *et al.*, 2009). Although less is known about mode of action of ToxC, chlorosis is probably related to the decreased chlorophyll a (*Chla*) and b (*Chlb*) similar to the chlorosis induced by ToxB, and is light-dependent and involves the disruption of photosynthesis and possibly the photooxidation of chlorophyll (Strelkov *et al.*, 1998; Kim *et al.*, 2010).

Nitrogen (N) is an essential element for plant growth. It is assimilated as inorganic N forms such as ammonium (NH_4^+) and nitrate (NO_3^{-2}) (Li *et al.*, 2015), and plays a key role in plant health and yield (Malhi *et al.*, 2001). N is an element necessary to build chlorophyll molecules, and is involved in most of plants' physiological processes, such as the production of amino acids, proteins, enzymes, hormones, phytoalexins and phenolic compounds among other cell components (Huber *et al.*, 1987; Huber & Thompson, 2007). It promotes vigorous plant growth, delays maturity and affects cell size and wall thickness (Huber, 1978, 1980; Huber & Thompson, 2007). In general, N metabolism genes are strongly affected by pathogen infection, probably as a result of both defense activation and attempted pathogen manipulation of host metabolism for nutritional purposes (Fagard *et al.*, 2014)

N is an essential part of physiological processes and at least 75% of N is distributed in the chloroplast organelles (Evans & Clarke, 2019). The impact of pathogen infection on primary metabolism involves cost-intensive plant defense; pathogen manipulation of plant metabolism (up take of sugars and amino acids) (Berger *et al.*, 2007), and reduction of photosynthetic activity and chloroplast metabolism pathways, mainly at the infection site, due to the development of chlorotic and necrotic areas. The main effects observed are reductions in gas exchange rates, impairment of energy dissipation via chlorophyll (Chl) a

fluorescence, increases leaf temperature, structural damages to the chloroplasts causing lower pigment concentration, disruption of carbon and nitrogen metabolism, reduction of mesophyll conductance and biochemical constraints (Berger *et al.*, 2007; Debona *et al.*, 2012; Rios *et al.*, 2017; Fortunato *et al.*, 2018).

It is well known that the N fertilization is involved in susceptibility of plants to pathogens (Huber & Thompson, 2007; Fagard *et al.*, 2014; Mur *et al.*, 2017). In recent decades, many studies have demonstrated that increases in the amount of N fertilizer applied decrease or increase the development of diseases, and that the form of N supply (ammonium or nitrate) affects the diseases intensity (Huber *et al.*, 1987; Huber & Thompson, 2007). In particular, tan spot management through fertilization especially with nitrogen (N), has been studied. Fleitas *et al.* (2018) and Castro *et al.* (2018) found that high N fertilization and fungicide application under field conditions increased the grain yield and reduced tan spot severity.

There is limited information about the physiological alterations due to photoinhibition, damage to the PSII, and chlorophyll alteration induced by *Ptr* races 1 and 2 (effect of nitrogen content and disease damage). Challenge of wheat plants by *Ptr* races 1 and 2 may cause affect in energy dissipation via chlorophyll (Chl) a fluorescence due to the toxin production during host-pathogen interaction, but N rates reduce tan spot severity. Therefore, the present study examined the effect of nitrogen rates using urea as ammonium source, on contrasting wheat genotypes during the infection process of *Pyrenophora tritici-repentis* isolated races 1 and 2, by quantifying tan spot resistant components and changes in Chl a fluorescence parameters and chlorophyll content.

2 MATERIALS AND METHODS

2.1 Plant material and growth

Two wheat (*Triticum aestivum*) cultivars TBIO Audaz (Biotrigo[®]) and TBIO Tibagi (Biotrigo[®]), were chosen among regionally adapted cultivars with similar anthesis and maturity dates, but contrasting resistance to tan spot, the former being more resistant. Seeds were surface sterilized in 10% (vol/vol) NaOCl for 2 min and rinsed in sterilized water for 3 min. Pre-germination was conducted in water stage for 12 h and dry stage for 12 h at 20°C in the dark for 2 days. Then, 5

germinated seeds were transferred to biodegradable seed nursery bags (14×18cm) (Huvai®, USA) containing 475g of soil and 100g of seed starter (Carolina Soil®, Brazil), and kept in a plastic tray (47 × 25 × 10 cm) (Supporting information, Figure S1). After seedling emergence, they were thinned to two plants per bag (experimental units). The plants were grown in a greenhouse with relative humidity of $80 \pm 5\%$ and temperature of $25 \pm 2^\circ\text{C}$.

2.1.2 Soil characteristics and nitrogen treatment

The soil used in the experiment was collected in the experimental area of Pelotas Federal University, located in the municipality of Capão do Leão, Rio Grande do Sul. The physicochemical characteristics of the soil were as follows: 658g kg⁻¹ of sand, 242 g kg⁻¹ of clay; 101g kg⁻¹ of silt; 1.0% of organic matter; 1.5 g kg⁻¹ of N; 6.64 g kg⁻¹ of NO₃⁻; 1.93 g kg⁻¹ of NH₄⁺; 47.7 ppm of phosphorus; 143 mg dm⁻³ of potassium; 2.7 cmolc dm⁻³ of calcium; 1.4 cmolc dm⁻³ of magnesium; 0.9 mg dm⁻³ of copper; 0.8 mg dm⁻³ of zinc; 12.3 mg dm⁻³ of manganese; and pH_{H₂O} of 5.5.

Plant fertilization was performed using a nutritive solution applied in the substrate of each bag. The nutritive solution was adjusted to wheat requirement according to (Silva *et al.*, 2017), composed of 30 kg ha⁻¹ of phosphorus and 100 kg ha⁻¹ of potassium to achieve a yield of 4 tonne ha⁻¹. The nitrogen requirement was applied with nitrogen solution for each treatment adjusted to obtain the three rates under study, classified as low N: 70 kg ha⁻¹; recommended N: 130 kg ha⁻¹; and high N: 200 kg ha⁻¹. The fertilization was applied weekly from the third week after plant emergence at ZGS20 (main shoot) until ZGS33 (third detectable node) in the seventh week. The first nutrient solution was composed of 12.97 g L⁻¹ of phosphorus (KH₂PO₄) and 15.62 g L⁻¹ of potassium (KCl). A volume of 63.5 ml of the nutrient solution (wt/vol) was applied to each bag in the third and fourth week. The three nitrogen solutions (granular urea (wt/vol), N, 45%) were prepared containing: 0.147 g L⁻¹, 0.294 g L⁻¹, or 0.442 g L⁻¹ for low N, recommended N or high N, respectively. A volume of 40 mL of each nitrogen solution was applied per bag of treatment from the fifth to seventh week. All nutrient solutions were prepared using deionized water. The plants were irrigated as needed with deionized water.

2.1.3 Experimental design and treatments

The experimental designs were completely randomized in three-way and four-way factorial with six replicates. For experiment 1 and 2 (resistance components and concentration of photosynthetic pigments), the factorial scheme was $2 \times 3 \times 3$, consisting of two winter wheat cultivars (TBIO Audaz and TBIO Tibagi), three nitrogen doses (low N: 70 kg ha^{-1} , recommended N: 130 kg ha^{-1} and high N: 200 kg ha^{-1}), and plant inoculations (with isolate of *P. tritici-repentis* race 1, race 2, or sprayed with water (mock inoculation)), with six replications. For experiment 3 (determination of Chla fluorescence parameters), the factorial scheme was $2 \times 3 \times 3 \times 12$, consisting of the same two winter wheat cultivars, three nitrogen doses and three plant inoculations, with 12 sampling times (before inoculation (0) and at 24-h intervals from 48 to 312 hai). For nitrogen concentration, the factorial scheme was 2×3 , consisting of the same two winter wheat cultivars and three nitrogen doses and three plant inoculations. Each replication was a bag with two plants. The experiments were performed twice.

2.2 Inoculum production and inoculation procedure

Two pathogenic isolates of *P. tritici-repentis* (BRPtr8 and BRPtr7), classified as race 1 and race 2, respectively, (Bertagnolli *et al.*, 2019), provided by Passo Fundo University, were used to inoculate the plants. The fungal isolates were maintained as PDA mycelium disks at -20°C in a freezer. The isolates were reactivated in PDA for a week, after which a 5 mm diameter mycelial plug was cut from the margin of actively growing colonies and transferred to Petri dishes with modified V8–agar medium (3.0 g L^{-1} of calcium carbonate (Synth, Diadema, Brazil), 150 mL L^{-1} of tomato sauce (Fugini®, Brazil), 15 g L^{-1} of agar (Kasvi, Curitiba, Brazil) and distilled water).

The fungal growth was performed according to the method described by Dorneles *et al.* (2017). Briefly, after fungal growth in the modified V8–agar medium for five days in a growth chamber at $25 \pm 1^{\circ}\text{C}$ in darkness, the fungal colony was stressed by mycelium scraping. Then the fungal colony was exposed for 24 h to light in the growth chamber at $25 \pm 1^{\circ}\text{C}$ to allow development of conidiophores, followed by a further 24 h of darkness at $15 \pm 1^{\circ}\text{C}$ necessary for conidia formation. At the end of seven days, conidia were carefully removed from the Petri dishes

with a soft bristle brush using water containing gelatin (1% wt/vol) and Tween 20. The conidial suspension was adjusted to obtain a concentration of 3×10^3 conidia ml^{-1} .

The conidial suspension was sprayed using a hand-held sprayer (Tecblas, REF: 300 mL/Porto Alegre, Brazil) on the adaxial surface of the leaves of 60-day-old wheat plants at flag leaf stage (GS39) until runoff. After inoculation, the plants were transferred to a plastic mist growth chamber (MGC) inside a greenhouse. The MGC was constructed using plastic pipes (0.95 m wide, 0.90 m high and 0.95 m long) and covered with transparent plastic (150 μm thickness) (Supporting information, Figure S2). The temperature inside the MGC ranged from $25 \pm 3^\circ\text{C}$ (day) to $22 \pm 2^\circ\text{C}$ (night). The relative humidity was maintained at $95 \pm 3\%$ using a misting system (Mondial Confort Air 6 Ua-07) in which a 280 mm \varnothing hosepipe sprayed a constant mist above the plant canopy, and the photoperiod of 12 h during 48 h. Mock-inoculated plants were sprayed with distilled water containing gelatin (1% wt/vol) and Tween 20, and exposed to the same conditions as the inoculated ones. After 48 h, the plants were transferred to a greenhouse with temperature of $25 \pm 3^\circ\text{C}$, relative humidity of $80 \pm 5\%$, and photoperiod of 12 h.

2.3 Disease assessment

Six variables were evaluated on the fourth and flag leaf of the main tiller of each plant, according Pazdiora *et al.*(2018): incubation period (IP), relative infection efficiency (RIE), area under lesion size curve (AULSC), final lesion size (LS), severity (SEV) and area under disease progress curve (AUDPC).

The IP (hours) was assessed by examining leaves every eight hours after inoculation using a 20 \times a magnifying lens, and was defined as the interval between inoculation and the onset of visible symptoms. The RIE was expressed as the ratio between the number of lesions per cm^2 of leaf and the estimated number of conidia per cm^2 after inoculation. To obtain this metric, four slides (26 \times 76 mm) with three pieces of double-sided tape (10 \times 10 mm) were placed randomly on the upper surface of leaves before inoculation, and 24 h later the number of viable conidia deposited on each slide was determinate using a CX-41 light microscope (Olympus[®]). A conidium was considered viable when the germ tube was longer than its central width. The number of lesions per cm^2 was

determined 48 h after IP at five sites (1.0 cm²) defined at random in the central region of each fourth and flag leaf. Five lesions were randomly selected 24 h after IP, identified and monitored daily to measure their individual lengths (mm) using a digital caliper (150 mm, YuanSen[®], 02KC4PR7P1995). The area under the lesion size progress curve (AULSPC) was computed using trapezoidal integration of the lesion size data overtime using the formula proposed by (Shaner & Finney, 1977). The LS was obtained by measuring five lesions randomly per plant at 312 hours after inoculation.

The fourth and flag leaves of each plant (per replication for each treatment) were marked and used to evaluate the tan spot severity visually at 24 h intervals from 48 to 312 h after inoculation (hai) using the Horsfall-Barratt scale at the midpoint (Horsfall & Barratt, 1945). The area under disease progress curve (AUDPC) for each leaf was computed using trapezoidal integration of the tan spot progress curve overtime using the formula according the formula proposed by (Shaner & Finney, 1977). Immediately after the last disease assessment, digital leaf images were obtained at 600 dpi using a scanner (Epson/L395), and final disease severity (SEV) was measured using the digital image analysis software Quant (Vale *et al.*, 2003).

2.4 Chlorophyll a fluorescence (CF)

The CF was determined in the fourth leaf and flag leaf on plants previously marked at ZGS39. The first measurement was performed before inoculation and denominated as 0 h. After plant inoculation, measurements were conducted daily from 48 to 312 hai. The leaves were placed 30 minutes in darkness before the measurements, during 7:30 to 9:30 a.m. The OJIP fluorescence transient was measured using a handheld portable fluorometer (FluorPen FP110, Photon Systems Instruments, Drásov, Czech Republic). The measurements were carried out according Ajigboye *et al.*(2016), including fluorescence intensity at 50 ms, considered as the initial fluorescence value (F_0). The maximum fluorescence level of the OJIP transient (F_m) was measured under saturating light conditions, while intermediate fluorescence values were measured at 300 ms, 2 ms, and 60 ms, and labeled as F_{300ms} , F_j and F_i respectively (Strasser *et al.*, 2000). Polyphasic CF transient was induced by saturating light of 3.000 $\mu\text{mol m}^{-2} \text{s}^{-1}$ and the kinetics

were recorded. The different steps of the OJIP transient were determined with the FluorPen 1.0.0.6 software (Photon Systems Instruments). The parameters obtained from the OJIP analyses were: the maximum efficiency of PSII photochemistry (F_v/F_m), dissipated energy flux (Dlo/RC), electron transport flux (ETo/RC), absorbed photon flux (ABS/RC), trapped energy flux (TRo/RC), probability that a trapped exciton moves an electron further than Q^-A (ψ_o), and quantum yield of electron transport (ϕE_o).

2.5 Determination of the concentration of photosynthetic pigments

The concentrations of chlorophyll *a* (Chla), chlorophyll *b* (Chlb) and carotenoids were determined using dimethyl sulfoxide (DMSO) as extractor (Wellburn, 1994). Five squares (10 × 10 mm) were punched from each fourth and flag leaf in each mock-inoculated and inoculated plant at the end of the experiment. The collected squares were immersed in Falcon tubes containing 5 mL of a saturated DMSO solution and 5 g L⁻¹ calcium carbonate (CaCO₃) (Santos *et al.*, 2008), and kept in the dark for 24 h. The absorbances of the extracts were read at 480, 649 and 665 nm using a saturated solution of DMSO and CaCO₃ as a blank in a spectrophotometer (model UV-UM51-Bel[®]). Data from the concentrations of Chla, Chlb and carotenoids were used to calculate the total chlorophyll concentration (Chla+b) and the total chlorophyll (Chla+b)/carotenoids ratio.

2.6 Nitrogen determination

Leaf samples were taken at the end of experiment. The samples were dried at 60°C for 72 h and ground using a mill (Tecnal R-TE-350). A subsample of 5 g was used for the determination of plant levels of nitrogen (total nitrogen, g kg⁻¹); nitrate (NO₃⁻, g kg⁻¹), and ammonium (NH₄⁺, g kg⁻¹) according to the micro-Kjeldahl method (Bremner & Mulvaney, 1982).

2.7 Data analyses

The statistical analyses were conducted with R version 4.0.4. (RStudio, 2021). The data of the two experiments were analyzed separately. Before the analyses, data assumptions were verified by qq-plots for data normality and plots of fitted values *versus* the residuals to verify homoscedasticity. For experiment 1

and 2, a generalized linear model (GLM) with a logit link and Gaussian family was used to analyses IP, RIE, AUDPLS, AUDPC, and concentration of photosynthetic pigments using 'glm' function of the lme4 package (Bates *et al.*, 2014). After this procedure, data assumptions were verified graphically using the 'simulateResiduals' function from the DHARMA package (Hartig, 2021). For experiment 3, the Chl *a* fluorescence parameters were analyzed by generalized least squares (GSL) using the 'gls' function of the nlme package (Pinheiro *et al.*, 2021) using the residual maximum likelihood (REML) for compute the coefficients. For nitrogen concentration, Levene's test was used to assess whether homoscedasticity could be assumed. After applying parametric ANOVA, the Shapiro-Wilk test was used to ascertain normality of the fitted residuals. These data were analyzed using the base *lm* of R. The mean values of all experiments were estimated with the emmeans package (Lenth, 2021) and compared by the Tukey test ($p < 0.05$) using 'cld' of the multcomp package (Hothorn *et al.*, 2008).

3 RESULTS

3.1 Disease intensity

The factors cultivar, N rate and race were significant ($p < 0.05$) for both tan spot final severity (SEV) and AUDPC (Table 1, Figure 1 and 2). Cultivar was also significant for RIE and LS, while N rate was significant for all resistance components evaluated (Table 1). The interactions cultivar \times race and nitrogen \times race were significant ($p < 0.05$) only for IP and RIE, respectively (Table 1). The RIE and LS were 24 and 17% lower, respectively, for TBIO Audaz compared to TBIO Tibagi (Table 2). The tan spot SEV and AUDPC of TBIO Audaz were significantly lower, by 14 and 19%, respectively, compared with TBIO Tibagi (Table 2 and Figure 1). Nitrogen rates were associated with differences of IP, RIE, LS, AUDPLS, SEV and AUDPC (Table 2). IP was 13% higher with application of high N than low N, but there were no differences between high N and recommended N (Table 2). RIE, LS and AUDPLS were 36, 34, and 32% lower at high compared to low N, but there were no differences between high N and recommended N (Table 2). The SEV on the leaves of high N plants was significantly lower by 39% compared with the low N plants (Table 2, Figure 1A). The AUDPC was reduced by 22 and 15% for the high N and recommended N plants, respectively, in

comparison with the low N plants (Table 2, Figure 1B). The SEV for race 2 was higher by 14% than race 1 (Table 2, Figure 1A, 2 and 3). Likewise, the AUDPC of race 2 was higher by 9% than the AUDPC of race 1 (Table 2, Figure 1A). At high N the lesions were smaller in both cultivars, associated with the higher IP observed (Figure 2).

3.2 Chlorophyll a fluorescence (CF)

The factor cultivar was significant for Fv/Fm , TRo/RC , ETo/RC , Dlo/RC , and Ψ_o , while N rate was significant only for Fv/Fm and TRo/RC (Table 3). Plant inoculation and evaluation time were significant for all parameters (Fv/Fm , ABS/RC , TRo/RC , ETo/RC , Dlo/RC , Ψ_o , and ϕE_o), except ϕE_o for evaluation time (Table 3). Several interactions were also significant ($p < 0.05$).

Fv/Fm , TRo/RC , and ETo/RC were lower for TBIO Tibagi than TBIO Audaz. In turn, Dlo/RC , and Ψ_o were higher for plants of cultivar TBIO Tibagi (Table 4, Figure 4, 5 and 6). At low N rates, Fv/Fm decrease by 2% compared with high N, but there were no differences between recommended and high N rate for all evaluated parameters (Table 4). As a result of tan spot development, changes in Fv/Fm , ABS/RC , TRo/RC , ETo/RC , Dlo/RC , Ψ_o , and ϕE_o were observed in inoculated plants compared with mock-inoculated (Table 4). Plants inoculated with races 1 and race 2 had 5% decreases in Fv/Fm by compared to plants receiving mock-inoculated. Decreases in the Fv/Fm values started at 96 hai, just before to the appearance of the first symptoms, especially in TBIO Tibagi, but remained stable until 192 hai (Table 4, Figure 3). At 216 hai, the Fv/Fm decreased in both cultivars, while at 312 hai, significant decreases by 8 % were observed compared to 0 h (plants before inoculation) (Figure 3). Fv/Fm did not differ between race 1 and race 2 (Table 4).

However, there were differences between the CF parameters in plants inoculated with both races. ABS/RC , ETo/RC , and Dlo/RC values increases by 8 and 5%, 4 and 3%, and 14 and 9% in plants inoculated with race 1 and race 2, respectively, whereas TRo/RC increased by 5% in plants inoculated with both races compared to plants mock-inoculated (Table 4, Figure 4). The values of Ψ_o and ϕE_o decreased by 5 and 7 %, and 6 and 8 % in plants inoculated with race 2 and race 1, respectively, compared to plants mock-inoculated (Table 4, Figure 5).

The ABS/RC increased at 168 hai and 312 hai ABS/RC by 6 and 7 % compared to 0 h (Table 4, Figure 4A). The TRo/RC values, increased by 6 and 7% at 168 hai and 312 hai, respectively, compared to 0 h (Table 4, Figure 4B). The ETo/RC values increase by 5% at 168 hai and 8% at 312 hai compared to 0 h (Table 4, Figure 4C). An increase of 8% in Dlo/RC values was observed at 168 hai compared to 0 h, and thereafter the values were constantly higher by 14% until 312 hai (Table 4, Figure 4D). The Ψ_o value was 8% lower at 96 hai by compared to 0 hai, while from 120 to 312 hai, the Ψ_o values were constant (Table 4, Figure 5A). ϕE_o values decreased with time and the highest decrease was observed at 72 hai by 8 % compared to 0 hai. The values then remained constant until 288 hai, but at 312 hai a decrease of 9 % was observed in comparison with 0 hai (Table 4, Figure 5B).

3.3 Concentration of photosynthetic pigments

The factors cultivar (C) and inoculation (I) and the C \times I interaction were significant for the concentrations of Chla, Chlb, Chla+b, and the Chla+b/carotenoids ratio ($p < 0.05$). The C \times NR \times I interaction was significant ($p < 0.05$) for Chla (Table 5, Figure 6 and 7).

The concentrations of Chla, Chlb, carotenoids, Chla+b, and the Chla+b/carotenoids ratio were significantly higher, by 3, 10, 9, 6 and 1%, respectively, for cultivar TBIO Audaz in comparison with TBIO Tibagi (Table 6, Figure 6 and 7B). The concentrations of Chla, Chlb, carotenoids, and Chla+b, as well as the Chla+b/carotenoids ratio in plants inoculated with race 1 and race 2 were significantly lower, by 92 and 31%, 288 and 78%, 193 and 82%, 115 and 45%, 26 and 15%, respectively, compared to plants mock-inoculated (Table 6, Figure 6 and 7). In plants inoculated with race 1, the concentrations of Chla, Chlb, carotenoids, Chla+b, and the Chla+b/carotenoids ratio were lower by 47, 119, 61, 66 and 10% compared to plants inoculated with race 2 (Table 6, Figure 6 and 7).

3.4 Leaf N concentration

The nitrogen concentration in plants varied according the N rates being significantly ($p < 0.05$) for total nitrogen, NH_4^+ and NO_3^- whereas the C \times N interaction was significant ($p < 0.05$) for NH_4^+ and NO_3^- (Table 7, Figure 8). The total

nitrogen was different for cultivars, being 5% higher for TBIO Audaz compared to TBIO Tibagi. However, there were no differences of NH_4^+ and NO_3^- between cultivars. The total nitrogen at recommended and high N were higher by 22 and 29% compared to low N. NH_4^+ concentration was higher by 134 and 70% compared with low and recommended N (Table 7). The C \times N interaction showed that the NH_4^+ concentration was higher TBIO Audaz and TBIO Tibagi at high N by 221 and 83% compared to TBIO Audaz and TBIO Tibagi at low N, respectively. For NO_3^- , the concentration was higher for TBIO Audaz at high N by 77% compared to TBIO Audaz at low N. The concentration of NO_3^- in TBIO Audaz and TBIO Tibagi at other N rates was not different (Figure 8).

4 DISCUSSION

Tan spot is an important wheat disease worldwide. The pathogen exhibits wide genetic variability, which explains its ability to cause different symptoms in a differential series of genotypes, which are used to classify the races of *Ptr*. In this experiment, the differences observed in severity caused by races 1 and 2 of *Ptr* were associated with the differences in partial resistance between the two cultivars as well as the nitrogen rates supplied. The higher RIE and LS in TBIO Tibagi demonstrated its higher susceptibility to *Ptr*. This observation agreed with previous reports that increases in the tan spot severity were associated with high RIE and LS in susceptible cultivars affected by *Ptr* (Dorneles *et al.*, 2017, 2018; Pazdiora *et al.*, 2018).

Higher nitrogen rates were associated with less severe damage. Also, increments in IP, and reduction in RIE, LS, and AUDPLS indicated that *Ptr*, regardless of the races, developed slower in plants receiving higher N rates. These findings are consistent with those of Fleitas *et al.* (2018), who reported reduction in AUDPC of tan spot at high N. Some studies had been reported that higher nitrogen rates increase the green leaf area index (GLAI) and prompting delay in senescence due to higher radiation interception and radiation use efficiency (RUE), in turn reducing the disease severity (Hawkesford, 2014; Schierenbeck *et al.*, 2016; Fleitas *et al.*, 2018). In this sense, the increment in the resistance components to tan spot at higher N may be associated with the modification of the plant structure, whereas *Ptr* takes advantage of the initially colonized senescent

tissues with less N content instead of healthy tissues (Bockus & Davis, 1993). Furthermore, higher N content effects on the pathogen may be related to the N form (Huber & Thompson, 2007), and the activation of different signaling pathways. We observed that NH_4^+ was the form with greatest concentration at higher nitrogen rate after its absorption by the plant, suggesting that higher NH_4^+ concentration may be associated with the reduction of *Ptr* development in plant tissue. In contrast, for some pathosystems, higher NH_4^+ was found to increase the severity, such as the case of rice blast (*Piricularia oryzae*) (hemibiotroph), while NO_3^- increased the severity of *Blumeria graminis* (biotroph), suggesting that nitrogen-induced susceptibility depends on physiological changes (Huber & Thompson, 2007). However, further studies are necessary to confirm these results.

The effects on PSII as well as the effect of the concentration of photosynthetic pigments were evident, as indicated by the changes in chlorophyll a fluorescence. The pigments' concentration was lower for TBIO Tibagi (susceptible) than TBIO Audaz (moderate resistant). This effect is associated with the photooxidative conditions caused by pathogens in the infected tissue, particularly the reduced concentration of photosynthetic pigments (Murchie & Horton, 1997). Also, it is associated with the fact that *Ptr* ToxA affected chloroplasts, altering the function of a ROS-detoxifying enzyme in the chloroplasts (Manning *et al.*, 2009; Ciuffetti *et al.*, 2014). Furthermore, the differences in concentrations of Chla, Chlb, Chla+b, carotenoids and the Chla+b/carotenoids ratio indicated that these parameters declined more in plants exposed to race 1 than race 2, although, the little to higher severity, associated with the race 2 in TBIO Tibagi. Nevertheless, both races possess the same ToxA, Friesen *et al.* (2003) suggested that race 2 possesses a host range determinant or other determinants than *Ptr* ToxA, indicating that race 2 only carries *Ptr* ToxA, so it may be a virulence factor rather than a pathogenicity factor at least for some wheat genotypes, and it is mainly influenced by the rate of lesion formation. However, this observation has not been confirmed so far. In this sense, it is suggested that the susceptibility may be associated with cultivar and the interaction with nitrogen rates, and the virulence of race 2 is associated with the rapid attack and colonization of senescent tissues, allowing the rapid spread to healthy tissue, resulting in a little

higher increase in severity compared to race 1. Further studies are needed to determine the races effects on cultivars.

The difference observed in chlorophyll *a* fluorescence between mock-inoculated and *Ptr* inoculated plants indicated strong stresses caused by *Ptr* in PSII. Mock-inoculated plants showed values of *Fv/Fm* between 0.8 and 0.83, but in *Ptr*-inoculated plants this value was lower due to stressed plants increasing the photoinhibition and damage to PSII (Björkman & Powles, 1984). As a result, daily evaluations showed that *Fv/Fm* reduces in both cultivars, but for TBIO Tibagi, the reduction was higher at low N due to the higher RIE and LS caused by *Ptr*. Those results are similar to previous observation on *Bipolaris sorokiniana* in wheat by Rios *et al.*(2017) who reported that infected plants suffered a progressive decrease of photosynthesis (measured by *Fv/Fm* and photochemical yield of photosystem II (Φ PSII)) correlated with the expansion of lesions as well as a progressive loss of chlorophyll. The greatest decrease of *Fv/Fm* was observed at 312 hai, but no significant differences were observed between the *Ptr* races, indicating that the severity differs according the nitrogen concentration and cultivar susceptibility.

In addition, in this study, we observed that Ψ_o and ϕE_o were lower in plants inoculated with race 2 than race 1 while ABS/RC, TRo/RC, ETo/RC, and DIo/RC were more strongly affected in plants inoculated with race 1. In this case, the interaction between components of the PSII complex and toxins produced by *Ptr* during the attack affected the active PSII reaction centers, reducing the photosynthesis efficiency. This observation agreed with the fact that ToxA induced cell death due to the disruption of photosystems (PSI and II) (Manning *et al.*, 2009). As a result, the biotic stress caused by the infection of a necrotrophic pathogen may first cause reduction of *Fv/Fm*, Ψ_o , and ϕE_o and then an increase of DIo/RC, ABS/RC, ETo/RC, and TRo/RC during the evaluation. These effects may be associated with the accumulation of inactive reaction centers, increasing the efficiency of dissipation of absorbed light as heat, as shown by the significantly higher values of DIo/RC, ABS/RC, ETo/RC, and TRo/RC, indicating the activation of non-photochemical processes, similar to reports of Pérez-Bueno *et al.* (2019) and Ajigboye *et al.* (2016).

Furthermore, the increased photooxidative damage in inoculated plants of cultivar TBIO Tibagi was also associated with the progressive increase of Dlo/RC values, declined of Fv/Fm and alteration in chlorophylls content in comparison with cultivar TBIO Audaz demonstrated an ineffective regulatory mechanism of photoprotection. In this way, to avoid the photooxidative damage, some mechanism such as xanthophyll cycle and carotenoids, for example, lutein, play a role in PSII heat dissipation (Pogson et al., 1998; Demmig-Adams & Adams, 1993; Gilmore & Yamamoto, 2001). Our results suggest that xanthophyll cycle can be involved in dissipating excess excitation energy.

In this study, the effect of the higher RIE and LS in a susceptible cultivar was associated with lower Fv/Fm and loss of chlorophyll pigments due to the effect of *Ptr*. The evaluation of chlorophyll *a* fluorescence indicated that decreases Fv/Fm , Ψ_o and ϕE_o and increases of Dlo/RC, ABS/RC, ETo/RC and TRo/RC were associated with the damage to PSII caused by *Ptr* races 1 and 2. At low N, the reduction of Fv/Fm was associated with higher severity, because weaker plants are unable to defend themselves, while high N and N equal to the recommended dose altered the resistance components, reducing *Ptr* damage regardless the race. Therefore, wheat management with the incorporation of nitrogen at the recommended rate (130 kg ha^{-1}) is necessary, because it will improve chlorophyll *a* fluorescence parameters while promoting the resistance components in cultivars with moderate resistance, as well as in susceptible ones.

ACKNOWLEDGEMENTS

The authors are thankful to the Office to Coordinate Improvement of Higher Education Personnel (CAPES) for financial support and the student scholarships (finance code 001) to A. R. and L. J. D. were supported by fellowships from the Brazilian National Council for Scientific and Technological Development (CNPq) (grant number 308149/2018-1). We thank to Passo Fundo University for providing the *P. tritici-repentis* isolates used in the experiments, Grow Green for the preparation of spreadsheets of fertilization recommendation for the experiments, and BIOTRIGO for providing wheat seeds for the experiments.

REFERENCES

- Aboukhaddour, R., Turkington, T.K. & Strelkov, S.E. (2013) Race structure of *Pyrenophora tritici-repentis* (tan spot of wheat) in Alberta, Canada. *Canadian Journal of Plant Pathology*, 35, 256-268.
- Ajigboye, O.O. Bousquet, L., Murchie, E.H. & Ray, R.V. (2016) Chlorophyll fluorescence parameters allow the rapid detection and differentiation of plant responses in three different wheat pathosystems. *Functional plant biology*, 43, 356-369.
- Dos Anjos, L., Oliva, M.A. & Kuki, K.N. (2012) Fluorescence imaging of light acclimation of Brazilian Atlantic forest tree species. *Photosynthetica*, 50, 95-108.
- Bates, D., Mächler, M., Bolker, B. & Walker, S. (2014) Fitting linear mixed-effects models using lme4. *arXiv preprint, arXiv:1406.5823*.
- Berger, S., Sinha, A.K. & Roitsch, T. (2007) Plant physiology meets phytopathology: plant primary metabolism and plant-pathogen interactions, *Journal of Experimental Botany*, 58, 4019-4026.
- Bertagnolli, V.V. Ferreira, J.R., Liu, Z., Rosa, A.C. & Deuner, C.C. (2019) Phenotypical and genotypical characterization of *Pyrenophora tritici-repentis* races in Brazil. *European Journal of Plant Pathology*, 154, 995-1007.
- Björkman, O. & Powles, S.B. (1984) Inhibition of photosynthetic reactions under water stress: interaction with light level. *Planta*, 161, 490-504.
- Bockus, W.W. & Davis, M.A. (1993) Effect of nitrogen fertilizers on severity of tan spot of winter wheat. *Plant Disease*, 77, 508.
- Bremner, J.M. & Mulvaney, Y.C. (1982) Nitrogen total, in *Methods of Soil Analysis. Part 2. Chemical and Microbiological Properties. Agronomy Monograph 9*. Madison, WI, USA: American Society Agronomy and Soil Science Society America, pp. 595-624.
- Castro, A.C., Fleitas, M.C., Schierenbeck, M., Gerard, G.S. & Simón, M.R. (2018) Evaluation of different fungicides and nitrogen rates on grain yield and bread-making quality in wheat affected by *Septoria tritici* blotch and yellow spot. *Journal of Cereal Science*, 83, 49-57.
- Ciuffetti, L.M., Manning, V.A., Pandelova, I., Betts, M.F., & Martinez, J.P. (2010) Host-selective toxins, *Ptr ToxA* and *Ptr ToxB*, as necrotrophic effectors in the *Pyrenophora tritici-repentis*-wheat interaction. *New Phytologist*, 187, 911-919.
- Ciuffetti, L.M., Manning, V.A., Pandelova, I., Faris, J.D., Friesen, T.L., Strelkov, S.E., Weber G.L., Goodwin S.B., Wolpert T.J. & Figueroa, M. (2014) *Pyrenophora tritici-repentis*: a plant pathogenic fungus with global impact. In: Dean R., Lichens-Park A., Kole C. (Eds.) *Genomics of Plant-Associated Fungi: Monocot Pathogens*. Berlin: Springer, pp. 1-39.

- Danelli, A.L., Reis, E.M. & Fiallos, F.R. (2011) Etiologia e intensidade de manchas foliares em cultivares de trigo em três locais do Rio Grande do Sul, Brasil. *Scientia Agropecuaria*, 2, 149-155.
- Debona, D., Rodrigues, F.Á., Rios, J.A. & Nascimento, K.J. (2012) Biochemical changes in the leaves of wheat plants infected by *Pyricularia oryzae*. *Phytopathology*, 102, 1121-1129.
- Demmig-Adams, B. & Adams, W.W. (1993). The xanthophyll cycle. In: *Carotenoids in photosynthesis*. Dordrecht: Springer, pp. 206-251.
- De Wolf, E.D., Effertz, R.J., Ali, S. & Francl, L.J. (1998) Vistas of tan spot research. *Canadian Journal of Plant Pathology*, 20, 349-370.
- Dorneles, K.R., Dallagnol, L.J., Pazdiora, P.C., Rodrigues, F.A. & Deuner, S. (2017) Silicon potentiates biochemical defense responses of wheat against tan spot. *Physiological and Molecular Plant Pathology*, 97, 69-78.
- Dorneles, K.R., Pazdiora, P.C., Hoffmann, J.F., Chaves, F.C., Monte, L.G., Rodrigues, F.A. & Dallagnol, L.J. (2018) Wheat leaf resistance to *Pyrenophora tritici-repentis* induced by silicon activation of phenylpropanoid metabolism. *Plant Pathology*, 67, 1713-1724.
- Evans, J.R. & Clarke, V.C. (2019) The nitrogen cost of photosynthesis. *Journal of Experimental Botany*, 70, 7-15.
- Fagard, M., Launay, A., Clément, G., Courtial, J., Dellagi, A., Farjad, M., Krapp, A., Soulié M.C. & Masclaux-Daubresse, C. (2014) Nitrogen metabolism meets phytopathology. *Journal of Experimental Botany*, 65, 5643-5656.
- Fleitas, M.C., Schierenbeck, M., Gerard, G.S., Dietz, J.I., Golik, S.I. & Simón, M.R. (2018) Breadmaking quality and yield response to the green leaf area duration caused by fluxapyroxad under three nitrogen rates in wheat affected with tan spot. *Crop Protection*, 106, 201-209.
- Fortunato, A.A., Debona, D., Aucique-Pérez, C.E., Fialho Corrêa, E. & Rodrigues, F.A. (2018) Chlorophyll a fluorescence imaging of soya bean leaflets infected by *Corynespora cassiicola*. *Journal of Phytopathology*, 166, 782-789.
- Friesen, T.L., Ali, S., Kianian, S., Francl, L.J. & Rasmussen, J.B. (2003) Role of host sensitivity to *Ptr* ToxA in development of tan spot of wheat. *Phytopathology*, 93, 397-401.
- Friesen, T.L., Xu, S.S. & Harris, M.O. (2008) Stem Rust, tan spot, stagonospora nodorum blotch, and hessian fly resistance in langdon durum–synthetic hexaploid wheat lines. *Crop Science*, 48, 1062.
- Gilmore, A.M. & Yamamoto, H.Y. (2001). Time-resolution of the antheraxanthin and pH-dependent chlorophyll a fluorescence components with photosystem II energy dissipation in *Mantoniella squamata*. *Photochemistry and Photobiology*, 74, 291-302.

- Hartig, F. (2021) DHARMA: Residual diagnostics for hierarchical (multi-level/mixed) regression models. R package version 0.4.1. Available at: <https://cran.r-project.org/package=DHARMA%0A>.
- Hawkesford, M.J. (2014) Reducing the reliance on nitrogen fertilizer for wheat production. *Journal of Cereal Science*, 59, 276-283.
- Horsfall, J.G. & Barratt, R.W. (1945) An improved grading system for measuring plant diseases, *Phytopathology*, 35, 65.
- Hothorn, T., Bretz, F. & Westfall, P. (2008) Simultaneous inference in general parametric models. *Biometrical Journal*, 50, 346-363.
- Huber, D.M., Lee, T.S., Ross, M.A. & Abney, T.S. (1987) Amelioration of tan spot-infected wheat with nitrogen. *Plant Disease*, 71, 49-50.
- Huber, D. & Thompson, I. (2007) Nitrogen and plant disease, in Datnoff, L., Elmer, W., and Huber, D. (eds) *Mineral Nutrition and Plant Disease*. St Paul, MA: APS Press, pp. 31-44.
- Kim, Y.M., Bouras, N., Kav, N.N. & Strelkov, S.E. (2010) Inhibition of photosynthesis and modification of the wheat leaf proteome by *Ptr* ToxB: a host-specific toxin from the fungal pathogen *Pyrenophora tritici-repentis*. *Proteomics*, 10, 2911-2926.
- Lamari, L. & Bernier, C.C. (1989) Evaluation of wheat lines and cultivars to tan spot [*Pyrenophora tritici-repentis*] based on lesion type. *Canadian Journal of Plant Pathology*, 11, 49-56.
- Lamari, L. & Strelkov, S.E. (2010) Minireview/ Minisynthèse The wheat/*Pyrenophora tritici-repentis* interaction: progress towards an understanding of tan spot disease. *Canadian Journal of Plant Pathology*, 32, 4-10.
- Lenth, R. (2021) emmeans: Estimated Marginal Means, aka Least-Squares Means. R package version 1.6.0'. Available at: <https://cran.r-project.org/package=emmeans>.
- Li, Y., Ouyang, J., Wang, Y.Y., Hu, R., Xia, K., Duan, J. & Zhang, M. (2015) Disruption of the rice nitrate transporter OsNPF2.2 hinders root-to-shoot nitrate transport and vascular development. *Scientific Reports*, 5, 1-10.
- Malhi, S.S., Grant, C.A., Johnston, A.M. & Gill, K.S. (2001) Nitrogen fertilization management for no-till cereal production in the Canadian Great Plains: a review. *Soil and Tillage Research*, 60, 101-122.
- Manning, V.A., Chu, A.L., Steeves, J.E., Wolpert, T.J. & Ciuffetti, L.M. (2009) A host-selective toxin of *Pyrenophora tritici-repentis*, *Ptr* ToxA, induces photosystem changes and reactive oxygen species accumulation in sensitive wheat. *Molecular Plant-Microbe Interactions*, 22, 665-676.
- Manning, V.A. & Ciuffetti, L.M. (2005) Localization of *Ptr* ToxA produced by *Pyrenophora tritici-repentis* reveals protein import into wheat mesophyll cells. *The Plant Cell*, 17, 3203-3212.

- Meinhardt, S.W. (2002) Role of the arginyl-glycyl-aspartic motif in the action of *Ptr ToxA* produced by *Pyrenophora tritici-repentis*. *Plant Physiology*, 130, 1545-1551.
- Moffat, C.S. & Santana, F.M. (2019) Diseases affecting wheat: tan spot. In: Oliver, R. (Ed.) *Integrated disease management of wheat and barley*. Cambridge, UK: Burleigh Dodds Science Publishing Limited, pp. 1-13.
- Mur, L.A.J., Simpson, C., Kumari, A., Gupta, A.K. & Gupta, K.J. (2017) Moving nitrogen to the centre of plant defence against pathogens. *Annals of Botany*, 119, 703-709.
- Murchie, E.H. & Horton, P. (1997) Acclimation of photosynthesis to irradiance and spectral quality in British plant species: chlorophyll content, photosynthetic capacity and habitat preference. *Plant, Cell and Environment*, 20, 438-448.
- Pandelova, I., Betts, M.F., Manning, V.A., Wilhelm, L.J., Mockler, T.C. & Ciuffetti, L.M. (2009) Analysis of transcriptome changes induced by *Ptr ToxA* in wheat provides insights into the mechanisms of plant susceptibility. *Molecular Plant*, 2, 1067–1083.
- Pazdiora, P.C., da Rosa Dorneles, K., Forcelini, C.A., Del Ponte, E.M. & Dallagnol, L.J. (2018) Silicon suppresses tan spot development on wheat infected by *Pyrenophora tritici-repentis*. *European Journal of Plant Pathology*, 150, 49-56.
- Pérez-Bueno, M.L., Pineda, M. & Barón, M. (2019) Phenotyping plant responses to biotic stress by chlorophyll fluorescence imaging. *Frontiers in Plant Science*, 10, 1135.
- Pinheiro, J., Bates, D., DebRoy, S. & Sarkar, D. (2021) *nlme: Linear and nonlinear mixed effects models, R package version 3.1-152*. Available at: <https://cran.r-project.org/package=nlme> [Accessed: August 10, 2021].
- Pogson, B., Niyogi, K.K., Bjorkman, O. & Dellapenna, D. (1998). Altered xanthophylls compositions adversely affect chlorophyll accumulation and nonphotochemical quenching in *Arabidopsis* mutants. *Proceedings of National Academy of Sciences, USA* 95, 13324-13329.
- Rios, J.A., Aucique-Pérez, C.E., Debona, D., Cruz Neto, L.B. M., Rios, V.S. & Rodrigues, F.A. (2017) Changes in leaf gas exchange, chlorophyll a fluorescence and antioxidant metabolism within wheat leaves infected by *Bipolaris sorokiniana*. *Annals of Applied Biology*, 170, 189-203.
- RStudio (2021) RStudio: Integrated Development Environment for R. RStudio, PBC, Boston, MA'. Available at: <http://www.rstudio.com/>.
- Santos, R.P., Cruz, A.C., Iarema, L., Kuki, K.N. & Otoni, W.C. (2008) Protocolo para extração de pigmentos foliares em porta-enxertos de videira micropropagados. *Ceres*, 55, 356-364.
- Schierenbeck, M., Fleitas, M.C., Miralles, D.J. & Simón, M.R. (2016) Does radiation interception or radiation use efficiency limit the growth of wheat

inoculated with tan spot or leaf rust?. *Field Crops Research*, 199, 65-76.

Shaner, G. & Finney, R.E. (1977) The effect of nitrogen fertilization on the expression of slow-mildewing resistance in knox wheat. *Phytopathology*, 67, 1051–1056.

Silva, S.R., Bassoi, M.C. & Foloni, J.S.S. (2017) *Informações Técnicas para Trigo e Tricale- Safra 2017*. Brasília: Embrapa. Available at: <http://ainfo.cnptia.embrapa.br/digital/bitstream/item/155787/1/Informacoes-Tecnicas-para-Trigo-e-Triticale-Safra-2017-OL.pdf>.

Strasser, R.J., Srivastava, A. & Tsimilli-Michael, M. (2000) The fluorescence transient as a tool to characterize and screen photosynthetic samples. *Probing photosynthesis: mechanisms, regulation and adaptation*. London: Taylor and Francis, pp. 445–483.

Strelkov, S.E., Lamari, L. & Ballance, G.M. (1998) Induced chlorophyll degradation by a chlorosis toxin from *Pyrenophora tritici-repentis*. *Canadian Journal of Plant Pathology*, 20, 428-435.

Turner, J.A., Chantry, T., Taylor, M.C. & Kennedy, M.C. (2021) Changes in agronomic practices and incidence and severity of diseases in winter wheat in England and Wales between 1999 and 2019. *Plant Pathology*, 70, 1759-1778.

Wellburn, A.R. (1994) The spectral determination of chlorophylls a and b, as well as total carotenoids, using various solvents with spectrophotometers of different resolution. *Journal of Plant Physiology*, 144, 307-313.

TABLE 1. Summary statistics of the effects of cultivar (C), three nitrogen rates (NR), race (Ra), incubation period (IP), relative infection efficiency (RIE), area under lesion size curve (AULSC), final lesion size (LS), area under disease progress curve (AUDPC), and final severity (SEV) of tan spot on the leaves of the cultivars TBIO Audaz and TBIO Tibagi grown in soil fertilized with three N rates (low:70, recommended:130, and high: 200 kg ha⁻¹) and inoculated with race 1 or 2 of *Pyrenophora tritici-repentis*.

Treatments	Df	IP	RIE	LS	AULSC	SEV (%)	AUDPC
Cultivar (C)	1	4.46ns	24.98**	10.63*	6.53ns	403.71***	41.86***
Nitrogen rate (NR)	2	29.42***	24.24***	25.16***	18.14**	902.08***	816.64***
Race (Ra)	1	4.46ns	0.34ns	3.16ns	3.53ns	489.35***	473.82***
C × NR	2	1.0ns	1.01ns	0.52ns	0.56ns	3.54ns	4.27ns
C × Ra	1	26.42***	2.11ns	0.15ns	1.64ns	16.43ns	0.02ns
NR × Ra	2	0.61ns	13.98**	3.28ns	5.25ns	1.77ns	5.37ns
C × NR × Ra	2	1.80ns	1.67ns	0.63ns	1.12ns	1.45ns	5.84ns

Significant at *** $p = 0.001$; ** $p = 0.01$; * $p < 0.05$; ns = not significant

TABLE 2. Mean squares and standard errors of effect of cultivar (C), nitrogen rate (NR), and race (Ra) on incubation period (IP), relative infection efficiency (RIE), area under lesion size curve (AULSC), final lesion size (LS), area under disease progress curve (AUDPC), and final severity (SEV) of tan spot on the leaves of the cultivars TBIO Audaz and TBIO Tibagi grown in soil fertilized with three N rates (low:70, recommended:130, and high: 200 kg ha⁻¹) and inoculated with race 1 or 2 of *Pyrenophora tritici-repentis*.

Treatments	IP	RIE	LS	AULSC	SEV (%)	AUDPC
Cultivar (C)						
TBIO Audaz	90 ± 1.12	37.4 ± 1.62 b	5.22 ± 0.22 b	170 ± 7.93	17.7 ± 0.17 b	182 ± 0.61 b
TBIO Tibagi	86 ± 1.12	48.9 ± 1.62 a	6.26 ± 0.22 a	199 ± 7.93	20.5 ± 0.17 a	208 ± 0.61 a
Nitrogen rate (NR)						
Low N	80 ± 1.37 b	53.9 ± 1.99 a	7.32 ± 0.28 a	231 ± 9.71a	23.2 ± 0.20 a	219 ± 0.74 a
Recommended N	93 ± 1.37 a	40.9 ± 1.99 b	5.10 ± 0.28 b	160 ± 9.71 b	17.2 ± 0.20b	186 ± 0.74 b
High N	92 ± 1.37 a	34.7 ± 1.99 b	4.80 ± 0.28 b	158 ± 9.71b	16.7 ± 0.20b	180 ± 0.74 c
Race (Ra)						
Race 1	90 ± 1.12	43.8 ± 1.62	6.02 ± 0.22	174 ± 7.93	17.8 ± 0.17 b	185 ± 0.61 b
Race 2	86 ± 1.12	42.5 ± 1.62	5.46 ± 0.22	194 ± 7.93	20.8 ± 0.17 a	204 ± 0.61a

TABLE 3. Summary statistics of the maximum efficiency of PSII photochemistry (F_v/F_m); dissipated energy flux (Dlo/RC), electron transport flux (ETo/RC), absorbed photon flux (ABS/RC), trapped energy flux (TRo/RC), probability that a trapped exciton moves an electron further than Q⁻A (ψ_o) and quantum yield of electron transport (ϕE_o) of the leaves of the cultivars TBIO Audaz and TBIO Tibagi grown in soil fertilized with three N rates (low: 70, recommended: 130, and high: 200 kg ha⁻¹), inoculated with water (mock-inoculated) or with race 1 or 2 of *Pyrenophora tritici-repentis* at several interval as after plant inoculation.

Treatments	Df	F_v/F_m	ABS/RC	TRo/RC	ETo/RC	Dlo/RC	Ψ_o	ϕE_o
Cultivar (C)	1	269***	6ns	604***	2197***	280***	369.7***	6.4ns
Nitrogen rate (NR)	2	543***	1ns	7***	3ns	3.3ns	4.2ns	6.7ns
Inoculation (I)	2	7155***	1796***	109***	948***	3833.7***	969.5***	1210.7***
Evaluation time (Etm)	12	940**	100***	251***	204***	97.9***	88.8***	91.8**
C*NR	2	1ns	2ns	17***	11**	23.5***	34.3***	13.7**
C*I	2	117**	40***	19***	56***	91.9***	2.1ns	10.4**
NR*I	4	160*	15**	3***	9**	6***	16.5***	13.4***
C*Etm	12	9***	12***	32***	17***	26.7**	4.4ns	18.5***
NR* Etm	24	77***	3ns	1.4ns	1***	2.1**	7***	5.9**
I* Etm	24	275***	16***	15***	49***	23.2***	22.3**	15.1***
C*NR*I	4	6***	13***	4ns	1ns	0.4ns	7.5ns	11.1**
C*NR* Etm	24	5***	2**	2ns	3***	2.6**	1.7ns	4.1***
C*I* Etm	24	7***	5***	9***	16***	12.2***	7.1***	23***
NR*I* Etm	48	27ns	3*	9ns	3**	1.9ns	3.8ns	48ns
C*NR*I* Etm	48	4ns	1ns	3ns	3ns	2.6ns	3.1ns	49ns

Significant at *** $p = 0.001$; ** $p = 0.01$; * $p < 0.05$; ns = not significant

TABLE 4. Mean squares and standard errors of effect of the maximum efficiency of PSII photochemistry (Fv/Fm); dissipated energy flux (Dlo/RC), electron transport flux (ETo/RC), absorbed photon flux (ABS/RC), trapped energy flux (TRo/RC), probability that a trapped exciton moves an electron further than Q^-A (ψ_o) and quantum yield of electron transport (ϕEo) of the leaves of the cultivars TBIO Audaz and TBIO Tibagi grown in soil fertilized with three N rates (low: 70, recommended:130, and high: 200 kg ha⁻¹), inoculated with water (mock-inoculated) or with race 1 or 2 of *Pyrenophora tritici-repentis* at several intervals after plant inoculation.

Treatments	Fv/Fm	ABS/RC	TRo/RC	ETo/RC	Dlo/RC	ψ_o	ϕEo
Cultivar (C)							
TBIO Audaz	0.793 ± 0.0002 a	2.52 ± 0.002	2.31 ± 0.001 a	1.23 ± 0.0007 a	0.47 ± 0.0001 b	0.57 ± 0.0005 b	0.47 ± 0.0005
TBIO Tibagi	0.788 ± 0.0002 b	2.51 ± 0.002	2.26 ± 0.001 b	1.18 ± 0.0007 b	0.48 ± 0.0001a	0.56 ± 0.0005 a	0.46 ± 0.0005
Nitrogen rate (NR)							
Low N	0.782 ± 0.0003 b	2.51 ± 0.002	2.30 ± 0.003	1.20 ± 0.001	0.48 ± 0.0001	0.57 ± 0.0006	0.46 ± 0.0006
Recommended N	0.793 ± 0.0003 a	2.52 ± 0.002	2.29 ± 0.003	1.21 ± 0.001	0.48 ± 0.0001	0.57 ± 0.0006	0.47 ± 0.0006
High N	0.794 ± 0.0003 a	2.52 ± 0.002	2.29 ± 0.003	1.21 ± 0.001	0.48 ± 0.001	0.57 ± 0.0009	0.47 ± 0.0006
Inoculation (I)							
Mock inoculation	0.814 ± 0.0002a	2.42 ± 0.002c	2.27 ± 0.002 b	1.18 ± 0.0001 c	0.44 ± 0.001 c	0.59 ± 0.0006 a	0.49 ± 0.0009 a
Race 1	0.780 ± 0.0003 b	2.60 ± 0.002a	2.30 ± 0.002 a	1.23 ± 0.0001a	0.51 ± 0.001 a	0.54 ± 0.0005 c	0.45 ± 0.0007c
Race 2	0.777 ± 0.0003 b	2.54 ± 0.002 b	2.30 ± 0.002 a	1.22 ± 0.0001 b	0.48 ± 0.001 b	0.56 ± 0.001 b	0.46 ± 0.0009 b
Evaluation time (ETm)							
0	0.821 ± 0.0005a	2.40 ± 0.004g	2.18 ± 0.004h	1.16 ± 0.003 g	0.44 ± 0.001g	0.60 ± 0.001 a	0.49 ± 0.001 a
48	0.811 ± 0.0005b	2.48 ± 0.004 f	2.21 ± 0.004g	1.17 ± 0.003 f	0.47 ± 0.001 ef	0.58 ± 0.001 b	0.47 ± 0.001d
72	0.799 ± 0.0005 c	2.52 ± 0.004 cd	2.24 ± 0.004 f	1.18 ± 0.003 e	0.47 ± 0.001ef	0.55 ± 0.001 bcd	0.45 ± 0.001 e
96	0.796 ± 0.0005d	2.53 ± 0.004cde	2.26 ± 0.004e	1.20 ± 0.003 d	0.47 ± 0.001 f	0.55 ± 0.001f	0.46 ± 0.001 cd
120	0.796 ± 0.0005d	2.53 ± 0.004cd	2.29 ± 0.004d	1.20 ± 0.003 d	0.47 ± 0.001 f	0.56 ± 0.002 de	0.45 ± 0.001 e
144	0.794 ± 0.0005d	2.51 ± 0.004e	2.32 ± 0.004c	1.21 ± 0.003 c	0.48 ± 0.001d	0.57 ± 0.002 bcd	0.47 ± 0.001 bcd
168	0.786 ± 0.0005 d	2.54 ± 0.004 bcd	2.31 ± 0.004 c	1.21 ± 0.003 c	0.48 ± 0.001 d	0.57 ± 0.001 bc	0.47 ± 0.001 bc
192	0.794 ± 0.0005d	2.55 ± 0.004ab	2.32 ± 0.004c	1.21 ± 0.003 c	0.48 ± 0.007 de	0.57 ± 0.001 cd	0.47 ± 0.002 b

216	0.786 ± 0.0005 e	2.53 ± 0.004 bcd	2.32 ± 0.004 c	1.211 ± 0.003 c	0.48 ± 0.001 de	0.57 ± 0.001 cd	0.47 ± 0.001 bc
240	0.786 ± 0.0005 e	2.53 ± 0.004 ab	2.32 ± 0.004 bc	1.227 ± 0.003 b	0.49 ± 0.001 c	0.56 ± 0.002 e	0.47 ± 0.001 cd
264	0.768 ± 0.0005 f	2.54 ± 0.004 bc	2.36 ± 0.004 a	1.22 ± 0.003 b	0.49 ± 0.001 bc	0.57 ± 0.001 cd	0.47 ± 0.001 cd
288	0.762 ± 0.0005 g	2.55 ± 0.004 ab	2.32 ± 0.004 c	1.23 ± 0.003 b	0.49 ± 0.001 b	0.57 ± 0.001 cde	0.46 ± 0.001 bcd
312	0.7558 ± 0.0005 h	2.57 ± 0.004 a	2.34 ± 0.004 b	1.25 ± 0.003 a	0.51 ± 0.001 a	0.56 ± 0.001 f	0.45 ± 0.001 f

TABLE 5. Summary statistics of the effects of cultivar (C), nitrogen rate (NR), inoculation (I), and their interactions on chlorophyll *a* (Chla), chlorophyll *b* (Chlb), carotenoids, total chlorophyll (Chla+b), and total chlorophyll (Chla+b)/carotenoids ratio.

Treatments	Df	Chla	Chlb	Carotenoids	Chla+b ($\mu\text{gcm}^{-2}\text{FM}$)	Chla+b/carotenoids ratio ($\mu\text{gcm}^{-2}\text{FM}$)
Cultivar (C)	1	17.65***	19.31***	40.84***	13.09***	4.33*
Nitrogen rate (NR)	2	0.80ns	0.14ns	0.22ns	0.44ns	0.91ns
Inoculation (I)	2	79.83***	64.42***	147.94***	45.84***	74.56***
C × NR	2	1.24ns	0.04ns	0.24ns	0.40ns	0.41ns
C × I	2	3.49**	3.58*	3.06ns	4.22*	1.09ns
NR × I	4	1ns	0.20ns	0.66ns	0.34ns	0.97ns
C × NR × I	4	1.64ns	0.52ns	0.68ns	0.98ns	0.46ns

Significant at *** $p = 0.001$; ** $p = 0.01$; * $p < 0.05$; ns = not significant

FM= Fresh matter

TABLE 6. Mean squares and standard errors of concentration of chlorophyll *a* (Chla), chlorophyll *b* (Chlb), carotenoids, total chlorophyll (Chla+b), and total chlorophyll (Chla+b)/carotenoids ratio of cultivars TBIO Audaz and TBIO Tibagi inoculated with water (mock-inoculated) or *Pyrenophora tritici-repentis* races 1 or 2.

Treatments	Chla	Chlb	Carotenoids	Chla+b ($\mu\text{gcm}^{-2}\text{FM}$)	Chla+b/carotenoids ratio ($\mu\text{gcm}^{-2}\text{FM}$)
Cultivar (C)					
TBIO Audaz	1.53 ± 0.053 a	1.07 ± 0.078 a	0.84 ± 0.034a	2.41 ± 0.12a	3.72 ± 0.05 a
TBIO Tibagi	1.48 ± 0.047b	0.97 ± 0.069b	0.77 ± 0.030 b	2.28 ± 0.11 b	3.68 ± 0.04 b
Inoculation (I)					
Mock inoculation	1.98 ± 0.051 a	1.67 ± 0.08 a	1.29 ± 0.03a	3.15 ± 0.12 a	4.16 ± 0.05 a
Race 1	1.03 ± 0.063c	0.43 ± 0.96c	0.44 ± 0.04 c	1.46 ± 0.15c	3.30 ± 0.06c
Race 2	1.51 ± 0.063 b	0.94 ± 0.96b	0.72 ± 0.04 b	2.42 ± 0.15 b	3.63 ± 0.06b

FM= Fresh matter

TABLE 7. Summary statistics, mean squares, and standard errors of the effects of cultivar (C) and nitrogen rate (NR) on total nitrogen (g kg^{-1}), ammonium (NH_4^+), and nitrate (NO_3^-) concentration.

Treatments	Total nitrogen (g kg^{-1})	NH_4^+ (mg kg^{-1})	NO_3^- (mg kg^{-1})
Cultivar (C)			
TBIO Audaz	29.2 ± 0.37 b	47.6 ± 1.22 b	11.2 ± 0.44
TBIO Tibagi	30.5 ± 0.37 a	52.6 ± 1.22 a	10.4 ± 0.44
<i>p value</i>	0.021	0.007	0.52504
Nitrogen rate (NR)			
Low N	25.5 ± 0.46 b	29.8 ± 1.49 c	10.3 ± 0.54
Recommended N	31.0 ± 0.46 a	50.7 ± 1.49 b	9.6 ± 0.54
High N	33.0 ± 0.46 a	69.8 ± 1.49 a	12.6 ± 0.54
<i>p value</i>	<0.0001	<0.0001	0.051
C × N			
<i>p value</i>	0.121	<0.0001	0.006

Significant at *** $p = 0.001$; ** $p = 0.01$; * $p < 0.05$; ns = not significant

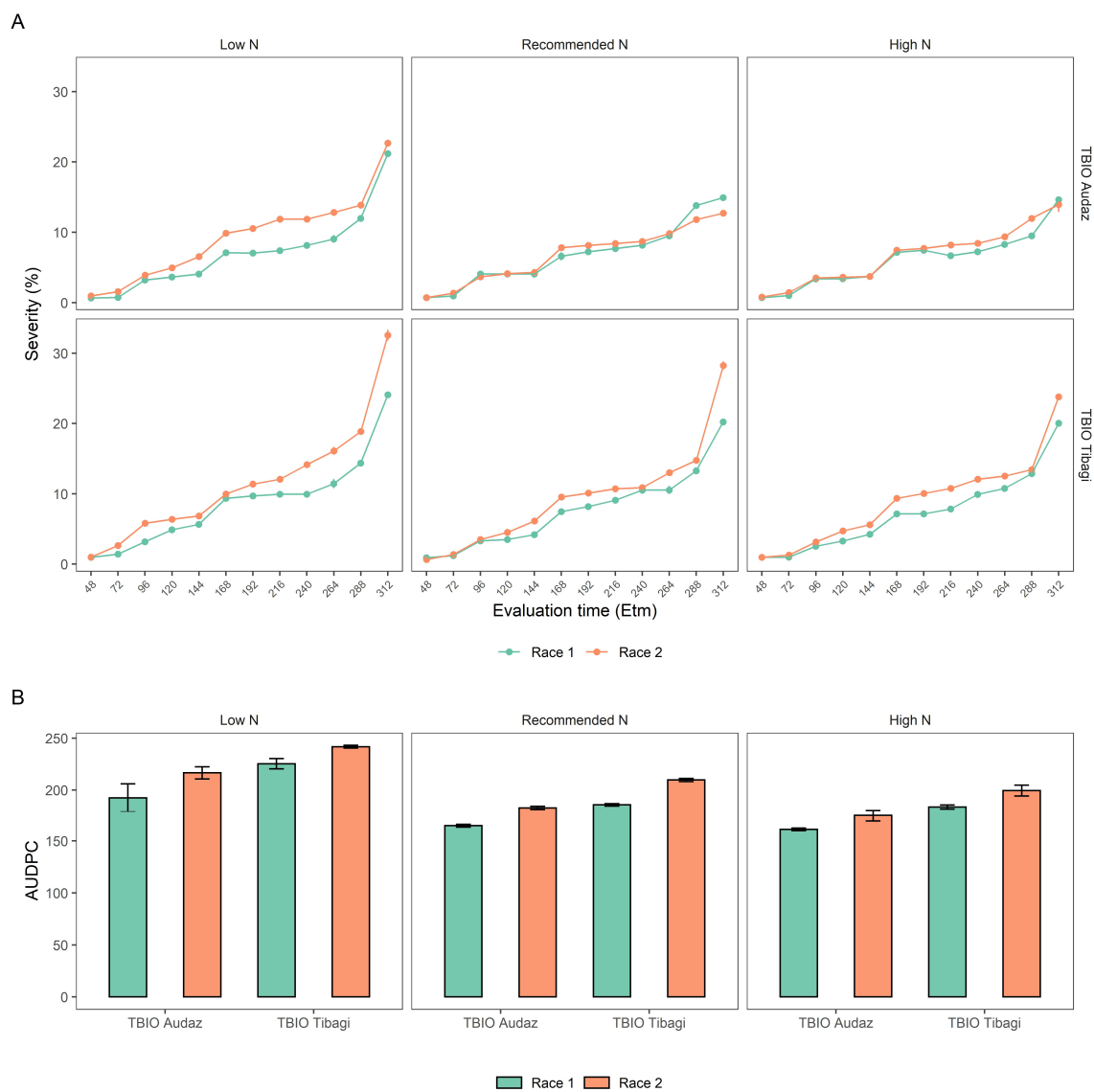


FIGURE 1 Severity (A) and area under disease progress curve AUDPC (B) of tan spot in the wheat cultivars TBIO Audaz and TBIO Tibagi grown in soil fertilized with three N rates (low N: 70, recommended N: 130 and high N: 200 kg ha⁻¹) and inoculated with *Pyrenophora tritici-repentis* race 1 or 2. Data points are the mean and error bars represent standard deviation of means from two pooled experiments (n = 12).

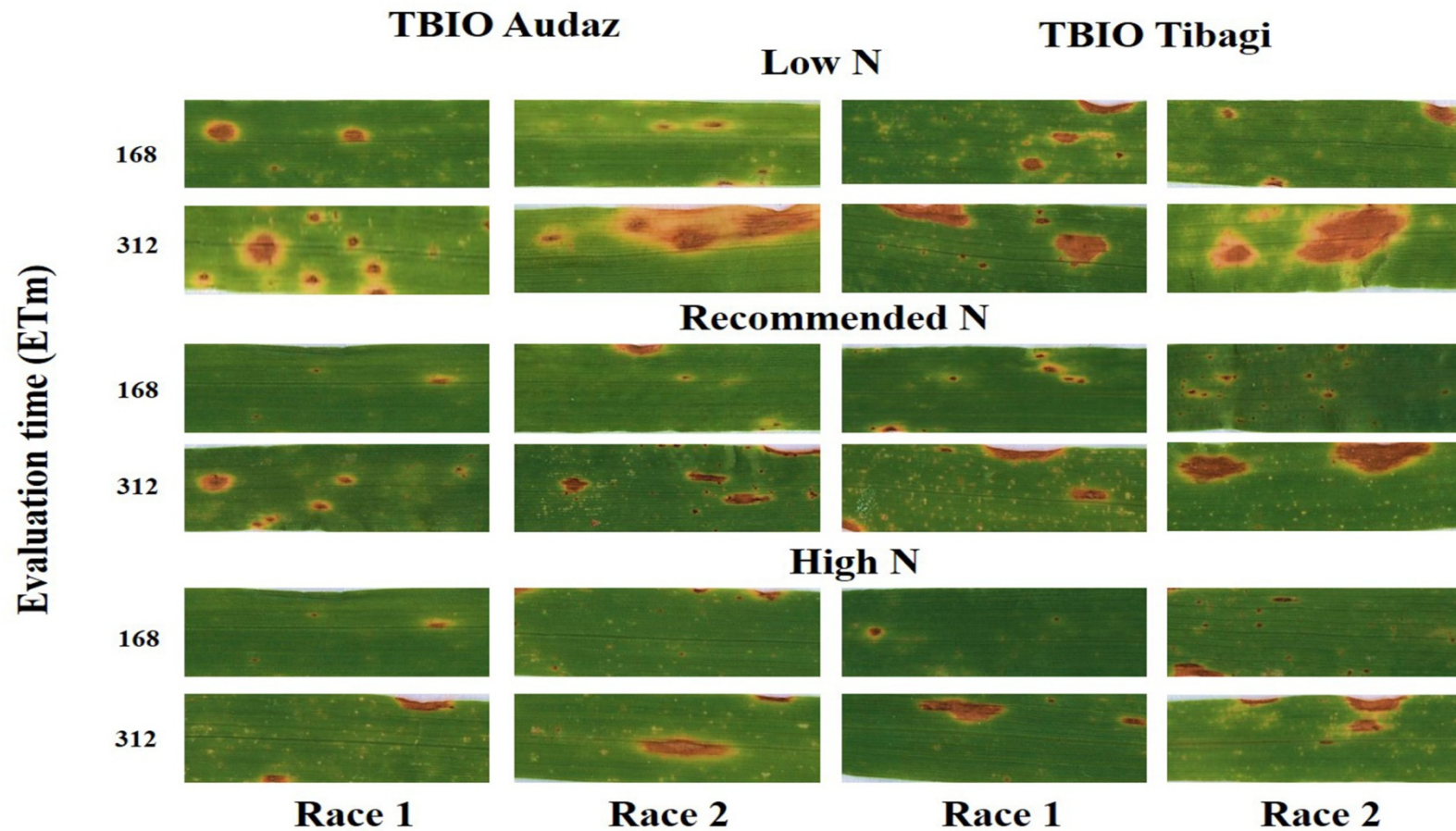


FIGURE 2 *Pyrenophora tritici-repentis* race 1 and race 2 symptoms at 168 and 312 hai on fourth leaf of wheat cultivars TBIO Audaz and TBIO Tibagi grown in soil fertilized with three N rates (low N: 70, recommended N: 130 and high N: 200 kg ha⁻¹).

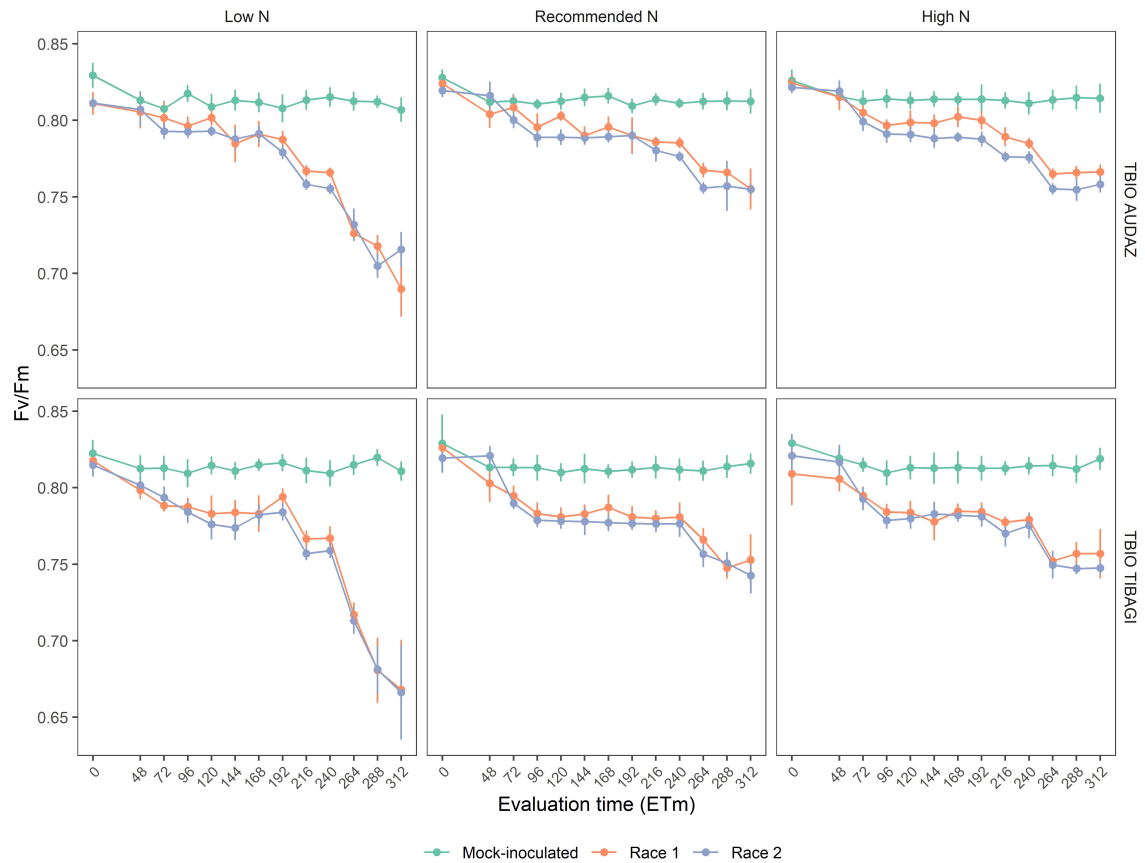


FIGURE 3 The maximum efficiency of PSII photochemistry (F_v/F_m) from 0 to 312 hours of evaluation time (ETm) of wheat cultivars TBIO Audaz and TBIO Tibagi grown in soil fertilized with three N rates (70, 130 and 200 kg ha⁻¹). Data points are the mean and error bars represent standard deviation of means from two pooled experiments (n = 12).

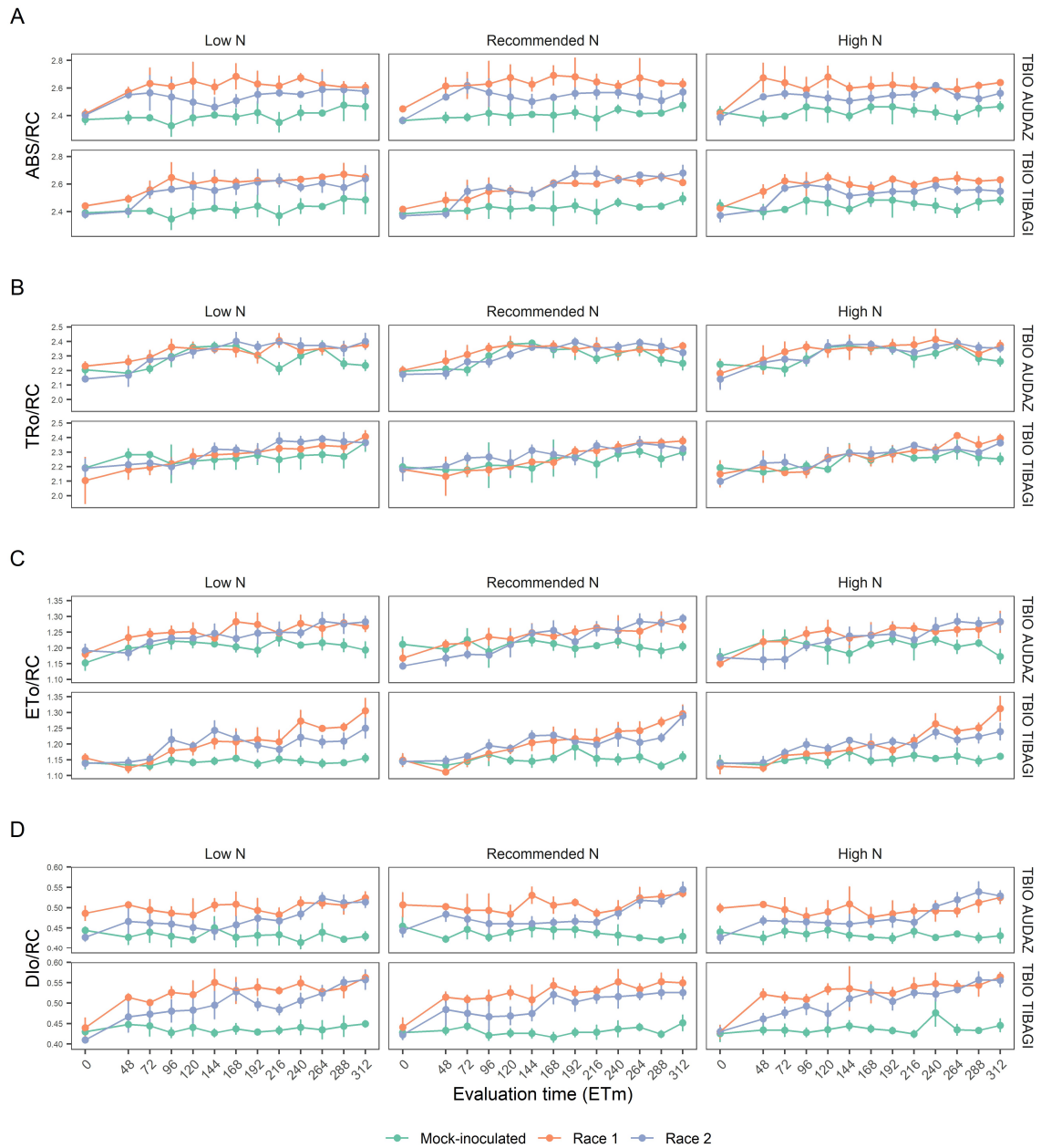


FIGURE 4 Absorbed photon flux (ABS/RC) (A), trapped energy flux (TRO/RC) (B), dissipated energy flux (DIO/RC) (C), electron transport flux (ETO/RC) (B) over 0 to 312 hours of evaluation time (ETm) of the wheat cultivars TBIO Audaz and TBIO Tibagi grown in soil fertilized with three N rates (70, 130 and 200 kg ha⁻¹). Data points are the mean and error bars represent standard deviation of means from two pooled experiments (n = 12).

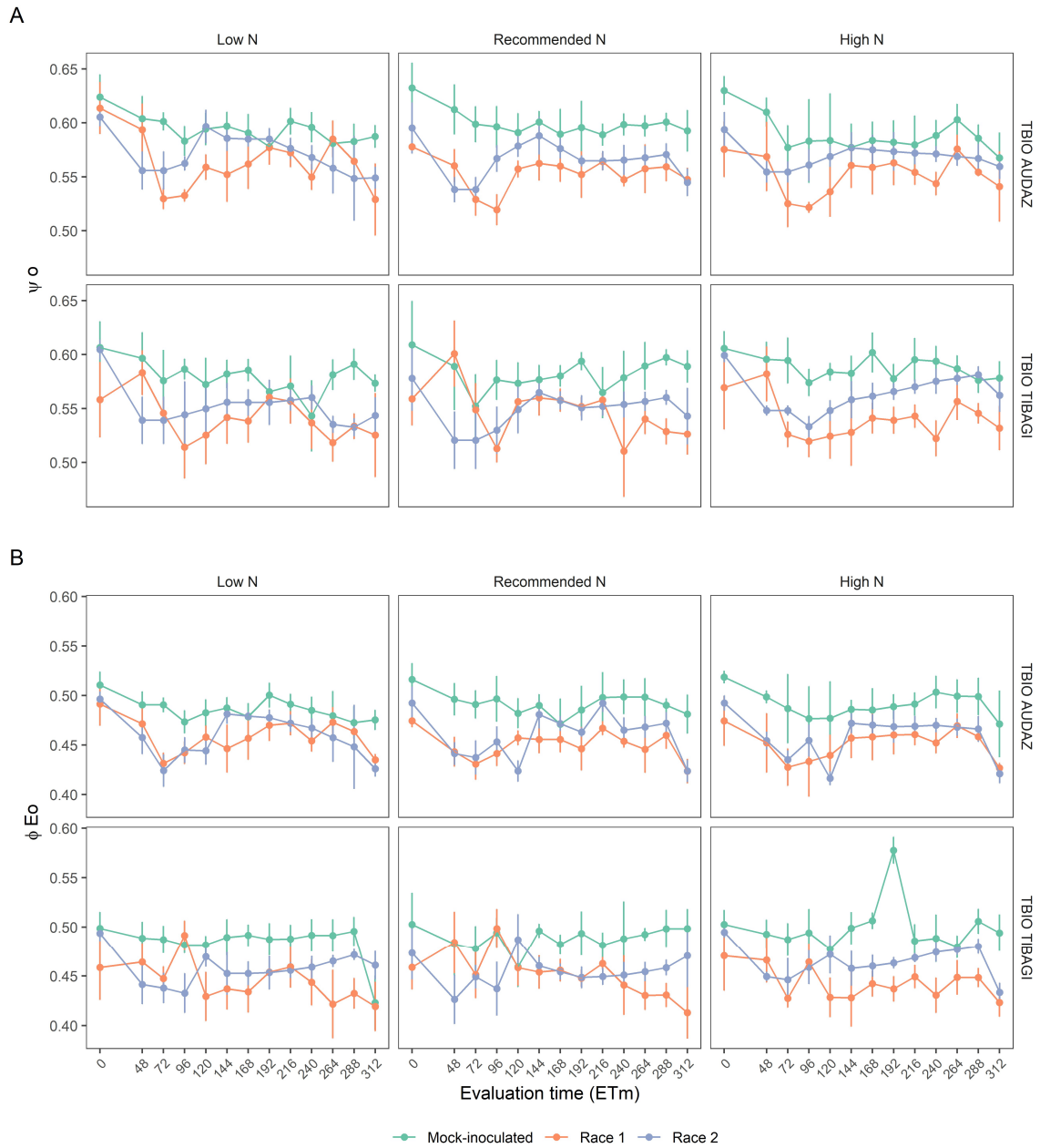


FIGURE 5 Probability that a trapped exciton moves an electron further than $Q^{\bar{A}}$ (ψ_o) (A) and quantum yield of electron transport (ϕE_o) (B) over 0 to 312 hours of evaluation time (ETm) of the wheat cultivars TBIO Audaz and TBIO Tibagi grown in soil fertilized with three N rates (70, 130 and 200 kg ha⁻¹). Data points are the mean and error bars represent standard deviation of means from two pooled experiments (n = 12).

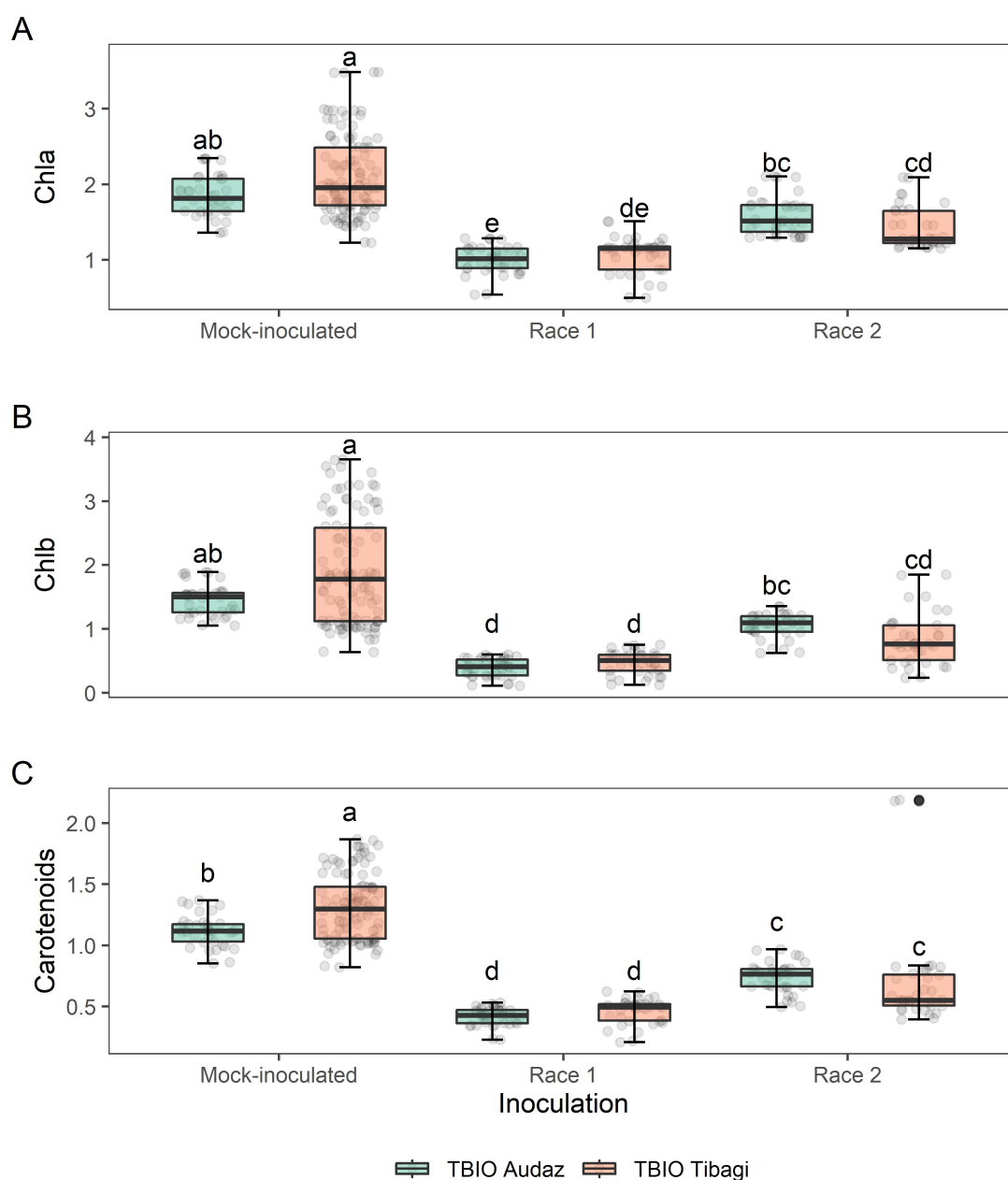


FIGURE 6 Effect of the cultivar \times inoculation interaction on chlorophyll *a* (Chla)(A), chlorophyll *b* (Chlb)(B), and carotenoid (C) concentrations. The horizontal line inside the box represents the median, the limits of the box represent the lower and upper quartiles, and the circles represent the observation of each treatment. Data points from two pooled experiments ($n = 8$) are the median and error bars represent standard deviation of means. Point (\bullet) corresponds to outliers. Different lowercase letters indicate statistical differences according to the Tukey test at $p < 0.05$.

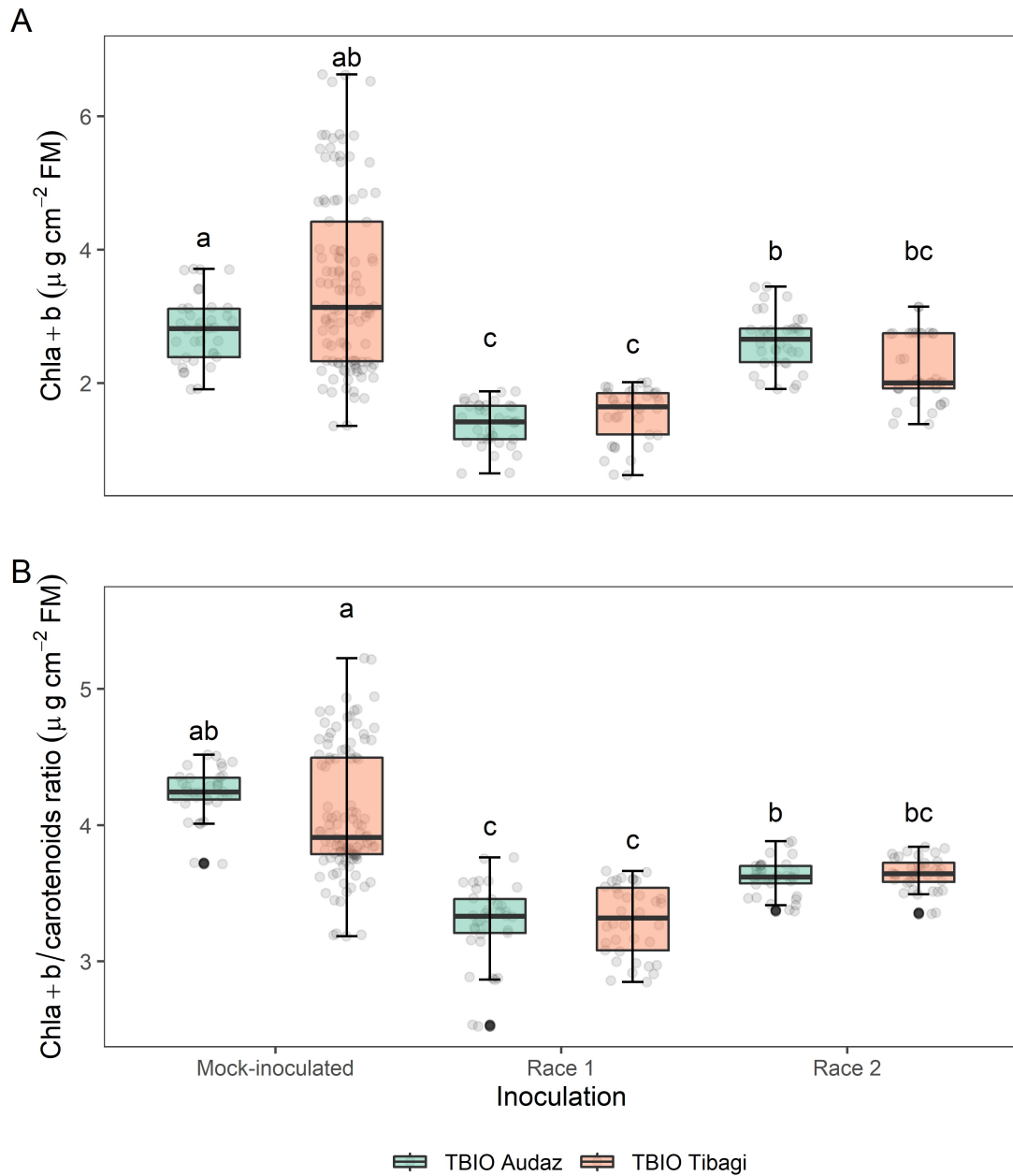


FIGURE 7 Effect of the cultivar \times inoculation interaction on total chlorophyll concentration (Chla+b), and Chla+b/carotenoid ratio (B). The horizontal line inside the box represents the median, the limits of the box represent the lower and upper quartiles, and the circles represent the observation of each treatment. Data points from two pooled experiments ($n = 8$) are the median and error bars represent standard deviation of means. Point (\bullet) corresponds to outliers. Different lowercase letters indicate statistical differences according to the Tukey test at $p < 0.05$. FM: fresh mater.

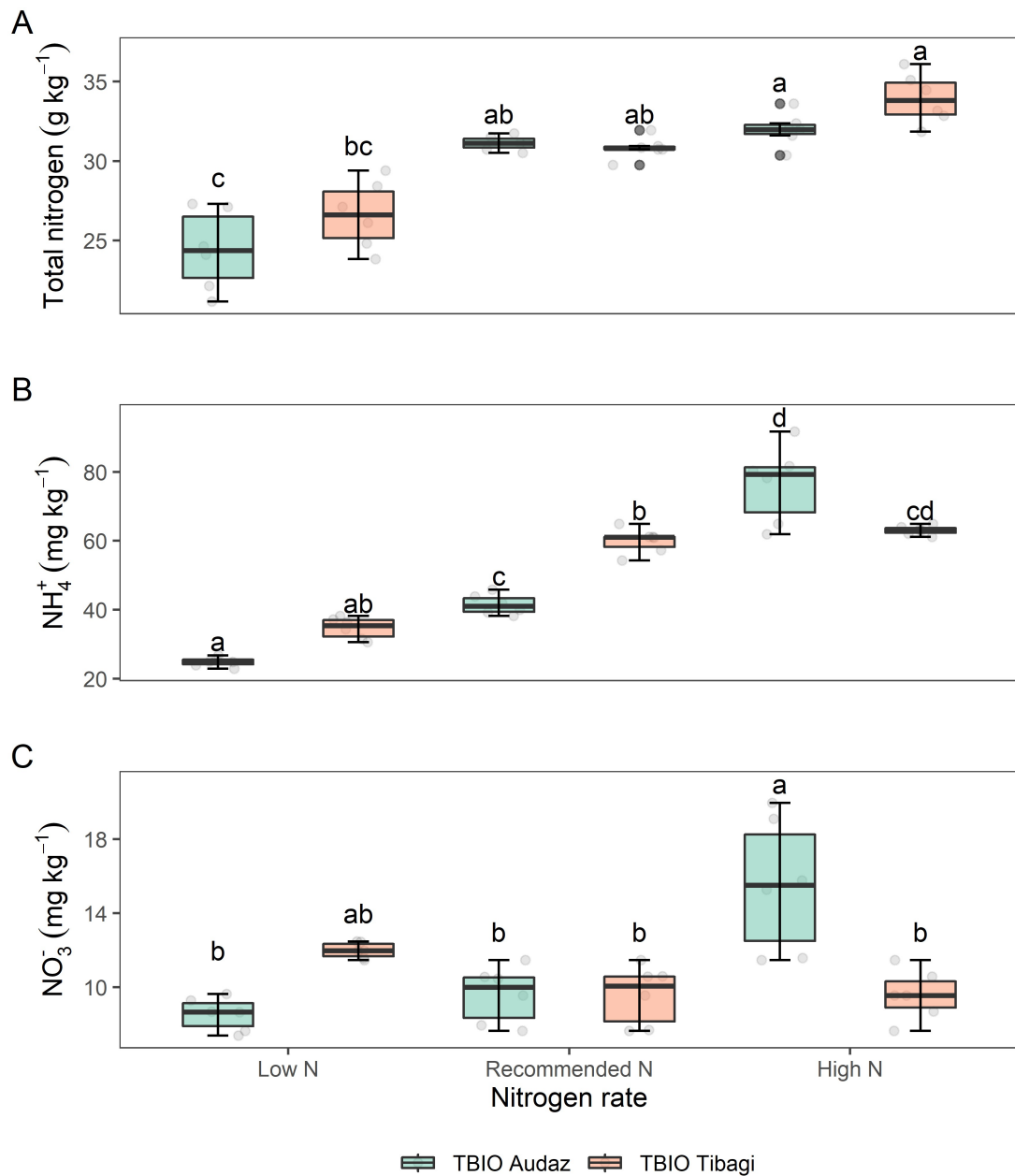
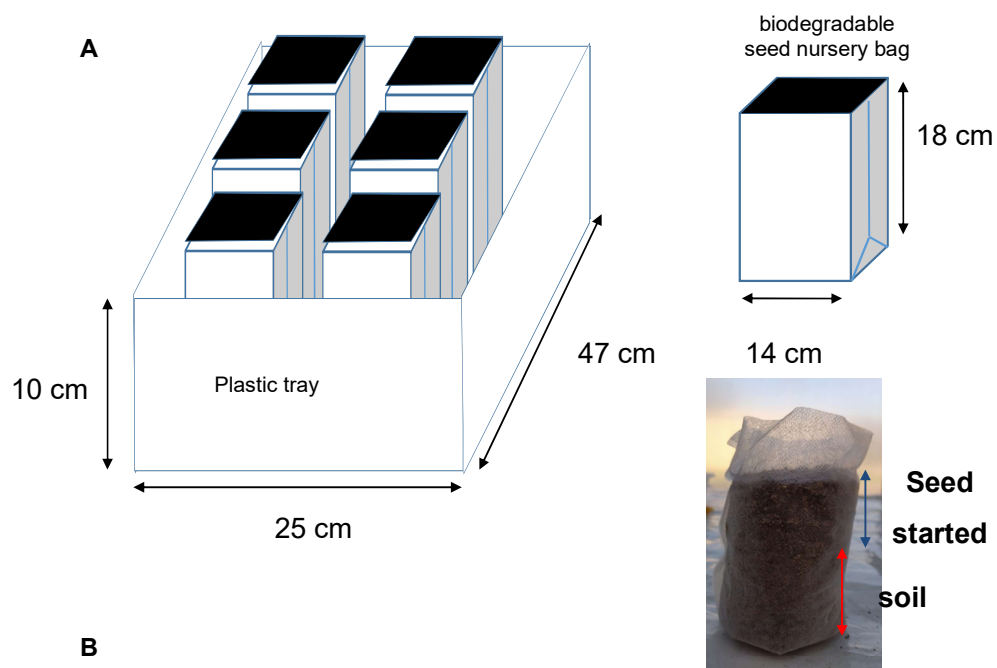
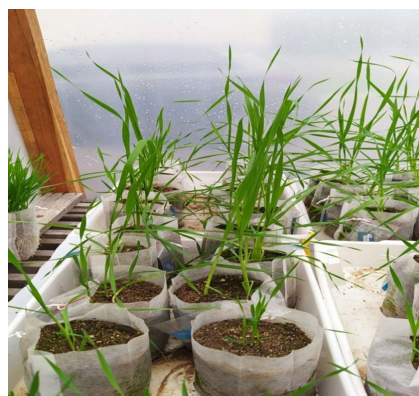


FIGURE 8. Effect of the cultivar × nitrogen interaction on total nitrogen (g kg⁻¹), ammonium (NH₄⁺), and nitrate (NO₃⁻). Data points from two pooled experiments (n = 6) are the median and error bars represent standard deviation of means. Point (•) corresponds outliers. Different lowercase letters indicate statistical differences according to the Tukey test at *p*<0.05.



Plastic tray with the nursery bags before wheat sowing



Plants growing in a greenhouse

Figure S1. Plant material and growth. A) Material used for experiment and bag nursery distributed in a plastic trail. B) Plants experiments growing in a greenhouse.

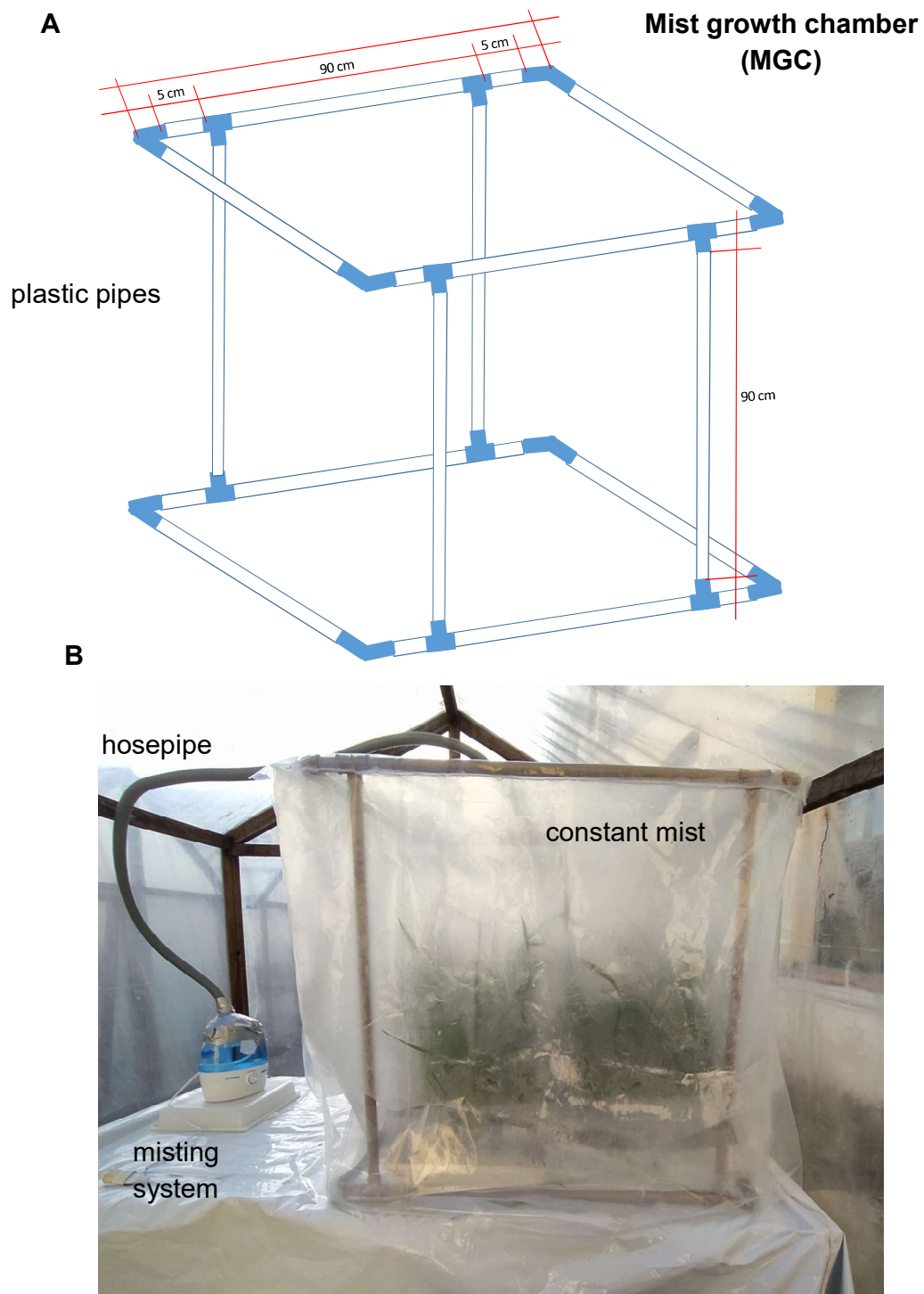


Figure S2. Plants inoculated in constant mist. A) Plastic mist growth chamber (MGC) design. B) Plants inoculated in a plastic mist growth chamber (MGC) inside a greenhouse.

The chapter 5 was formatted under the guidelines of the **Plant Pathology**

Cytological and biochemical responses in wheat leaves infected by *Pyrenophora tritici-repentis* mediated by nitrogen and silicon

Andrea Román^{1,3}, Daniel Debona², Eduardo Rodríguez⁴ and Leandro José Dallagnol^{1*}

¹ Federal University of Pelotas, Eliseu Maciel Faculty of Agronomy, Crop Protection Department, Laboratory of Plant Pathogen Interaction, 96010-900, Pelotas, Rio Grande do Sul, Brazil.

² Universidade Tecnológica Federal do Paraná - Campus Santa Helena, Agronomy Department, 85892-000, Santa Helena, Paraná, Brazil.

³ Bolívar State University, Agricultural Sciences Natural Resources and the Environment Faculty, Laboratory of Phytopathology, EC020150, Guaranda, Ecuador.

⁴ Grow green Agricultural Technologies, EC060103, Riobamba, Ecuador.

***Corresponding author:** leandro.dallagnol@ufpel.edu.br

Abstract

Nitrogen (N) and silicon (Si) play key roles in plant health and yield, especially in grasses. Both elements have been demonstrated to decrease tan spot, caused by *Pyrenophora tritici-repentis* (*Ptr*), in wheat. Despite these reports the N-Si interaction effect on wheat resistance to tan spot remains elusive. Here, we investigated the effect of N and Si on the histo-cytological and biochemical responses of defense triggered during the *Ptr* infection in leaves of wheat with Si amended and fertilizer with low and high N rate. Plants supplied with Si and low N displayed higher activity of superoxide dismutase (14%), catalase (56%) and peroxidase (36%) 48 to 60 hours after inoculation (hai). By contrast, the phenylalanine ammonia-lyase activity was reduced by 36% at high N despite the Si amendment. Accumulation of hydrogen peroxide was increased by 37% in response to the *Ptr* infection in plants supplied with Si and low N, whereas callose deposition was observed at 32 to 48 hai in the same treatment, with 80% higher accumulation. However, at high N, the +Si concentration declined by 21% in leaves. Those results indicated that Si and N may act in an independent way in the activation of plant defense responses and the activation of antioxidative mechanisms.

KEYWORDS: callose, hydrogen peroxide, necrotrophic, plant defense, tan spot.

1 INTRODUCTION

Tan spot, caused by the necrotrophic fungus *Pyrenophora tritici-repentis* (*Ptr*) (Died.) *Drechs.*, is one of the most important diseases of wheat (*Triticum aestivum* L.) worldwide (Ciuffetti *et al.*, 2014). In southern Brazil, the main Brazilian wheat producing region, *Ptr* it is the main leaf spot disease, and the *Ptr* race 1 (Tox A and Tox C), which induces necrosis and chlorosis, is a common race found under field conditions (Bertagnolli *et al.*, 2019). Recent studies of *Ptr*-wheat interaction have shown that the activation of defense response varies with the levels of susceptibility of wheat cultivars, and biochemical defense mechanisms as well as histo-cytological defense responses are more robust in genotypes with moderate resistance (Dorneles *et al.*, 2017, 2018). During *Ptr* attack, the accumulation of hydrogen peroxide (H₂O₂) is known to be a pathogen-triggered response, inducing cell death in the host through toxins (Ciuffetti *et al.*, 2014). In susceptible cultivars, late accumulation (>24 hours after inoculation) of H₂O₂ in the epidermal and mesophyll cells was observed, as well as delayed fluorescence in epidermal cells (Dorneles *et al.*, 2017). Contrarily, in moderately resistant cultivars, lower infection efficiency was observed, which was associated with earlier accumulation of H₂O₂ in the epidermal cells, as a defense mechanism against pathogen attack, along with alteration of the activities of enzymes such as superoxide dismutase (SOD), catalase (CAT), peroxidase (POX), chitinase (CHI), and phenylalanine ammonia-lyase (PAL); early and intense fluorescence of epidermal cells, in turn, associated with the accumulation of phenylpropanoid derivatives at the infection site (Dorneles *et al.*, 2017, 2018).

The fertilization effect related to *Ptr* management through the use of nitrogen (N) (Castro *et al.*, 2018; Fleitas *et al.*, 2018) and silicon (Si) (Dorneles *et*

al., 2017, 2018; Pazdiora *et al.*, 2018, 2021) has been studied in recent years. These studies have demonstrated a reduction of tan spot damage when calcium silicate, a source of soluble Si, was included in the soil or high N fertilization was used.

Nitrogen (N) is an essential element for plant growth and plays a key role in plant health and yield (Huber & Thompson, 2007; Simon *et al.*, 2020). Several studies have shown contrasting effects of plant tissue N concentration on disease development (Huber & Thompson, 2007; Veresoglou *et al.*, 2013). Meanwhile, Si is considered a non-essential plant nutrient, although it plays a beneficial role in promoting plant growth and increasing yield by alleviating biotic and abiotic stresses in many plant species (Debona *et al.*, 2017; Dallagnol *et al.*, 2020).

Overall, Si mediates cell wall fortification as well as induces or enhances defense responses, increasing plant disease resistance (Debona *et al.*, 2012; Dallagnol *et al.*, 2015; Dorneles *et al.*, 2017, 2018; Pazdiora *et al.*, 2018), whereas N is involved in the photosynthesis capacity, increasing plant chlorophyll content and the activity of PAL (Moriwaki *et al.*, 2019). While both elements alone can be associated with resistance or susceptibility of host plants to diseases (Simon *et al.*, 2020; Huber & Thompson, 2007; Dorneles *et al.*, 2017; Pazdiora *et al.*, 2018, 2021), the effect of interaction between N and Si fertilization has only been evaluated on resistance to pests and yield in crops such as rice, sugarcane, and wheat (Wu *et al.* 2017; White *et al.*, 2017; Shahrtash, 2017). Little information on the interaction of N and Si related with plant diseases has been reported. For example, White *et al.* (2017) and Shahrtash (2017) showed that N and Si did not have any interactive effect on wheat yield, Si uptake or leaf rust development. Furthermore, Si fertilization alone or combined with N may have a significant role

in improving yield and abiotic stress resistance only in areas with highly weathered soils that contain low levels of soluble Si (White *et al.*, 2017).

Nitrogen fertilizers are an integral part of most crop production systems, and it is essential to understand the interactions between N and Si regarding plant disease management. In this context, no previous study has investigated the interaction between both elements regarding the *Ptr* infection process or the *Ptr*-wheat interaction. Therefore, the aim of this study was to investigate the effect of Si amendment and its interaction with N on the histo-cytological and biochemical responses of defense mechanisms triggered during *Ptr* infection in wheat.

2 MATERIALS AND METHODS

2.1 Plant material and growth

Wheat (*Triticum aestivum*), cultivar TBIO Tibagi (Biotrigo®), susceptible to tan spot, was used in the experiment. Seeds were surface sterilized in 10% (vol/vol) NaOCl for 2 min and rinsed in sterilized water for 3 min. Pre-germination was conducted in wet/dry cycles of 12 h, at 20°C, in the dark for 2 days. Then, 5 g of germinated seedlings was transferred to biodegradable seed nursery bags (14×18 cm) (Huvai®, USA) containing 475 g of soil and 100 g of seed starter (Carolina Soil®, Brazil), and kept in a plastic tray (47 × 25 × 10 cm) (Figure S1). Plants were grown in a greenhouse with relative humidity of 80 ± 5% and temperature of 25 ± 2°C.

2.2.1 Soil characteristics, silicon amendments, and nitrogen treatment

The soil used in the experiment was collected in the experimental area of Federal University of Pelotas, Capão do Leão, Rio Grande do Sul, Brazil, with the

following physicochemical characteristics: 658 g kg⁻¹ of sand; 242 g kg⁻¹ of clay; 101g kg⁻¹ of silt; 1% organic matter; nitrogen, 1.5 g kg⁻¹; NO₃, 6.64 g kg⁻¹; NH₄, 1.93 g kg⁻¹; phosphorus, 47.7 ppm; potassium, 143 mg dm⁻³; calcium, 2,7 cmolc dm⁻³; magnesium, 1,4cmolc dm⁻³; copper, 0.9 mg dm⁻³; zinc, 0.8 mg dm⁻³; manganese, 12.3 mg dm⁻³; pH_{H2O}: 5.5; CTC, 10.4 cmolc dm⁻³; H + Al, 0.3 cmolc dm⁻³; and base saturation, 48.1%. The concentration of available Si (extracted with 0.01 M CaCl₂) was 6.0 mg dm⁻³, determined according to standard colorimetric analysis method.

The source of Si was calcium silicate (Agrosilício[®], Agronelli Insumos Agrícolas, Uberaba, Brazil), which is composed of 10.5% Si, 25.0% calcium and 6.0% magnesium. Calcium silicate was mixed with the soil at a rate of 13.2 ton ha⁻¹ in order to increase the soil pH to 6.0. To standardize the amount of calcium and magnesium supplied to the plants in the calcium silicate treatment, the soil in the control treatment was mixed with extra-fine limestone at the rate of 11.0 ton ha⁻¹. The extra-fine limestone (Dagoberto Barcelos, Caçapava do Sul, Brazil) was composed of 26.5% calcium and 15.0% magnesium. Calcium carbonate (Synth, Diadema, Brazil) and magnesium carbonate (Synth, Diadema, Brazil) were used to adjust the concentration of calcium and magnesium, respectively. After complete soil homogenization in each treatment, water was added to reach 80% of field capacity, followed by 30 days of incubation in plastic bags.

Plant fertilization was adjusted using chemical fertilizer as nutritive solution, applied to the substrate in each bag according to wheat plant requirement, of 30 (phosphorus) and 100 (potassium) kg ha⁻¹ to achieve a yield of 4 ton ha⁻¹ (Silva *et al.*, 2017). Nitrogen was applied as a nutrient solution in each treatment and adjusted to obtain the two doses under study, low N: 70 kg ha⁻¹, and high N: 200 kg ha⁻¹. The fertilizer was applied weekly from the third week after plant

emergence at ZGS20 (main shoot) until ZGS33 (third detectable node) in the seventh week. The first nutrient solution contained 12.97 g L⁻¹ of phosphorus (KH₂PO₄) and 15.62 g L⁻¹ of potassium (KCl). A volume of 63.5 ml of this nutrient solution (wt/vol) was applied to each bag in the third and fourth week. Two nitrogen solutions [granular urea (wt/vol), N, 45%] were prepared containing: 0.147 g L⁻¹, and 0.442 g L⁻¹ for low N and high N, respectively. A volume of 40 ml of one or the other nitrogen solution was applied per bag, in the fifth to seventh week. All nutrient solutions were prepared using deionized water. Plants were watered as needed with deionized water.

2.2.2 Experimental design and treatments

The experimental design was completely randomized in a 2 × 2 × 8 factorial, consisting of two nitrogen rates (70 or 200 kg ha⁻¹), two silicon treatments (not supplied (-Si) or supplied (+Si)), and 8 sampling times (ST) (8, 16, 24, 32, 48, 60, 72 and 96 hai), with four replicates. For enzymatic activity, a fourth factorial was considered by including the inoculation as a factor (mock-inoculated and *Ptr*-inoculated). The experiments were repeated twice.

2.3 Inoculum production and inoculation procedure

The isolate of *P. tritici-repentis* (BRPtr8), classified as race 1 (Bertagnolli *et al.*, 2019), provided by Passo Fundo University, was used for leaf inoculation. The fungus was maintained as a PDA mycelium disk at -20 °C in a freezer. The fungus was reactivated in PDA during a week, after which a 5 mm diameter mycelial plug was cut from the margin of actively growing colonies and transferred to Petri dishes containing modified V8-agar medium (3.0 g L⁻¹ of calcium carbonate

(Synth, Diadema, Brazil), 150 mL L⁻¹ of tomato sauce (Fugini[®], Brazil), 15 g L⁻¹ of agar (Kasvi, Curitiba, Brazil) and distilled water).

The fungal growth was performed according to the method described by Dorneles *et al.* (2017). Briefly, after fungal growth in the modified V8-agar medium during five days at 25 ± 1 °C in darkness, the fungal colony was stressed by mycelium scraping. Then, the fungal colony was exposed for 24 h to light at 25 ± 1°C to allow development of conidiophores, followed by a further 24 h of darkness at 15 ± 1°C, necessary for conidia formation. At the end of seven days, conidia were carefully removed from the Petri dishes with a soft bristle brush using water containing gelatin (1% wt/vol) and Tween 20. The conidial suspension was adjusted to obtain a concentration of 3 × 10³ conidia ml⁻¹.

The fourth leaves of 50-day-old wheat plants with the flag leaf just visible (ZGS37) were used in the experiment. For this, leaves were sampled and immediately placed in 10% (vol/vol) NaOCl for 2 min, followed by washing three times with sterilized water for 3 min, and air drying for 5 min. The conidial suspension was sprayed with a hand-held sprayer (Tecblas, REF: 60 mL/Porto Alegre, Brazil) on the adaxial surface of the leaves. After inoculation, six leaves were transferred to a plastic Petri dish (150 × 15 mm) with water - agar medium (Figure S2). Mock-inoculated plants (control) were sprayed with distilled water and exposed to the same conditions as *Ptr*-inoculated ones. The plastic Petri dishes with *Ptr*-inoculated and mock-inoculated leaves were incubated at 25 ± 1 °C, relative humidity of 80 ± 5%, and photoperiod of 12 h (Figure S2).

2.4 Disease assessment

Disease assessments were performed at 96 hai. For this purpose, four areas (1 cm² of leaf each) of six leaves were chosen to quantify the number of lesions per cm² (NLs). The final lesion size (FLS) was quantified at four points of one cm² of leaf by randomly measuring five lesions with a digital caliper (150 mm, YuanSen®, 02KC4PR7P1995). The final disease severity (SEV), defined as the percentage of total leaf area affected by the disease (necrotic and chlorotic tissue) was determined in six inoculated leaves. For this purpose, digital leaf images were obtained at 600 dpi using a scanner (Epson/L395), and final disease severity (SEV) was measured using the digital image analysis software Quant® software (UFV, Brazil).

2.5 Detection of hydrogen peroxide

For detection of hydrogen peroxide, inoculated leaves were collected at 8, 16, 24, 32, 48, 60, 72 and 96 hai, according to the method described by Shi *et al.* (2010). Briefly, fragments of 1 cm² were cut from the middle of each leaf, discarding the tip and base of the leaf, and immediately vacuum infiltrated in diaminobenzidine (DAB) (Acros Organics, USA) solution (wt/vol) for 15 min (1 mg ml⁻¹, pH 3.8, adjusted using 0.1 N HCl), which was freshly made in 10 mM phosphate buffer (pH 5). Leaf samples were incubated in the solution at room temperature and exposed to light (fluorescent tube [Osram 40 W]) for 8 h. Finally, the leaf samples were discolored in boiling 70% ethanol. After this period, the leaf samples were kept in 5 mL of 70% ethanol in Falcon tubes for further documentation.

2.5.1 Microscopic analysis, DAB image acquisition, and quantification of epidermal cells affected

For microscopic analysis, 16 leaf samples of 1cm² per treatment were examined at each sampling time. Leaf samples were placed on slides with the adaxial side up containing drops of 20% glycerol and covered by a coverslip, and observed under a CX-41 light microscope (Olympus®) at 200× magnification. The number of epidermal cells showing brown staining (DAB polymerized), indicating the presence of H₂O₂, was counted at each infection site. For each sampling time, at least 20 appressorial sites were randomly observed and photographed for further analyses. Leaf image acquisition was performed using a digital camera with 3.1MP (USB 2.0 Color CMOS Digital Eyepiece Microscope Camera, AmScope) linked to the PC via USB interface. The AmScope 4.11.software was used as an interface for DAB image acquisition. All photographs were acquired with 2038 × 1536 resolution and saved as JPEG files.

After this, a set of reference images with a visible H₂O₂ reaction at the infection site caused by *Ptr* were selected to determine the intensity profile (value between 0-255 RGB). For this purpose, the 'magic wand' and histogram tools of the Adobe Photoshop CS6® software was used to manually select visible H₂O₂ reactions and determine the intensity scale (IS) based on a previous categorical color intensity scale, according to Dorneles *et al.* (2017). In this way, the IS was established considering three color intensities: low intensity or wall of the epidermal cells slightly brownish (LI; range between 111 and 131 RGB); medium intensity or wall of epidermal cells encircled by a dark brownish color (MI; range between 91 and 110 RGB); and high intensity or whole epidemic cells dark brown (HI; values ≤ 90 RGB). Based on the IS from the training images, a total of 12

images for each treatment were evaluated. The histogram analysis tool of ImageJ/Fiji 1.46 software was used, which allows obtaining an intensity profile for RGB images. For each image, the number of pixels was quantified according to the IS. At the end of these analyses, the pixels of IS of image evaluated were expressed as percentage of H₂O₂ reaction based on the ratio between the total number of pixels at each IS and the total number of pixels into which each image was decomposed.

2.6 Aniline blue staining

For detection *in situ* of callose, inoculated leaves were sampled at 8, 16, 24, 32, 48, 60, 72 and 96 hai, and stained with aniline blue (Sigma-Aldrich) as described by Schenk & Schikora (2015), with some modification. Briefly, leaf samples (1 cm²) were discolored in 1:3 [acetic acid: ethanol 95% (vol/vol)]. Each 12 h, the saturated destaining solution was replaced, if necessary, until all tissues were transparent. Then, leaf samples were washed in 0.07 mM phosphate buffer (pH = 9) for 30 min. Next, the destained leaf samples were incubated in the dark for at least 8 h in staining solution containing 0.001 mg mL⁻¹ aniline blue fluorochrome (wt/vol) (Sigma-Aldrich) in 0.07 mM phosphate buffer (pH = 9), and kept in a Falcon tube. After incubation, leaf samples were washed again in 0.07 mM phosphate buffer (pH = 9), placed in 70% ethanol for fixation and finally embedded in 50% glycerol (vol/vol) in the dark for conservation. After this procedure, leaf segments at each sampling time were placed and fixed with the adaxial side up on slides containing drops of EntellanTM new rapid mounting medium (Sigma-Aldrich) and a drop of 50% glycerol (vol/vol), and maintained in the dark for further microscopic analysis.

2.6.1 Microscopic analysis, image acquisition, and callose quantification

For microscopic analysis, 16 leaf samples of 1cm² per treatment at each sampling time were visualized for callose deposition through epifluorescence microscopy (Eclipse Ts2-FL, Nikon) using a DAPI filter (wavelength of 385 nm and maximum emission of 420 nm). The Capture 2.2 software was used for documentation. The images were acquired at 1300 × 1030 resolution with adjustment of brightness at 300 ms exposure time, and saved the as JPEG files.

Once again, a set of reference photographs was used for determination of intensity profile (value between 0-255 RGB). For this purpose, the 'magic wand' and histogram tools of the Adobe Photoshop CS6® software were used to select manually the callose intensity, which ranged between 139 and 176 RGB. Based on the intensity range identified from the training images, a total of 12 images for each treatment were evaluated, using the histogram analysis tool of the ImageJ/Fiji 1.46 software, which allows obtaining the number of pixels and intensity profile at the range of each RGB image. The callose deposition area was recorded as corresponding pixels of range intensity (139 and 176 RGB) of the total number of pixels into which each image was decomposed.

2.7 Enzyme activity

Inoculated leaves (*Ptr*-inoculated and mock-inoculated) were sampled at 8, 16, 24, 32, 48, 60, 72 and 96 hai, flash-frozen using liquid nitrogen, and then stored at -80°C until further analysis. Each leaf sample (300 mg) was ground with a mortar and pestle and the resulting fine powder was used for enzyme analysis. The crude extract used for enzyme activity determination was obtained according to the method described in Dallagnol *et al.* (2015).

The activities of catalase, peroxidase and superoxide dismutase were determined according to the methods described in Dallagnol *et al.* (2015). The activity of catalase (CAT, EC 1.11.1.6) was determined by quantifying the degradation of hydrogen peroxide (H_2O_2) (Merck, São Paulo, Brazil) and expressed as micromoles of H_2O_2 degraded $\text{min}^{-1} \text{mg}^{-1}$ of protein. The activity of peroxidase (POX, EC 1.11.1.7) was determined based on the colorimetric quantification of pyrogallol (Sigma-Aldrich, São Paulo, Brazil) oxidation, and expressed as moles of purpurogallin produced $\text{min}^{-1} \text{mg}^{-1}$ of protein using an extinction coefficient of 2.47 mM cm^{-1} . The superoxide dismutase (SOD, EC 1.15.1.1) activity was estimated based on the colorimetric quantification of the photoreduction of nitroblue tetrazolium (NBT) (Sigma-Aldrich, São Paulo, Brazil). The specific activity of SOD was expressed in units of SOD mg^{-1} of protein, considering that one unit of SOD was the amount required to inhibit the photoreduction of NBT by 50%. Phenylalanine ammonia-lyase (PAL, EC 4.3.1.5) activity was determined by colorimetric quantification of transcinnamic acid formed from phenylalanine (Sigma-Aldrich) and expressed as μmol of transcinnamic acid produced per $\text{min}^{-1} \text{mg}^{-1}$ of protein.

For each enzyme activity, three separate extractions were performed for samples from each treatment. Each extraction was read in a spectrophotometer (model UV-UM51- Bel®). The soluble protein concentrations of the extracts were measured by the standard Bradford method, using bovine serum albumin as the standard protein.

2.8 Analyses of N in leaf tissues

Leaf samples were collected at the end of experiment, dried at 60°C for 72 h, and ground using an R-TE-350 mill. A subsample of 1.0 g was used for determination of the plant nitrogen concentration (g kg^{-1}) according to standard micro-Kjeldahl method.

2.9 Analyses of Si in leaf tissues

The leaves were collected at the end of experiment to determine the Si concentration (g kg^{-1}). Samples were rinsed with deionized water, dried for 72 h at 65°C, and ground to pass through a 40-mesh screen using a mill. The foliar Si concentration was determined by standard colorimetric analysis from 0.1 g of alkali-digested tissue.

2.10 Data analyses

The statistical analyses were conducted with R version 4.0.4. (RStudio, 2021). Before the analyses, data assumptions were verified by qq-plots for data normality and plots of fitted values versus the residuals to verify homoscedasticity. Also, data assumptions were verified graphically by using the 'simulateResiduals' function of the DHARMA package. Data of FLs, NLs, and SEV were analyzed by a generalized linear model (GLM) with a logit link and Gaussian family using the 'glm' function of the lme4 package. Data of DAB reaction, callose deposition, and enzyme activity were analyzed by generalized least squares (GSL) using the 'gls' function of the nlme package using the residual maximum likelihood (REML) to compute the coefficients. For nitrogen and silicone concentration, Levene's test was used to assess whether homoscedasticity could be assumed.

After applying parametric ANOVA, the Shapiro-Wilk test was applied to ascertain normality of the fitted residuals. These data was analyzed using the base *lm* of R. The mean values of all experiments were estimated with the *emmeans* package and compared by the Tukey test ($p < 0.05$) using 'cld' of the *multcomp* package.

3 RESULTS

3.1 Disease intensity

The factors Si and N rate and their interaction were significant ($p < 0.05$) for FLS, NLs and AA (Table 1, Figure 1). FLS, NLs, and SEV were decreased by 21, 27 and 13%, respectively, in leaves of +Si plants compared with -Si ones. Accordingly, high N decreased FLS, NLs, and SEV by 17, 26 and 24%, respectively; compared with the low N (Table 1). With respect to the Si \times NR interaction, FLS, NLs and SEV were significantly reduced by 35, 70, and 21% in leaves with +Si plants and low N compared to -Si plants and low N (Figure 1).

3.2 Effect of N rates and Si on hydrogen peroxide accumulation

The DAB reaction, used for quantification of H₂O₂ accumulation, revealed that the intensity of the H₂O₂ accumulation varied over time (hours after inoculation), and the factors N and Si as well as its interaction were significant ($p < 0.05$) (Table 2; Figure S3).

The intensity of H₂O₂ accumulation varied between treatments with Si and N. Low DAB reaction was observed at 8 hai, classified as LI in treatment supplied with Si, whereas the reactions classified as MI and HI were only observed at 16 hai in all treatments (Table 3, Figures 2). The greatest intensities of H₂O₂ accumulation were observed from 24 to 72 hai, with higher values at 48 and 60 hai (Table 3). The treatments with Si had more intense DAB reaction for HI and LI, but

there were no differences for MI between leaves from +Si and -Si plants (Table 3). In contrast, the treatments with low N resulted in a more intense DAB reaction of LI, MI and HI, by 12, 35 and 26%, respectively, compared with high N. As a result, the Si × NR × ST interaction showed that leaves from +Si plants with low N had a more intense DAB reaction at HI, MI, and LI for accumulation of H₂O₂ by 12 and 37% at 48 and 60 hai, respectively, compared with +Si plants with high N (Figure 3).

3.3 Effect of N rates and Si on callose accumulation

The Si, N rates, and their interaction, as well as the sampling times, were significant ($p < 0.05$) for callose accumulation (Table 2, Figure 4). Callose accumulation was observed at 24 hai, with the greatest accumulation observed at 32 hai, decreasing afterwards (Table 3, Figure 4A; Figure S4). Leaves from Si supplied plants showed higher accumulation of callose by 90% compared to -Si plants (Table 3, Figure 4A). However, leaves from plants supplied with low N showed a 50% higher accumulation of callose compared with high N plants (Table 3). Furthermore, the Si × NR interaction showed that leaves from +Si plants with low N had higher callose accumulation by 80% compared to -Si plants with high N (Figure 4B).

3.4 Effect of N and Si on enzyme activity

The effects of N rate, plant inoculation and sampling time were significant ($p < 0.05$) for CAT, POX, SOD, and PAL activities, while Si was only significant ($p < 0.05$) for SOD, POX, and PAL (Table 4). All leaves from inoculated plants showed higher activities of SOD, CAT, POX, and PAL compared with mock-inoculated plants (Tables 4 and 5; Figure 5). In general, the SOD, CAT, POX, and

PAL activities increased over time after plant inoculation, reaching the highest values at 48 hai, then remaining constant until 72 hai for CAT and POX, except for a slight decrease of SOD and PAL activities after 60 hai in low N and +Si amended plants (Figure 5). SOD activity of high N and Si amended plants was constant from 48 until 96 hai, but PAL activity was higher at 48 hai and decreased after 60 hai (Table 5, Figures 5A and 5D). There were no significant differences for CAT and POX between +Si and -Si plants (Figure 5B and 5C). Moreover, CAT and POX activities were higher at 48 hai in the treatment with high N and +Si, but CAT activity continued to increase until 72 hai (Figure 5B) and POX activity decreased after 60 hai in the same treatment (Figure 5C). On the other hand, in leaves from plants with low N, there were increases of the activities of SOD, CAT, POX, and PAL by 20, 6, 17 and 13%, respectively, compared to leaves from plants with high N (Table 5).

In the Si × NR × ST interaction, in leaves from +Si plants with low N, the SOD and CAT activities increased by 14 and 56% at 48 hai, while POX activity increased by 36% at 60 hai compared with +Si with high N (Figures 5A, B and C). In contrast, the PAL activity decreased by 36% in leaves from +Si plants with high N at 60 hai compared with +Si with low N (Figure 5D).

3.5 Leaf nitrogen and silicon concentrations

The leaf concentrations of N and Si varied according to the treatment applied. Significant differences ($p < 0.05$) were observed for Si, NR and the Si × NR interaction (Table 6). Additionally, there was no observed effect on macro and micronutrients in plant tissue (Supporting information; Table S7). The Si concentration increased by 27% in leaves of +Si plants compared to -Si ones, but

the Si amendment had no significant ($p < 0.05$) effect on the N concentration in the leaves (Table 6). In contrast, the increase in the N rate reduced the leaf Si concentration by 13% and increased the N leaf concentration by 16% (Table 6). Therefore, the interaction of Si \times NR showed that the increase in the N rate reduced the leaf Si concentration up to 21% (Table 6), and N concentration in the leaves was not affected regardless of Si incorporation (Table 6).

4DISCUSSION

In this study the soil amendment with Si and N fertilization were found to affect wheat resistance to race 1 of *Ptr* by affecting histo-cytological and biochemical responses of defense mechanisms. The early and higher H₂O₂ accumulation, callose deposition and increased enzymatic activity in treatments were found to be related to the reduction in tan spot intensity.

The higher Si concentration in plants with low N showed an enhanced effect of Si compared to higher N, resulting in earlier and stronger activation of defense responses, indicating a higher beneficial role of the element under low availability of N in potentiating the plant defense against the pathogen. The higher SOD activity indicated that that plants supplied with Si and low N responded rapidly to pathogen infection probably by regulating the reactive oxygen species concentration. This observation was also reported by Dorneles *et al.* (2017) that found the early accumulation of H₂O₂ in wheat epidermal cells associated with the plant's defense mechanism, as opposed to the accumulation of H₂O₂ later in the infection, and mainly in the parenchymal cells, as a result of the action of *Ptr* toxins. Likewise, the increase in the activity of CAT and POX, observed in +Si and low N plants, showed that plants supplied with Si activated those enzymes due to the increment in H₂O₂ to protect cells against oxidative stress caused by the

*Ptr*infection, indicating better homeostasis in the concentration of ROS in the plant cells. These results agree with previous reports by Dorneles *et al.* (2017, 2018).

Regarding the PAL activity, it has been observed that in plants receiving low N, the activity increases, but only slightly, while at high N the activity decreases (Moriwaki *et al.*, 2019). Results of our study corroborate this finding, since the plants supplied with low N had increased PAL activity. PAL is a key enzyme of the phenylpropanoid pathway, which leads to increase in the synthesis of resistance-related phenolics (Dixon & Paiva, 1995). In this line, Dorneles *et al.* (2018) reported that plants supplied with Si, had higher PAL activity, thereby resulting in the accumulation of phenylpropanoid derivatives at infection sites, related to reduced *Ptr* damage.

On the other hand, at higher N rate, the *Ptr* damage was lower, but the PAL activity was still low. Despite this contrary finding, we believe that higher N reduces *Ptr* damage, as was previously reported by Castro *et al.* (2018) and Fleitas *et al.* (2018). In this sense, at high N, the PAL activity may not be the principal effect of the resistance to *Ptr*. Indeed, in response to necrotrophic pathogens and pathogens triggering resistance, more genes of N metabolism are up- or down-regulated than in response to biotrophic pathogens, suggesting that many of the observed gene modulations are associated with cell death and/or plant defense (Fagard *et al.*, 2014; Sanmartín *et al.*, 2020). Overall, N metabolism genes are strongly affected by pathogen infection, probably as a result of both defense activation and attempted pathogen manipulation of host metabolism for nutritional purposes (Fagard *et al.*, 2014). For instance, the necrotrophic habit of *Ptr* leads to the capacity to break down plant cell elements, allowing the use of a wide range of N sources (Simón *et al.*, 2020). At higher N, the colony structure of

necrotrophic pathogens results in a denser and more branched mycelium, enabling the fungus to exploit the substrate (Fleitas *et al.*, 2018; Simon *et al.*, 2020). Indeed, this fact may explain at least why some authors have reported that tan spot preferably colonizes weak and senescent tissues (Bockus & Davis, 1993; Snoeijers *et al.*, 2000). These observations also agree with the fact that at higher N, the N modifies the crop structure, increasing the green leaf area index (GLAI) and delaying senescence due to a higher radiation interception and radiation use efficiency (RUE) affecting the disease severity (Schierenbeck *et al.*, 2016; Fleitas *et al.*, 2018).

Nevertheless, observations of enzymatic activity and the accumulation of H₂O₂, and callose deposition may be associated with the effect of N. Callose deposition is promoted by indole glucosinolates (IGSs) and reactive oxygen species (ROS) (Wang *et al.*, 2021). Furthermore, the activation of abscisic acid (ABA) signaling induces or primes callose deposition and is influenced by carbohydrate metabolism (Sanmartín *et al.*, 2020; Wang *et al.*, 2021). In our study, the response activated at low N was observed at 24 hai and the major callose deposition occurred at 32 hai. Indeed, the highest callose accumulation and H₂O₂ accumulation were observed in leaves infected by *Ptr* of plants receiving Si amendment and low N, suggesting that the activation of these defenses may be associated with Si rather than N incorporation. These results suggest that low N reduces the capacity for sucrose formation, as previously reported by Rufty *et al.* (1988). However, Si incorporation probably is involved in maintaining the sucrose concentration despite the *Ptr* effect. This observation agrees with the finding of Araújo *et al.* (2019), who reported that Si improved the source-sink relationship of infected leaves due to alteration in the activities of the enzymes

acid invertase and sucrose phosphate synthase in leaves and spikes of wheat challenged by *Pyricularia oryzae*. This observation is in line to the fact that at higher N rate, despite Si amendment, the infection by *Ptr* was delayed from 48 to 72 hai, associated with lesser callose deposition. This result suggests that the effect of +Si and low N may have influenced the accumulation of H₂O₂, which probably induced the deposition of callose as a defense response.

Associated with this observation, Si concentration in leaves decreased with high N rate. At least two factors may have influenced this outcome: first, the increase in biomass with higher N, which lead to dilution of Si in the plant tissue; and second, changes in the soil pH caused by the higher N rate affected Si uptake. In this context, the acidification of soil at high N rates in this experiment may affect the Si absorption, which is mainly through active transport mechanisms inherent to the roots (Bélanger *et al.*, 2016), resulting in the less Si content at high N. This observation agrees with Murozuka *et al.* (2015), who reported that differences in leaf Si concentration among wheat genotypes were partially explained by differences in the soil pH.

Overall, this is the first report of the effect of N × Si interaction in wheat challenged by *Ptr*. At low N, the Si concentration was higher in plants, demonstrating the effect on *Ptr* due to increases in plant defenses. However, more research on this topic needs to be undertaken to clearly understand the association between N and Si. The finding of this study, suggests that Si and low N increase the callose deposition in a compatible reaction (susceptible host). There were no synergistic effects between the two elements. These findings agree with White (2017) and Shahrtash (2017), who reported that N and Si did not have any interactive effect on wheat yield. Under field conditions, Si (silicate slag

application) effectively raised soil pH, and the availability of the essential N nutrient (nitrate, NO_3^-). However, nitrogen at 145 kg ha^{-1} had a greater impact on wheat yield than silicate slag application (White *et al.*, 2017). This observation may explain why Si application reduced N fertilization by approximately 50% in wheat ($195\text{-}200$ to 100 kg ha^{-1}) (Galindo *et al.*, 2021). These findings agree with those of Wu *et al.* (2017), who reported antagonistic interaction between Si and N accumulation in rice, because high N fertilization reduced Si accumulation in rice leaves, a decrease due, at least in part, to a decrease in the expression of Si transporters *OsLsi1* and *OsLsi2*.

Despite the greater effect on *Ptr* control of higher N, the N fertilization should be used with caution when Si is incorporated in the soil during crop management. Nitrogen application and soil amendment with silicon are strategies that activate the plant's defense mechanisms independently, because exceeding the nitrogen dose affects silicon absorption, reducing the plant's defense responses to *Ptr* exposure. In conclusion, the +Si and low N treatment increased the activity of SOD, CAT, and POX, conferring protection to cells against oxidative stress caused by *Ptr* infection. In addition, the greater accumulation of H_2O_2 and deposition of callose in leaves infected by *Ptr* suggests the activation of these defenses was associated with Si.

ACKNOWLEDGEMENTS

The authors are thankful to the Office to Coordinate Improvement of Higher Education Personnel (CAPES) for financial support and the student scholarships (finance code 001) to A. R and L. J. D. were supported by fellowships from the Brazilian National Council for Scientific and Technological Development

(CNPq)(grant number 308149/2018-1). We thank to Passo Fundo University for providing the *P. tritici-repentis* isolates used in the experiments, Grow Green for the preparation of spreadsheets of fertilization recommendation for the experiments and BIOTRIGO for providing wheat seeds for the experiments.

REFERENCES

- Araújo, M.U., Rios, J.A., Silva, E.T. & Rodrigues, F.Á. (2019) Silicon alleviates changes in the source-sink relationship of wheat plants infected by *Pyricularia oryzae*. *Phytopathology*, 109, 1129-1140.
- Bélanger, R. Deshmukh, R., Belzile, F., Labbé, C., Perumal, A. & Edwards, S.M. (2016) Plant with increased silicon uptake. Patent Application No. 15/574,414.
- Bertagnolli, V.V., Ferreira, J.R., Liu, Z., Rosa, A.C. & Deuner, C.C. (2019) Phenotypical and genotypical characterization of *Pyrenophora tritici-repentis* races in Brazil. *European Journal of Plant Pathology*, 154, 995-1007.
- Bockus, W.W. & Davis, M.A. (1993) Effect of nitrogen fertilizers on severity of tan spot of winter wheat. *Plant Disease*, 77, 508.
- Castro, A.C., Fleitas, M.C., Schierenbeck, M., Gerard, G.S. & Simón, M.R. (2018) Evaluation of different fungicides and nitrogen rates on grain yield and bread-making quality in wheat affected by *Septoria tritici* blotch and yellow spot. *Journal of Cereal Science*, 83, 49-57.
- Ciuffetti, L.M., Manning, V.A., Pandelova, I., Faris, J.D., Friesen, T.L., Strelkov, S.E., Weber G. L., Goodwin S. B., Wolpert T.J. & Figueroa, M. (2014) *Pyrenophora tritici-repentis*: a plant pathogenic fungus with global impact. In: Dean R., Lichens-Park A., Kole C. (Eds.) *Genomics of Plant-Associated Fungi: Monocot Pathogens*. Berlin: Springer, pp. 1–39.
- Dallagnol, L.J., Rodrigues, F. Á., Pascholati, S.F., Fortunato, A.A. & Camargo, L.E.A. (2015) Comparison of root and foliar applications of potassium silicate in potentiating post-infection defences of melon against powdery mildew. *Plant Pathology*, 64, 1085-1093.

- Dallagnol, L.J., Román, A.E. & da Rosa Dorneles, K. (2020) Silicon Use in the Integrated Disease Management of Wheat: Current Knowledge. *Current Trends in Wheat Research*. [Online First], IntechOpen, Available from: <https://www.intechopen.com/online-first/74509>. [Accessed: July 5, 2021].
- Debona, D., Rodrigues, F.Á., Rios, J.A. & Nascimento, K.J.T.(2012) Biochemical changes in the leaves of wheat plants infected by *Pyricularia oryzae*. *Phytopathology*, 102, 1121-1129.
- Debona, D., Rodrigues, F.A. & Datnoff, L.E. (2017) Silicon's role in abiotic and biotic plant stresses. *Annual Review of Phytopathology*, 55, 85-107.
- Dixon, R.A. & Paiva, N.L. (1995) Stress-induced phenylpropanoid metabolism. *The plant cell*, 7, 1085.
- Dorneles, K.R., Dallagnol, L.J., Pazdiora, P.C., Rodrigues, F.A. & Deuner, S. (2017) Silicon potentiates biochemical defense responses of wheat against tan spot. *Physiological and Molecular Plant Pathology*, 97, 69-78.
- Dorneles, K.R., Pazdiora, P.C., Hoffmann, J.F., Chaves, F.C., Monte, L.G., Rodrigues, F.A. & Dallagnol, L.J. (2018) Wheat leaf resistance to *Pyrenophora tritici-repentis* induced by silicon activation of phenylpropanoid metabolism. *Plant Pathology*, 67, 1713-1724.
- Fagard, M., Launay, A., Clément, G., Courtial, J., Dellagi, A., Farjad, M., Krapp, A., Soulié, M.C. & Masclaux-Daubresse, C. (2014) Nitrogen metabolism meets phytopathology. *Journal of Experimental Botany*, 65, 5643-5656.
- Fleitas, M.C. Schierenbeck, M., Gerard, G.S., Dietz, J.I., Golik, S.I. & Simón, M.R. (2018) Breadmaking quality and yield response to the green leaf area duration caused by fluxapyroxad under three nitrogen rates in wheat affected with tan spot. *Crop Protection*, 106, 201-209.
- Galindo, F.S. Pagliari, P.H., Rodrigues, W.L., Fernandes, G.C., Boleta, E.H., Santini, J.M. & Teixeira Filho, M.C.(2021) Silicon amendment enhances agronomic efficiency of nitrogen fertilization in maize and wheat crops under tropical conditions. *Plants*, 10, 1329.

- Huber, D. & Thompson, I. (2007) Nitrogen and plant disease. In Datnoff, L., Elmer, W., and Huber, D. (Eds.) *Mineral Nutrition and Plant Disease*. USA: American Phytopathological Society, pp. 31-44.
- Moriwaki, T., Falcioni, R., Tanaka, F.A, Cardoso, K.A., Souza, L.A., Benedito, E., Nanni, M.R., Bonato, C. & Antunes, W.C. (2019) Nitrogen-improved photosynthesis quantum yield is driven by increased thylakoid density, enhancing green light absorption. *Plant Science*, 278, 1-11.
- Murozuka, E., De Bang, T.C., Frydenvang, J., Lindedam, J., Laursen, K.H., Bruun, S., Magid, J. & Schjoerring, J.K.(2015) Concentration of mineral elements in wheat (*Triticum aestivum* L.) straw: Genotypic differences and consequences for enzymatic saccharification. *Biomass and Bioenergy*, 75, 134-141.
- Pazdiora, P.C., da Rosa Dorneles, K., Forcelini, C.A., Del Ponte, E.M. & Dallagnol, L.J. (2018) Silicon suppresses tan spot development on wheat infected by *Pyrenophora tritici-repentis*. *European Journal of Plant Pathology*, 150, 49-56.
- Pazdiora, P.C., da Rosa Dorneles, K., Morello, T.N., Nicholson, P. & Dallagnol, L.J. (2021) Silicon soil amendment as a complement to manage tan spot and fusarium head blight in wheat. *Agronomy for Sustainable Development*, 41, 1-13.
- RStudio (2021) RStudio: Integrated development environment for R. RStudio, PBC, Boston, MA. Available at: <http://www.rstudio.com/>. [Accessed: August 11, 2021].
- Rufty Jr, T.W., Huber, S.C. & Volk, R.J. (1988) Alterations in leaf carbohydrate metabolism in response to nitrogen stress. *Plant Physiology*, 88, 725-730.
- Sanmartín, N., Pastor, V., Pastor-Fernández, J., Flors, V., Pozo, M.J. & Sánchez-Bel, P. (2020) Role and mechanisms of callose priming in mycorrhiza-induced resistance. *Journal of Experimental Botany*, 71, 2769-2781.
- Schenk, S. & Schikora, A. (2015) Staining of callose depositions in root and leaf tissues. *Bio-protocol*, 5, e1429–e1429.

- Schierenbeck, M., Fleitas, M.C., Miralles, D.J. & Simón, M.R. (2016) Does radiation interception or radiation use efficiency limit the growth of wheat inoculated with tan spot or leaf rust?. *Field Crops Research*, 199, 65-76.
- Shahrtash, M. (2017) *Effects of silicon and nitrogen fertilization on growth, yield, and leaf rust disease development in wheat*. Louisiana State University. Available at: https://digitalcommons.lsu.edu/gradschool_theses/4470. [Accessed: March 8, 2021].
- Shi, J. Fu, X.Z., Peng, T., Huang, X.S., Fan, Q.J. & Liu, J.H. (2010) Spermine pretreatment confers dehydration tolerance of citrus in vitro plants via modulation of antioxidative capacity and stomatal response. *Tree Physiology*, 30, 914-922.
- Silva, S.R., Bassoi, M.C. & Foloni, J.S. (2017) *Informações Técnicas para Trigo e Tricale- Safra 2017*. Brasília: Embrapa. Available at: <http://ainfo.cnptia.embrapa.br/digital/bitstream/item/155787/1/Informacoes-Tecnicas-para-Trigo-e-Triticale-Safra-2017-OL.pdf>. [Accessed: January 5, 2021].
- Simón, M.R., Fleitas, M.C., Castro, A.C. & Schierenbeck, M. (2020) How foliar fungal diseases affect nitrogen dynamics, milling and end-use quality of wheat. *Frontiers in Plant Science*, 11, 1568.
- Snouijers, S.S., Pérez-García, A., Joosten, M.H. & De Wit, P.J. (2000) The effect of nitrogen on disease development and gene expression in bacterial and fungal plant pathogens. *European Journal of Plant Pathology*, 106, 493-506.
- Veresoglou, S.D., Barto, E.K., Menexes, G. & Rillig, M.C. (2013) Fertilization affects severity of disease caused by fungal plant pathogens. *Plant Pathology*, 62, 961-969.
- Wang, Y., Li, X., Fan, B., Zhu, C. & Chen, Z. (2021) Regulation and function of defense-related callose deposition in plants. *International Journal of Molecular Sciences*, 22, 2393.
- White, B., Tubana, B.S., Babu, T., Mascagni, H., Agostinho, F., Datnoff, L.E. & Harrison, S. (2017) Effect of silicate slag application on wheat grown under

two nitrogen rates. *Plants*, 6, 47.

Wu, X., Baerson, S.R., Song, Y., Liang, G., Ding, C., Niu, J., Pan, Z. & Zeng, R. (2017) Interactions between nitrogen and silicon in rice and their effects on resistance toward the brown planthopper *Nilaparvata lugens*. *Frontiers in Plant Science*, 8, 28.

TABLE 1. Summary statistics, mean squares and standard errors of final lesion size (FLS), number of lesions per cm² (NLs) and severity (SEV) of tan spot, at 96 hours after inoculation with *Pyrenophora tritici-repentis*, on leaves of wheat plants grown in soil supplied with calcium silicate (+Si) or extra-fine limestone (-Si) receiving 70 (Low N) or 200 (High N) kg ha⁻¹ of nitrogen.

Treatment	FLS (mm)	NLs (number)	SEV (%)
Silicon (Si)			
+Si	0.660 ± 0.03 b	8.12 ± 0.97 b	12 ± 0.33 a
-Si	0.839 ± 0.03 a	11.12 ± 0.97 a	13.5 ± 0.33 b
<i>p value</i>	<0.001	0.033	0.002
Nitrogen rate (NR)			
Low N	0.819 ± 0.03 a	11.04 ± 0.97 a	14.5 ± 0.33 b
High N	0.680 ± 0.03 b	8.21 ± 0.97 b	11.1 ± 0.33 a
<i>p value</i>	0.005	0.044	<0.001
Si × NR	0.041	0.006	<0.001

Significant at *** $p = 0.001$; ** $p = 0.01$; * $p < 0.05$; ns = not significant

TABLE 2. Summary statistics of the effects of silicon (Si), nitrogen rate (NR) and sampling time (ST) on DAB reaction, classified as low intensity (LI), medium intensity (MI) and high intensity (HI), and for callose accumulation (# pixels) on leaves of wheat plants grown in soil supplied with calcium silicate (+Si) or extra-fine limestone (-Si) receiving 70 (Low N) or 200 (High N) kg ha⁻¹ of nitrogen and inoculated with *Pyrenophora tritici-repentis*.

Treatment	df	DAB			Callose (# pixels)
		H1 (%)	MI (%)	LI (%)	
Silicon (Si)	1	52.39***	7.58**	224.23***	4979.40***
Nitrogen rate (NR)	1	1099.38***	1058***	132.31**	5119.69***
Sampling time (ST)	7	978.89**	1363.07**	1016.86*	19225.98**
Si × NR	1	147.97**	418.36**	69.39*	611.27*
Si × ST	7	105.86*	40.75*	8.96*	2657.82*
NR × ST	7	247.85*	34.33*	22.11*	2394.53*
Si × NR × ST	7	546.44**	169.28**	55.79*	956.14**

Significant at *** $p = 0.001$; ** $p = 0.01$; * $p < 0.05$; ns = not significant

TABLE 3. Mean squares and standard errors of effect of silicon (Si), nitrogen rate (NR) and sampling time (ST; hours after inoculation with *Pyrenophora tritici-repentis*) on DAB reaction classified as low intensity (LI), medium intensity (MI) and high intensity (HI), and callose (# pixels) on leaves of wheat plants grown in soil supplied with calcium silicate (+Si) or extra-fine limestone (-Si) receiving 70 (Low N) or 200 (High N) kg ha⁻¹ of nitrogen.

Treatment	DAB			Calose (# pixels)
	HI (%)	MI (%)	LI (%)	
Silicon (Si)				
-Si	0.503 ± 0.005 b	8.05 ± 0.25	11.7 ± 0.35 b	4046 ± 52.8 b
+Si	0.731 ± 0.005 a	7.85 ± 0.25	13.5 ± 0.35 a	7694 ± 52.8 a
Nitrogen rates (NR)				
Low N	0.634 ± 0.005 a	9.12 ± 0.25 a	13.3 ± 0.35 b	7120 ± 52.8 a
High N	0.547 ± 0.005 b	6.78 ± 0.25 b	11.9 ± 0.35 a	4620 ± 52.8 b
Sampling time (ST)				
8	0.000 ± 0.01 g	0 ± 0.10 g	0.886 ± 0.17 f	0 ± 106 f
16	0.347 ± 0.01 f	5.37 ± 0.10 f	9.63 ± 0.17 e	0 ± 106 f
24	0.563 ± 0.01 e	7.75 ± 0.10 e	12.89 ± 0.17 d	6833 ± 106 c
32	0.717 ± 0.01 d	9.77 ± 0.10 c	13.23 ± 0.17 d	29720 ± 106 a
48	0.864 ± 0.01 b	9.55 ± 0.10 cd	16.99 ± 0.17 a	7747 ± 106 b
60	0.912 ± 0.01 a	9.18 ± 0.10 d	15.30 ± 0.17 c	1891 ± 106 d
72	0.734 ± 0.01 d	11.60 ± 0.10 a	16.07 ± 0.17 b	770 ± 106 f
96	0.807 ± 0.01 c	10.60 ± 0.10 b	16 ± 0.17 bc	0 ± 106 f

TABLE 4. Summary statistics of the effects of silicon (Si), nitrogen rate (NR), sampling time (ST) and inoculation (I) on activities of superoxide dismutase (SOD), catalases (CAT), peroxidases (POX), and phenylalanine ammonia-lyase (PAL)

Treatment	df	SOD	CAT	POX	PAL
Silicon (Si)	1	169.25***	0.9 ns	8.63**	283.92***
Nitrogen rate (NR)	1	461.02***	362.4***	585.65***	58.80*
Sampling time (ST)	7	353.51***	478.9***	987.45***	310***
Inoculation (I)	1	774.55**	625.6**	2021.28**	1307.16**
Si × NR	1	1.60ns	2.5ns	104.96***	605.39**
Si × ST	7	60.82**	41.5**	23.79*	71.49***
NR × ST	7	36.95**	16***	38.29**	133.68***
Si × I	1	38.04**	0.4ns	12.89**	12.38**
NR × I	1	2.29ns	24.6***	57.33*	3.9**
ST × I	7	16.17**	40.3**	85.18**	45.34**
Si × NR × ST	7	62.99**	66.7**	209.77***	24.25**
Si × NR × I	1	18.72ns	4.8*	80.70**	3.15ns
Si × ST × I	7	27.54*	2.2*	35.87*	33.88*
NR × ST × I	7	6.40ns	8.7ns	30.60ns	21.42ns
Si × NR × ST × I	7	4.62ns	17.7ns	43.63ns	21.10ns

Significant at *** $p = 0.001$; ** $p = 0.01$; * $p < 0.05$; ns = not significant

TABLE 5. Mean squares and standard errors of effect of silicon (Si), nitrogen rate (NR), sampling time (ST; hours after inoculation with *Pyrenophora tritici-repentis*), and inoculation (I) on activities of superoxide dismutases (SOD), catalases (CAT), peroxidases (POX), and phenylalanine ammonia-lyase (PAL) in leaves of wheat plants grown in soil supplied with calcium silicate (+Si) or extra-fine limestone (-Si) receiving 70 (Low N) or 200 (High N) kg ha⁻¹ of nitrogen.

Treatment	SOD	CAT	POX	PAL
Silicon (Si)				
-Si	123 ± 1.76 b	19.1 ± 0.22	0.899 ± 0.0062	0.105 ± 0.0012 b
+Si	145 ± 1.76 a	19.2 ± 0.22	0.874 ± 0.0062	0.131 ± 0.0012 a
Nitrogen rates (NR)				
Low N	146 ± 1.76a	19.7 ± 0.22 a	0.957 ± 0.0062 a	0.125 ± 0.0012 a
High N	122 ± 1.76 b	18.5 ± 0.22 b	0.816 ± 0.0062 b	0.111 ± 0.0012 b
Inoculation (I)				
<i>Ptr</i> -inoculated	157 ± 2.28 a	20 ± 0.26 a	1.015 ± 0.008 a	0.149 ± 0.149 a
Mock -inoculated	111 ± 1.02 b	18.3 ± 0.18 b	0.758 ± 0.004 b	0.868 ± 0.087 b
Sampling time (ST)				
8	87.1 ± 3.53 e	17.8 ± 0.15d	0.540 ± 0.012 e	0.0719 ± 0.0024 e
16	77.5 ± 3.53 e	18.3 ± 0.15 d	0.640 ± 0.012 d	0.0791 ± 0.0024 de
24	116.7 ± 3.53 d	18.1 ± 0.15d	0.735 ± 0.012 c	0.0800 ± 0.0024 de
32	154.3 ± 3.53 bc	19.7 ± 0.15 c	0.833 ± 0.012 b	0.1214 ± 0.0024 c
48	182.6 ± 3.53 a	21.8 ± 0.15 a	1.143 ± 0.012 a	0.1696 ± 0.0024a
60	158.9 ± 3.53 b	20.5 ± 0.15b	1.160 ± 0.012 a	0.1753 ± 0.0024 a
72	156.3 ± 3.53 b	21.5 ± 0.15 a	1.169 ± 0.012 a	0.1561 ± 0.0024 b
96	139.2 ± 3.53 c	15.4 ± 0.15 e	0.871 ± 0.012 b	0.0891 ± 0.0024 d

Table 6. Mean squares and standard errors of effect of silicon (Si) and nitrogen rate (NR) effect on leaf silicon concentration (Si) and leaf nitrogen concentration (N) of wheat plants grown in soil supplied with calcium silicate (+Si) or extra-fine limestone (-Si) receiving 70 (low N) or 200 (high N) kg ha⁻¹ of nitrogen.

Treatment	Si (g kg⁻¹)	N (g kg⁻¹)
Silicon (Si)		
+Si	23.1 ± 0.26 a	29.5 ± 0.21b
-Si	17.5 ± 0.26 b	30.6 ± 0.21 a
<i>p value</i>	<0.0001	<0.0001
Nitrogen rate (NR)		
Low N	21.8 ± 0.26 a	27.7 ± 0.21b
High N	18.8 ± 0.26 b	32.4 ± 0.21 a
<i>p value</i>	<0.0001	<0.0001
Si × NR		
+Si × Low N	25.6 ± 0.35 a	26.8 ± 0.30 c
+Si × High N	20.7 ± 0.35 b	32.9 ± 0.30 a
-Si × Low N	18.1 ± 0.35 c	29.4 ± 0.30 b
-Si × High N	16.9 ± 0.35 c	31.9 ± 0.30 a
<i>p value</i>	<0.0001	<0.0001

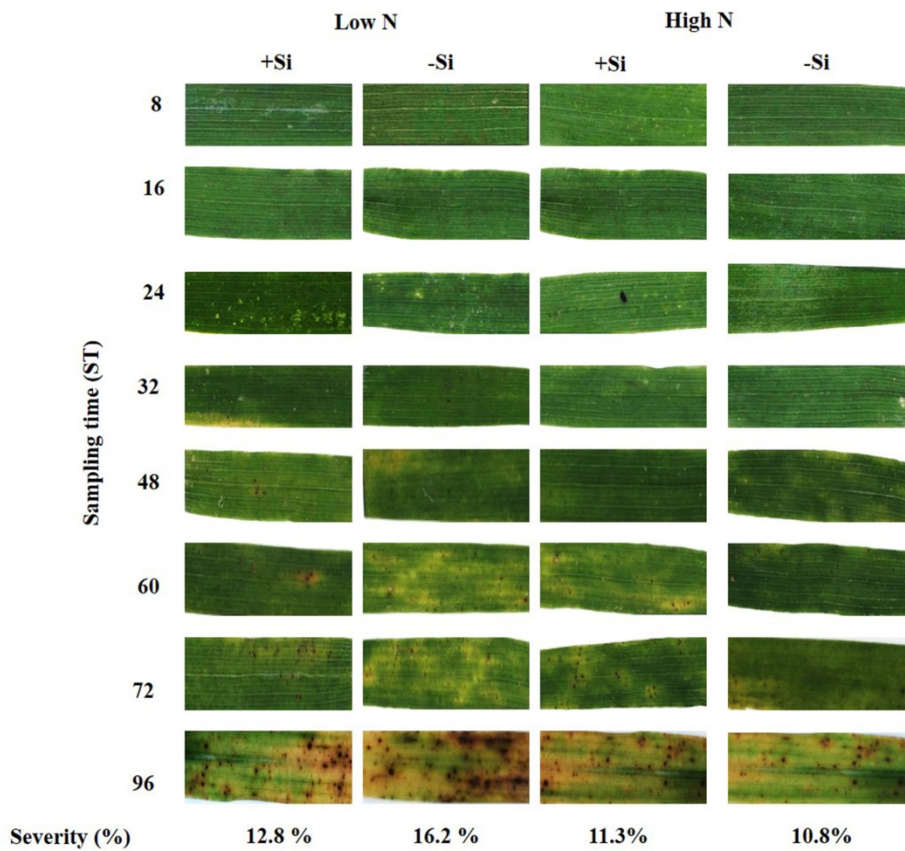


FIGURE 1 Tan spot symptoms at 8 to 96 hours after inoculation of *Pyrenophora tritici-repentis* race 1 on leaves of TBIO Tibagi wheat plants grown in soil supplied with calcium silicate (+Si) or extra-fine limestone (-Si) receiving 70 (Low N) or 200 (High N) kg ha⁻¹ of nitrogen.

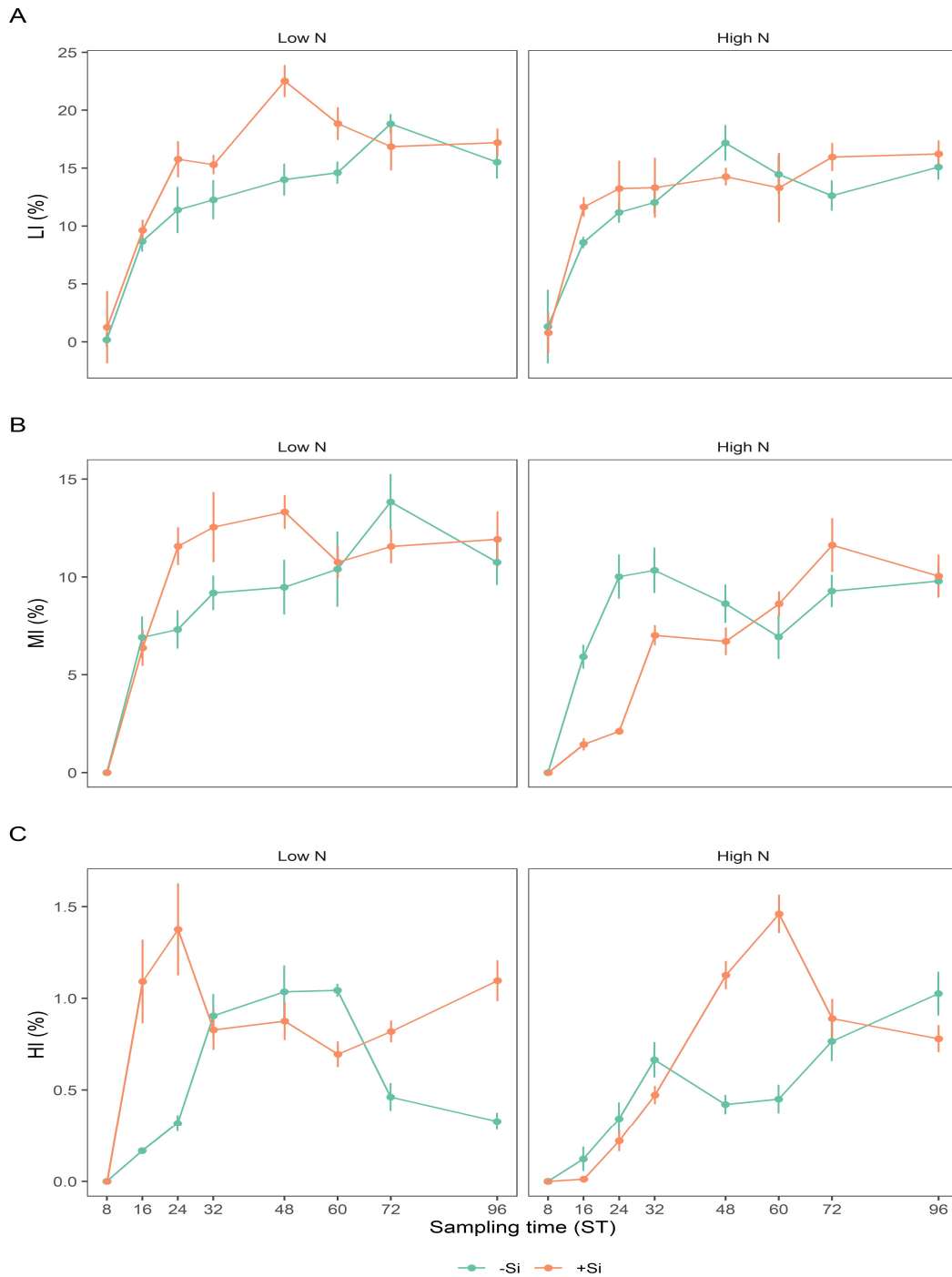


FIGURE 2 Silicon (Si) × nitrogen rate (NR) × sampling time (ST) interaction for DAB reaction classified as low intensity (LI) (A), medium intensity (MI) (B) and high intensity (HI) (C) after *Pyrenophora tritici-repentis* inoculation on leaves of wheat plants grown in soil supplied with calcium silicate (+Si) or extra-fine limestone (-Si) receiving 70 (Low N) or 200 (High N) kg ha⁻¹. Data point from two pooled experiments (n = 24) are the median and error bars represent standard deviation of means.

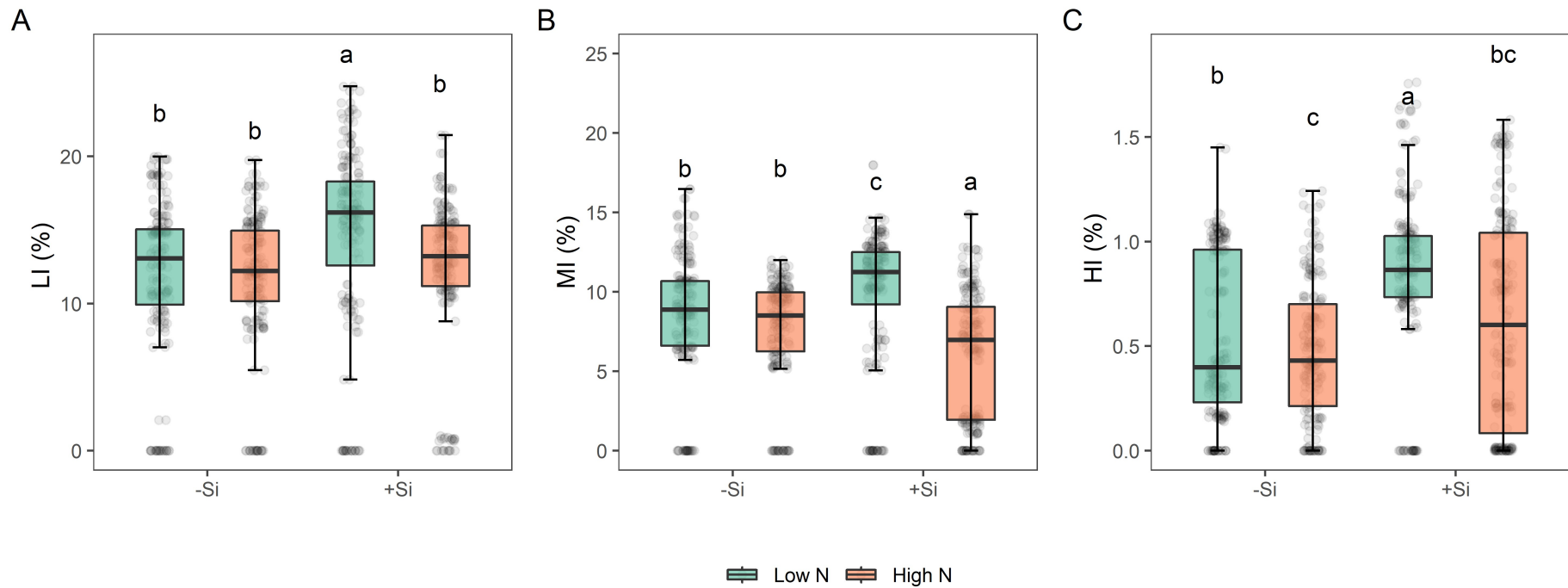


FIGURE 3 Silicon (Si) × nitrogen rate (NR) interaction for DAB reaction classified as low intensity (LI) (A), medium intensity (MI) (B), and high intensity (HI) (C) on leaves of wheat plants grown in soil supplied with calcium silicate (+Si) or extra-fine limestone (-Si) receiving 70 (Low N) or 200 (High N) kg ha⁻¹ of nitrogen and inoculated with *Pyrenophora tritici-ripentis*. Data points (•) from two pooled experiments (n = 24) are the median and error bars represent standard deviation of means. Different lowercase letters indicate statistical differences according to Tukey test at $p < 0.05$.

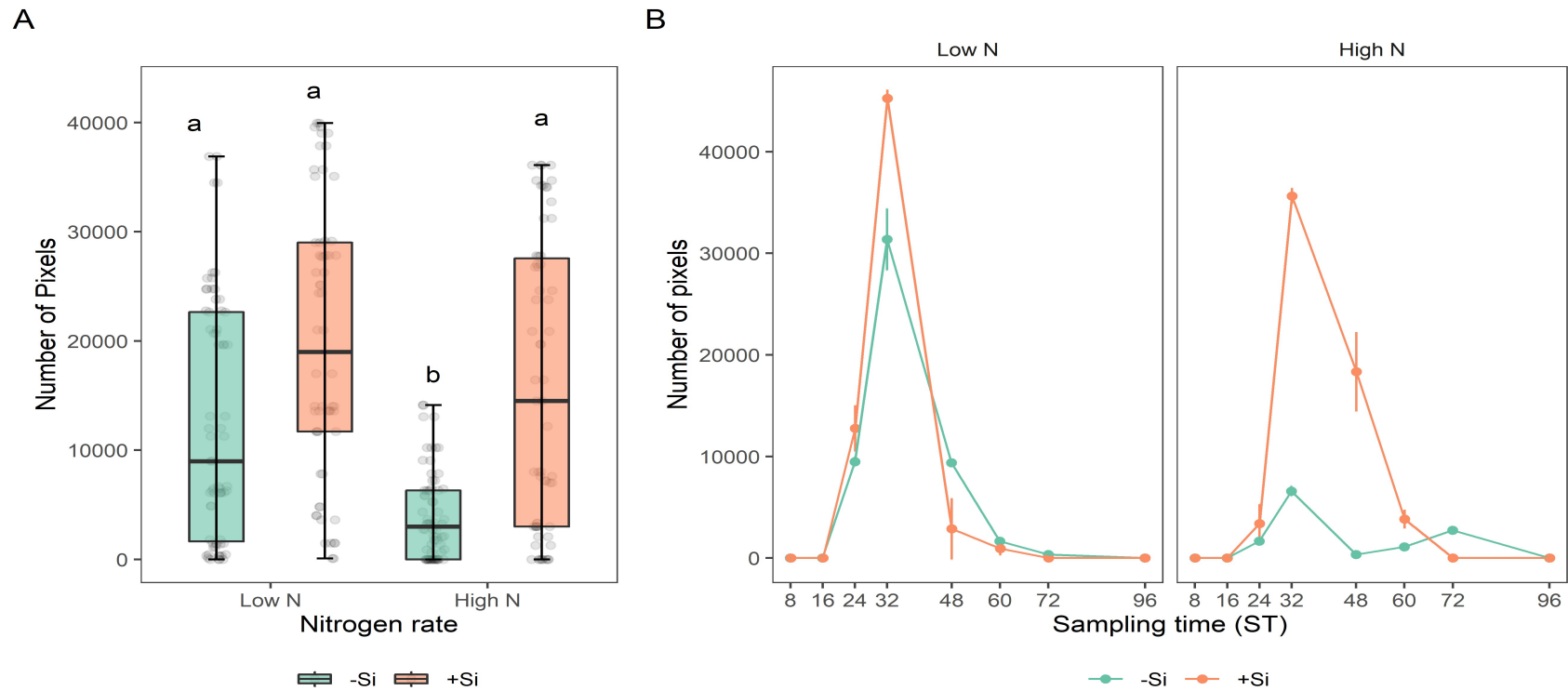


FIGURE 4 Silicon (Si) × nitrogen rate (NR) interaction of number of pixels of callose deposition (A); and Si × NR × sampling time (ST) interaction of callose deposition (B) on leaves of wheat plants grown in soil supplied with calcium silicate (+Si) or extra-fine limestone (-Si) receiving 70 (Low N) or 200 (High N) kg ha⁻¹ of nitrogen and inoculated with *Pyrenophora tritici-repentis*. Data points from two pooled experiments (n = 24) are the median and error bars represent standard deviation of means. Different lowercase letters indicate statistical differences according to Tukey test at $p < 0.05$.

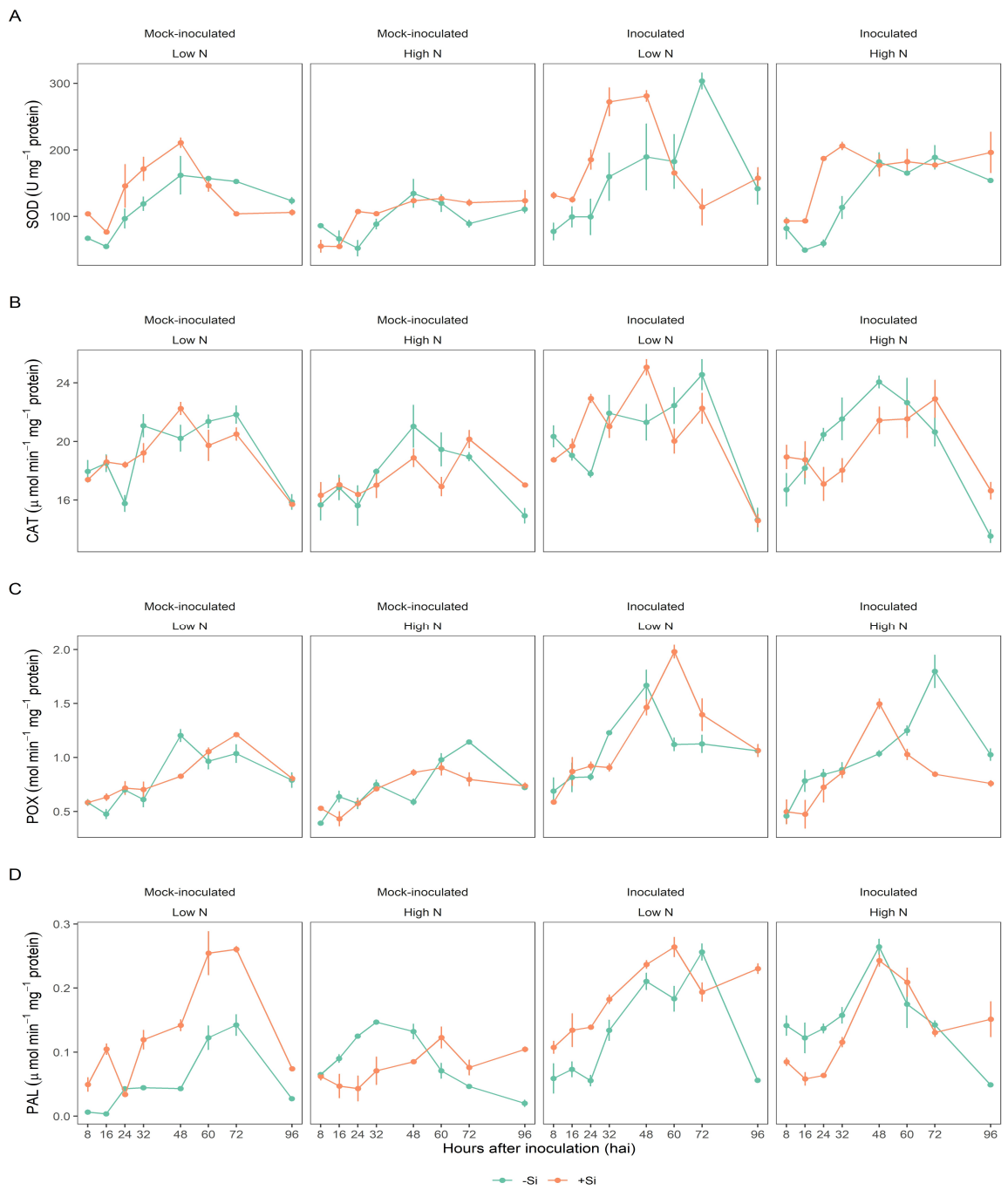
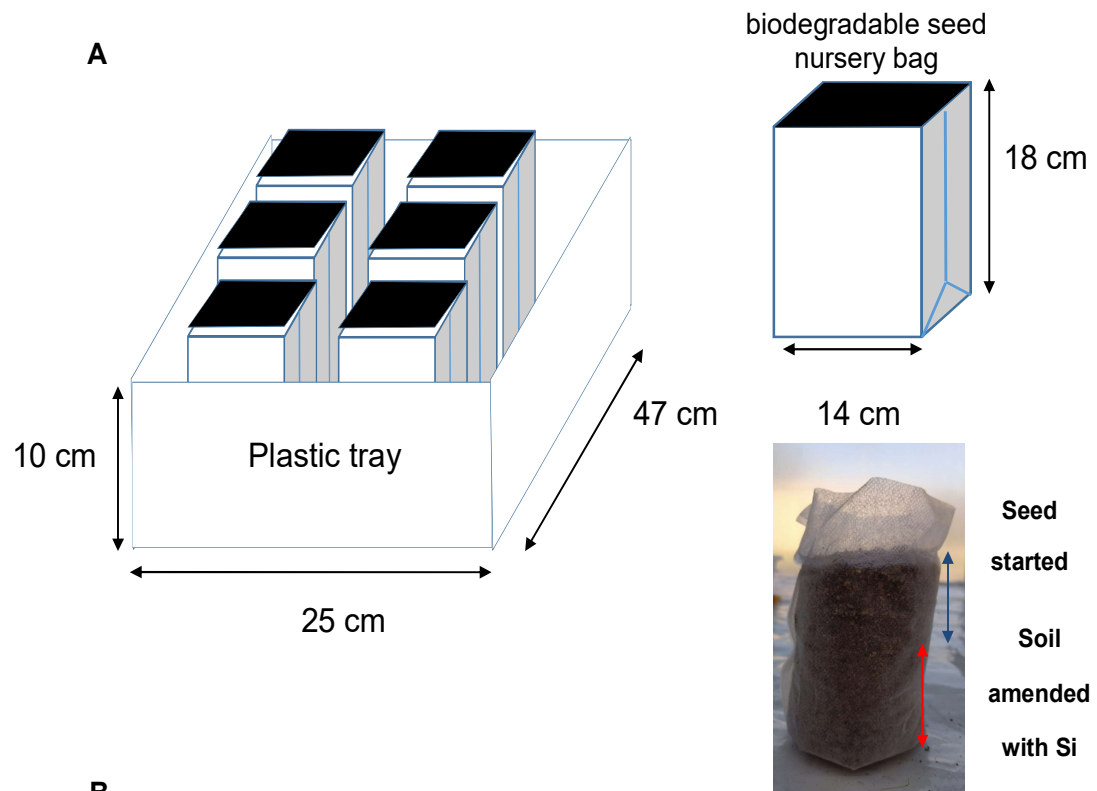


FIGURE 5 Activity of superoxide dismutase (SOD) (A), catalases (CAT) (B), peroxidases (POX) (C), and phenylalanine ammonia-lyase (PAL) (D) on leaves of wheat plants grown in soil supplied with calcium silicate (+Si) or extra-fine limestone (-Si) receiving 70 (Low N) or 200 (High N) kg ha⁻¹ of nitrogen at sampling time (ST; hours after inoculation with *Pyrenophora tritici-repentis*). Data point from two pooled experiments (n = 8) are the median and error bars represent standard deviation of means.

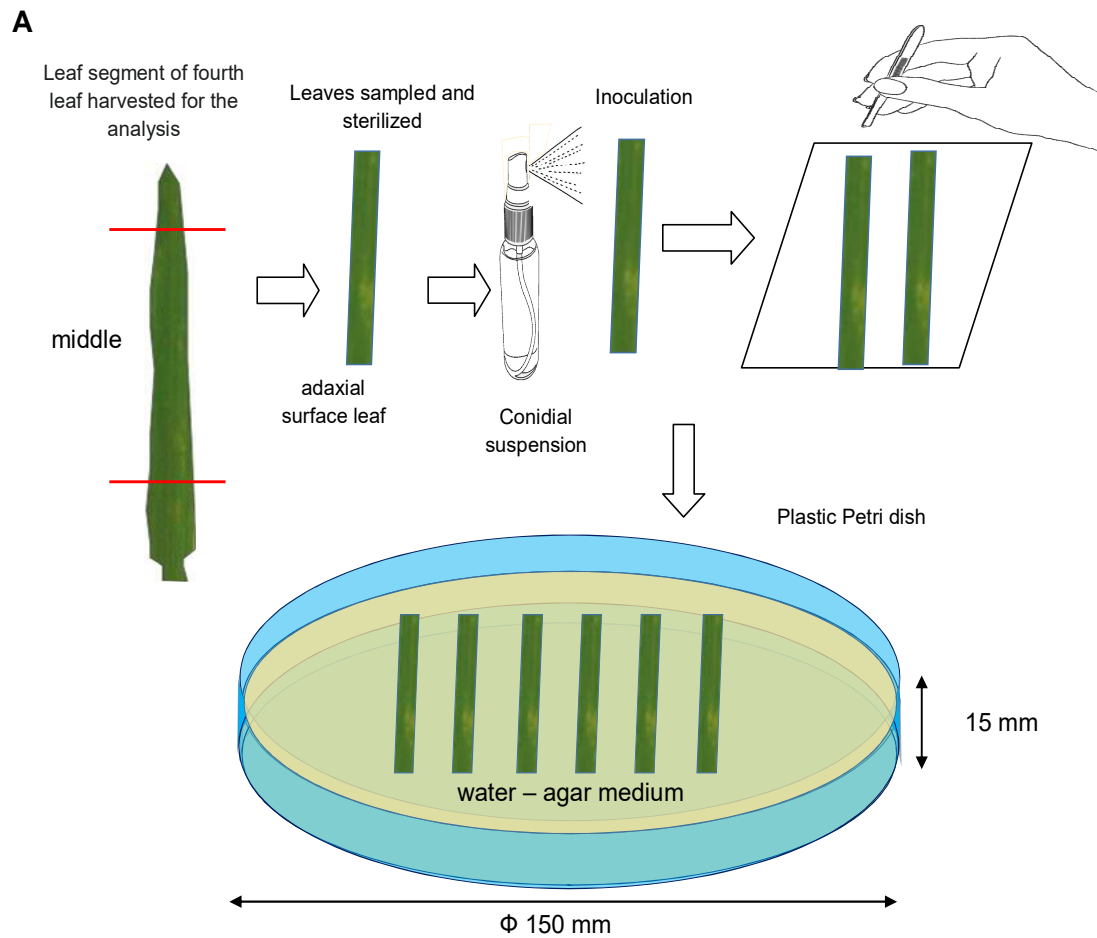


B



Supporting information

Figure S1. Plant material and growth. A) Material used for experiment and bag nursery distributed in a plastic tray. B) Plants growing in a greenhouse before inoculation.



B



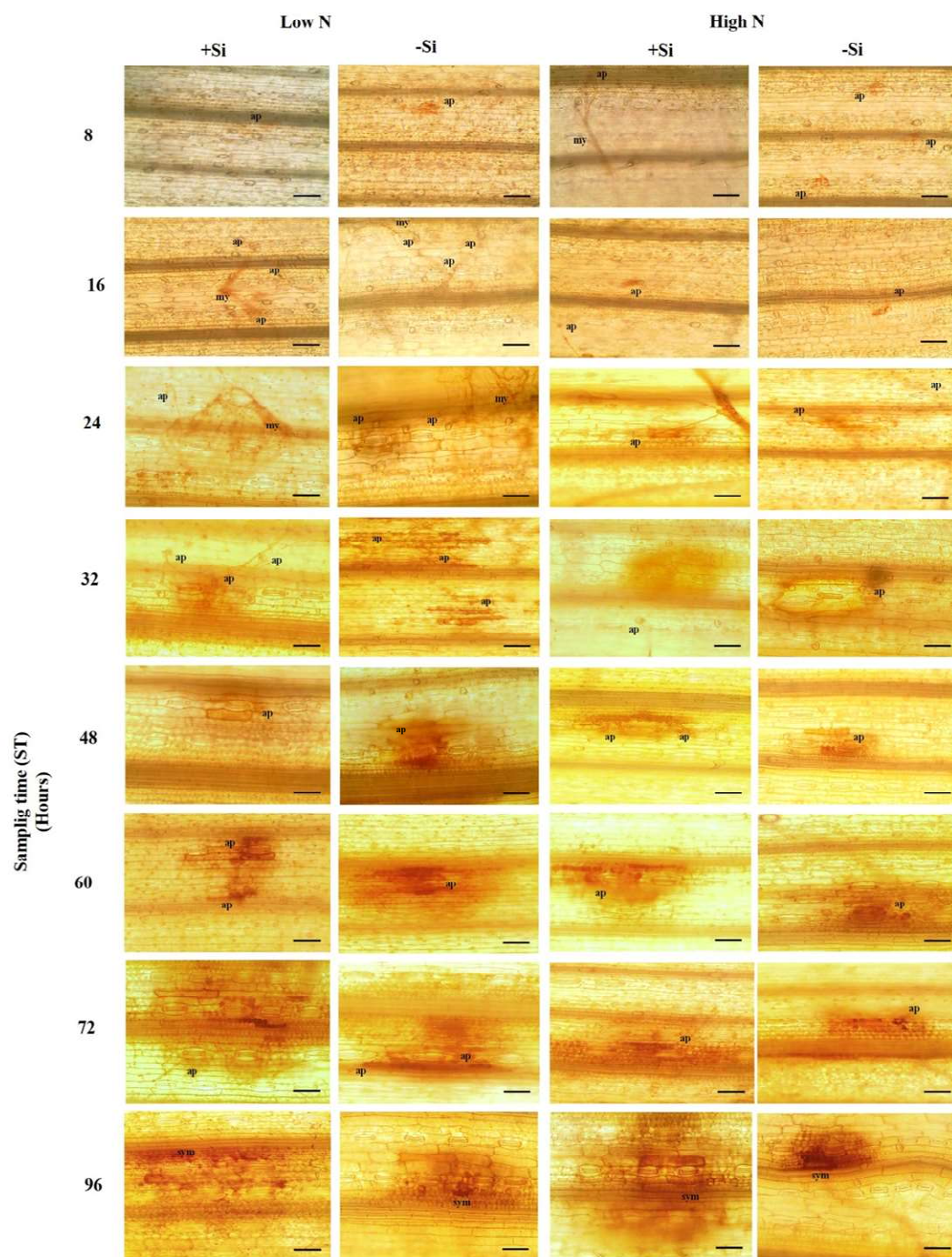
Leaves arrangement in plastic Petri dish with water- agar



The plastic Petri dishes with *Ptr*-inoculated and mock-inoculated leaves

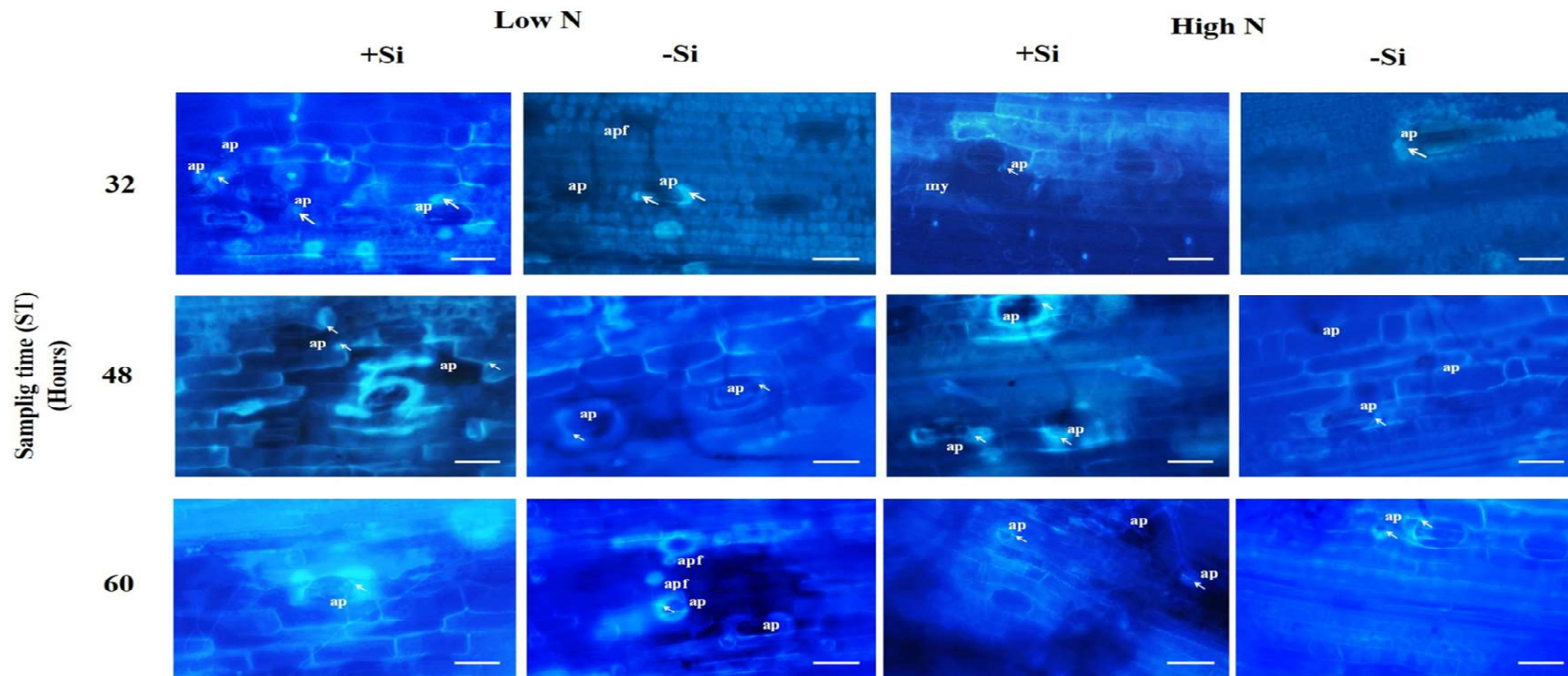
Supporting information

Figure S2. Inoculation procedure. A) The fourth leaf of 50-day-old of wheat plants at the flag leaf just visible (ZGS37) used for inoculation. B) Plastic Petri dishes with *Ptr*-inoculated and mock-inoculated leaves incubated at 25 ± 1 °C, relative humidity of $80 \pm 5\%$, and photoperiod of 12 h.



Supporting information

Figure S3 DAB reaction observed from 8 to 96 hours after inoculation (hai) with *Pyrenophora tritici-repentis* on leaves of wheat plants grown in soil supplied with calcium silicate (+Si) or extra-fine limestone (-Si) receiving 70 (Low N) or 200 (High N) kg ha⁻¹ of nitrogen. Scale bar 50 μm: my: mycelium; ap: appressorium; sym: symptoms.



Supporting information

Figure S4. Callose deposition in wheat leaves from 32 to 60 hours after inoculation (hai) with *Pyrenophora tritici-repentis* of wheat plants grown in soil supplied with calcium silicate (+Si) or extra-fine limestone (-Si) receiving 70 (Low N) or 200 (High N) kg ha⁻¹ of nitrogen. Scale bar 50 μm; my: mycelium; apf: appressorium formation; ap: appressorium; callose deposition (white arrow).

TABLE S7. Concentration of nutrients in leaves of wheat plants at third node detectable (ZGS33)

Macronutrients	Units	Low N		High N	
		+Si	-Si	+Si	-Si
Nitrogen (N)	g kg ⁻¹	26.65	30.81	33.64	34.11
Phosphorus (P)	g kg ⁻¹	2.64	2.91	3	3.15
Potassium (K)	g kg ⁻¹	19.66	18.99	17.99	19.72
Calcium (Ca)	g kg ⁻¹	3.8	3.38	3.09	3.17
Magnesium (Mg)	g kg ⁻¹	2.43	2.16	2.34	2.47
Sulfur (S)	g kg ⁻¹	2.9	2.9	2.86	3.3
Micronutrients					
Boron (B)	mg kg ⁻¹	19.57	16.87	12.28	14.25
Copper (Cu)	mg kg ⁻¹	9.14	25.99	11.18	14.43
Iron (Fe)	mg kg ⁻¹	186.14	537.65	214.08	322.95
Manganese (Mn)	mg kg ⁻¹	52.37	56.83	46.04	40.05
Molybdenum (Mo)	mg kg ⁻¹	4.99	3.72	12.38	4.2
Zinc (Zn)	mg kg ⁻¹	11.41	12.36	4.44	13.4

General conclusions

A positive linear relationship was recorded for primary inoculum and the presence of the disease, showing that an amount greater than 1000 pseudothecia per m² were associated with cases of severity or incidence in 2019 and 2020. Collectors at 30 cm height captured the largest portion of *Drechslera* sp. conidia, and the highest conidial frequencies occurred during early seedling growth (ZGS13), tillering (ZGS20) and after flowering (ZGS65) stages. As a result, *Ptr* management should be associated with the stubble management, since the successive wheat planting for more than the two years favored the increase in the inoculum from pseudothecia. The findings about the initial inoculum *Ptr* have implications for tan spot integrated management in the South region of Brazil.

It was determined that the recommended N rate (130 kg ha⁻¹) increased yield and HAD, and improved tan spot control. In this sense, these results associated with economic and cost efficiency analysis indicate that the use of a moderately resistant cultivar and low N or recommended N maintained adequate nitrogen use efficiency (NUE) and economic returns.

AUDPC of tan spot, powdery mildew, and leaf rust were positively associated with ash content (AC), and higher PC, DG, WG, AC, and falling number (GFN), resulting in changes in whole flour color. However, fungicide application increased the lightness and the yellow tendency of color parameters. The integrated diseases management that involves use of moderately resistant cultivar, fungicide application, and nitrogen showed an effect reducing the area under disease progress curves (AUDPCs) and higher *Fv/Fm* (adequate

physiological process), while guaranteeing adequate levels of yield components and grain quality.

The use of high N increased the incubation period (IP) and reduced the tan spot damage due to the higher maximum photosystem II quantum yield (F_v/F_m). Race 1 caused reduction of Chl a , Chl b , carotenoids, total chlorophyll (Chl $a+b$), and total chlorophyll (Chl $a+b$)/carotenoids ratio compared to race 2. The damage caused by necrotrophic *Ptr* race 1 and 2 decreased F_v/F_m , the probability of a trapped exciton moving an electron further than Q_A^- (Ψ_o), and quantum yield of electron transport (ϕE_o), which, in turn, increased flux of dissipated (Dl o /RC), absorbed (ABS/RC), transported (ET o /RC), and trapped (TR o /RC) energy per active reaction center. The results indicated that the application of recommended N and the use of moderately resistant cultivars reduced the effect of *Ptr* while maintaining adequate CF parameters.

Nitrogen and silicon fertilization demonstrated that +Si applied and low N increased the activity of superoxide dismutases (SOD), catalases (CAT), peroxidases (POX) and phenylalanine ammonia-lyase (PAL). The enzymatic activity was associated with higher H $_2$ O $_2$ accumulation (high intensity) in response to the *Ptr* infection in treatment with +Si and low N, whereas the callose deposition was observed at 32 to 48 hai in the same treatment, with higher accumulation. However, at high N, the +Si concentration declined in leaves. Those results indicated that each element may act in an independent way in the activation of plant defense responses and the activation of antioxidative mechanism.

Data availability statement

All data, including graphical work, were processed and analyzed with R version 4.0.4. (RStudio, 2021). Scripts were prepared in R Markdown and organized as a research compendium available at https://osf.io/kz492/?view_only=5dd31d76891047b5b6f8885ff34a587c

Citation as:

Román Ramos, A. E. (2022). Partial resistance, fungicide and mineral nutrition on wheat: effect on cytological and biochemical defenses, chlorophyll a fluorescence, yield and technological grain quality. Retrieved from osf.io/kz492.